UNIVERSITY "MEDITERRANEA" OF REGGIO CALABRIA
AGRARIA DEPARTMENT
Ph.D. Course in Agricultural, Food and Forestry Sciences
Cycle XXXIV, DSS: AGR/07

DISSECTING THE PHYSIOLOGICAL AND MOLECULAR MECHANISMS OF NITROGEN USE EFFICIENCY (NUE) IN TOMATO

Ph.D. THESIS

Ph.D. Candidate
Meriem Miyassa Aci

Tutor
Prof. Francesco Sunseri

Co-Tutor
Prof. Maria Rosa Abenavoli

Ph.D. Coordinator
Prof. Marco Poiana

Academic Years 2018-2021

Table of content

Abstract

Nitrogen (N) is a limiting factor of plant growth, crop yield and quality being a structural component of amino acids, nucleic acids, and other N-containing biomolecules. In the last decades, to maintain high yield for meeting global food demands, the N fertilizers have been massively applied with a negative impact on environment and human health. In this regard, understanding and improving the nitrogen use efficiency (NUE) of crop plants is an important challenge for a sustainable agriculture. Modern varieties of many crops, including tomato, have been selected under high input conditions with a possible decline of the N uptake and utilization efficiency. Thus, exploiting the genetic diversity in traditional cultivars, as long storage tomato ecotypes, represent a promising strategy to identify useful traits for improving NUE. In this respect, the morpho-physiological and molecular responses of different tomato genotypes in response to nitrate (NO_3^-) limiting condition were assessed. In the first step, a NUE contrasting pair, Regina Ostuni (RO, high-NUE) and UC82 (low-NUE), based on morpho-physiological traits and biomass production, was identified. To understand the molecular mechanisms conferring high NUE, several NO_3^- metabolism related genes (assimilation, transport, remobilization, and storage/sequestration), at short and long-term limiting NO_3^- exposure, in root and shoot, were assayed. At short-term, RO exhibited a higher NO_3^- storage (*SlCLCa*) and remobilization (*SlNRT1.7*) abilities compared to UC82, whereas at long-term, the N-use efficient genotype seemed to store less NO_3^-, which was more allocated and assimilated into the shoot (*SlNRT1.5* and *SlNR*). In the second step, after 5 days of N-deprivation, RO and UC82 short-term (0h, 8h and 24h) transcriptomic responses to low (LN) and high (HN) NO_3^- resupply, in both root and shoot, were compared. The significant Differentially Expressed Genes (DEGs) for G (Genotype), G×N (N supply) and G×N×T (sampling Time) were identified by the analysis of variance (ANOVA) using a multivariate linear model. The N-responsive genes were selected according to their expression profiles across the time-course. In addition, to detect the modules significantly correlated to LN in RO, a Weighted Gene Co-expression Network Analysis (WGCNA) was performed. In both tissues, one co-expressed module was highly correlated to 24h LN resupply in RO. In shoot, the hub genes were enriched in vegetative phase change, carbohydrate mediated signaling, response to nutrient, cytokinin biosynthetic process and carbon fixation in photosynthetic organism's biological process GO terms, while, in root, any metabolic process was significantly enriched. In addition, the regulatory network analysis identified the key LN-

related genes in each module, which might be responsible for the differential regulation of early LN responses between genotypes. In the last step, RO and UC82 transcriptomes in response to long-term (7 d) LN and HN resupply and the co-expression modules correlated to the phenotypic traits, in both tissues, were investigated by WGCNA. Different comparisons were performed to identify both genotype and NO_3^- effects. Interestingly, most of the LN-induced differential expression in RO compared to UC82 affected genes involved in the photosynthetic process. Finally, the WGCNA revealed the co-expression modules highly correlated with the morpho-physiological traits including NUE and its components, in both tissues. Functional analysis of the hub modules showed a significant enrichment in photosynthesis and transmembrane transport activity biological process GO terms in shoot and root, respectively, and some key NUE and NUpE related genes were also identified. In conclusion, our study provided a detailed framework of the molecular regulatory networks modulating tomato responses to N limiting condition, identifying novel key genes useful for improving NUE in tomato.

Keywords: Nitrate, abiotic stress, N-stress, RNAseq, time-course, Weighted Gene Coexpression Network Analysis (WGCNA).

Riassunto

L'azoto (N) è il nutriente maggiormente limitante la crescita, la produttività e la qualità delle piante, in quanto componente strutturale di amminoacidi, acidi nucleici e biomolecole. Nelle ultime decadi, i fertilizzanti azotati sono stati utilizzati in modo massiccio per garantire un'alta produzione rispondendo alla crescente richiesta di cibo, causando un impatto negativo sull'ambiente e sulla salute umana. A tal fine, comprendere e migliorare l'efficienza d'uso dell'azoto (NUE) nelle specie coltivate è fondamentale per un'agricoltura sostenibile. Le moderne varietà, incluso il pomodoro, sono state selezionate in condizioni di alto N determinando una riduzione dell'efficienza di assorbimento e utilizzazione. In quest'ottica, esplorare la diversità genetica di *landraces*, quali le varietà da serbo in pomodoro, rappresenta una strategia vincente per identificare tratti utili per migliorare la NUE. A tale scopo, sono stati comparati differenti genotipi di pomodoro sulle base delle loro risposte morfo-fisiologiche e molecolari a limitanti livelli di nitrato. Nel primo *step* sono stati identificati due genotipi contrastanti per la NUE, Regina Ostuni (RO, alta-NUE) and UC82 (bassa-NUE) in base ad analisi morfo-fisiologiche e produzione di biomassa. Successivamente, per individuare i meccanismi molecolari alla base della diversa efficienza, sono stati analizzati i livelli di espressione di alcuni geni del metabolismo dell'azoto (assimilazione, trasporto, rimobilizzazione e stoccaggio) in radice e germoglio, in risposta a breve- e lungo termine di esposizione a basso (LN) ed alto (HN) NO_3^-. Nelle prime ore di esposizione a LN, RO mostrava un alto livello di espressione dei geni relativi allo stoccaggio (*SlCLCa*) ed alla rimobilizzazione (*SlNRT1.7*), mentre a lungo termine, evidenziava alti livelli di espressione dei geni *SlNRT1.5* e *SlNR*, suggerendo una maggiore assimilazione. Nel secondo *step*, e dopo 5 giorni in assenza di N, sono state analizzate le risposte trascrittomiche a breve-termine (0, 8, 24h) dei due genotipi esposti a LN ed HN, in radici e germoglio. Sono stati individuati DEGs per G (Genotipo) e le interazioni G×N (livello di N) e G×N×T (Tempo di campionamento) con l'analisi della varianza (ANOVA), adottando un modello multivariato lineare. Inoltre, attraverso una WGCNA (*Weighted Gene Co-expression Network Analysis*), sono stati rilevati i moduli correlati al trattamento LN nel genotipo RO. Nel germoglio come nelle radici è stato identificato un modulo correlato al trattamento LN dopo 24h di esposizione. I maggiori *biological process GO terms* del modulo identificato nel germoglio erano *vegetative phase change*, *carbohydrate mediated signaling*, *response to nutrient* and *cytokinin biosynthetic process* e *carbon fixation in photosynthetic organisms*, mentre nella radice nessun *GO term* era significativo. L'analisi network ha permesso di identificare i geni piu connessi in ciascun

modulo, che potrebbero spiegare le differenti risposte tra genotipi. Nell'ultimo *step*, la risposta trascrittomica è stata analizzata dopo lunga esposizione a LN ed è stata effettuata una correlazione tra moduli e caratteri morfo-fisiologici tramite WGCNA. Diversi confronti sono stati effettuati per determinare gli effetti di G e N, ed individuare risposte (DEGs) genotipo e LN-specifiche, molti dei geni identificati mostravano un coinvolgimento nel processo fotosintetico. L'analisi WGCNA ha permesso di identificare i moduli altamente correlati con tratti morfo-fisiologici inclusa la NUE e le sue componenti in entrambi i tessuti. I *GO terms* significativi erano *photosynthesis process* nel germoglio e *transmembrane transport activity* nella radice, e geni correlati alla NUE e NUpE sono stati identificati. In conclusione, questo studio fornisce un quadro dettagliato della regolazione a livello molecolare che modula la crescita e lo sviluppo del pomodoro a limitata disponibilità azotata, identificando alcuni *geni candidati* utili al miglioramento della NUE in pomodoro.

Keywords: Nitrato, stress abiotici, N-stress, RNAseq, *time-course,* Weighted Gene Coexpression Network Analysis (WGCNA).

General Introduction

1. Role of Nitrogen in Crop systems

In plants, Nitrogen (N) represents an essential constituent of many macromolecules, such as DNA, chlorophyll, phytohormones, primary and secondary metabolites, required for plant growth and development (Hawkesford *et al*., 2012). N is also a sensing and signal molecule affecting many plant processes including root and leaf functionalities, abiotic and biotic stress responses, seed germination, and hormone balance (Vidal *et al*., 2010; Alvarez *et al*., 2012; Xu *et al*., 2012). For this reason, after carbon (C), N (about 1–5% of total plant dry matter) is the element required in largest amount by plants, thus representing one of the most important nutrients limiting crop productivity (Marschner, 2012).

In soil, N is present as inorganic forms, such as nitrate (NO_3^-) and ammonium (NH_4^+), and as organic forms, mainly consisting of urea, free amino acids, and short peptides. The availability of these different forms considerably fluctuates in both space and time, due to soil heterogeneity and dynamic microbial conversions, agricultural practices and environmental conditions (Bloom, 2015). Among them, NO_3^- and NH_4^+ are the major N sources acquired by root. In agricultural soil, NO_3^- is present in higher concentrations (1-5 mM) compared to NH_4^+ (20-200 mM), and it is more mobile than other N forms in soil solution. Therefore, it is readily available to plants but also easily lost in the root zone by leaching and, consequently, its soil concentration is very variable (Miller and Cramer, 2004). By contrast, NH_4^+ becomes a dominant form in some acidic and/or anaerobic and/or uncultivated soils, as well as in acid forest and rice paddy soils (Kronzucker *et al*., 2000). However, high NH_4^+ concentration is toxic for many sensitive crops, causing stunted growth, leaf chlorosis, and poor root development (Miller and Cramer, 2004). For an optimal growth, most crops require both NO_3^- and NH_4^+ availability, and the best ratio depends on plant species, developmental phase and environmental conditions (Miller and Cramer, 2005; Esteban *et al*., 2016).

In addition, plants can acquire amino acids, small peptides, and (partial) proteins from the soil, whose concentration ranged from 0.1 to 100 μM (Jones *et al*., 2002; Jämtgård *et al*., 2010). In low N-input and cold environment, pools of amino acid N represent a primary factor in ecosystem function and vegetation succession (Warren, 2006). In recent years, many studies proved that the amino acids supply could sustain by itself the plant growth. Recently, amino acid transport systems for root uptake have been partly characterized in *Arabidopsis* and crops (Yao *et al*., 2020).

In soil, urea occurs at very low concentrations (Miller and Cramer, 2004) and it is generally subject to rapid microbial conversion in NH_4^+ and NO_3^- (Cantarella *et al*. 2018). Recently, the urea acquisition by root, operated by dedicated transporters, has been evidenced, demonstrating the plant's ability to use urea as a direct N-source (Zanin *et al*. 2014). The high affinity transporter DUR3, selective for urea, has been identified as the major transporter, at low urea concentrations, in *Arabidopsis* (Liu *et al*. 2003, Kojima *et al*. 2007) and maize (Zanin *et al*, 2014).

Finally, the N_2 fixation from the air to plant-available ammonium by symbiotic bacteria is another important N source in agriculture (Xu *et al*., 2012), quantified approximately 50-70 Tg (Herridge *et al*., 2008). However, although natural mechanisms of N fixation in soil occur in some plants, it is not sufficient to satisfy global population growth and food demand (Crews and Peoples, 2004). In the last decades, to improve crop production, N-based fertilizers, especially urea, were largely employed in crop systems but its very rapid conversion to ammonia (NH_3) and CO_2 in moist soil (Fisher *et al*., 2016) resulting in high losses.

N fertilization can be considered as one of the most common practices to maintain and/or improve crop yield and quality to human consumption. Indeed, more than 110 Tg of N fertilizers are annually applied for meeting the increasing food demand (Chen *et al*., 2020). A large amount of world energy use (about 2%) is dedicated to the massive N fertilizer production by “Harber-Bosch” process (Sutton *et al*., 2013). However, depending on crops and soils, plants take up less than half of the applied N fertilizer (Yang *et al*., 2015; Zhu *et al*., 2016), and the remaining soil N, estimated in a range of 50-70%, was loss into the environment (Hodge *et al*., 2000; Tilman *et al*., 2002). It may contaminate aquatic systems through runoffs or leached water (Vitousek *et al*., 2009) or undergo to denitrification and released into the atmosphere as nitrous oxide, a powerful greenhouse gas (Reay *et al*., 2012), causing a reactive N species increase (Austin *et al*., 2013). These induce the O_3 formation in the troposphere (Butterbach-bahl *et al*., 2011), affecting human health (Von Mutius, 2000; Mulvaney *et al*., 2009; McAllister *et al*., 2012) and ecosystem biodiversity (Wedlich *et al*., 2012). Furthermore, N soil accumulation affects soil quality including erosion, acidification, salinization, and organic matter reduction (Velthof *et al*., 2011). In particular, N fertilizer applications determine a decrease in pH soil (Guo *et al*., 2010; Lu *et al*., 2014; Mahler and Harder, 1984), thereby inducing the development of infertile soils. In addition, soil acidification caused the heavy metals release in soil solution, which may lead to nutrient disorders and toxic effects in plants (Sutton *et al*., 2013).

In vegetable crops, N fertilization has significant impact with marked effects on fruit quality and their shelf life. In the last decades, research about N effect on vegetable quality was intensified. In particular, low nitrogen levels reduced protein content and fruit quality vegetables, whereas increasing N application often decreases the concentration of vitamin C, soluble sugar, soluble solids, while increasing the titratable acidity in tomato (Wang *et al*., 2008), overall, optimum N level improves also the quality of edible plant part.

However, although the N application achieved higher crop yield and quality due to an increased soil N availability (Halvorson and Reule, 2007), an over-fertilization reduced yield in many crops (Albronoz, 2016) and quality, affecting some agronomic and physiological traits (Figure 1). Furthermore, it leads a higher cost of investment in agricultural inputs by farmers, and greater food and nutrition insecurity (Dimkpa *et al*., 2020). Moreover, a balanced dynamic between N supply and food demand in crop systems need to be achieved, and an efficient N use could be crucial for enhancing productivity and cost-effectiveness of the cropping systems, but also decreasing the risk for the environment and human health.

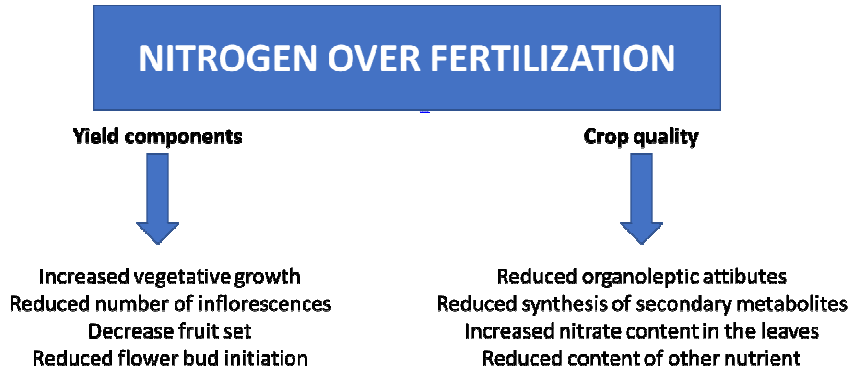

Figure 1. Schematic representation of the primary effects of N over-fertilization on yield parameters and produce quality.

2. Nitrogen Use Efficiency

The improvement of N use efficiency (NUE) together with an integrated N management strategies and practices are crucial to maximize crop yield, reducing cost of production, environmental pollution, and human damages (Zhang *et al*., 2015; Anas *et al*., 2020).

Nitrogen use efficiency (NUE) is a complex multigenic trait, in which several intricate physiological and molecular processes are involved and affected by many genetic and environmental factors. Two components contribute to plant NUE: N uptake efficiency (NUpE) and N utilization efficiency (NUtE) (Xu *et al*., 2012).

N uptake efficiency (NUpE) is the ability of plant to take up N from the soil, whereas N utilization efficiency (NUtE) is the ability of plant to convert the N taken up from the soil into harvestable grain (Moll *et al*., 1982; Good *et al*., 2004; Moose and Below, 2009) (Figure 2).

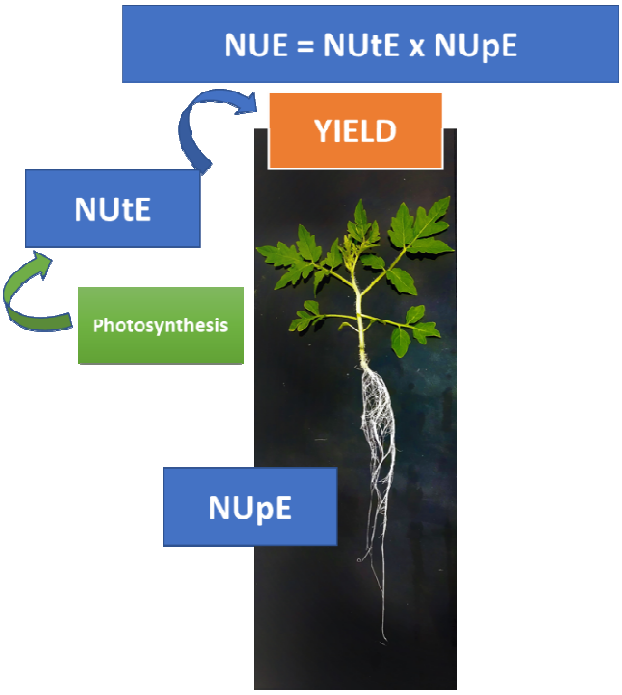

Figure 2.Schematic representation of NUE and its components (Nitrogen Utilization Efficiency, NUtE; Nitrogen Uptake Efficiency, NUpE)

NUpE is controlled by many factors including soil N forms, soil structure, plant N status, root architecture, N assimilation, and N metabolites (Nacry *et al*., 2013). For example, a large and deep root, with an appropriate architecture and a high stress tolerance (high plant density, drought, and N deficiency), underlies high NUE in maize production (Peng *et al*. 2020). However, a crucial strategy to improve NUE is to enhance N uptake by root through N-transporters (Miller *et al*., 2007; Xu *et al*., 2012; Krapp *et al*., 2014), whose efficiency reduces economic cost of crop production and environmental damage (Fageria and Baligar, 2005). So that, NUpE appears to be a relevant limiting factor to improve NUE in many crops (Le Gouis *et al*., 2000; Schroeder *et al*., 2013).

NUtE is regulated by N uptake, metabolism, allocation, and remobilization (Tsay *et al*., 2011; Nacry *et al*., 2013). Thus, the genetic manipulations of N metabolic processes have been already used to improve this trait (Good *et al*., 2007; Pena *et al*., 2017; Perchlik and Tegeder, 2017). However, as NUtE is a multigenic trait, the transgenic overexpression of N assimilation genes did not lead to an improved NUE (Pathak *et al*., 2011; Sinha *et al*., 2018).

In the last decades, different researches focused on understanding the molecular processes involved in NUE (Good *et al*., 2004; Fageria and Baligar, 2005; Fan *et al*., 2007; Hirel *et al* 2007; Garnet *et al*., 2009; Robertson and Vitousek, 2009; Masclaux-Daubresse *et al*., 2010; Xu *et al*., 2012; Han *et al*., 2015), mainly through both cropping systems management and breeding innovations (Cormier *et al*., 2016; Martinez-Feria *et al*., 2018). For this reason, numerous approaches have been proposed to calculate NUE with distinctive definitions and functions (Fageria *et al*., 2005; Ernst *et al*., 2020; Congreves *et al*., 2021).

Firstly, NUE can be defined as grain yield per unit of available N in soil (Moll *et al*., 1982):

$$NUE = Gw/Ns = (Nt/Ns)/(Gw/Nt) \quad [1]$$

where Gw is the grain yield, Ns is the available N in soil and Nt is the total N in plants when they are mature. In the equation [1] NUE is also the product of NUpE and NUtE.

Moreover, Berendse and Aerts (1987) defined NUE as produced dry weight per unit of N taken up:

$$NUE = A/Ln \quad [2]$$

where A is the N productivity (g dry weight g-1 N) and 1/Ln is the mean residence time of N in plants. In details, A is the dry matter production rate per unit of N in plants, and 1/Ln represents the period when N is used for carbon fixation. In *Arabidopsis thaliana*, Chardon *et al*. (2010) defined NUE as the ratio of dry matter over N concentration:

$$NUE=DM/N\% \quad [3]$$

where DM is the total shoot dry matter and N% is the total N concentration in plant.

Xu *et al*. (2012) reported many other indexes related to NUE: apparent N recovery rate (ANR), agronomy efficiency of fertilizer N (AE), N physiological use efficiency (NpUE), N transport efficiency (NTE), and N remobilization efficiency (NRE), but previously Good *et al*. (2004) described different equations related to specific contest (Table 1).

Recently, Congreves *et al*. (2021) collected the numerous NUE indices, commonly used in agricultural research, into groups by denominator such as fertilizer-based, plant-based, soil-based; but also by approaching isotope-based or systems-based NUEs.

Table 1.Definitions and formulae used to describe nutrient use efficiency in plants (Good *et al*., 2004)

Eqn	Term	Formula	Definition	Comments
1	Nitrogen use efficiency	NUE = Sw ÷ N	SW, shoot weight (DW); N, nitrogen content of shoot (DW)	Dose not account for biomass increases
2	Usage index	UI = Sw × (Sw ÷N)	Sw, shoot weight; N, nitrogen in shoot	Take into account absolute biomass increase
3	Nitrogen use efficiency (grain)	NUE = Gw ÷ Ns	Gw, grain weight; Ns, nitrogen supply (g per plant)	Reflects increased yield per unit
4	Uptake efficiency	UpE = Nt ÷Ns	Nt, total nitrogen in plant; Ns, nitrogen supply (g per plant)	Measures efficiency of uptake of nitrogen into plant
5	Utilization efficiency	UtE = Gw ÷ Nt	Gw, grain weight; Nt, total nitrogen in plant	Fraction of nitrogen converted to grain
6	Agronomic efficiency	$AE = (Gw_F – Gw_C) ÷ N_F$	N_F, nitrogen fertilizer applied; Gw_F, grain weight with fertilizer; Gw_C, grain weight of unfertilized control	Measures the efficiency of converting applied nitrogen to grain yield
7	Apparent nitrogen recovery	$AR = (N_F\text{uptake} – N_C \text{ uptake}) ÷ N_F × 100$	N_F uptake = plant nitrogen (fertilizer); N_C uptake = plant nitrogen (no fertilizer); N_F = Nitrogenfertilizer applied	Measures the efficiency of nitrogen capture from soil
8	Physiological efficiency	$PE = (Gw_F – Gw_C) ÷ (N_F\text{uptake} – N_C \text{ uptake})$	Gw_F, grain weight (fertilizer); Gw_C, grain weight (no fertilizer)	Measures the efficiency of plant nitrogen capture in grain yield

Good *et al*. (2004) stated the need of combining traditional breeding, marker assisted selection followed by genetic modification to improve specific NUE aspects. Moreover, breeding strategies must be performed at low N input (Ceccarelli, 1996), since the best performing crop cultivars, at high N input, are different from those at low (Gallais and Coque, 2005). Indeed, breeding plants with increased NUE, at limiting N input, is currently one of the key goals of research on plant nutrition for sustainable agriculture (Hirel *et al*. 2007; Hirel *et al*. 2011).

However, NUE is an important parameter commonly used to assess relative efficiency of fertilizer input to farmland (Andrews and Lea, 2013).

Among different species and within each one, genetic variations for NUE were already detected in *Arabidopsis* (Chardon *et al*., 2010), wheat (Chatzav *et al*., 2010), tomato (Abenavoli *et al*., 2016) and eggplant (Mauceri *et al*., 2020). Studies on the genetic variation, at both seedling and plant maturity, under controlled and field conditions, resulted in the identification of high NUE genotypes in many crops possessing high yield under low N condition (Le Gouis *et al*., 2000; Vijayalakshmi *et al*., 2015; Mauceri *et al*., 2020; Aci *et al*., 2021).

In addition, plant responsiveness to N depends also on the N fertilization levels, in which NUE as well as NRE are higher at low than at high N supplies. At high N, NUE variations are

mainly due to N uptake as reported in maize and *Arabidopsis*, whereas at low N, the remobilization of nitrogen and overall NUtE seem to play a predominant role (Xu *et al*. 2012). Phenotypic and genotypic variability for QTL mapping to identify genomic regions related to NUE have been applied on different food crops such as rice, wheat, maize and sorghum (Vijayalakshmi *et al*., 2013; Malleswari, 2013; Yu *et al*., 2015; Mahjourimajd *et al*., 2016). However, the role of the regulatory elements and signal transduction as well as NUE relationships with genes involved in root architecture, N uptake and assimilation, N-storage and re-translocation and genes involved in the regulation of these processes could have a critical impact on NUE (Xu *et al*., 2012).

Although many genes involved in NUE improvement are being proposed in both crops and *Arabidopsis* (Hirel *et al*., 2007), the causal intrinsic relationships to NUE have yet to be demonstrated.

In conclusion, the improvement of NUE is a challenging target because crop yield depends on many variables, including genetic traits and their variation among and within plant species (G), environmental factors (E), and agronomic and management practices (M) (timing, amount, forms and place of N application) (Nguyen *et al*., 2017; Martinez-Feria *et al*., 2018; Nguyen and Kant, 2018; Plett *et al*., 2020). The interaction and combination of these variables (G×E×M) will allow NUE improvement for a sustainable and safe crop production (Swarbreck *et al*., 2019; Hawkesford and Riche, 2020; Peng *et al*., 2020). Also, the integration of genomic and phenomic data, including as well meta-analysis, to find quantitative traits loci (QTLs) can provide novel molecular markers for assisting the selection of high NUE varieties in several crops, including tomato. Furthermore, specific approaches integrating transcriptomic, metabolomic, phenomic, functional genomics, quantitative genetics and soil nutrient dynamics will be useful to decipher the mechanisms underlying NUE.

3. Nitrate uptake, assimilation, and remobilization

To understand NUE, N transport and homeostasis must be considered as key points during life plant cycle. Although N is present in different inorganic and organic forms in soil solution, NO_3^- is usually the most abundant N source in aerobic soils, and its availability significantly affects crop productivity (Miller and Cramer, 2005). Nitrate can be assimilated in root or translocated to shoot via the xylem. Then, it is reduced to nitrite by nitrate reductase (NR) and further to ammonium by nitrite reductase (NiR) before incorporation into the amino acids

(Stitt, 1999). Otherwise, NO_3^- could also be stored, mainly in the vacuoles (Miller and Smith, 2008), in both root and shoot for further remobilization when its availability becomes scarce.

The major adaptations to NO_3^- availability consist in the modulation of the root system architecture (RSA) and in the uptake activity changes. An efficient N uptake depends on root/shoot ratio (R/S), root size, and root distribution in soil profile, such as root branching, which reduces N losses to deeper soil layers and groundwater (Lynch, 2013). The NO_3^- availability role in the root adaptation has been recently demonstrated by the invariably increases in the total root size in all maize genotypes under N starvation (Sinha *et al*, 2020). Furthermore, NO_3^- acts as a signal in the regulation of lateral roots (LR) development, which in turn considerably contributes to RSA. Furthermore, low NO_3^- can determine both stimulatory and inhibitory effects on LR development, while high nitrate supply has an inhibitory effect on LR development (Sun *et al*., 2017).

Four families of NO_3^- transporters in plants regulate N uptake, remobilization, or storage (Figure 3): Nitrate Transporter 2 (NRT2) (Orsel *et al*., 2002; Krapp *et al*., 2014), Nitrate Transporter 1/Peptide Transporter Family (NPF), (Léran *et al*., 2014), Chloride Channel Family (CLC) (Barbier-Brygoo *et al*., 2011) and Slow Anion Associated Channel Homolog (SLAC/SLAH) (Negi *et al*., 2008).

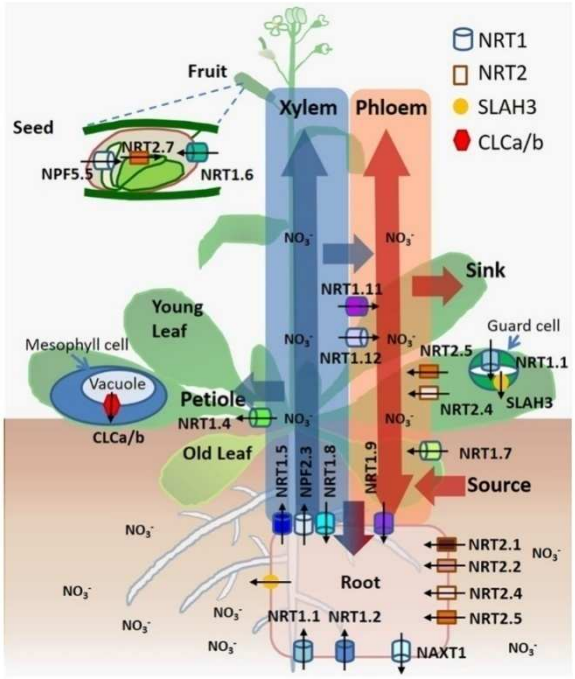

Figure 3.Spatio-temporal functionality of NO_3^- transporters/channels and NO_3transport routes in Arabidopsis (from Guan, 2017).

3.1. Nitrate uptake

NO_3^- fluctuation in the soil solution, both in time and space, can make it a limited resource; therefore, plants must adapt to NO_3^- soil availability maximizing uptake efficiency in different environments (Miller *et al.*, 2007). In plants, NO_3^- uptake by root is mediated by the NPF (previously named NRT1/PTR family) and the NRT2 family transporters, which in *Arabidopsis* consist of 53 and 7 members, respectively (Léran *et al.*, 2014).

NO_3^- uptake involves a complex set of membrane transport systems that includes specific affinity transporters, but the net uptake rates can be strongly influenced by the NO_3^- availability, plant N status and NO_3^- efflux from root cells (Forde, 1999). In particular, N uptake occurs thanks to membrane transporters, which are classified according to the affinity for their substrate. In plants, two transport systems can be detected: the High-Affinity Transport Systems (HATS) and the Low-Affinity Transport Systems (LATS) (Forde *et al.*, 2000). They operate at low (< 0.5 mM) and high (> 0.5 mM) NO_3^- external nitrate concentrations, respectively (Glass *et al.*, 2002) (Figure 4).

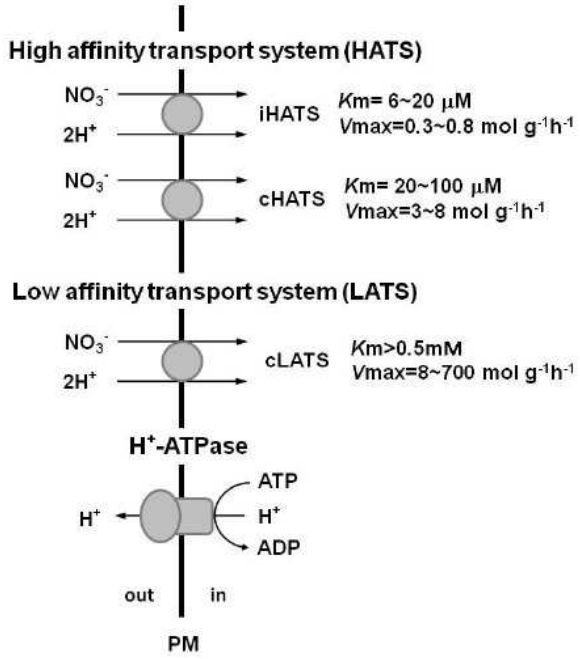

Figure 4.Proposed model of two-component high-affinity nitrate transport system.

Furthermore, within each of these systems, a constitutive (cHATS) and an inducible NO_3^- transport system (iHATS), regardless N concentration, co-exist (Glass *et al.* 1992; Noguero and Lacombe, 2016). The activity of both systems is regulated by cellular energy expressed as proton electrochemical gradient (Siddiqi *et al.*, 1990; Miller *et al.*, 2007). Considering *Arabidopsis thaliana*, as plant model, the main NO_3^- transporters are reported in Table 2.

3.1.1. Low Affinity Transport Systems (LATS)

Many genes are included in the NPF family (previously named NRT1), which can transport NO_3^- and other molecules. In *Arabidopsis*, this family consist of 53 members belonging to low affinity transporters, which operate at high NO_3^- concentration (Léran *et al*., 2014). Among these, the NPF6.3/NRT1.1/CHL1 is first member identified (Tsay *et al*., 1993), involved in various functions such as NO_3^- uptake from soil (Crawford, 1995; Munos *et al*., 2004) and NO_3^- translocation into the shoot (Léran *et al*., 2013). It is expressed in primary and secondary roots, root hairs as well as in young leaf and flower buds (Guo *et al*., 2002; Remans *et al*., 2006, Krouk *et al*., 2010).

Furthermore, NRT1.1 plays a key role as NO_3^- sensor, controlling several plant responses to NO_3^- by a signaling cascade, mechanism partly elucidated (Maghiaoui *et al*., 2020). The NPF6.3 is also considered a double affinity transporter revealing the ability to switch to the high-affinity activity, at low NO_3^- conditions, by the Thr 101 phosphorylation (Liu *et al*., 1999; Liu and Tsay, 2003; Ho *et al*., 2009), included in CIPK23-CBL9 protein complex (Figure 5). However, the mechanism is even more complex, involving other proteins such as ABI2 (belonging to protein phosphatase 2C family from the clade A), which modulates transport activity by preventing phosphorylation of CIPK23-CBL1 complex (Léran *et al*., 2015). Moreover, by using crystallization studies, the role of His 356 residues, as a nitrate-binding site, was also revealed (Parker and Newstead, 2014; Sun *et al*., 2014).

Table 2. Summary of the physiological functions and regulations of identified NO_3^- e transporters in *Arabidopsis thaliana* (modified from Wang *et al*. 2012).

Gene	**Function**	**Nitrate response**	**N starvation**	**Other regulations**
CHL1	Nitrate sensing	Induction	Repression	Nitrite (long-term) and high pH repression
(NRT1.1)	High and low-affinity nitrate uptake			Auxin, light, sugar, and nitrite (short-term) induction
NRT1.2	Low affinity nitrate uptake	Constitutive	Not known	Not known
NRT1.3	Not known	Induction (shoot)	Not known	Light induction
NRT1.4	Leaf nitrate homeostasis	Constitutive	Not known	Not known
NRT1.5	Root xylem loading	Induction	Not known	High pH and potassium limitation repression; Sugar induction
NRT1.6	Delivery of nitrate to developing embryos	Not known	Induction	Not known
NRT1.7	Nitrate remobilization from old to young leaves	Not known	Induction	Sucrose induction
NRT1.8	Xylem unloading and cadmium resistance	Induction	Not known	Cadmium induction
NRT1.9	Nitrate loading into root phloem	Constitutive	Not known	Not known
NAXT1	Root nitrate efflux	Not known	Not known	Acidic pH induced at protein level
NRT2.1	High-affinity nitrate uptake	Induction	Induction	Ammonium and glutamine repression; Light and sugar induction
NRT2.2	High-affinity nitrate uptake	induction	Not known	Not known
NRT2.4	High-affinity nitrate uptake at low nitrate concentration	Repression	Induction	Ammonium repression; Light induction
NRT2.7	Nitrate storage in mature embryos	Constitutive	Not known	Not known
CLCa	Nitrate accumulation in vacuoles	Induction	Not known	Not known
CLCb	Nitrate accumulation in vacuoles	Not knwon	Not known	Not known

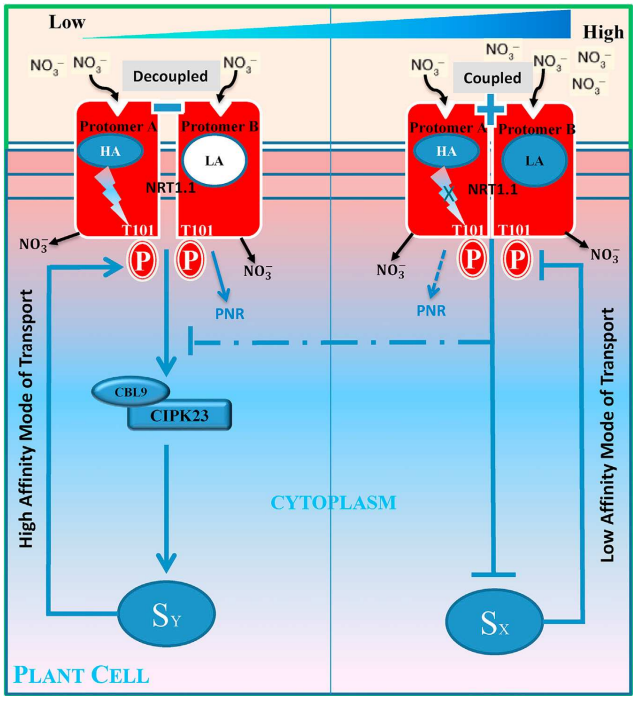

Figure 5.A Model of Phosphorylation Switch of the NPF6.3 transporter (Rashid *et al.*, 2018)

Another NO_3^- transporter belonging to NPF family, involved in the NO_3^- uptake, is the NPF4.6/NRT1.2/AIT1, which is localized in root epidermis and characterized by low affinity activity (Liu *et al*., 1999). Finally, others NPFs (i.e., NPF7.2, NPF7.3, and NPF2.3) have been identified and characterized, although their role appears restricted to NO_3^- translocation and distribution (Lin *et al*., 2008, Li *et al*., 2010; Taochy *et al*., 2015).

3.1.2. High Affinity Transport Systems (HATS)

Seven members of the NRT2 family, with an affinity around 0.2-0.5 mM NO_3^-, are included in the HATS, as reported by many authors (Orsel *et al*., 2002; Kiba *et al*., 2012; Lezhneva *et al*., 2014; Krapp *et al*., 2014; Kiba and Krapp, 2016). The most studied member of this family is NRT2.1, localized in the epidermal and cortical cells of roots, whose activity seems to be regulated by different factors. Indeed, *NRT2.1* expression is induced by NO_3^- itself and under limiting NO_3^- condition (Crawford and Glass, 1998; Cerezo *et al*., 2001), representing a classical inducible high affinity transport system model (Filleur and Daniel-Vedele, 1999), but it is repressed by high NO_3^-/N concentrations (Crawford, 1995). Among the members, only *NRT2.1* exhibited significant correlations between transcript abundance and high-affinity nitrate influx in *Arabidopsis* (Okamoto *et al*., 2003). In addition, recent studies also suggested a role of this transporter in water balance by regulating root hydraulic conductivity (Li *et al*., 2016).

Another NO_3^- transporter, with the same regulation in response to this anion, is the NRT2.2 member, localized close to the *NRT2.1* genomic region (*NRT2.1*: At1g08090 and *NRT2.2*: At1g08100) in *Arabidopsis*. Both *AtNRT2.1* and *AtNRT2.2* encoded the iHATS, usually making a small contribution to the system, which becomes evident when *NRT2.1* function is lost. Furthermore, the disruption of both *AtNRT2.1* and *AtNRT2.2*, using both KO mutants (*atnrt2.1* and *atnrt2.2*), highlighted that the iHATS was reduced by up to 80%, the cHATS up to 30% whereas the LATS fluxes were unaffected (Li *et al*, 2007). So, at low concentration, the NO_3^- uptake ability is partly guaranteed by the presence of cHATS (Cerezo *et al*., 2001; Miller *et al*., 2007) or other transporters, such as NRT2.4 (Kiba *et al*., 2012). Indeed, this transporter, expressed in epidermis of the lateral roots, contributes to maintain a residual NO_3^- uptake in root, at very low NO_3^- level (25 µM), and restores the absorption activity in *nrt2.1/nrt2.2* double mutant (Kiba *et al*., 2012). The use of a triple mutant (nrt2.1/nrt2.2/nrt2.4), at low NO_3^- level, suggested the existence of other high affinity transporters, among others the NRT2.5, which assured the NO_3^- uptake ability. Its role was

confirmed by using the quadruple mutant *nrt2.1/nrt2.2/nrt2.4/nrt2.5* in which finally the HATS activity was strongly reduced (Lezhneva *et al*., 2014). In addition, the increased *NRT2.4* and *NRT2.5* transcripts are characterized by a very high-affinity and are strongly induced by N deprivation, but rapidly repressed by NO_3^- and NH_4^+, suggesting their primary role in the earliest influx of NO_3^- (Lezhneva *et al*., 2014).

Moreover, the NO_3^- transport activity of the NRT2 members is regulated by the interaction with the protein NAR2/NRT3 in *Arabidopsis* (Orsel *et al*., 2006; Li *et al*. 2007) as demonstrated in oocyte gene co-expressions in which a positive effect of the NAR2.1 was observed in NO_3^- uptake (Kotur *et al*., 2012). This interaction was also observed in other plant species such as barley (Tong *et al*., 2005), maize (Lupini *et al*., 2016) and rice (Yan *et al*., 2011). Finally, NAR2.1 seems to be implicated in the NRT2.1 localization or stabilization in the plasma membrane (Wirth *et al*., 2007).

From a physiological perspective, NO_3^- uptake is always active, mediated by a $2H^+/1\ NO_3^-$ symport mechanism, coupled to a favorable H^+-electrochemical gradient created by the plasma membrane (PM) H^+-ATPase. Root PM-H^+-ATPase activity displayed a similar time-course pattern as that of NO_3^- uptake in maize (Santi *et al*., 1995). However, higher plants have multiple PM H^+-ATPase isoforms, with tissue specificity and co-presence in a specific cell type. In maize, MAH3 and MAH4, member of the PM-H+-ATPase subfamily II, responded to NO_3^- supply, although to different degree, MAH4 more sensitive than MAH3, with a greater up- and down- regulation in response to the treatment (Santi *et al*., 2003; Sorgonà *et al*., 2010 and 2011).

3.1.3.CLC channels

The name of chloride channel family (CLC, ChLoride Channel) derives from the first protein identified, CLC-0, in the electric organs of the marine ray *Torpedo californica* (Miller and White, 1980). Afterwards, the *CLC-0* cloning by Jentsch *et al*. (1990) led to the identification of a wide family, which includes either anion channels or anion/proton exchangers (Figure 6), being present in bacteria and all eukaryotic organisms. In plants, CLC proteins are involved in different physiological processes as stomatal movements, anion transport from cytoplasm to vacuole, osmoregulation, and resistance to biotic and abiotic stresses. However, they play a critical role in vesicular transport by regulating the internal pH and membrane potential of organelles (Von der Fecht-Bartenbach *et al*., 2007).

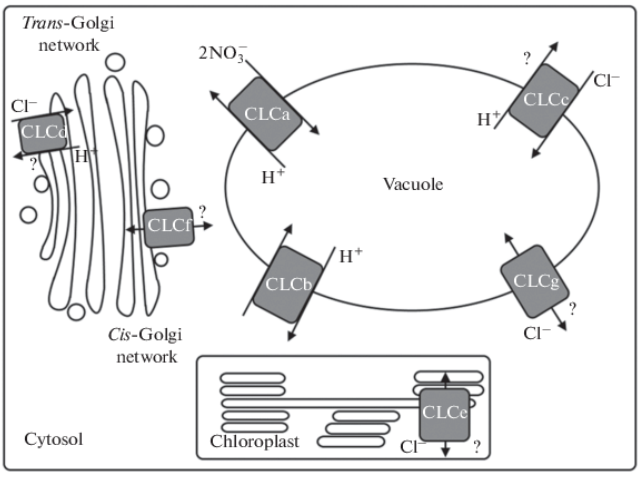

Figure 6. Intracellular localization of CLC family proteins in *A. thaliana* (Nedelyaeva *et al*., 2020).

In particular, these transporters are involved in NO_3^- transport into vacuoles, probably mediated by the nitrate/proton antiport machinery (De Angeli *et al*, 2009), in endomembrane vesicles (Zifarelli and Pusch, 2010), and in NO_3^- vacuolar remobilization (Schumaker and Sze, 1987). To date, the identified *AtCLCa* was expressed in both root and shoot appearing responsible for NO_3^- accumulation into vacuoles (Geelen *et al*., 2000; De Angeli *et al*., 2006). In particular, *AtCLCa* transports NO_3^- in two directions: from the cytoplasm to the vacuole and viceversa depending on cell demand, suggesting that its physiological role is not limited to vacuolar NO_3^- pool but participates also in the reuse of that previously accumulated. The *AtCLCa* disruption led to approximately 50% decrease in vacuolar NO_3^- confirming its important role in NO_3^- accumulation in this organelle (Geelen *et al*., 2000; De Angeli *et al*., 2006).

Other genes of the CLC family are involved in restoring the ionic balance in tissues by the mutation in *CLCa*. For example, in *Arabidopsis clca* mutant, the *AtCLCb–AtCLCd*, *AtCLCf*, and *AtCLCg* expression increased while *AtCLCe* decreased, demonstrating that the mechanisms related to CLC genes expression and NO_3^- transporters remain unclear (Monachello *et al*., 2009). Moreover, Brunaud *et al*. (2001) showed that the anion flux through AtCLCa is regulated by PP2A phosphatase (Protein Phosphatase 2A), which interacts with AtCLCa in *Arabidopsis*.

3.1.4. Slow Anion Associated Channel Homolog (SLAC/SLAH)

The existence of slow-type anion channels (SLACs), showing preference for NO_3^-, was demonstrated by patch-clamp experiments (Schroeder and Keller, 1992; Schmidt and

Schroeder, 1994). The protein, involved in these anion channels, belongs to the small SLAC/SLAH gene family (Negi *et al*., 2008; Vahisalu *et al*., 2008). Five genes (*SLAC1* and *SLAH1-SLAH4*) are included in this family displaying a common structure of 10 transmembrane α-helices (Negi *et al*., 2008), but only *SLAC1* and *SLAH3* have a NO_3^- transport activity (Geiger *et al*., 2011).

3.2. Nitrate assimilation

Nitrate needs to be reduced to ammonia for assimilation into the amino acids, in both root and shoot (Logan and Thomas, 1999). The efficiency of this process depends on the regulation of the different enzymes involved in the amino acid synthesis and their ultimate conversion into more complex N-containing molecules supporting growth.

The first step in NO_3^- reduction into nitrite (NO_2^-) occurs in both root and shoot by the cytoplasmic FAD-dependent NO_3^- reductase (NR) enzyme (Meyer and Stitt, 2001), by the following reaction:

$$NO_3^- + 8H^+ + 8e^- \rightarrow NH_3 + 2H_2O + OH^-$$

NR activity is tightly regulated by many environmental and physiological factors (Campbell 1999) and nitrate reduction represents the most important checkpoint in the metabolism of N compounds. Briefly, the NR holoenzyme is a dimer of two identical polypeptide chains, each of about 900 amino acids containing three prosthetic groups: FAD, haem-Fe, and Mo-pterin, all of which are bound into structurally independent domains. Each 100-kDa monomer has two active sites: one located at the C-terminus (the FAD-domain), which accepts electrons from NAD(P)H and the other at the N-terminus (the Mo-pterin domain) for the reduction of bound NO_3^- to NO_2^-. Both are connected to a central heme (cyt-b) domain (Figure 7).

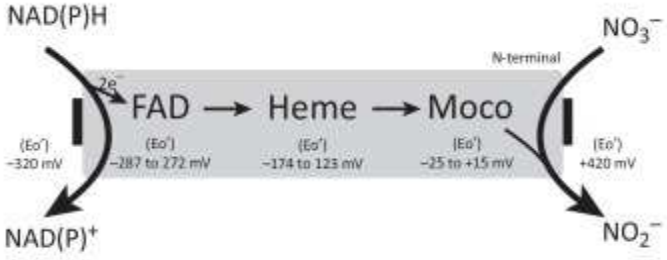

Figure 7.NR structure (from Chamizio-Ampudia *et al*., 2017)

In higher plants, NR is inducible (iNR) by nitrate itself, and if NO_3^- uptake exceeds assimilation by root, it will be transported to the shoot and leaves; in addition, the induction of

NR is affected by other signals such as light, carbohydrate, and phytohormones. The NR central role in the assimilation process was demonstrated in *Arabidopsis* by inverse genetic approaches in which *nr* null mutant was unable to use NO_3^- when it was the sole N source (Wang *et al*., 2004). Afterwards, an interplay between NR and nitrate transporters (NRT1.1 and NRT2.1) was also demonstrated (Filleur *et al*., 1999; Loqué *et al*., 2003).

After NO_3^- reduction, NO_2^- is translocated from the cytoplasm to the chloroplast, by specific transporters, where it is reduced to NH_4^+ by nitrite reductase (NiR), the second enzyme of this pathway (Figure 8). Consequently, NH_4^+ assimilation requires the availability of carbon skeletons and promotes carbon flow in the TCA cycle to produce different amino acids *via* the GS/GOGAT cycle (the enzymes glutamine synthetase (GS) and glutamate synthase or glutamate-2-oxoglutarate amino-transferase (GOGAT) (Turpin *et al*. 1988) (Figure 8). The GS fixes NH_4^+ in a glutamate molecule to form glutamine (Stitt 1999), which in turn reacts with oxoglutarate to form two molecules of glutamate. Therefore, NO_3^- is assimilated into the amino acids via the GS-GOGAT pathway, resulting in glutamine and glutamate as primary N organic compounds (Tobin *et al*. 1985; Lea and Forde, 1994).

Two GS isoforms are present in plants: GS1 and GS2 (Bernard and Habash, 2009). The cytosol located GS1 isoform is involved in N recycling in senescence leaves and N traslocation during seed germination, whereas the chloroplastic GS2 isoform is considered responsible for NH_4^+ assimilation (Masclaux-Daubresse *et al*. 2010). The role of GS1 and GS2 isozymes as potential marker to predict and select genotypes with enhanced NUE has been proposed in winter wheat (Zhang *et al*., 2017).

In higher plants, GOGAT uses either NADH or ferredoxin (Fd) as the electron carrier (Lam *et al*. 1996). These two isoforms are located in distinct organelles: NADH-GOGAT in plastids of non-photosynthetic tissues where plays a pivotal role in the N primary assimilation and NH_4^+ recycling (Sechley *et al*. 1992), whereas Fd-GOGAT in chloroplast where it is involved in light regulated processes (Suzuki *et al*. 1982).

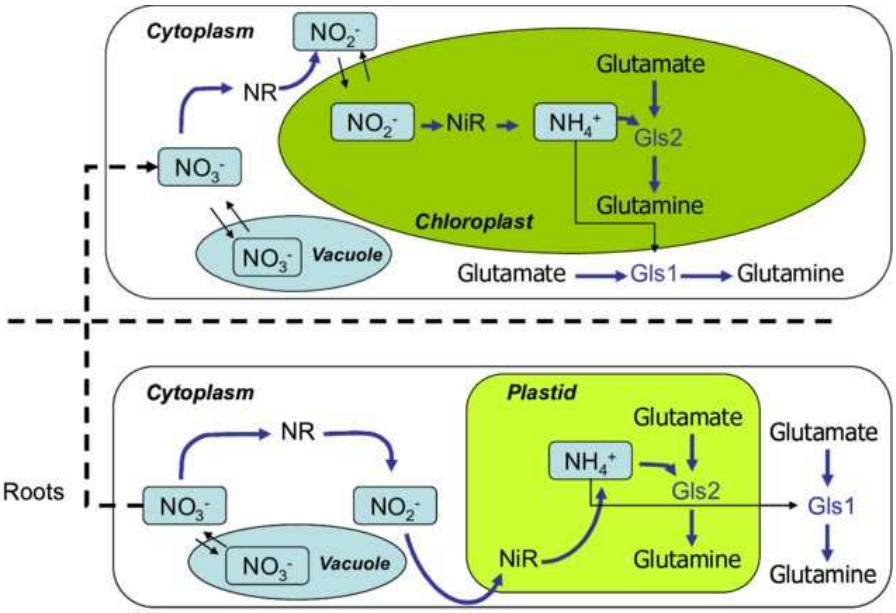

Figure 8.Schematic and simplified representation of the nitrate uptake, transport, and assimilation in plants (from Antonacci *et al*, 2007).

In addition to the GS/GOGAT cycle, another enzyme participates in ammonium assimilation. Indeed, ammonium or glutamine can be also used as substrate for asparagine synthetase (AS) enzyme for an ATP-dependent production of asparagine (Lam *et al*. 2003). Moreover, by amino-transferases different amino acids can be biosynthesized (Forde and Lea, 2007).

Finally, to form organic N compounds, carbon skeletons are essential, thereby photosynthesis, respiration and photorespiration are also essential for N assimilation (Masclaux-Daubresse *et al*., 2010).

3.3. Nitrate remobilization

N-remobilization allows a rapid increase in endogenous N availability. A switch from sink to source, during life cycle, regulates the remobilization process. In particular, at the senescence stage, old leaves become sink and leaf protein are degraded providing an important N source for plant organs (young leaves) (Diaz *et al*., 2008) and for grain filling (Salon *et al*., 2001). Breeze *et al*. (2011) confirmed that primary N assimilation decreases with senescence while N recycling and remobilization enzymes are stimulated. N-remobilization occurs through proteolysis and amino acids release, amino acid deamination and NH_4^+ release, and from catabolism of other N-rich compounds stored in the vacuole (Bigot *et al*., 1991). For example, the proteins degradation represents a huge N source, accumulated during vegetative stage, which will be remobilized and transported in other part of plant (Xu *et al*., 2012). Up to 95% of seed proteins derive from amino acids exported to seed after the degradation of existing

proteins in leaves (Xu *et al*., 2012), while the remaining is absorbed from the soil (Yoneyama *et al*., 2016). N metabolism and its remobilization processes, within the plant, are regulated by internal factors, such as NR and GS activities and affected by external factors, such as heat, drought, and salinity (Tian *et al*., 2016; Zandalinas *et al*., 2016).

Some GS1, NADH-glutamate dehydrogenase (GDH) and asparagine synthetase (AS) isoforms are strongly activated during N remobilization (Masclaux-Daubresse *et al*., 2010). The nature of the amino acid transporters in phloem loading during senescence is poorly understood (Okumoto and Pilot, 2011). In addition, the mitochondrial GDH plays a major role in reassimilation of photorespiratory ammonia and can alternatively incorporate ammonium into glutamate in response to high ammonium levels under stress (Masclaux-Daubresse *et al*., 2010).

Many authors demonstrated that different NRT transporters are involved in the N remobilization. In *Arabidopsis*, N remobilization *via* phloem, from source to developing tissues, occurs by NPF1.1/NPF1.2 and NPF2.13 transporters (Fan *et al*., 2009; Hsu and Tsay, 2013). Other members are organ specific such as NPF2.12, which is expressed in the vascular reproductive tissues and involved in seed N accumulation (Almagro *et al*., 2008).

4. Nitrate: a signal for plant growth

As plants are sessile organisms, they have implemented a series of mechanisms to ensure an efficient NO_3^- uptake to cope its spatial and temporal fluctuation in soil solution due to leaching and microbial activity (Miller and Cramer, 2004). In particular, plants have evolved elaborate adaptive sensing, signaling and regulatory network in response to NO_3^- availability, making it a signal for plant growth and development (Crawford, 1995; Wang *et al*., 2012; Remans *et al*., 2006; Ho *et al*., 2009; Ruffel *et al*., 2011; Marchive *et al*., 2013; Vidal *et al*., 2015). Indeed, NO_3^- triggers local and systemic signaling pathways, modulating gene expression, metabolism, and physiological processes in response to NO_3^- availability, N-status, photosynthesis and hormones (Nacry *et al*., 2013; Vidal *et al*., 2015; Krouk *et al*., 2016; O'Brien *et al*., 2016). Thus, many transporters are also involved in sensing and regulating gene expression, including the primary nitrate response (PNR) and nitrate-regulated root development (Remans *et al*., 2006; Ho *et al*., 2009; Gojon *et al*., 2011). Among them, at least two transporters, NRT1.1 and NRT2.1, are involved in nitrate-sensing in *Arabidopsis*. The first signal discovered in plants in response to NO_3^- availability is the switch mechanism of NPF6.3 (NRT1.1) by the T101 residue phosphorylation, which involved

protein kinase CIPK23, a plant-specific calcium sensor (Ho *et al*., 2009; Hu *et al*., 2009). Many studies demonstrated the role of NPF6.3 (CHL1/NRT1.1) as sensor required for PNR regardless uptake function (Remans *et al*., 2006; Ho *et al*., 2009; Wang *et al*., 2009), defining it as "transceptor" (Ho *et al*., 2009). In addition, NRT2.1 was proposed as sensor able to modify root growth in response to NO_3^- level (Remans *et al*., 2006).

In addition, there are also other genes not directly involved in PNR, as calcium-dependent protein kinases (CPKs), which play a fundamental role in nitrate-regulated root and shoot growth (Liu *et al*., 2017). Recently, the CPK translocation from cytoplasm to nucleus activating a NPL transcription factor was detected (Liu *et al*., 2017). These signal responses should be considered as intracellular NO_3^--related mechanisms, in which CPKs orchestrate N metabolism. In fact, by gene cloning and *Arabidopsis* mutants deficient in different regulatory proteins, specific functions were detected. For instance, nitrate transporters NPF6.3 and NRT2.1, NR, NIR, GLN2, glucose-6-phosphate dehydrogenase (G6PDH3) enzymes were markedly regulated by protein kinase CIPK8 (Hu *et al*., 2009).

Moreover, the identification of specific sequences in *Arabidopsis*, belonging to the promoters of nitrate-inducible genes, suggests the existence of transcription factors (TFs) involved in nitrate signaling (Konishi and Yanagisawa, 2010). The segments of promoters detected and recognized were named nitrate-responsive cis-elements (NRE).

TFs control metabolism and development, playing important roles in regulating the expression of NO_3^--responsive genes, including sentinel genes such as NRT1.1/NPF6.3, NRT2.1, NRT2.2, NIA1, NIA2, and NIR. To date, different TFs involving in nitrate responses were identified. Guan (2017) reported transcriptional regulators, including ANR1, NLP6, NLP7, LBD37/LBD38/LBD39, SPL9, HNI9, NAC4, bZIP1, TGA1/TGA4, TCP20, HRS1, NRG2, BT1/BT2 and NLP8 families, in which some TFs are nitrate-responsive, many from NLP6, NLP7, HNI9, TCP20, NRG2, BT1/BT2, and NLP8. For instance, ANR1 was the first TF detected in lateral root apices of *Arabidopsis* stimulating root growth in NO_3^- rich soils (Zhao and Forde, 1998). NPLs are involved in primary nitrate signaling, and NPL7 was found in nucleus via a CPK-dependent phosphorylation (Marchive *et al*., 2013; Liu *et al*., 2017). The TCPs (Teosinte branched1/Cycloidea/Proliferating cell factor1) are specific main regulators of plant morphology and architecture, playing a direct control on hormone activity (Guan, 2017).

Finally, many important factors are to be discovered yet for elucidating the different nitrate-sensing mechanisms and understanding their spatio-temporal crosstalk, at the cell-, organ-,

and organism-level. However, many regulatory networks with an impact on plant form and function, remain to be fully mapped and understood (Figure 9).

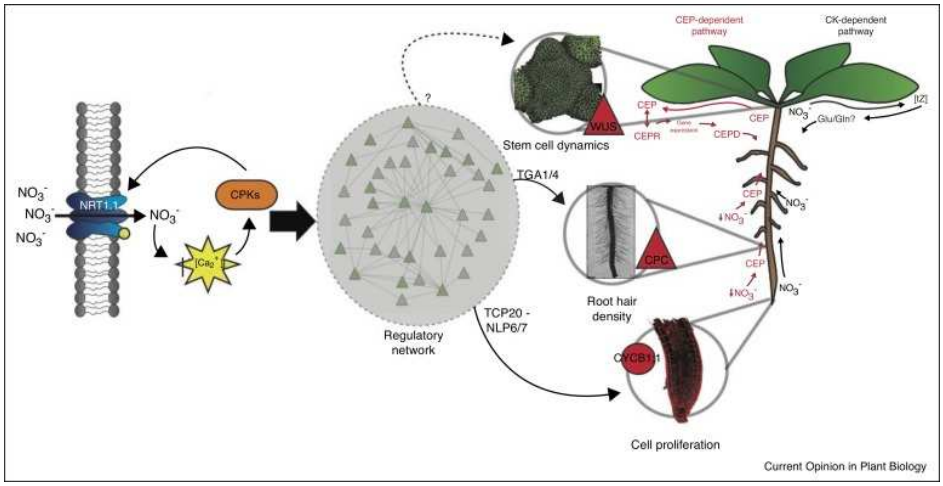

Figure 9. Nitrate signalling control cellular programs with an impact on plant form and function (from Fredes *et al*., 2019)

4.1. Nitrate controlled shoot growth

Nitrate regulates shoot growth and by consequence plant biomass in response to nitrate fluctuations in the environment. In particular, nitrate-induced shoot growth was correlated to the hormone cytokinin (CK) translocation from root to shoot, and this communication has been proposed as a model of systemic signaling for nutrient status (Sakakibara, 2006; Ruffel *et al*., 2011; Poitout *et al*., 2018). Some authors demonstrated that the key enzyme linked to cytokinin biosynthesis IPT3, as well as several response regulators (ARR), which were specifically regulated by NO_3^- in *Arabidopsis* during the primary responses (Takei *et al*., 2004; Wang *et al*., 2004). In addition, to depict the dynamic complexity of interactions, CK and auxin also exert feedback controls on nitrate uptake and assimilation, modulating shoot growth (Guo *et al*., 2002; Krouk, 2016). Some results suggested that CK signaling allowed buds to escape auxin-mediated apical dominance; and NO_3^- simulating CK-dependent increased some PIN-FORMED (PIN) proteins in shoot (Müller *et al*., 2015; Waldie and Leyser, 2018). Recently, observations on the NO_3^- regulation of vegetative growth by modulating cell size and endo-replication have been reported, wherethe authors identified the LGO gene, a CDK inhibitor, as a key cell cycle regulatory factor influencing ploidy and cell-size depending on external nitrate (Moreno *et al*., 2020).

4.2. Nitrate-induced root system architecture modulation

Among nutrients, NO_3^- modulates root system architecture (RSA) to optimize its acquisition (Forde, 2014). The RSA modification in response to NO_3^- depends firstly on its concentration and involves the action of different cell types with high dynamism underpinning root plasticity. At molecular level, the gene activity is different in relation to localization, expression timing, and environmental responsiveness, as observed in *Arabidopsis* (Walker *et al*., 2017). Several regulatory factors have been implicated in RSA modulation (Figure 10).

The NPF6.3/NRT1.1 transporter modulates RSA being involved in auxin transport in lateral root primordium (Krouk *et al*., 2010). A point mutation in the Th101 residue of *NPF6.3* transporter determined a repression of lateral root development at low NO_3^- concentrations, highlighting that the nitrate-dependent regulation of root development relayed on the protein phosphorylation (Bouguyon *et al*., 2015). Afterwards, the same authors showed that *NPF6.3* acted differentially on protein accumulation, depending on the tissues considered, modulating auxin accumulation in lateral primordia (Bouguyon *et al*., 2016). However, in these responses several kinases were also involved, such as CIPK8, CIPK23, CPK10/30/32 (Liu *et al*., 2017; Varala *et al*., 2018). In addition, the involvement of NO_3^- signaling in RSA modulation by scaffold proteins such as BT1 and BT2, the negative regulator GARP-type transcription factors NIGT/HRS1 and Cytokinin Response Factor 4 (CRF4) have been demonstrated (Kiba *et al*., 2018; Varala *et al*., 2018).

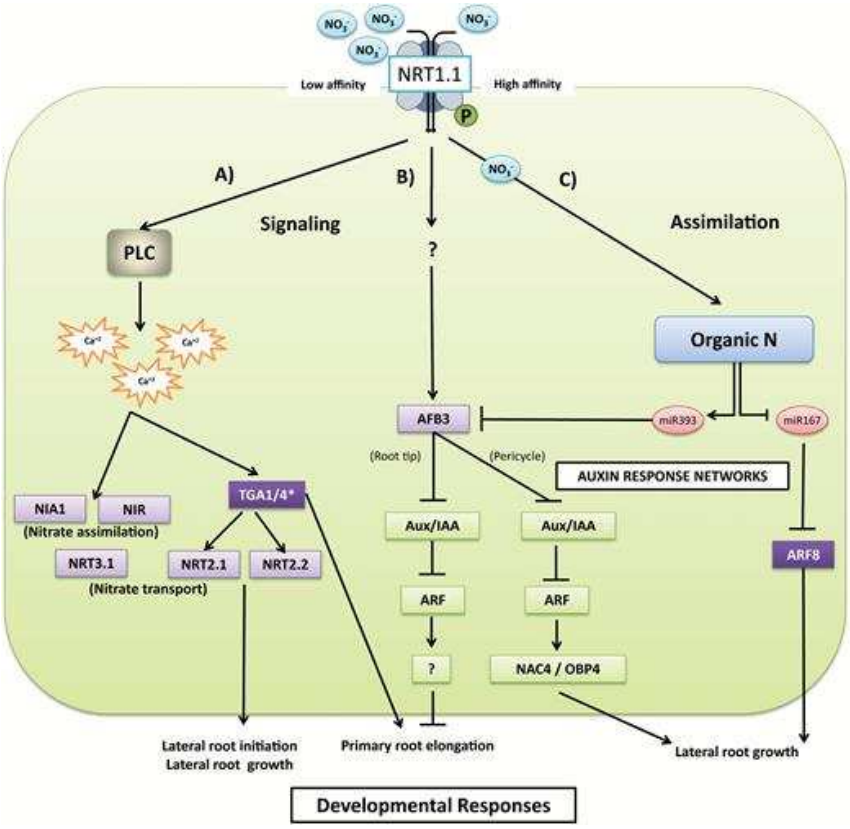

Figure 10. Summary of NO_3^- signaling and assimilation (from Undurraga *et al*., 2017)

Other TFs are reported to be involved in root modulation by NO_3^- such as NLP6/7, TGACG Sequence-Specific Binding Protein 1 and 4 (TGA1/4), NAC Domain containing protein 80 (NAC4), hormone signaling components including the auxin receptor Auxin Signaling F-Box 3 (AFB3) (Vidal *et al*., 2010; Fredes *et al*., 2019). Furthermore, TCP20 TF can be also considered as a master regulator of RSA. Indeed, plants exposed to N-starvation showed an interaction between TPC20 and NPL6/7, useful to modulate nitrate-responsive genes by controlling cell cycle genes, redirecting root growth to nitrate rich-zones (Guan *et al*., 2017).

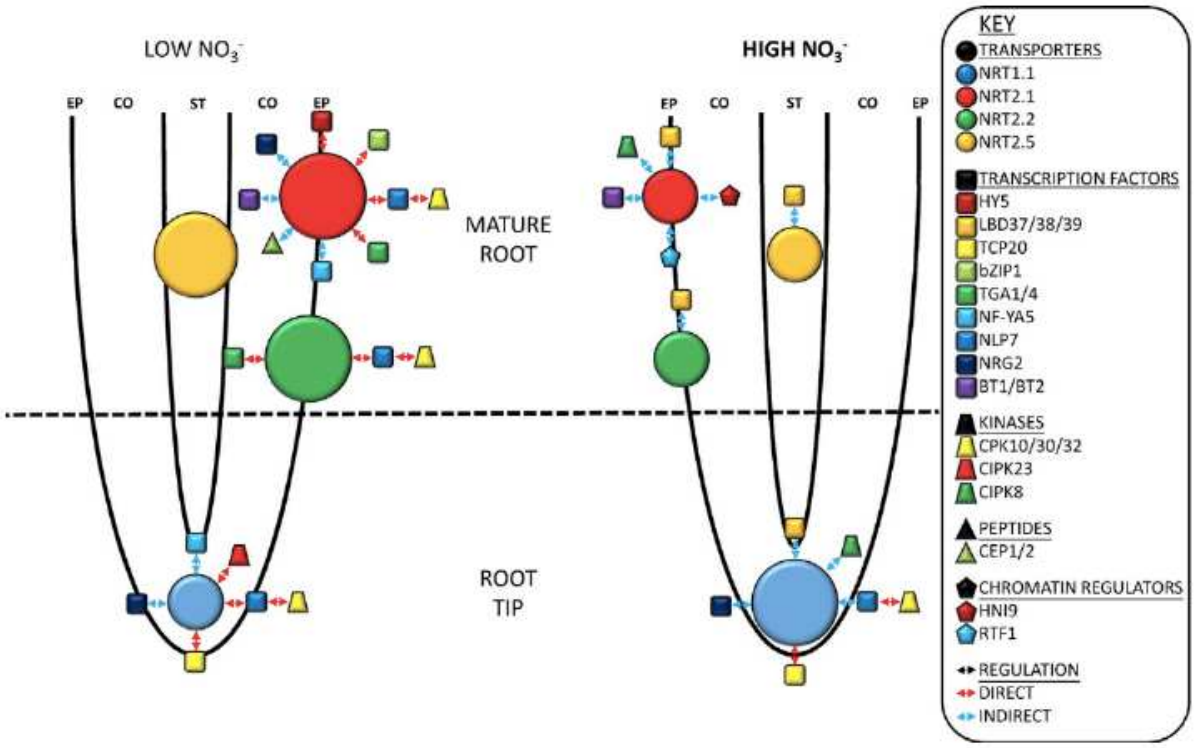

Figure 11. Summary of key transporters and regulators mediating NO_3^- in plant root (Plett *et al*., 2018)

As already reported, nitrate-induced effects on RSA depend on root type (primary, lateral) as well as on nitrate availability (low or high) (Figure 11). Many studies demonstrated that primary root is insensitive to normal NO_3^- level (Walch-Liu and Forde, 2008; Tian *et al*., 2014), but its increasing caused root growth inhibition, probably regulated by AFB3 and NAC (Forde, 2014). Ruffel *et al*. (2011) demonstrated as cytokinin was involved in root development into heterogeneous NO_3^- conditions. In particular, NO_3^- triggers an active trans-zeatin accumulation in roots, which translocats to shoot acting in the nitrate-derived systemic signaling pathway (Poitout *et al*., 2018). More recently, an interaction between NO_3^- and CK signals in primary root growth has been observed (Naulin *et al*., 2019).

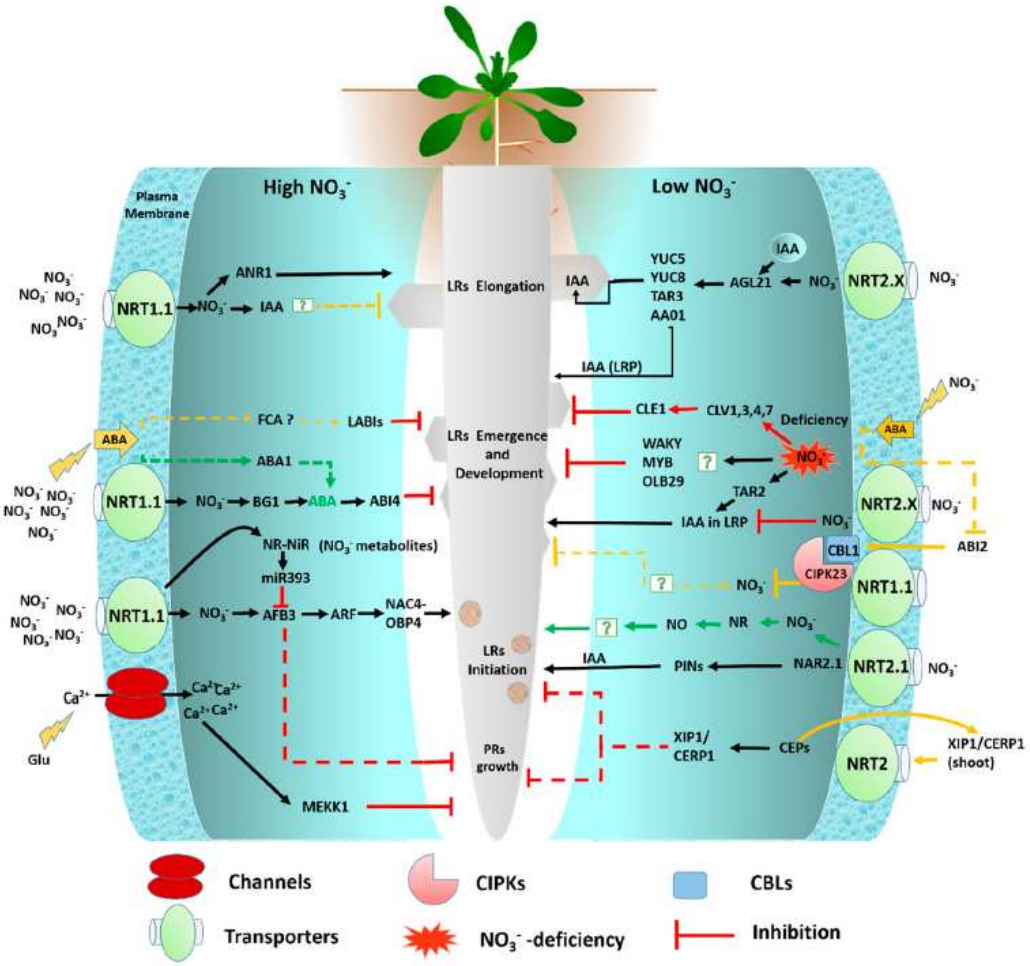

Figure 12. Schematic diagram presents the multiple pathways regulating the root system architecture responses by NO_3^- supply (Asim *et al*., 2020).

By contrast, lateral roots are strongly affected by NO_3^- in different ways (Figure 12). In particular, there are two evident morphological adaptations: under moderate NO_3^- conditions, the lateral root length (LRL) is significantly stimulated, but when exposed to severe NO_3^- deficiency or high NO_3^- level, the total LRL and branching were reduced as well as its formation (Krouk *et al*., 2010; Tian *et al*., 2014; Sun *et al*., 2017). Lateral root (LR) development contributes considerably to RSA being more sensitive than primary roots (PRs) to nutrient variations (Tian *et al*., 2014). Nitrate heterogeneity determines also a stimulatory effect on LR development in NO_3^-- rich zone (Sun *et al*., 2017). In particular, low NO_3^- increases lateral root development by auxin biosynthesis and the nitrate-dependent RSA modulation by interacting with *TAR2*, which encodes for auxin biosynthesis (Sun *et al*., 2017). A repressed auxin accumulation in LR primordia and their reduced emergence and numbers under low N conditions in the *Arabidopsis tar2* mutant have been already observed (Ma *et al*., 2014). The transcriptional profile showed that *TAR2* and *PIN7* expressions are highly correlated with NLP7-activated and NO_3^-- assimilation genes (Marchive *et al*., 2013;

Liu *et al*., 2017). Moreover, NLP7-regulated auxin efflux *via* PIN7 could determine lateral root numbers as previously supposed (Overvoorde *et al*., 2010). In addition, another nitrate responsive gene, BBX16 (bobby sox homolog), affects LRL in response to NO_3^- (Gaudinier *et al*., 2018). Moreover, under NO_3^-- deficiency, the AGL17-clad MADs-box gene (*AGL21*) is induced to promote LRs in *Arabidopsis*, whereas the *agl21* mutant results significantly impaired in the LR elongation (Forde, 2014; Yu *et al*., 2014).

Finally, NO_3^- induces root hair density that increases nutrient uptake capacity by increasing the soil surface area explored. The molecular mechanism includes *NPF6.3/NRT1.1* and the *TGA1/TGA4* transcription factors *via* a MYB named CAPRICE (*CPC*), involved in the root hair cell (Canales *et al*., 2017). Recently, Liu *et al* (2020) showed that the root hair development is under control of both local and systemic NO_3^- signaling effects.

5. Plant responses to nitrogen deficiency

Physiological and metabolic adaptations to low nutrient concentrations are important for a sessile plant to accomplish their life-cycle even under harsh growth conditions. For example, plants are able to adjust their root morphology and metabolism for growing into nitrogen-depleted soil (Hodge, 2004). Long-term N deficiency affects the whole plant, thus, the morpho-physiology and biochemistry of both root and shoot is adjusted to cope with limiting N-conditions. This includes the increased expression of high-affinity N uptake systems (*e.g.*, AMTs and NRTs), the reduction of growth and photosynthesis, N remobilization from mature to growing tissues and the accumulation of abundant photo-damage-protecting anthocyanin pigments (Peng *et al*., 2007; Krapp *et al*., 2011).

The adaptations responses to low N firstly involve early transcriptome adjustments well elucidated by microarray experiments in *Arabidopsis*, rice and tomato (Wang *et al*., 2001; Scheible *et al*., 2004; Peng *et al*., 2008; Krapp *et al*., 2011). N-depletion leads to a coordinate repression of the major genes assigned to photosynthesis, chlorophyll and plastid protein synthesis, while an induction of many genes involved in the secondary metabolism, and reprogramming of mitochondrial electron transport was observed (Scheible *et al*., 2004). The adaptation to limiting N is concentration-dependent as mild N-stress triggers transcriptional down-regulation only of a small gene set. Within two days N deficiency, hundreds of genes are regulated in both root and shoot (Krapp *et al*., 2011). This involves also changes in the expression of regulatory *miRNAs* upon N-starvation (Liang *et al*., 2012). Remarkably, in most studies, a prevalent down-regulation of gene expression with advancing N-deficiency was

always observed. Transcriptomic impacts of long-term ammonium depletion prior to ammonium resupply are rather unspecified. Even less is known about the earliest responses to depletion of each nitrogen compound from the nutrient solution. Nutrient deprivation from root can elicit rapid responses similar to those observed with the phosphorus deprivation, which elicits rapid and robust up- and down-regulation of multiple genes as early as within a few minutes (Lin *et al*., 2011).

6. Tomato as model plant

Many plant species of high economic importance such as tomato, potato, tobacco, pepper and eggplant belong to the *Solanaceae*, extensively studied family among the Euasterids. Tomato (*Solanum lycopersicum* L.) is the most intensively studied member of this family, mainly due to its short generation time, elementary diploid genetics, a well-known genetic transformation methodology, inbreeding tolerance, and a vast well-characterized genetic resource (Van der Hoeven *et al*., 2002; Barone *et al*., 2008). Originated from South America, it was spread around the world to become one of the most extensively used vegetable crops. Besides its economic value, it has interesting developmental features, such as compound leaves, fleshy fruits, and sympodial shoot branching (Schmitz and Theres, 1999; Townsley and Sina, 2012). For its behavior, tomato has known an exciting phase of research development, in which huge amount of genomic, proteomic and metabolomics datasets have been gathered. These advantages make tomato an excellent model plant for both basic and applied research.

The whole genome sequencing of tomato was completed in 2012 as an initiative of the Tomato Genome Consortium, including more than 90 research institutions (Tomato Genome Consortium, 2012). The genome sequence, its epigenome and other extensive resequencing data are available from the Sol Genomics Network (SGN: https://solgenomics.net). Furthermore, the Tomato Genomics Resources Database (TGRD: https://59.163.192.91/tomato2/) houses RNA-seq and microarray data for tomato as well as some metabolite data. These databases allow an interactive browsing of tomato genes, micro RNAs, simple sequence repeats (SSRs), quantitative trait loci (QTL) and the Tomato-EXPEN 2000 genetic map (Suresh *et al*., 2014). There are extensive genetic resources for mutant collections (Tomato Genetic Resource Center, TGRC University of California, Davis: https://tgrc.ucdavis.edu/), several excellent TILLING (Targeting Induced Local Lesions IN Genomes), populations for mutant discovery (UC Davis in Heinz-1706; INRA Bordeaux in MicroTom, INRA Versailles in M82), Red Setter and Money Maker (phenotypes available

through SGN and LycoTILL) and a phenotypic library of additional mutations catalogued in "The Genes that Make Tomato", available through SGN.

Compared to other model plants, tomato studies have been facilitated by the development of specialized variety such as MicroTom, characterized by a short growth cycle and reduced plant size. This cherry tomato variety has been used for fundamental research to be then transferred to large-sized, globe tomato varieties (Dan *et al*., 2006). In addition, the establishment of the *S. lycopersicum*×*S. pennellii* introgression lines (ILs) (and now, other IL populations including *S. lycopersicum*×S. *lycopersicoides, S. lycopersicum*×*S. pimpinellifolium, S. lycopersicum*×*S. sitiens, S. lycopersicum*×*S. chilense*, and *S. lycopersicum*×*S. habrochaites=hirsutum*) provided unique genetic resources to identify loci controlling important traits (Frary *et al*., 2000; Kushibiki and Tabata, 2005; Powell *et al*., 2012).

As in other model organisms, methods for stable and transient expression/silencing of target genes in tomato are well developed (Hannon, 2002; Orzaez *et al*., 2009). Recently, with the emergence of the new breeding technologies of genome editing, new alleles can be created directly into the desired genetic background, to supply beneficial quantitative variation for tomato breeding (Rodríguez-Leal *et al*., 2017). In particular, Clustered Regularly Interspaced Short Palindromic Repeats (CRISPR)/CRISPR-associated protein 9 (Cas9) genome editing has been proved to be particularly efficient in tomato breeding for improving fruit yield and quality, increasing stress resistance and accelerating the domestication of wild tomato (Brookes *et al*., 2014; Li *et al*., 2018; Wang *et al*., 2019; Tran *et al*., 2021) (Figure 13). Besides transcriptomics and genome editing, proteomics has become one of the largest areas to study functional genomics (Park, 2004). The importance to study the dynamic and complex plant proteomes relies on the identification of proteins and their modifications in stress conditions to develop crop improvement (Hu *et al*., 2015; Kilambi *et al*., 2016). Proteome databases contain the protein sequences diverged from predicted genomic gene models and unigene transcripts. Nowadays, the tomato database (v.3.2), maintained by the international tomato annotation group (iTAG), contained 30,868 annotated genes, from which 2,300 genes were user curated. Other proteomics and genomics databases for tomato are available by Phytozome (https://phytozome-next.jgi.doe.gov/), Plant Genome and Systems Biology (PGSB) (https://pgsb.helmholtzmuenchen.de/plant/tomato), and the Tomato Genomic Resources Database (TGRD) (https://59.163.192.91/tomato2).

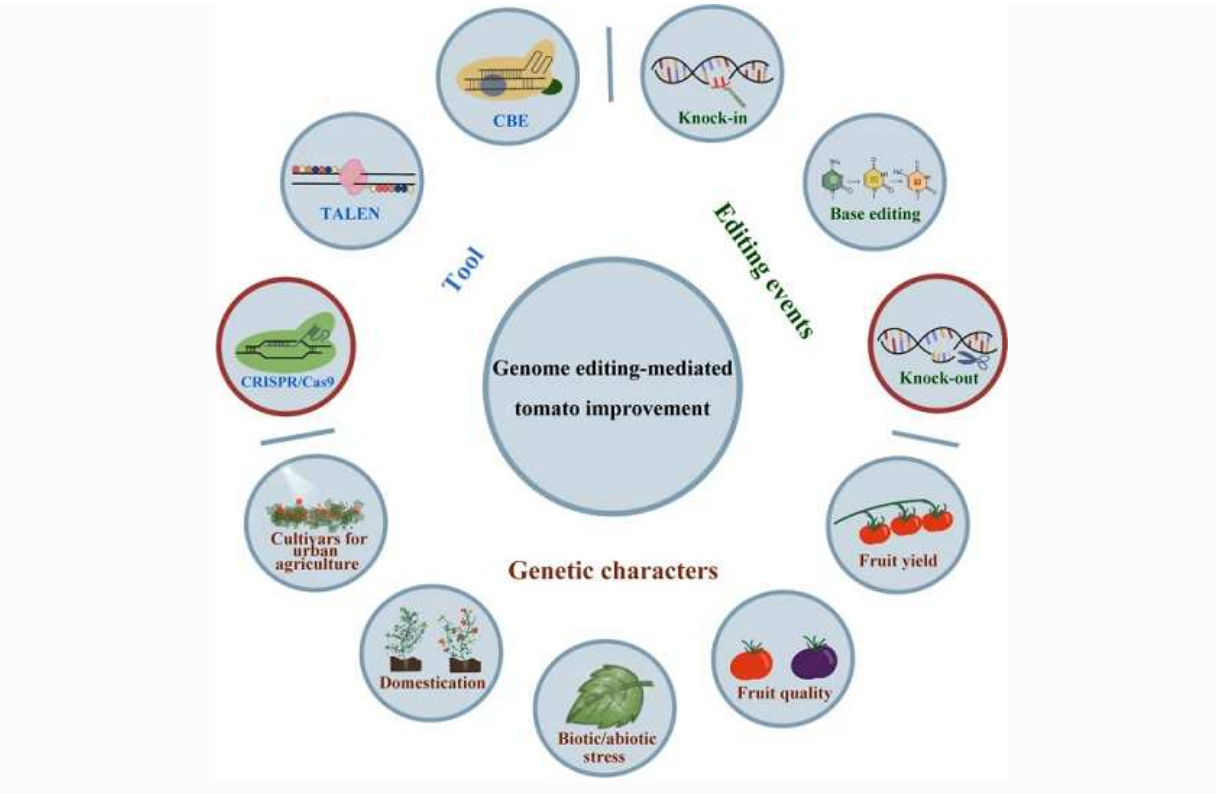

Figure 13.A chart illustrating the applications of genome editing in tomato improvement (from Xia *et al.*, 2021)

Recently, SGN has created an initiative to map the tomato secretom (https://solgenomics.net/secretom), created as a support to study the proteins of the cell wall, proteins secreted in the exterior of the plasma membrane, considered part of the secretory pathway. Secretom proteins are involved in communication, responses to stress and plant development (Krause *et al.*, 2013). The secretom is especially important for fleshy fruits, considering the relationship of the mechanical and chemical characteristics of the cell wall and fruit texture (Konozy *et al.*, 2013). SecreTary is another tool developed by the SGN, which allows the accurate computational prediction of proteins of the secretom, which datasets are available through FTP on the Secretom website.

Additionally, recent progress in tomato metabolomics provides extensive information about its primary and specialized metabolism and the pathways involved in their synthesis and turnover (Luo, 2015; Tieman *et al.*, 2017; Zhu *et al.*, 2018). During the past 15 years, the integration of metabolic profiling with transcriptome data has proven to be highly effective for identifying gene functions and elucidating metabolic pathways in plants (Luo, 2015). For example, pioneering work by Carrari *et al.* (2006) combined gas chromatography-mass spectrometry (GC-MS) with parallel transcriptome analysis to dissect metabolic changes during tomato fruit development.

To evaluate how breeding has changed the tomato fruit metabolome, different research groups have recently generated and analyzed large datasets encompassing genomes, transcriptomes, and metabolomes from hundred tomato genotypes (Tieman *et al*., 2017; Zhu *et al*., 2018; Zhao *et al*., 2019). Through metabolite genome-wide association studies (mGWAS), researchers have identified a large number of genetic loci that affect the concentrations of important metabolites in tomato fruit (Tieman *et al*., 2017; Zhao *et al*., 2019).

7. Objectives and organization of the thesis

In intensive cropping systems, farmers massively apply N fertilizer to sustain high yield. Unfortunately, crops utilize 40% of the supplied N and the remaining is lost into the environment becoming a cue for the ecosystems. Crops modern varieties have been selected in high-input conditions for maximize yields, whereby the favorable traits for N uptake and assimilation in these varieties could decline under an N limited supply. Therefore, the exploitation of genetic diversity within the landraces is considered a promising strategy to enhance NUE. Long-storage tomato ecotypes, cultivated in the Mediterranean basin and resilience to many abiotic stresses, represent good candidates to identify high NUE genotypes and study the molecular mechanisms underlying this complex trait. In this respect, the core research objective of this thesis focused on morpho-physiological and molecular responses in two NUE-contrasting tomato genotypes in response to low NO_3^- availability.

In Chapter I, we evaluated the performances of four tomato genotypes at low NO_3^- (LN). They were compared for root and shoot morphological traits, biomass production, chlorophyll content, NUE and its components, NUpE (Nitrogen Uptake Efficiency) and NUtE (Nitrogen Utilization Efficiency) performances (Chardon *et al*., 2010; Siddiqi and Glass, 1981). In particular, we identified a pair of NUE-contrasting tomato genotypes, Regina Ostuni (RO, high-NUE) and UC82 (low-NUE), confirming our previous results (Abenavoli *et al*., 2016). Furthermore, the relative expression of some NO_3^- metabolism related genes over time and in both tissues suggested that NUtE component as the most responsible for NUE enhancement compared to NUpE. In particular, we focused on genotypes abilities to modulate long-distance NO_3^- transport, assimilation, remobilization and vacuolar storage.

In Chapter II, after five days of N-deprivation, RO and UC82 short-term (0h, 8h and 24h) transcriptome responses to low (LN) and high (HN) NO_3^- resupply, were compared in both roots and shoots. For this purpose, we generated 60 RNA libraries taking into account three variables: genotypes (G), NO_3^- condition (N) and time (T) for each tissue. The resulting Reads

per kilobase of transcripts per million mapped reads (RPKM) were normalized using DEseq2 R package. To take into consideration all the variables, firstly data were modeled using an ANOVA multivariate linear model to identify the differentially expressed genes (DEGs) for each variable and their interactions. We focused on the significant DEGs between genotypes (G), but also for G×N and G×N×T interactions. Then, the significant temporal expression profiles and genes associated with these profiles as well as a comparison of genes behavior across multiple conditions were analyzed by STEM software. This analysis permitted to screen for the significant N-responsive genes in RO and UC82 after 8 and 24h of N-resupply. Afterwards, DEseq2 R package was used to identify among the N-responsive genes those differentially expressed between genotypes (RO*vs.*UC82), highlighting the major pathways affected over time, in both root and shoot. Finally, a Weighted Gene Co-expression Network Analysis (WGCNA) was carried out to identify the co-expression modules significantly correlated to LN treatment in the high-NUE genotype (RO). In shoot, the LN-responsive metabolic processes specifically induced after 24h LN resupply in RO included the vegetative phase change, the carbohydrate mediated signaling, the response to nutrient, the cytokinin biosynthetic process and the carbon fixation in photosynthetic organisms. By contrast, any metabolic process was significantly affected in root. Finally, the regulatory network analyses allowed us to identify the key LN-related genes in each module, which might be responsible for the differential regulation of the early response to LN between genotypes.

In Chapter III, we compared the RO and UC82 transcriptome profiles in response to long-term (7 days) LN-stress, and a WGCNA was carried out to correlate the co-expression modules to the phenotypic traits analyzed in Chapter 1. In this respect, we generated RNA libraries from both root and shoot of each genotype after 7 days LN and HN resupply. Using DEseq2 R package, we first identified the DEGs between genotypes at each N condition to study the genotypic effect (RO*vs.*UC82-HN and RO*vs.*UC82-LN), and the DEGs between LN and HN in each genotype to study the N-effect (RO-LN*vs*.HN and UC82-LN*vs*.HN). Venn diagrams allowed us to identify the genotype-specific LN-responsive genes (DEGs related to RO-LN*vs*.HN and UC82-LN*vs*.HN comparisons), as well as the LN-specific DEGs related to the RO*vs*.UC82-LN comparison, excluding those shared with the RO*vs*.UC82-HN comparison. Interestingly, most of the LN-specific differential expressions observed in ROvsUC82 comparison affected genes involved in the photosynthesis process. Then, WGCNA investigated the co-expression modules highly correlated with the morpho-physiological traits as well as NUE and its components in both shoot and root. The hub

modules revealed a significant enrichment mainly in photosynthesis and transmembrane transport activity biological process GO term, in shoot and root, respectively. Finally, the regulatory network analysis of the hub modules revealed some key NUE and NUpE related genes in shoot and root, respectively, which might represent novel candidate genes for NUE improvement in tomato.

In conclusion, our study presented detailed analyses on two NUE-contrasting tomato genotypes responses to N limited availability. Furthermore, transcriptomic profiles comparisons showed genotype specific behavior as well as correlations between gene transcription, LN treatment and phenotypic traits. The different adaptive responses between N-use efficient and inefficient genotypes also opened novel insight into the LN-stress regulation in tomato. These findings represent guidelines to select for LN tolerance and NUE improvement through molecular assisted breeding and genome editing approach in tomato.

Chapter I

New insights into N-utilization efficiency in tomato (Solanum lycopersicum L.) under N limiting condition

Plant Physiology and Biochemistry 166 (2021) 634–644

Contents lists available at ScienceDirect

Plant Physiology and Biochemistry

journal homepage: www.elsevier.com/locate/plaphy

New insights into N-utilization efficiency in tomato (*Solanum lycopersicum* L.) under N limiting condition

M.M. Aci, A. Lupini, A. Mauceri, F. Sunseri, M.R. Abenavoli *

Dipartimento Agraria, Università Mediterranea degli Studi di Reggio Calabria, Feo di Vito, 89123, Reggio Calabria, Italy

ARTICLE INFO

Keywords:
Nitrogen deficiency
NUtE
Nitrate transport
Nitrate assimilation
Nitrate remobilization
Nitrate storage

ABSTRACT

Understanding Nitrogen Use Efficiency (NUE) physiological and molecular mechanisms in high N demanding crops has become decisive for improving NUE in sustainable cropping systems. How the Nitrogen Utilization Efficiency (NUtE) component contributes to the NUE enhancement under nitrate limiting conditions in tomato remains to be elucidated. This study deals with the changes in several important nitrate metabolism related gene expressions (nitrate assimilation, transport, remobilization and storage/sequestration) engendered by short and long-term limiting nitrate exposure in two selected NUE-contrasting genotypes, Regina Ostuni (RO) and UC82, efficient and inefficient, respectively. At short-term, nitrate limiting supply triggered higher *SlCLCa* and *SlNRT1.7* expressions in RO root and shoot, respectively, suggesting a higher nitrate storage and remobilization compared to UC82, explaining how RO withstood the nitrate deficiency better than UC82. At long-term, nitrate reductase (*SlNR*) and nitrite reductase (*SlNIR*) expression were not significantly different between nitrate treatments in RO, while significantly down-regulated under nitrate limiting treatment in UC82. In addition, *SlCLCa* and *SlNRT1.8* transcript levels were significantly lower in RO, while those of *SlNRT1.5* and *SlNR* appeared significantly higher. This suggested that the efficient genotype stored less nitrate compared to UC82, which was allocated and assimilated to the shoot. More interestingly, the expression of *SlNRT2.7* was significantly higher in RO shoot compared to UC82 and strongly correlated to RO higher growth as well as to NUE and NUtE component. Our findings underlined the differential regulation of N-metabolism genes that may confer to NUtE component a pivotal role in NUE enhancement in tomato.

1. Introduction

Nitrogen (N) fertilizers have largely contributed to vegetable crops high yield worldwide to meet the increasing food demands (Robertson and Vitousek, 2009). Tomato (*Solanum lycopersicum* L.) is one of the most important horticultural crops with 4.7 million cultivated hectares and 182 million producted tonnes in 2018 (FAOstat, 2020). The lowest N supply recommended for a high tomato yielding is about 100–150 kg ha^{-1} (Doorenbos and Kassam, 1986), but doses more than two fold higher are usually applied (Scholberg et al., 2000). However, crops utilize less than half of the applied N-fertilizer and the remaining amount is lost into the environment causing dangerous pollution as well as reducing nitrogen use effieciency (NUE) in crops (Socolow, 1999; Garnett et al., 2009; Xu et al., 2012). So, improving crop NUE, exploiting the genetic diversity for this trait, is considered one of the most promising strategy to enhance crop production sustainability (Lammerts van Bueren and Struik, 2017), minimizing the impact of high N-fertilization (Gutiérrez, 2012; Xu et al., 2012). In this context, long storage tomato ecotypes cultivated in the Mediterranean basin are of great interest being resilient to drought and N-limited conditions, typical of this area (Abenavoli et al., 2016). Besides, deep insights on both physiological and molecular mechanisms to cope low-N are required for an effective use of genetic and genomic approaches when improving NUE.

NUE is a complex trait in which physiological, developmental and environmental factors are involved; it encompasses the plant efficiency to absorbe (NUpE component), assimilate, transport and remobilize the available N into the soil (NUtE component) (Jackson et al., 2008; Xu et al., 2012). In tomato, physiological and molecular NUE-related traits were studied under contrasting N-supply, focusing mostly on root morphology, nitrogen uptake and transport systems (Abenavoli et al., 2016; Lupini et al., 2017), albeit further efforts should be addressed to nitrogen utilization efficiency (NUtE).

* Corresponding author.
E-mail addresses: mlyana.aci@unirc.it (M.M. Aci), antonio.lupini@unirc.it (A. Lupini), antonio.mauceri87@unirc.it (A. Mauceri), francesco.sunseri@unirc.it (F. Sunseri), mrabenavoli@unirc.it (M.R. Abenavoli).

https://doi.org/10.1016/j.plaphy.2021.06.046
Received 21 December 2020; Received in revised form 14 June 2021; Accepted 23 June 2021
Available online 25 June 2021
0981-9428/

1. Introduction

Nitrogen (N) fertilizers have largely contributed to vegetable crops high yield worldwide to meet the increasing food demands (Robertson and Vitousek; 2009). Tomato (Solanum lycopersicum L.) is one of the most important horticultural crops with 4.7 million cultivated hectares and 182 million producted tonnes in 2018 (FAOstat, 2020). The lowest N supply recommended for a high tomato yielding is about 100-150 kg ha^{-1} (Doorenbos and Kassam, 1986), but doses more than two fold higher are usually applied (Scholberg *et al*., 2000). However, crops utilize less than half of the applied N-fertilizer and the remaining amount is lost into the environment causing dangerous pollution as well as reducing nitrogen use effieciency (NUE) in crops (Socolow, 1999; Xu *et al*., 2012). So, improving crop NUE, exploiting the genetic diversity for this trait, is considered one of the most promising strategy to enhance crop production sustainability (Lammerts van Bueren and Struik, 2017), minimizing the impact of high N-fertilization (Gutiérrez, 2012, Xu *et al*., 2012). In this context, long storage tomato ecotypes cultivated in the Mediterranean basin are of great interest being resilient to drougth and N-limited conditions, typical of this area (Abenavoli *et al*., 2016). Besides, deep insights on both physiological and molecular mechanisms to cope low-N are required for an effective use of genetic and genomic approaches when improving NUE.

NUE is a complex trait in which physiological, developmental and environmental factors are involved; it encompasses the plant efficiency to absorbe (NUpE component), assimilate, transport and remobilize the available N into the soil (NUtE component) (Jackson *et al*., 2008, Xu *et al*., 2012). In tomato, physiological and molecular NUE-related traits were studied under contrasting N-supply, focusing mostly on root morphology, nitrogen uptake and transport systems (Abenavoli *et al*., 2016, Lupini *et al*., 2017), albeit further efforts should be addressed to nitrogen utilization efficiency (NUtE).

Nitrate (NO_3^-) is the major N source in well-aerated soil (Crawford and Glass, 1998). Once uptaken into the root cell, NO_3^- is either assimilated to organic nitrogen or stored/sequestred in root cell tonoplasts (Orsel *et al*., 2002); otherwise, it is loaded into the xylem vessels and then transported to above-ground organs (Marschner *et al*., 1997). In Arabidopsis, a higher NO_3^- allocation to the shoot was correlated with higher NUE (Lin *et al*., 2008). Tang *et al*. (2012 and 2013) suggested that the promotion of NO_3^- transport from root to shoot represents an “adventagous physiological adaptation”, which allows the utilization of solar energy for NO_3^- assimilation contributing to higher NUE. According to Hirose and Bazzaz (1998), high-

NUtE seems to be related to the ability of efficient genotypes to reallocate N to the best lighted leaves with an efficient photosynthetic activity useful for a more cost-effective assimiliation. Thus, NUtE is considered positively correlated to the photosynthetic activity (Smirnoff and Stewart, 1985; Tang *et al*., 2013).

The NO_3^- long and short-distance transport mechanisms are as well significantly involved in NUtE. In particular, the NRT1.5 and NRT1.8 genes regulate nitrate long-distance transport and its distribution between roots and shoots. In roots of *Brassica napus* and *Arabidopsis*, NRT1.5 is responsible for xylem NO_3^- loading, whereas NRT1.8 mediates xylem NO_3^- unloading (Lin *et al*., 2008, Li *et al*., 2010, Han *et al*., 2016). Their regulation is controlled by cytosolic NO_3^- concentration, which in turn depends on NO_3^- short-distance transport between cytosol and vacuole, mediated by chlorid channel protein (CLCa) in the tonoplast membrane (De Angeli *et al*., 2006, Han *et al*., 2016). Indeed, the NO_3^- sequestration in root cells vacuole prevents its assimilation and allocation to the shoots for further utilization (Han *et al*., 2015).

The N remobilization also plays a key role in NUtE improvement (Mickelson *et al*., 2003; Masclaux-Daubresse *et al*., 2008). Indeed, the N remobilization from the older to the younger leaves results essential to sustain plant vigorous growth under N deficiency (Rossato *et al*., 2001; Schiltz *et al*., 2005; Fan *et al*., 2009). During leaf senescence, organic N is the major remobilized form (Good *et al*., 2004; Masclaux-Daubresse *et al*., 2008); although, the stored NO_3^- can also be remobilized from older leaves to N demanding tissues as in Arabidopsis. In this species, NO_3^- remobilization is mediated by NRT1.7 gene, encoding a low affinity NO_3^- transporter, expressed in phloem source leaves minor veins and responsible for NO_3^- loading into the sink tissues (Fan *et al*., 2009; Chen *et al*., 2020). Another gene, NRT2.7 could be involved in NUE improvement. This high affinity NO_3^- transporter is responsible for its storage in Arabidopsis seeds (Chopin *et al*., 2007), and seems to play a role in NO_3^- efflux regulation in leaves, balancing NO_3^- assimilable amount by transporting back into xylem vessels any NO_3^- excess (Orsel *et al*., 2002). The NRT2.7 transcripts were also reported in N-stress tolerant sorghum genotype leaves (Gelli *et al*., 2014).

Recently, a genotypes pair contrasting for NUE was selected among some long-storage tomatoes, speculating about the key role which might play NUtE in NUE performance (Abenavoli *et al*., 2016). In the present work, NUE performance of both genotypes were confirmed by using different NUE definitions, in addition the NUtE component was deeply evaluated throughout the gene expression analysis of most NO_3^- metabolism related genes in both shoots and roots under NO_3^- limiting and non-limiting supply. In particular, we focused on the ability of N-efficient and inefficient genotypes to modulate long-distance N transport,

assimilation, remobilization and vacuolar sequestration based on the related genes expression. Finally, the correlation between NUE and its components and the N-metabolism-related gene expressions was highligthed.

2. Materials and Methods

2.1. Screening for NUE

2.1.1. Plant material and growth conditions

Seeds of three tomato landraces, namely Linosa and Piriddu from Sicily (University of Palermo, Italy), Regina Ostuni (RO) from Apulia (University of Bari, Italy) and a North American cultivar, UC82, from the Department of Plant Sciences (University of California Davis), were sterilized with 10% (v/v) NaClO for 15 min and then transferred in Petri dishes (Ø 90 mm) for 10 days as reported by Lupini *et al*. (2017). Seedlings of each genotype, with uniform size, were selected and transferred in an aerated hydroponic system containing a complete Hoagland solution supplied with 10 mM $Ca(NO_3)_2$, according to Abenavoli *et al*. (2016) with some modifications. Tomato seedlings were then placed in a growth chamber maintained at 25°C, 70% relative humidity and 16 h photoperiod with a light intensity of 350 µmol $m^{-2}s^{-1}$. The nutrient solution was renewed every two days and the pH was maintained at 5.8 with 1 M KOH. After 10 days, the half of each genotype was maintained in non-limiting N condition (5 mM $Ca(NO_3)_2$) (control), while the remaining was transferred in N-limiting condition (0.25 mM $Ca(NO_3)_2$), for one week. These two NO_3^- concentrations (0.5 and 10 mM) were previously established (Abenavoli *et al*. 2016).

2.1.2. Root and shoot morphology and biomass evaluation

Ten plants (27-d old) from each genotype and treatment (10 mM and 0.5 mM) were collected, divided into shoot and root, and weighted. Roots were dipped in 0.1% (w/v) toluidine blue (Sigma Aldrich, #89160) for 5 min, rinsed in deionized water, and then scanned at 1200 dpi resolution (WinRhizo STD 1600, Instruments Règent Inc., Quebec, Canada) to determine the total root length (TRL, cm) and root volume (RV, cm^3) using WinRhizo Pro System v. 2002a software, as reported by Lupini *et al*. (2016; 2017). Shoots were analyzed by IMAGE J software to measure plant height (cm), leaf number (#) and leaf area (cm^2). Then, shoots and roots were dried at 70°C for two days until their weight remained constant to determine their dry weight (SDW and RDW, respectively). Total dry weight (TDW, g) was calculated by adding SDW to RDW. Root length ratio, RLR (root length/whole plant dry weight, cm g^{-1}), root mass ratio, RMR (root dry weight/whole plant dry weight, g g^{-1}), root thickness or

fineness, RF (root length/root volume, cm cm^{-3}) and root density, RD (root dry weight/root volume, g cm^{-3}) were calculated.

2.1.3.Chlorophyll content

Chlorophyll content was also evaluated by SPAD meter (Minolta). Ten measurements per plants (five) for each genotype and treatment were performed on the adaxial surface of leaves.

2.1.4.Nitrogen content

Total nitrogen content (mg N, Nc) was determined in both shoot and root of each genotype by combustion method through a LECO-CNS-1000 analyzer (LECO Instruments Ltd., Mississauga, ON) as reported by Lupini *et al*. (2017), root/shoot Nc ratio was then calculated. The mean is the average N-content of five plants for each genotype and treatment.

2.1.5.Nitrogen Use Efficiency and its components

Nitrogen Use Efficiency (NUE, SDW $N\%^{-1}$, where N% is the g N (100 g $TDW)^{-1}$) (Chardon *et al*., 2010), Nitrogen Utilization Efficiency (NUtE, SDW^2 Nc^{-1}) (Siddiqi and Glass, 1981) and Nitrogen Uptake Efficiency (NUpE) (TDW x N concentration (g N g TDW^{-1}) (Chardon *et al*., 2010) were calculated. The mean is the average value of five plants for each genotype and treatment.

2.2. Gene expression analysis

2.2.1.Growth conditions

Since the internal nitrate concentration modifies the N response and its regulatory mechanisms (Forde and Clarkson, 1999), an experiment was carried out to define the nitrate starvation time in the NUE contrasting genotypes, RO and UC82. Thus, tomato seedlings (10 days old) grown in hydroponic system in non-limiting NO_3^- supply for 10 days, were transferred to N-free solution. Shoots and roots were sampled at 0, 1, 4 and 7 days of treatment, for Nc determination and results were evaluated by a nonlinear regression model. The recovery key time where the starvation was reached (minimum Nc value) was estimated at 5 days. The mean for each sampling time is the average of three plants (Figure S1).

2.2.2.RNA extractions and cDNA synthesis

Plants (20-d old) were starved in an N-free solution for 5 days and then exposed to 0.5 mM and 10 mM NO_3^- for 7 days. Shoots and roots were harvested separately after 0, 8, 24 h and one week N-treatments and immediately frozen in liquid nitrogen. Three biological replicates for each genotype, sampling time and N level were harvested, and each replicate was constituted of a pool of three plants. Total RNA from shoots and roots of both genotypes was isolated and purified using RNeasy Plant Mini Kit (Qiagen, Milano, Italy) according to the manufacturer's protocol. The total RNA was quantified using a NanoDrop 2000 (Thermo Scientific), and its integrity was assayed on 2% agarose gel electrophoresis. A first-strand cDNA was synthesized from 2 μg of total RNA using Maxima First Stand cDNA Synthesis Kit (Thermo Fisher Scientific Baltics UBA) according to the manufacturer instructions.

The primer specificity of candidate reference genes was detected through PCR, and the mixed cDNA was used as template. The PCR reaction mix included 12.5 μL 2×Dream Tap Green PCR Master Mix (Thermo Scientific), 1 μL forward/reverse primers (100 μM), 1ul cDNAs (50 ng/μL), and 9.5 μl ddH_2O supplement. The PCR reaction procedures were as follows: 35 cycles, 94°C for 3 min, 94°C for 30 sec, 59°C for 30 sec, followed by elongation at 72°C for 12 sec and extension for 5 min. At the end of the reaction, 2% agarose gel electrophoresis was used to detect primers specificity.

2.2.3.Quantitative Real-Time PCR (qRT-PCR)

Specific primers for nitrate and nitrite reductase (*SlNR and SlNIR*, respectively), chloroplastic glutamate synthetase (*SlGS2*) and glutamine synthase (*SlGOGAT*), low and high affinity NO_3^- transporters (*SlNRT1.5, SlNRT1.8, SlNRT1.7 and SlNRT2.7*) and chloride channel protein (*SlCLCa*) were designed together with the reference gene (*SlActin*) using primer 3 (http://primer3.u.ee/) (Table 3). The qRT-PCR was performed in 96-well plates on StepOne™ Real-Time PCR System (Applied Biosystems, foster, CA, USA) using PowerUp SYBR Green master mix (Applied Biosystems by Thermo Fisher Scientific) according to the manufacturer instructions. The qRT-PCR was carried out starting from 2 min at 50° C, 2 min 95° C (initial denaturation), then 40 cycles of 15 s at 95°C, 1 min at 59°C and finally 15 s at 95°C, 1 min at 60°C and 15s at 95°C. Three biological and two technical replicates were performed for each genotype, sampling time and NO_3^- level. The PCR efficiency of primer pairs was optimized in the range 92-105% with R^2-values of 0.997. The qPCR results were normalized adopting the $2^{-\Delta\Delta Ct}$ comparative method (Livak and Schmittgen, 2001) considering time 0 for each target gene as calibrator and where $\Delta\Delta C_T = (C_{T,Target} - C_{,Actin})_{Time\ x} - (C_{T,Target} - C_{,Actin})_{Time\ 0}$. In the formula, "Time x" and "time 0" represent any time point and the 1X expression of the target

gene normalized to the internal control gene (*SlActin*), respectively. The qPCR results at T0 are presented in the supplementary materials as the normalized relative quantity of each target gene's expression with respect to the reference gene *SlActin* ($2^{-\Delta Ct}$).

2.3. Statistical analysis

All the experiments were set up in a completely randomized design with at least five replications. The data were checked for normality (Kolmogorov–Smirnov test) and tested for the homogeneity of variance (Leven median test). The data were then analyzed by ANOVA, and the means were separated by Tukey's Honest Significant Difference (HSD) test ($p < 0.05$), using Systat software (Systat Software Inc., Chicago, IL, USA). The relative gene expressions ($2^{-\Delta\Delta Ct}$) within each time point were analyzed by ANOVA based on three biological replicates for each treatment by using R software version 3.5.0.

Table 3. Primers for qRT-PCR

Gene	Accession ID	Primer Sequences (5' to 3')		Amplicon length
SlNR	NM_001328498.1	Forward	5'-GGTGGATGGATGGCAAAGGA-3'	127
		Reverse	5'-TCCTCACCTCGGACATGGAA-3'	
SlGOGAT	XM_004234907.4	Forward	5'-GTGGTTTGGGCCATCTCTGA-3'	83
		Reverse	5'-CACGACTGTTGGCTGCTTTT-3'	
SlGS2cp	NM_001323669.1	Forward	5´-TGGAGTTGAGGTGTAATTGTTGG-3´	105
		Reverse	5´-CATTCGGAAAGAGCACACCA-3´	
SlNir	XM_004248688.4	Forward	5´-GGACAGGTTGCCCAAATACA-3´	67
		Reverse	5´-GTCAGGCATCCCATGAATCCG-3´	
SlNRT1.7	XM_004238712.2	Forward	5'- TCCCCGAAAACATGAGCAGT -3'	117
		Reverse	5'- GCCCATTTCCTCCCGTAGTG -3'	
SlNRT2.7	XM_004233279.4	Forward	5'-TCCTTCGTTCATTTCATGGCG-3'	101
		Reverse	5'-CATCAGGTAAGTCCTGGCCG-3'	
SlCLC-a	XM_004231738	Forward	5´-CGTCTCCCTTTTCACCTCCA-3´	93
		Reverse	5´-CCAGGACAGGACCCTTGAAT-3´	
SlNRT1.5	XM_004244498.4	Forward	5´-TCCTTAGTGTAGCAGGCGTC-3´	127
		Reverse	5´-ACCAGTCCAATACCCATCCG-3´	
SlNRT1.8	XM_010328990.3	Forward	5´-GCCTTTGTGCAGTGTCTCAA-3´	141
		Reverse	5´-CTGTTTTCATTGCAGCCCCT-3´	
SlActin[a)]	NM_001330119.1	Forward	5´AGGTATTGTGTTGGACTCTGGTGAT-3´	81
		Reverse	5´-ACGAGAATGGCATGTGGAA-3´	

a) Reference gene used as internal standard (Løvdal and Lillo, 2009)

3. Results

3.1. NUE evaluation

3.1.1. Biomass and morphological response to limiting NO_3^- supply

Plant growth of two tomato genotypes, RO and UC82, were analyzed under limiting and non-limiting NO_3^- supply (Figure S2). The biomass production, expressed as shoot dry weight (SDW), varied significantly between NO_3^- treatments and among tomato genotypes ($P < 0.05$) (Figure 14A). By contrast, root dry weight (RDW) did not differ significantly among genotypes and between N-treatments (Figure 14B). The SDW results indicated that RO was the less sensitive to NO_3^- limiting supply than UC82.

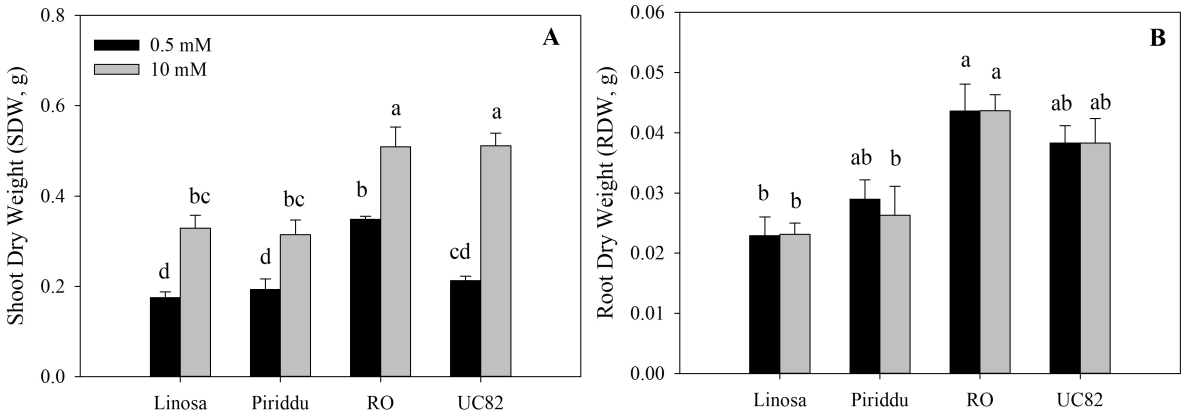

Figure 14. Shoot (A) and root (B) dry weight of four tomato genotypes grown under NO_3^- limiting (0.5 mM $Ca(NO_3)_2$) and non-limiting (10 mM $Ca(NO_3)_2$) supply ($P < 0.05$, n=5).

All the genotypes did not show any significant variation in response to different NO_3^- supply in total root length (TRL), root tissue density (RTD), root fineness (RF) and shoot length (SL), whilst root length ratio (RLR), root mass ratio (RMR), leaf number (# L) and leaf area (LA) varied significantly except for RO ($P < 0.05$) (Table 4), for which these parameters underlined RO lowest sensitivity to NO_3^- limiting supply (Table 4).

Table 4. Comparison of root and shoot morphology among four tomato genotypes grown under NO_3^- limiting (0.25 mM $Ca(NO_3)_2$) and non-limiting (5 mM $Ca(NO_3)_2$) supply. (**TRL,** Total Root Length; **RLR,** Root Length Ratio; **RMR,** Root Mass Ration**; RTD,** Root Tissue Density; **RF,** Root Fineness; **#L,** Leaves number; **LA,** Leaf Area; **SL,** Shoot Length). Different letters along column indicate statistical significant differences ($P < 0.05$).

Genotypes	$[NO_3^-]$	TRL (cm)	RLR (cm g^{-1})	RMR	RTD (g cm^{-3})	RF (cm cm^{-3})	# L	LA (cm^2)	SL (cm)
Linosa	0.5	845,74 c	6192,55 a	0,094 ab	0,07 abc	3595,78 abc	19,66 c	93,38 ab	17,52 ab
	10	1015,19 bc	2302,42 b	0,052 c	0,08 abc	3508,05 abc	33,66 ab	163,29 c	18,97 a
Piriddu	0.5	1006,94 bc	6456,08 a	0,101 ab	0,065 bc	4181,68 a	26,67 bc	83,72 a	13,57 cd
	10	727,77 c	2969,67 b	0,051 c	0,07 abc	4047,86 a	34,66 a	123,98 b	16,1 bc
R.O	0.5	1734,72 a	4846,31 ba	0,091 ab	0,081 ab	4006,72 a	36,66 a	168.91 c	10,20 e
	10	1780,38 a	3281,76 b	0,074 bc	0,092 a	3640,12 ab	39,66 a	180.26 c	10,61 e
UC82	0.5	1453,20 ab	5806,038 a	0,117 a	0,058 bc	2835,59 c	25,33 c	67,13 a	11,81 de
	10	1713,02 a	3104,09 b	0,057 c	0,055 c	3012,13 bc	38,67 a	126,72 b	14,96 bc

3.1.2.Chlorophyll content (SPAD)

Chlorophyll content was measured in tomato leaves of each genotype and treatment, the SPAD values showed significant differences in response to limiting and non-limiting NO_3^- conditions in all the genotypes, except for RO that exhibited similar values at both N-treatments. In addition, UC82 appeared the most sensitive genotype to N limitation (Figure 15).

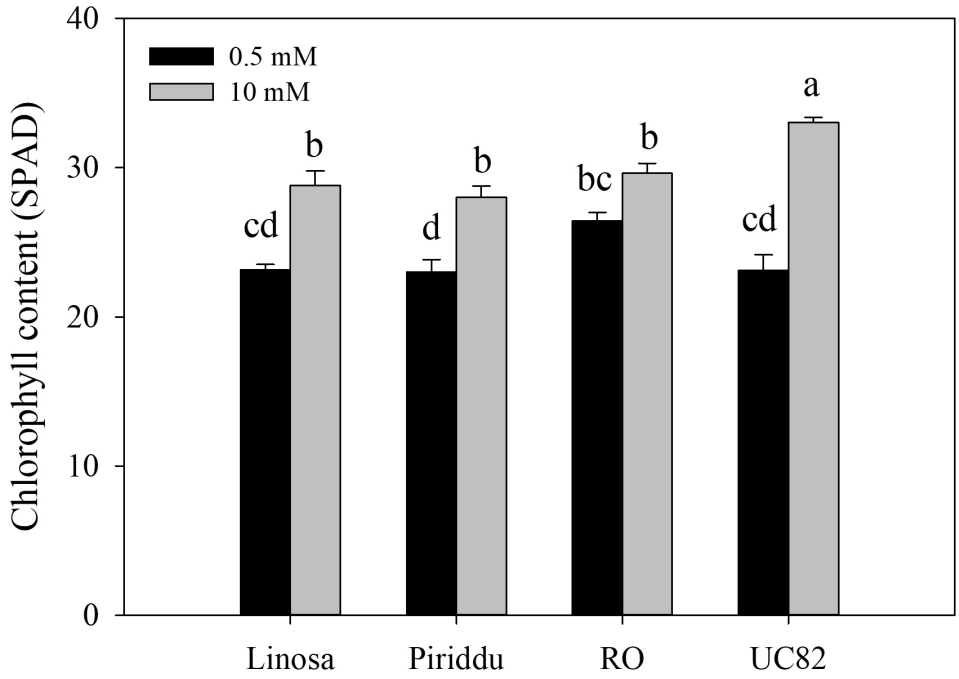

Figure 15. Chlorophyll content (SPAD values) in four tomato genotypes grown under NO3- limiting (0.5 mM $Ca(NO_3)_2$) and non-limiting (10 mM $Ca(NO_3)_2$) supply ($P < 0.05$, n=5).

3.1.3. Nitrogen content and nitrogen use efficiency

The N content (Nc) did not vary significantly in root of all the genotypes, except for RO, which showed a significant lower Nc under NO_3^- limiting condition; by contrast, significant differences were observed in the shoot of all the genotypes (Figure S3; Table S1). To further analyze N distribution in plant, the root/shoot Nc ratio (R/S Nc ratio) was also calculated. In NO_3^- limiting supply, RO exhibited the lowest R/S Nc ratio value indicating a lower N content in root compared to the other genotypes. By contrast, similar R/S Nc ratio values were observed under NO_3^- non-limiting condition among genotypes (Figure 16A). Under NO_3^- limiting supply, NUE increased significantly in RO respect to the control, while any significant difference was observed between treatments in the other genotypes. In the same condition, NUpE decrased in all the genotypes except for Linosa, while NUtE decreased significantly only in UC82, respect to the control. Overall, in NO_3^- limiting supply, RO showed significant higher NUE and NUtE, while UC82 exhibited a marked NUtE decrease compared to the other genotypes. (Figure 16B,C and D).

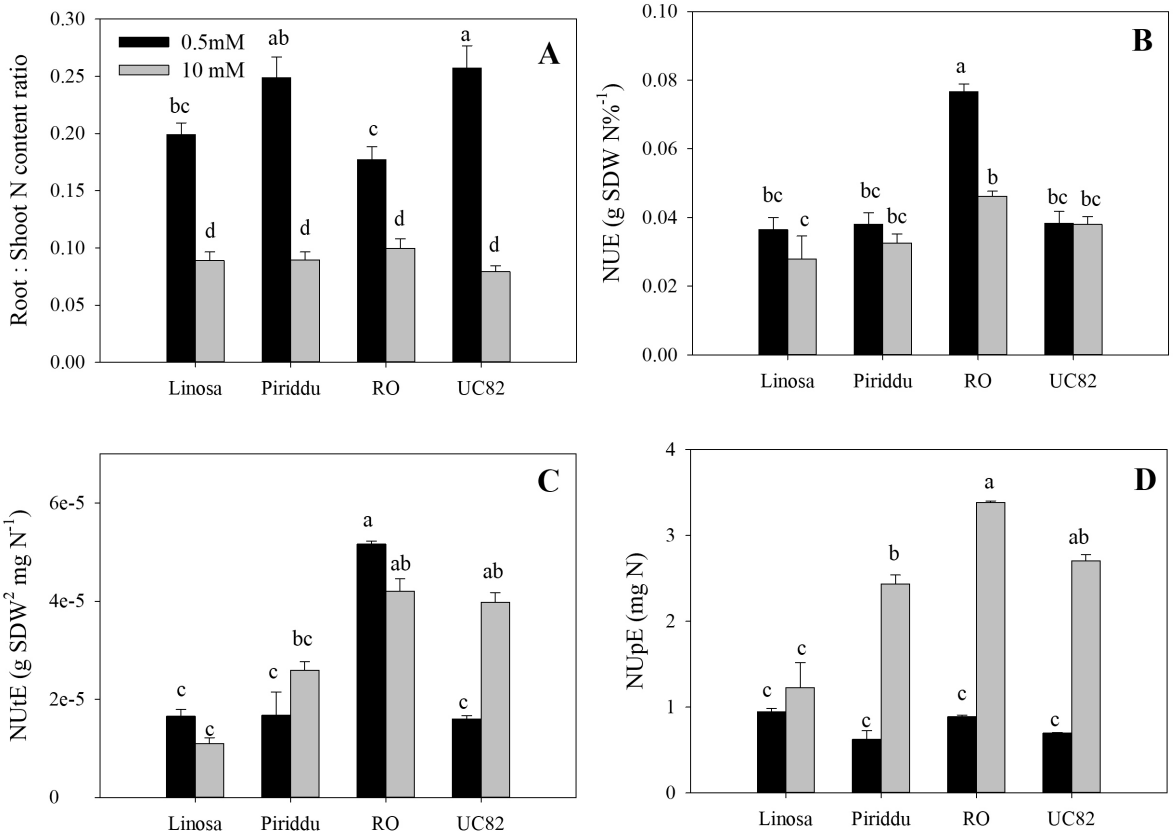

Figure 16. Root/shoot N content ratio (R/S ratio) (A), Nitrogen Use efficiency (NUE) (B), Nitrogen Utilization Efficiency (NUtE) (C) and Nitrogen Uptake efficiency (NUpE) (D) of four tomato genotypes grown under NO3- limiting (0.5 mM Ca(NO3)2) and non-limiting (10 mM Ca(NO3)2) supply ($P < 0.05$, n=5).

3.2. Gene expression analysis

Based on morphological and physiological traits, RO and UC82 were selected for their contrasting response in NO_3^- limiting conditions. The expression patterns of NO_3^- assimilation, allocation, remobilization and storage/sequestration related genes in root and shoot of both genotypes were analyzed at 0, 8 and 24 h (short-term response) and after one week (long term response) from NO_3^- recovery.

3.2.1. Short and long-term response to limited NO_3^- supply in shoot

The time-course of *SlNR*, *SlNIR*, *SlGS2*, *SlGOGAT*, *SlNRT1.7*, *SlNRT2.7* and *SlCLCa* expressions was assessed (Figure 17). Before NO_3^- recovery (0h), no significant differences were observed in gene expressions ($2^{-\Delta Ct}$) between the two genotypes except for SlNR and *SlGS2*, which were significantly more expressed in UC82 respect to RO ($P < 0.05$) (Figure S4A; Table S2).

After 8h from NO_3^- recovery, *SlNR* and *SlNRT1.7* expressions were significantly up-regulated in both genotypes (Figure 17A, E), while *SlNIR* and *SlGOGAT* were significantly down-regulated only in RO under NO_3^- limiting (0.5mM) compared to non-limiting (10mM) condition (Figure 17B,D). In turns, *SlCLCa* was significantly up- and down-regulated in RO and UC82, respectively, in NO_3^- limiting compared to the non-limiting condition ($P < 0.05$) (Figure 17G; Table S3). Furthermore, *SlGS2* and *SlNRT2.7* did not show significant differences between genotypes and N treatments (Figure 17C, F). Interestingly, the expression levels of *SlNRT1.7* was significantly higher in RO compared to UC82, while *SlNIR*, *SlGOGAT* and *SlCLCa* were significantly more expressed in UC82 compared to RO in the NO_3^- limiting condition ($P < 0.05$) (Table S3).

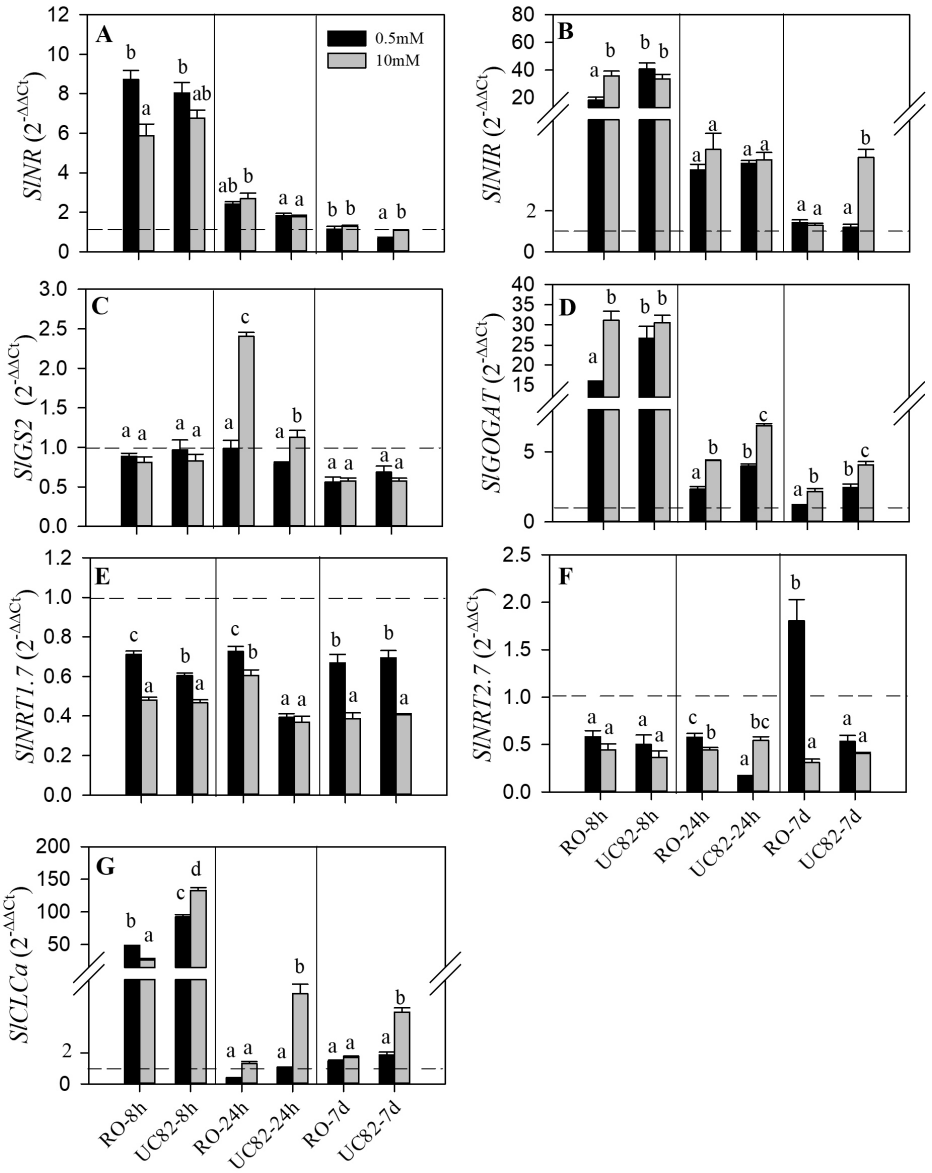

Figure 17. Differential relative expression of NO_3^- metabolism-related gene in shoot of RO and UC82 grown under NO_3^- limiting (0.25 mM $Ca(NO_3)_2$) and non-limiting (5 mM $Ca(NO_3)_2$) supply. Shoots of 32d old plants were sampled at 0h, 8h and 24 h after NO_3^- recovery. The mean fold change in expression of the target gene at each time point was calculated using the $2^{-\Delta\Delta Ct}$ method, where $\Delta\Delta CT = (C_{T,Target} - C_{,Actin})_{Time\ x} - (C_{T,Target} - C_{,Actin})_{Time\ 0,}$ SlActin was the internal control gene and time 0 was the calibrator. Means and standard errors are shown from the analysis of three biological replicates ($P < 0.05$, n=3) and different letters within each time point indicate significant differences at $P < 0.05$).

After 24h, *SlNR* and *SlNIR* expressions did not show significant differences between genotypes and treatments (Figure 17A, B). The *SlGS2* and *SlCLCa* expressions were significantly down-regulated in RO and UC82, respectively, under NO_3^- limiting compared to non-limiting condition ($P < 0.05$) (Figure 17C, G; Table S3). Further, *SlGOGAT* expression was significantly down-regulated in RO and UC82 at 0.5mM (Figure 17D), *SlNRT1.7* expression was significantly up-regulated in RO (Figure 17E), while *SlNRT2.7* expression was significantly up and down-regulated in RO and UC82, respectively under NO_3^- limiting

compared to non-limiting condition ($P < 0.05$) (Figure 17F; Table S3). At this recovery time, the *SlNRT1.7* and *SlNRT2.7* expression levels under NO_3^- limiting supply were significantly higher in RO compared to UC82 ($P < 0.05$) (Table S3).

After one week (7d) from NO_3^- recovery, the *SlNR* and *SlNIR* expression levels did not show any significant differences between NO_3^- treatments in RO, while both gene expressions were significantly down-regulated in UC82 at 0.5mM compared to non-limiting N-treatment ($P < 0.05$) (Figure 17A,B; Table S3). Furthermore, SlGS2 did not show significant differences between genotypes and N treatments (Figure 17C), while *SlGOGAT* and *SlNRT1.7* expressions were significantly down and up-regulated, respectively, in both genotypes (Figure 17D-E). Finally, *SlNRT2.7* was significantly up-regulated only in RO in NO_3^- limiting condition respect to the control ($P < 0.05$) (Figure 17F, Table S3). In addition, the SlNR and *SlNRT2.7* transcripts abundance was significantly higher in RO compared to UC82, while *SlGOGAT* expression level was higher in UC82 compared to RO, in NO_3^- limiting condition ($P < 0.05$) (Table S3).

3.2.2. Short and long-term response to limited NO_3^- supply in root

The time course of *SlNR*, *SlCLCa*, *SlNRT1.5* and *SlNRT1.8* expressions was assessed (Figure 18). Before NO_3^- recovery (0h), all the gene expression levels ($2^{-\Delta Ct}$) were significantly different between genotypes; in particular, *SlNR*, *SlCLCa* and *SlNRT1.5* were significantly more expressed in RO, while *SlNRT1.8* was significantly more expressed in UC82 ($P < 0.05$) (Figure S4B, Table S2).

After 8h from NO_3^- recovery, *SlNR* and *SlNRT1.8* expressions were significantly down-regulated in UC82 (Figure 18A,D), while *SlCLCa* expression was significantly up-regulated in RO under NO_3^- limiting compared to non-limiting condition (Figure 18B). Further, *SlNR* and *SlNRT1.5* were significantly more expressed in UC82 compared to RO, while *SlCLCa* expression level was significantly higher in RO ($P < 0.05$) (Figure 18A, B, Table S3).

After 24h, *SlNR*, *SlCLCa* and *SlNRT1.5* expressions were significantly down-regulated in both genotypes (Figure 18A,B,C), while *SlNRT1.8* appeared significantly down-regulated only in RO (Figure 18D) under NO_3^- limiting compared to non-limiting condition ($P < 0.05$) (Table S3). In addition, all the analyzed gene expressions were significantly more expressed in UC82 compared to RO under NO_3^- limiting condition ($P < 0.05$) (Table S3).

After one week (7d) from NO_3^- recovery, all the gene expressions were significantly down-regulated in both genotypes under NO_3^-limiting condition compared to non-limiting ones, except for *SlNRT1.8* ($P < 0.05$) (Figure 18, Table S3). Furthermore, under NO_3^- limiting condition, *SlNR* expression was not significantly different between genotypes (Figure 18A), *SlCLCa* and *SlNRT1.8* expression levels were significantly higher in UC82 compared to RO (Figure 18B,D), while *SlNRT1.5* expression level was significantly higher in RO compared to UC82 (Figure 18C, Table S3).

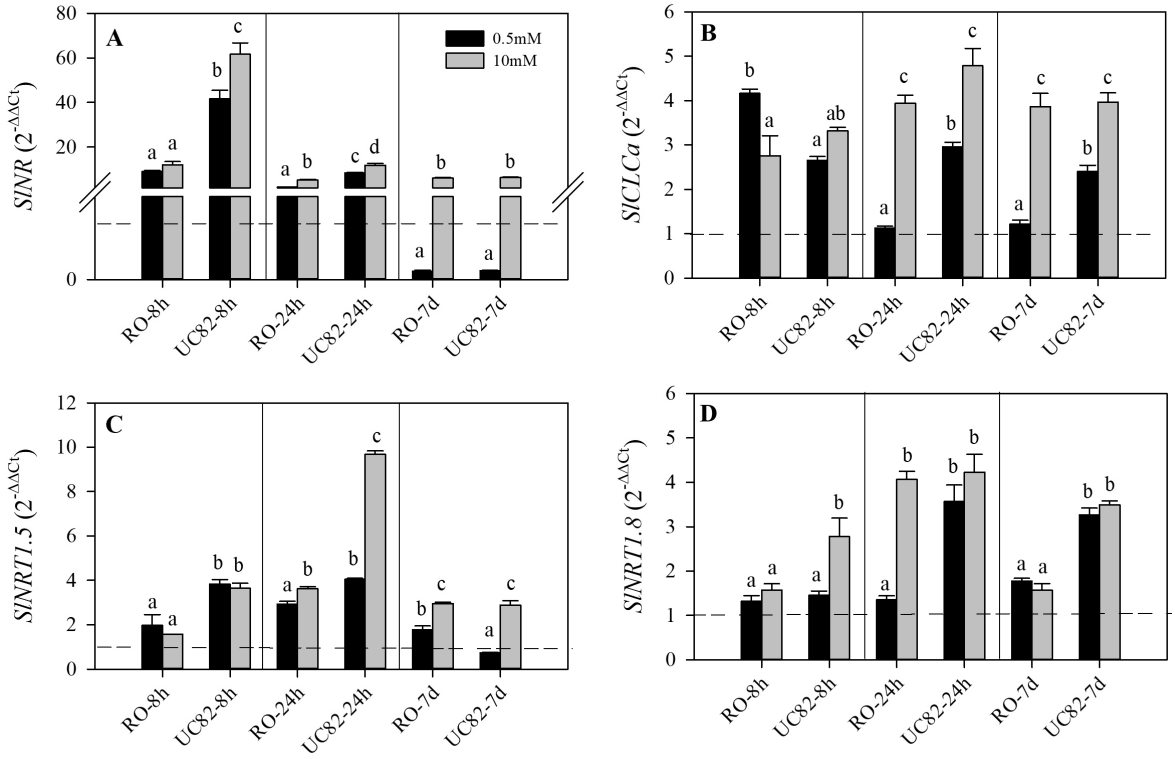

Figure 18. Differential relative expression of NO_3^- metabolism-related gene in root of RO and UC82 grown under NO_3^- limiting (0.25 mM $Ca(NO_3)_2$) and non-limiting (5 mM $Ca(NO_3)_2$) supply. Roots of 32d old plants were sampled at 0h, 8h and 24 h after NO_3^- recovery. The mean fold change in expression of the target gene at each time point was calculated using the $2^{-\Delta\Delta Ct}$ method, where $\Delta\Delta CT = (C_{T,Target} - C_{,Actin})_{Time\ x} - (C_{T,Target} - C_{,Actin})_{Time\ 0}$, SlActin was the internal control gene and time 0 was the calibrator. Means and standard errors are shown from the analysis of three biological replicates ($P < 0.05$, n=3) and different letters within each time point indicate significant differences at $P < 0.05$).

Moreover, the results obtained after one week of NO_3^- treatments on NUE and its components together with the molecular responses observed in both genotypes as well in root and shoot were highlighted in a heatmap (Figure 19). The observed differences in N use efficiency could be explained by *SlNR*, *SlCLCa* and *SlNRT2.7* expressions in shoot, and *SlNRT1.5* and *SlNRT1.8* in root displaying contrasting expressions between tomato genotypes in NO_3^- limiting condition (Figure 19).

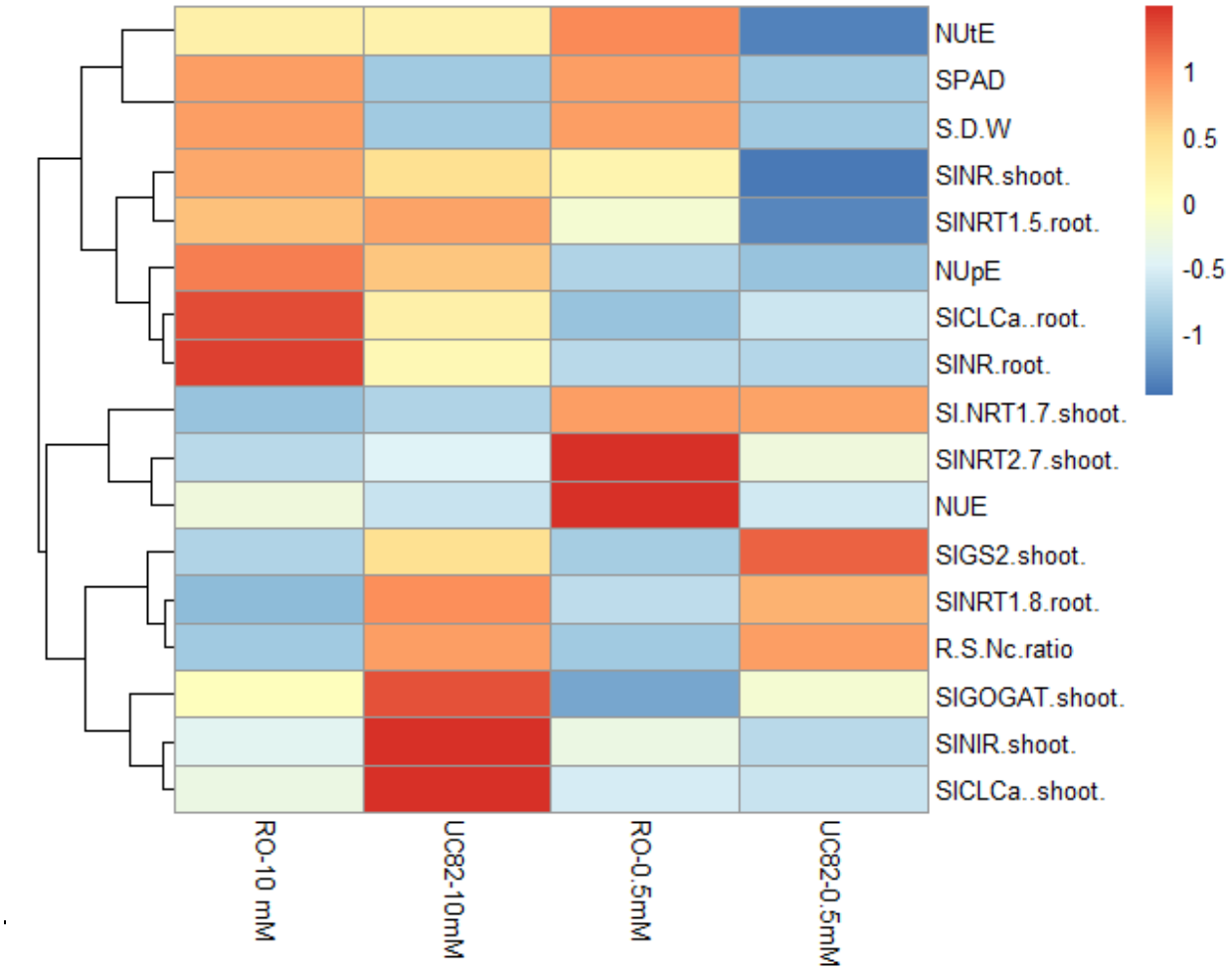

Figure 19.Heatmap of NO_3^- metabolism-related gene expressions in shoot and root, physiological NUE-related parameters and NUE and its components of RO and UC82 after one week under NO_3^- limiting (0.25 mM $Ca(NO_3)_2$) and non-limiting (5 mM $Ca(NO_3)_2$) supply.

3.2.3. NO_3^- metabolism-related genes expressions and NUE parameters correlations

Pearson correlation between genes expression and morpho-physiological traits (including NUE and its components) in shoot and root of both tomato genotypes after one week under limiting NO_3^- treatment is presented in Figure 20.

According to the matrix visualization, NUE, NUtE and NUpE showed a significant and positive correlation with SDW, as expected, but also with NO_3^- assimilation and efflux related genes expression (*SlNR*, *SlNIR* and *SlNRT2.7*) in shoot, and NO_3^- long-distance transporter gene expression (*SlNRT1.5*) in root. Otherwise, NUE and its components exhibited a negative correlation with *SlCLCa* expression in both shoot and root, *SlNRT1.8* expression in root and R/S Nc ratio. Moreover, *SlGOGAT* and *SlGS2* showed a significant negative correlation with NUE and its components (NUpE and NUpE).

The results highlighted also some specific negative correlations; in detail: a) *SlNIR* and *SlNRT2.7* expression in shoot as well as *SlNRT1.5* expression in root with NO_3^- storage related gene (SlCLCa) and *SlNRT1.8* in root; b) the chlorophyll content (SPAD) with the *SlCLCa* expression in root; .c) the R/S Nc ratio with SPAD values and NO_3^- assimilation and transporter gene expressions in both shoot and root (*SlNRT2.7*, *SlNIR* and *SlNR*); d) the SDW with *SlCLCa* and *SlNRT1.8* expressions in root (Figure 20).

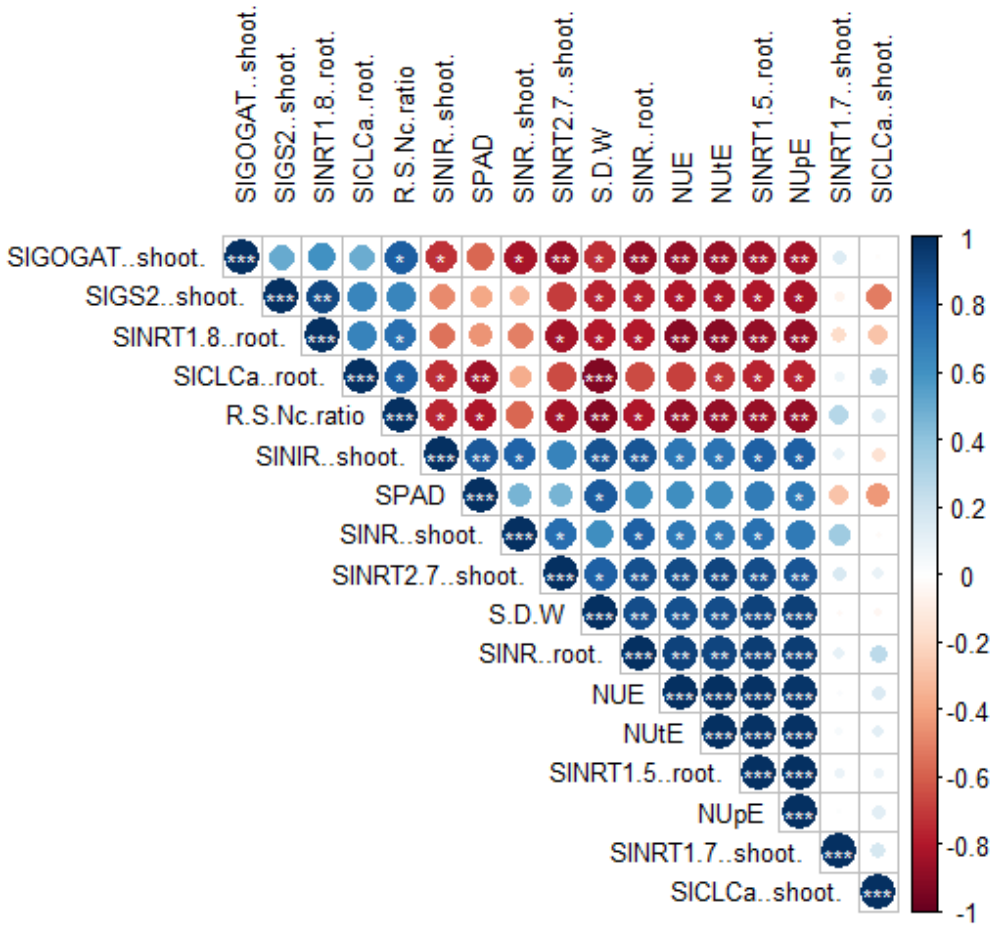

Figure 20.Correlation matrix visualization of the correlations between NUE related parameters and NO_3^- metabolism-related gene expressions of RO and UC82 after one week under NO_3^- limiting supply (0.25 mM $Ca(NO_3)_2$). * $0.01 < p \leq 0.05$; ** $0.001 < p < 0.01$; *** $p < 0.001$

4. Discussion

Limiting nitrogen availability drives specific and complex physiological, morphological and developmental responses in plants (Yang *et al*., 2011). These can differ among cultivars of the same species due to the genetic variation for N uptake (Rodgers and Barneix, 1988) and utilization (Chardon *et al*., 2010; Coque and Galleis, 2007), laying the foundations for improving Nitrogen Use Efficiency (NUE). The present study further confirms the existing differences among genotypes for a complex trait like NUE and its components in tomato.

Our findings confirmed RO and UC82 as the best NUE contrasting genotypes, namely N-use efficient and inefficient, respectively (Abenavoli *et al*., 2016). Previous researches showed that considerable variation in NUE occurs mainly for biomass production in tomato, barley, maize and cotton (Abenavoli *et al*, 2016; Lupini *et al*., 2017; Xu *et al*., 2016; Granato *et al*., 2014; Iqbal *et al*., 2020); in agreement, our results showed the highest RO biomass production (SDW) compared to the others, in turns it decreased considerably in UC82 mainly under limiting NO_3^- treatment. Accordingly, NUE appeared noticeably enhanced in RO under limiting NO_3^- supply, while UC82 exhibited the most significant decrease in NUtE level, compared to the other tomato genotypes.

The SPAD values, that predict crop nitrogen deficiency and the photosynthetic rates (Debaeke *et al.*, 2006; Reis *et al*., 2009), further emphasized the contrasting responses between RO and UC82 facing NO_3^- limitation, underlying the highest tolerance to N scarcity of RO throughout the photosynthetic efficiency and its positive correlation with higher biomass production (here measured as SDW) (Figure 20). Furthermore, under NO_3^- limiting condition, the R/S Nc ratio indicated that RO translocated more N to the shoot than the other genotypes supporting the positive correlation between NO_3^- shoot allocation (SlNRT1.5) and NUE (Figure 20), as well as between NUtE and the photosynthetic efficiency (Smirnoff and Stewart, 1985; Lin *et al*., 2008; Tang *et al*., 2013). Overall, our preliminary results suggested that the strategy adopted by RO to perform a considerable NUE enhancement seemed to be due to a high NUtE, while NUpE was of less importance in NUE performance, as already reported by Abenavoli *et al.* (2016).

As a signal molecule, NO_3^- regulates several plant physiological processes by inducing or repressing the expression of its transport, assimilation and remobilization related genes (Kant, 2017; Hachiya and Sakakibara, 2017). The identification of key metabolic pathways in genotypes able to optimize NO_3^- utilization under N-stress is essential for crop NUE improvement (Lian *et al*., 2005). In the present study, all the genes related to NO_3^- translocation, assimilation and storage were up-regulated whereas those encoding for NO_3^- remobilization and efflux appeared down-regulated during the early hours after NO_3^- re-supply, regardless NO_3^- concentration and plant tissue. Interestingly, the chloroplastic glutamine synthetase (*SlGS2*) expression level was maintained in both RO and UC82 throughout time in shoot, suggesting that the constitutive *SlGS2* expression was enough to support nitrogen metabolism in tomato under NO_3^- stress. Similar expression patterns were already observed in *Thellungiella halophila* and barley (Kant *et al*., 2008; Chen *et al*., 2018).

It is well known that nitrate reductase (NR) and nitrite reductase (NIR) are the first enzymes that reduce NO_3^- to NH_4^+ for sustaining N assimilation (Meyer and Stitt, 2001). Nitrate limiting condition triggered differences in NO_3^- assimilation between the NUE contrasting genotypes after one week of treatment. In agreement, *SlNR* and *SlNIR* did not exhibit significant differences between NO_3^- treatments in RO, while they were significantly down-regulated under NO_3^- limiting condition in UC82. Noterworthy, *SlNR* transcripts abundance was significantly higher in RO compared to UC82 in shoot. Both gene expressions were significantly correlated among them and to NUE and its components (NUpE and NUtE) (Figure 20). These results could sustain the higher NUtE maintained by RO under low N supply compared to UC82. In agreement, the same *NR* and *NIR* expression profiles in potato and barley under N-limiting condition were observed (Li *et al*., 2010; Chen *et al*., 2018; Kollaricsné Horvath *et al*., 2019).

Beside, the GS/GOGAT pathway is of critical importance for NO_3^- assimilation catalyzing the reactions that transform inorganic to organic nitrogen (Lea and Miflin, 1974). Therefore, the induction of both genes (GS2 and GOGAT) was identified as the major effector for NUE under NO_3^- limiting supply in many crops species (Quraishi *et al*., 2011; Chen *et al*, 2018; Mauceri *et al*., 2020). Conversely, our findings correlated lower GS/GOGAT gene expression to higher NUE under NO_3^- limiting conditions, as recently reported in Arabidopsis by Meyer *et al*. (2019). They suggested that this result could be related to the fact that good NUE definition in their study was essentially based on good biomass production under NO_3^- deficiency, as considered in our study. However, althought GS/GOGAT are important in NUE (Xu *et al*., 2012), the negative correlation found in our results could be related to the phenological stage in which the tomato plants were harvested for analysis, thereby indicating their marginal role in this stage compared to flowering onwards.

Nitrate remobilization was reported as another key factor for improving NUE (Masclaux-Daubresse *et al*., 2008). To discern NO_3^- remobilization role in tomato NUE, we evaluated the differential expression of *SlNRT1.7* between genotypes pair, based on its involvement in the stored NO_3^- remobilization from older leaves to N-demanding tissues through phloem (Fan *et al*., 2009; Chen *et al*., 2020). Nitrate limiting condition triggered a *SlNRT1.7* up-regulation in both genotypes compared to non-limiting N-supply. More interestingly, transcripts of *SlNRT1.7* were more abundant in RO respect to UC82 mainly after 8 and 24h of N-stress. Hence, the adopted strategy by RO during the early hours under NO_3^- limiting supply appeared of crucial importance for facing the long-term NO_3^- stress. Chen *et al*. (2020)

improved Arabidopsis, tobacco and rice NUE through a novel strategy aiming to specifically enhance *NRT1.7*-mediated NO_3^- remobilization.

Our results evidenced as well the strong correlation between both NUE and NUtE and *SlNRT2.7* expression level in the shoot of RO, the N-use efficient genotype (Figure 20). Until now, limited information have been reported on this high affinity NO_3^- transporter in shoot tissues. However, Orsel *et al*. (2002) stated that NRT2.7 was the only NRT2 family member not apparently involved in NO_3^- uptake from soil, showing a strong leaf tissue specific expression pattern in Arabidopsis under limiting NO_3^- supply, in agreement with our results. They suggested that, under N-starvation, NRT2.7 protein regulated NO_3^- efflux balancing the NO_3^- assimilable amount transporting back into the xylem any excess (Orsel *et al*., 2002).

Nitrate long-distance transport from root to shoot likely contributes to plant growth and NUE enhancement (Andrews, 1986; Tang *et al*., 2012; Han *et al*., 2016) since higher NO_3^- assimilation efficiency occurred in shoot tissues (Smirnoff and Stewart, 1985; Tang *et al*., 2013). This transport is regulated by NRT1.5 and NRT1.8 genes, which control xylem NO_3^- loading and unloading, respectively (Lin *et al*., 2008; Li *et al*., 2010; Han *et al*., 2016). However, NO_3^- long-distance transport was strongly affected by its storage/sequestration in vacuoles (Han *et al*., 2015; Han *et al*., 2016). This short-distance transport between cytosol and vacuole is mediated by CLCa, a NO_3^-/H^+ exchanger localized in the tonoplast and responsible for NO_3^- homeostasis maintenance in the cytosol (De Angelis *et al*., 2006; Wege *et al*., 2014).

After seven days of N-treatment, high-NUE was significantly correlated with a higher NO_3^- xylem uploading gene expression (*SlNRT1.5*) and thereby to a major NO_3^- allocation to the shoot and a higher assimilation guided by *SlNR* and *SlNIR* expression (Figure 20). By contrast, high-NUE was negatively correlated to both xylem NO_3^- unloading (SlNRT1.8) and its storage/sequestration in vacuoles (*SlCLCa*) in root (Figure 20). These results are in agreement with the statement that a higher CLCa activity in root induces a down- and up-regulation of *NRT1.5* and *NRT1.8* gene expressions, respectively (Lin *et al*., 2008; Han *et al*., 2016). Noticeably, our N-use efficient genotype RO exhibited a significant higher SlCLCa transcript abundance in root compared to UC82 at the first 8h of N-stress. These differential gene expressions suggested that high-NUE in RO could occur for a higher NO_3^- accumulation in root cell vacuoles during the short-term NO_3^- stress exposure, followed by a significant higher NO_3^- translocation to the shoot (guided by *SlNRT1.5* higher expression) under the long-term NO_3^- stress, compared to UC82 (Figure 21).

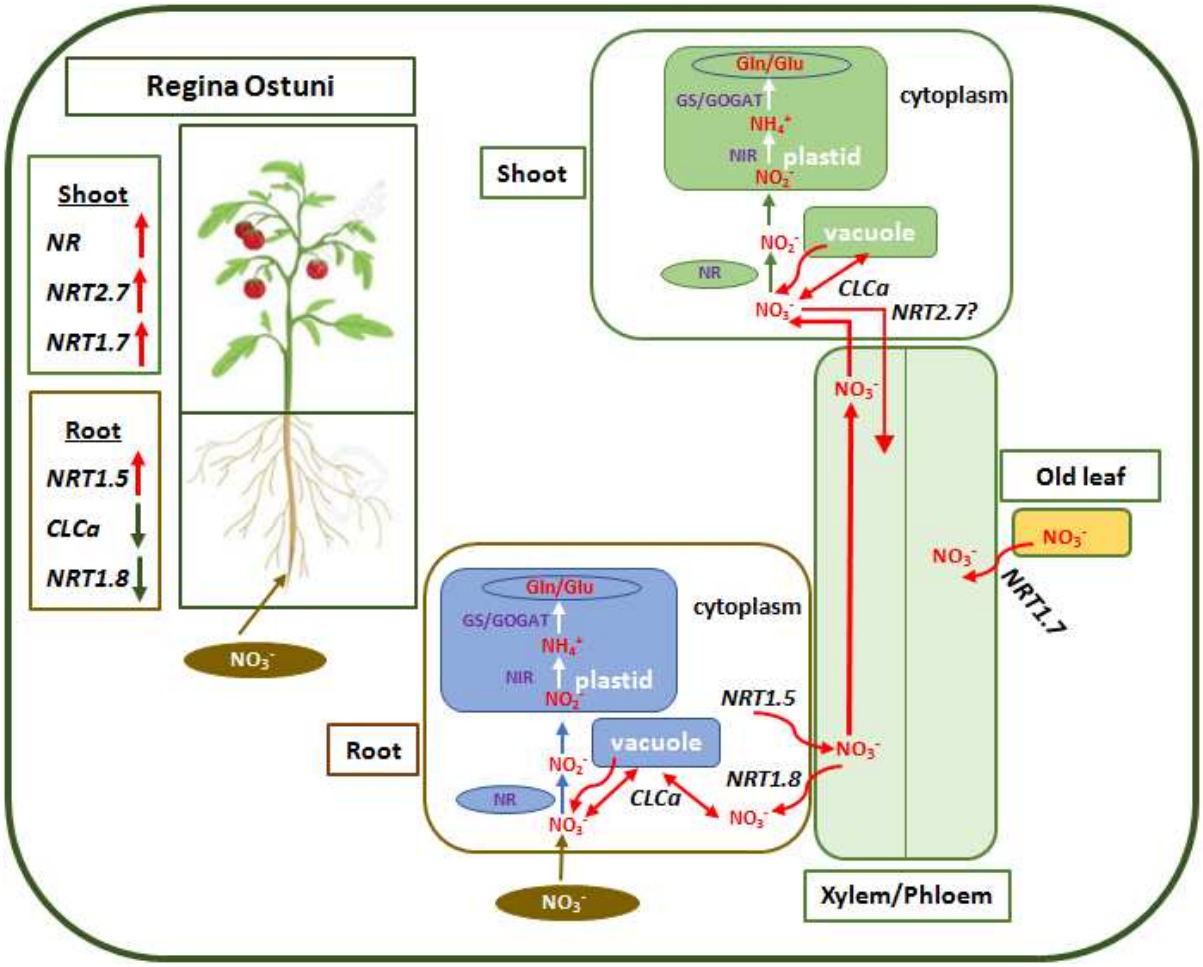

Figure 21. The proposed model describing Regina Ostuni high N-utilization efficiency (NUtE). In black and bold the different expressed key genes that could be involved in high NUE tomato genotype making it able to cope N-limiting supply. The gene expression increase or decrease are indicated with red and green arrows, respectively.

After long-term stress (7d), UC82 showed a higher NO_3^- storage/sequestration and NO_3^- xylem unloading in root (*SlNRT1.8* higher expression), thereby less NO_3^- amount was translocated to shoot and available for assimilation. Moreover, we observed a negative correlation between *SlCLCa* and *SlNR* expressions confirming that CLCa activity limits NO_3^- availability in the cytosol and reduces NR activity, as previously reported in Brassica napus (Han *et al*., 2015).

Finally, designing efficient breeding strategies for NUE improvement requires an integration of agronomy, physiology and molecular insights (Lammerts van Bueren and Struik, 2017) to identify discriminant traits useful for selecting efficient genotypes, especially under low N condition. According to these authors, our results emphasized the morpho-physiological and molecular markers strongly correlated with high NUE in RO, making it a valuable genetic resourse for future tomato NUE breeding programs.

5. Conclusion

Our experiment contributed to shed light on NUE enhancement mechanisms under limiting NO_3^- supply in tomato. The differential expressions of the most important nitrate metabolism related genes explained the RO higher N-utilization efficiency (NUtE) and consequently higher NUE, compared to UC82.

The results suggested a RO faster adaptation to NO_3^- limiting condition compared to the inefficient genotype, afterwards RO appears able to ensure high NO_3^- efficient storage in cell root vacuoles within the short-term N-stress as well as a constant NO_3^- remobilization. RO high NUE seems to rely also on a more efficient NO_3^- translocation to the shoot for a higher assimilation efficiency, compared to UC82.

Overall, our results revealed some aspect of the molecular adaptation to NO_3^- deficiency and suggested that NUE in tomato could be mainly determined by the genotype ability to regulate long-distance N transport, assimilation, remobilization and storage/sequestration genes.

Chapter II

Short-term transcriptome profiling of two NUE-contrasting tomato genotypes in response to low nitrate

1. Introduction

Plant growth and development requires nitrogen (N) as source for the biosynthesis of amino acids, nucleic acids, and other nitrogen-containing biomolecules, and its limited availability causes crops yield and quality decrease (Xu *et al*., 2012; Bloom, 2015; Kiba and Krapp, 2016; Wang *et al*., 2018; Fredes *et al*., 2019). Since the 1950s, increasing N fertilizer application has been a major management strategy driving high crop yields (Guo *et al*., 2010) whose consumption has approximately reached 60% of the total fertilizer produced every year (Wang *et al*., 2018). Because less than 50% of the applied N is absorbed and utilized by crops, the remaining is lost into the environment (Ueda *et al*., 2020), causing pollution, and indirectly, human health damages (Fox *et al*., 2017; Alfatih *et al*., 2020). Therefore, the development of cultivars with high N use efficiency (NUE) is an effective and promising approach to improve crop yield, reduce fertilizer applications and alleviate hazardous impact on the environment (Hu *et al*., 2018). The elucidation of the molecular mechanisms underlying N response in crops will quicken the development of new varieties with low N requirement.

Although nitrate (NO_3^-) and ammonium (NH_4^+) are the major inorganic N forms in the aerobic soils (Wang *et al*., 2018), NO_3^- is the most commonly used by plants (Tischner, 2001; Crawford and Forde, 2002). Besides its role as a nutrient, NO_3^- is a local and systemic signal molecule that coordinates its uptake with plant growth and development (Ruffel *et al*., 2011; Alvarez *et al*., 2012; Ruffel *et al*., 2014). NO_3^- induces changes in the expression of genes involved in the N acquisition and assimilation, as well as the production of reducing equivalents needed for N and C metabolism (Scheible *et al*., 2004; Vidal and Gutiérrez, 2008). Furthermore, it induces seed germination, regulates root growth and architecture, controls shoot growth and delays flowering (Remans *et al*., 2006; Liu *et al*., 2011; Vidal *et al*., 2014; Yuan *et al*., 2016).

To orchestrate all these adaptive responses, NO_3^- provokes the plant transcriptome reprogramming (Canales *et al*., 2014; Medici and Krouk, 2014; Vidal *et al*., 2015). This highly dynamic phenomenon causes changes in transcripts accumulation detected as quickly as within 3 minutes from NO_3^- exposure, appearing also cell- and tissue-specific (Krouk *et al*., 2010b; Walker *et al*., 2017; Varala *et al*., 2018).

Recently, the investigations on N signaling mechanisms, at the transcriptome level, have attracted considerable attention. Several transcription factors (TFs), from many families, have been characterized and found to be involved in N response, such as B-box containing proteins

(BBXs), MYeloBlastosis (MYBs), ethylene response factors (ERFs), basic leucine zipper (bZIPs), NIN-like proteins (NLPs), lateral boundary domain-containing proteins (LBDs), and BTB and TAZ domain proteins (BTs) (Wang *et al*., 2018; Gaudinier *et al*., 2018). These studies provided comprehensive information on the role played by these TFs in the regulation of gene expression in the primary nitrate response (PNR) (Marchive *et al*., 2013; Liu *et al*., 2017; Varala *et al*., 2018; Brooks *et al*., 2019). Furthermore, the dynamic changes in intracellular calcium signaling induced by NO_3^- to generate rapid control on the nitrate uptake and transcriptional PNR has been also elucidated (Hu *et al*., 2009; Léran *et al*., 2015; Liu *et al*., 2017).

In addition to the transcriptional regulation, NO_3^- signaling involves post-translational modifications such as protein phosphorylation and ubiquitination, and chromatin modification (Liu *et al*., 2017; Hu *et al*., 2019; Poza-Carrion and Paz- Ares, 2019). In particular, protein phosphorylation can lead to rapid, versatile, and reversible modifications that directly regulate the localization, stability, interaction, function, and enzymatic activity of target proteins (Yip Delormel and Boudsocq, 2019).

Although NO_3^--induced genes involved in its transport and metabolism have been largely described in many crops, the tomato early response to N-resupply has not been deepened. According to Wang *et al* (2001), NO_3^- application to N-starved tomato plants significantly increased the transcription levels of genes responsible for its transport and assimilation in the first 24h. Moreover, many metabolic enzymes, such as transaldolase, transketolase, malate dehydrogenase, asparagines synthase and histidine decarboxylase, and genes encoding for water channels, root phosphate and potassium transporters, ribosomal proteins, or involved in transcriptional regulation and stress responses were identified after NO_3^- exposure (Wang *et al*., 2001). Recently, integrative transcriptomic-physiological- and metabolomic analyses individuated several pathways and key regulatory genes in response to low NO_3^- (LN) in tomato (Renau-Morata *et al*., 2021). So far, data on comparative transcriptome profiling between two NUE-contrasting tomato genotypes in response to early LN resupply are not available yet. In this respect, the RNA-Seq technology has been adopted in the present study for transcriptome profiling, because of its low background noise, high sensitivity, reproducibility, dynamic range of expression, and base pair resolution.

This chapter should essentially shed the light on:

- The tissue specific transcriptome modifications in the high- (Regina Ostuni, RO) and low-NUE (UC82) genotypes in responses to short-term LN-resupply compared to N-optimal condition;

- The early differences in LN-induced responses between RO and UC82 through time-course analysis of gene expression;
- The metabolic pathways mostly involved in the early LN response in ROvsUC82
- The genes and transcription factors regulating the early LN-response as new putative candidates for tomato NUE.

2. Material and Methods

2.1. N-depletion experiment

Since the internal NO_3^- concentration affects the N regulatory mechanisms (Forde and Clarkson, 1999), a preliminary N-depletion experiment was conducted to define the approximate NO_3^- starvation time for the NUE contrasting pair, RO and UC82. It is an essential step allowing us to identify the N-recovery starting time-point, where the N-related processes are expected to be de-induced, to study the differentially N-induced responses and their regulatory mechanisms between RO and UC82. The N-depletion experiment (Figure 22) was conducted as described in chapter I (Aci *et al*., 2021) and the results confirmed that the best N-recovery starting time-point was after 5 days from the N-starvation starting-time in both tissues of each genotype (Figure 23) (Aci *et al*., 2021).

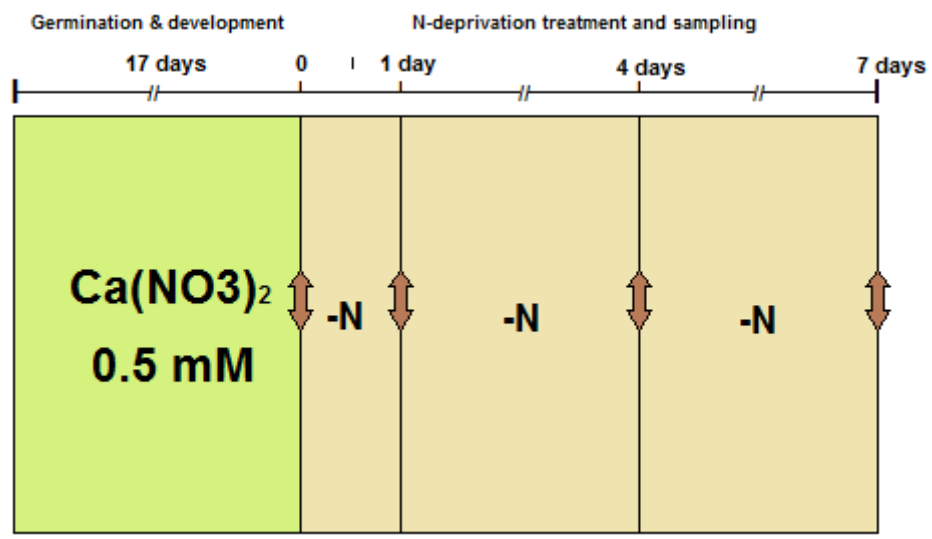

Figure 22. The N-depletion experimental setup and the schematic sampling-time.

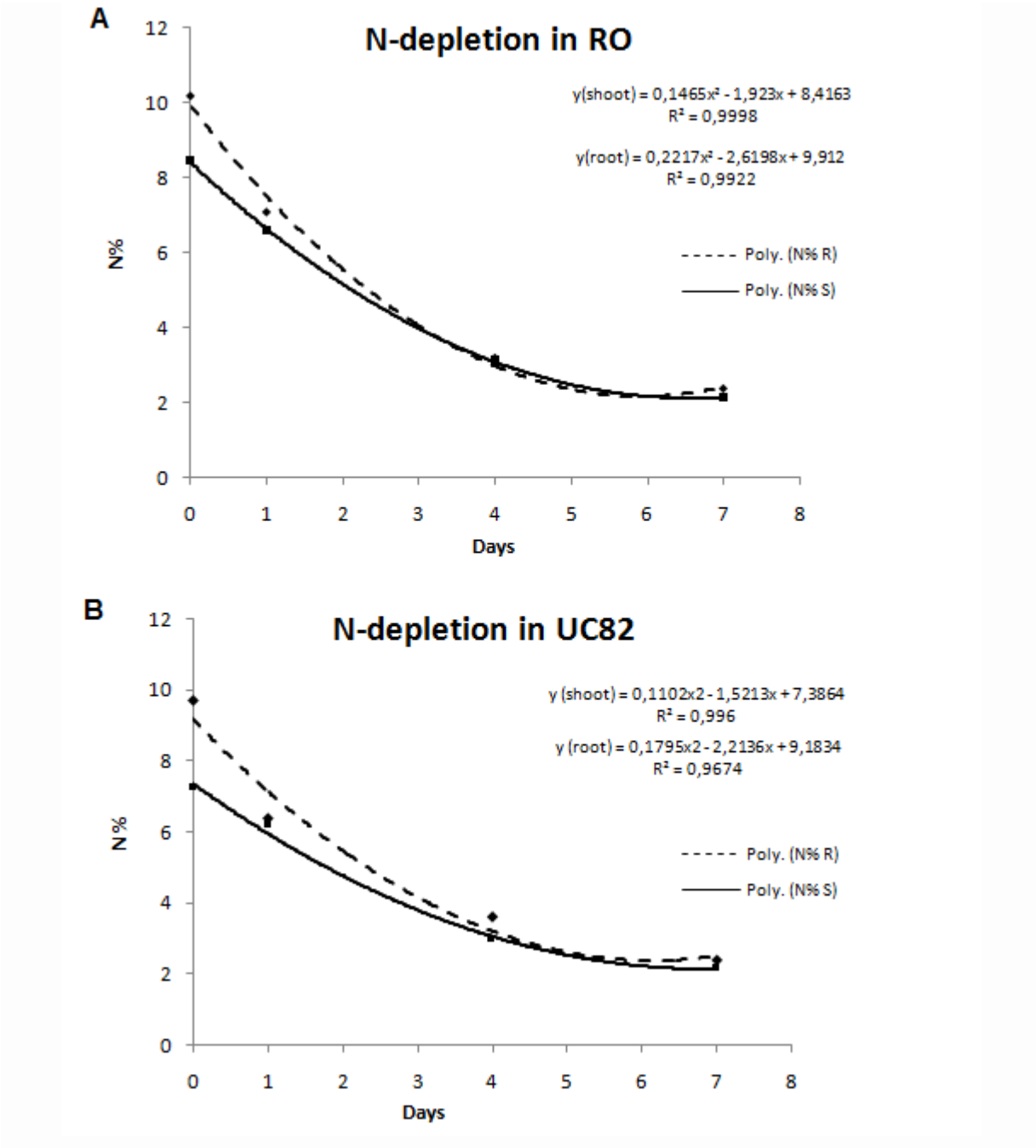

Figure 23.N-depletion of the two tomato genotypes grown in N-free solution. The data were plotted by a non-linear regression.

2.2. Transcriptome modulation analysis in response to short-term N treatment

2.2.1.Growth conditions at short-term N treatment

Seedlings (10-d old) from RO (high NUE) and UC82 (low NUE) were grown under non-limiting NO_3^- conditions for 10 days. Plants (20-d old) were starved for 5 days and then exposed to low (LN; 0.5 mM) and high NO_3^- (HN; 10 Mm). These two NO_3^- concentrations

(0.5 and 10 mM) were previously established for tomato (Abenavoli *et al*., 2016). Both shoot and root of each genotype were harvested at 0h, 8h and 24h after N resupply (HN and LN) (Figure 24) and three biological replicates were used for the transcriptome analysis, each consisting of a pool of three plants.

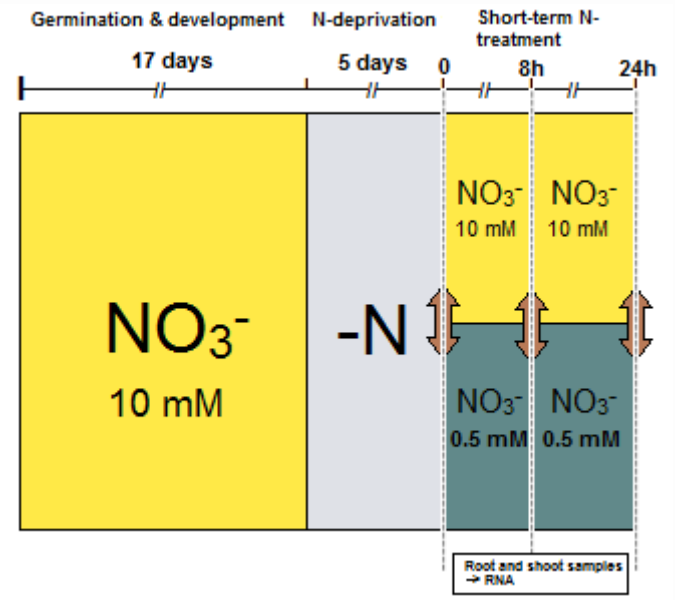

Figure 24. Experimental setup adopted for the short-term RNAseq analysis

2.2.2.RNA-seq analysis and data processing

Total RNA was extracted and purified using RNeasy Plant Mini Kit (Qiagen, Milano, Italy) following the manufacturer's protocol. RNA integrity was monitored on 1% denaturing RNA agarose gels and its purity checked using a NanoDrop 2000 (ThermoFisher Scientific, Wilmington, Delaware USA). Separate RNA-seq single-end sequencing libraries were prepared for each genotype (RO and UC82), treatment (HN and LN), tissue (shoot and root) and time point (0h, 8h and 24h) following the Transeq approach (Tzfadia *et al*. 2018). The 60 libraries were sequenced on six lanes HiSeq 2500 System (Illumina), using the SR60 protocol. The raw data were processed to obtain high quality clean reads, removing adapter sequences, reads with unknown N nucleotides larger than 5%, and low-quality sequences. Clean reads were mapped to the *Solanum lycopersicum* (tomato) genome (SL3.0) from Ensembl Plants (http://plants.ensembl.org/Solanum_lycopersicum/Info/Index) using TopHat v2.0.12 (http://ccb.jhu.edu/software/tophat/index.shtml) (Kim *et al*., 2013). Reads per kilobase of transcript per million mapped reads (RPKM) were used to calculate the expression levels of genes.

2.2.3. Modeling of gene expression patterns

To individuate the DEGs taking into account all the variables of our experimental setup, an ANOVA was performed on the normalized data in R environment (http://r-project.org/), using the following multivariate linear model:

$$Y = \alpha_1 G + \alpha_2 N + \alpha_3 T + \alpha_4 G*N + \alpha_5 G*T + \alpha_6 N*T + \alpha_7 G*N*T + \varepsilon$$

where G, N and T represent genotype, nitrate, and time factors, respectively, α_1 to α_7 the angular coefficient or effect of each factor (G, N, and T) and their interactions, and ε the random error. DEGs were determiner at FDR < 5%. Finally, the model was performed on root and shoot separately.

2.2.4. Time series clustering of gene expression after short term N-treatment

The short time-series expression miner (STEM) software (Ernst and Bar-Joseph, 2006) was used to examine the DEGs expression profiles and to identify significant N-responsive genes over time (0h, 8h and 24h) after N-resupply. This algorithm uses exclusive methods for clustering, comparing and visualizing data, and provides useful and statistically rigorous biological explanations of short time-series data due to its integration with GO. Each gene was assigned to the filtering criteria of the model profiles and the correlation coefficient was determined. We performed the standard hypothesis test using the true order of time-points, and determined the P value using the number of genes assigned to the model profile and the expected number of assigned genes (adjusted p-value, 0.05 by Bonferroni correction). The clustered profiles with a *P* value $\leq$ 0.05 were coloured and considered differentially expressed.

2.3. Differential gene expression analysis

To narrow the focus on genes regulated by NO_3^- over the entire data set, we selected all the clustered genes, which were up or down-regulated at least at 8h or 24h compared to the starting point (0h). The normalized counts of RO and UC82, at each time-point and for each tissue, were then compared using DESeq2 R package. A *P* value < 0.05 and an absolute $\log^2$ (fold change) value $\geq$ 1 were set to identify the N responsive DEGs.

2.4. Weighted Gene Co-expression Network Analysis (WGCNA)

A Weighted Gene Co-expression Network Analysis (WGCNA) was performed by using the RPKM values of the identified DEGs in RO*vs*UC82. The correlation between genes was performed by Pearson correlation coefficient (PCC), which was used to calculate the distance matrix. Both the WGCNA and distance matrix calculation were done using the WGCNA package v1.51 (Langfelder and Horvath, 2008). The distance matrix was then used for the dynamic hierarchical clustering and to build the edges (connections) between nodes (genes) in the regulatory networks.

2.4.1.Co-expression Network Construction

Eight treatment samples of both tissues were included in the WCGNA, namely RO-8h-LN, UC82-8h-LN, RO-24h-LN, UC82-24h-LN, RO-8h-HN, UC82-8h-HN, RO-24h-HN and UC82-24h-HN. The choice of soft thresholding value is a critical step to carry out the WGCNA, so we executed network topology research of 1 to 20 soft thresholding power using scale-free topology criteria for both tissues, and used a power of 16 and 14 to identify modules in shoot and root, respectively (Figure 34A and 35A). The minimum module size was set to 30, and the merge cut height was set to 0.15 (to merge modules with at least 85% of similarity). The correlations between one gene and all the others were incorporated into an adjacency matrix, which was then transformed into the topological matrix (TOM) (Yip and Horvath, 2007). After hierarchical clustering, highly correlated genes were assigned to the same module (Ravasz *et al*., 2002).

2.4.2.Identification of Significant Co-expression Modules

Once the treatment data were imported into the network, the module eigengene (ME), module membership (MM), and gene significance (GS) were calculated. The eigengenes are the representative genes in a module and the MEs represent the expression pattern of eigengenes, and the MM is the correlation degree between eigengenes and module. For MM close to 1, the eigengene is highly correlated with the module. GS is the association of a gene with the samples treatment information. A module is considered as a key module when it shows a high ME value with the samples treatment information (Langfelder and Horvath, 2008).

2.4.3.Identification and visualization of Hub genes

In a network, a hub gene is a node with a high degree of connectivity (many interactions with other nodes), and usually plays an important role in other genes regulation and biological processes (Yu *et al*., 2017). To deepen the analysis on differential behavior between the two NUE contrasting genotypes, we focused on the identification of hub genes that might regulate the early plant responses to LN. Thus, the DEGs in RO*vs*UC82 comparison, at the early stages (0h, 8h and 24h) after N-resupply in both tissues, were used to structure the co-expression networks. The hub genes were filtered for the MM and GS absolute values. After identifying the hub genes highly associated with LN treatment in the efficient genotype (RO), the functional analysis (GO, KEGG) of relevant modules was performed to identify the potential mechanisms involved in plant response to the corresponding treatment. Then, the regulatory network visualization and analysis for the highly connected genes were carried out by Cytoscape v3.8.2 software (Shannon *et al*., 2003).

2.5. Quantitative real-time PCR

Quantitative real-time PCR (RT-qPCR) was performed to validate the transcriptomic results on 10 chosen N-metabolism related genes. Total RNA was extracted and purified using TRIzol^{TM} reagent (Qiagen, Milano, Italy) according to the instructions provided by the manufacturer. The Maxima First Stand cDNA Synthesis Kit (Thermo Fisher Scientific Baltics UBA) was used to produce cDNA samples via reverse transcription according to the manufacturer instructions. Primer specificity of candidate genes was verified by melting curve using the mixed cDNA as template, and by 2% agarose gel electrophoresis analysis. The PowerUp SYBR Green master mix (Applied Biosystems by Thermo Fisher Scientific) and the StepOne™ Real-Time PCR System (Applied Biosystems, foster, CA, USA) were employed to perform qPCR with gene specific primers. Three biological and three technical replicates were adopted and the means of the relative gene expression (Ct) were normalized to the reference genes, Actin and Ef1-α (Lovdal and Lillo, 2009). Primers were designed using Primer3 (v0.4.0) and listed in Table S4. Results of the Pearson correlation between RNAseq data and qRT-PCR were plotted in a scatter plot which revealed a good and significant correlation ($r = 0.96$, $P < 0.0001$) (Figure S5).

3. Results

3.1. Transcriptome modulation analysis in responses to short-term N-treatment

3.1.1.RNA-seq analysis

We constructed 60 libraries to study the changes occurring in both shoot and root of RO and UC82 at the transcriptome level in response to short-term LN treatment at 3 different sampling times (0h, 8h and 24h after N-resupply). Up to 268 million clean reads were obtained and mapped to the tomato genome (SL3.0). Two hundred and six million reads were aligned to the reference genome, yielding an overall mapping percentage of 72.14% (Table S5). Finally, 35,845 transcripts were identified after assembly.

A Principal component analysis (PCA), on the whole transcriptome dataset, revealed a clear distinction between shoot and root samples (Figure 25). Thus, the downstream analyses were performed on root and shoot separately.

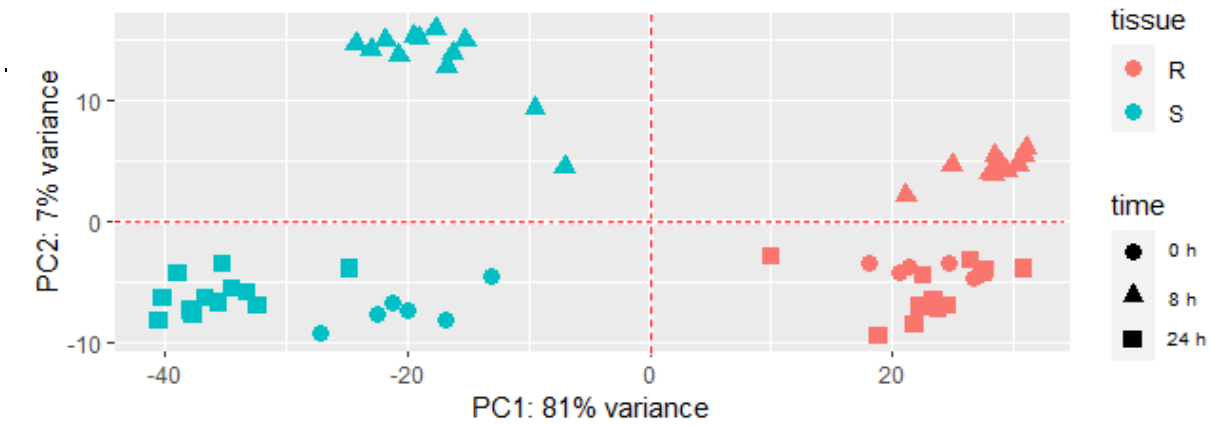

Figure 25. Principal component analysis (PCA) of the whole transcriptome data set.

3.1.2.Modeling of gene expression patterns

We analyzed the global gene expression patterns, at 0h, 8h and 24h after N-resupply, in all the possible combinations of G, N, T factors, using analysis of variance (ANOVA). In detail, the analysis identified the DEGs for each factor and 4812 and 4802 unique genes were differentially expressed among G, G*N, and G*N*T in shoot and root, respectively (P value < 0.05) (Table S6). The whole DEGs expression patterns in both tissues are presented in Figure 26.

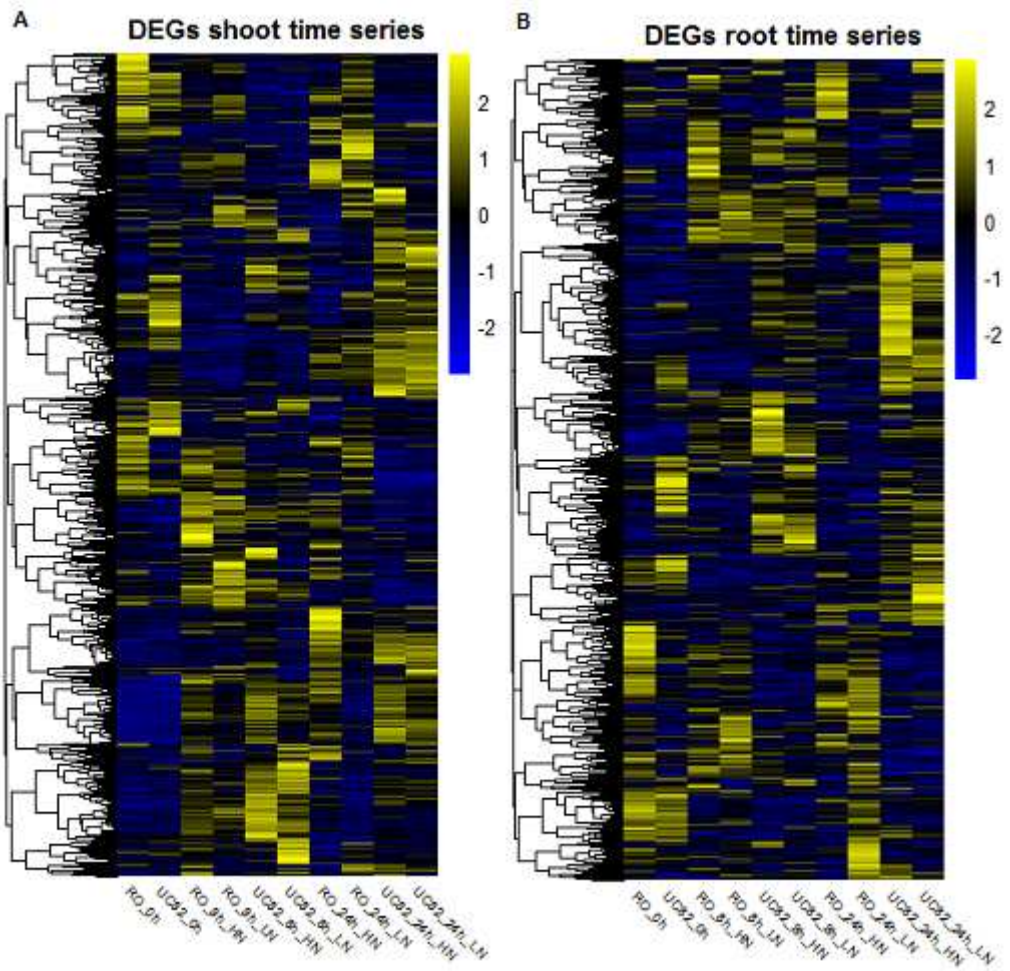

Figure 26. Hierarchical clustering of normalized expression levels of the differentially expressed genes (DEGs) between genotypes, times, N levels and their interactions.

3.1.3.Temporal gene expression patterns analysis and identification of N-responsive DEGs in response to short-term N-resupply

The DEG expression profiles overtime were examined using STEM software and 2041 and 3119 unique DEGs were significantly clustered in shoot and root, respectively (P-value < 0.05) (Table S7). The clustering patterns of all the DEGs were divided into 15 different profiles in both genotypes for each N condition and only the significant enriched temporal expression profiles were presented (Figure 27). The black lines in the profile boxes depict the gene expression patterns overtime (0h, 8h and 24h). The profile number on the top left corner of each profile box was assigned by STEM, the number on the bottom-left represents the adjusted p-value, and that on the bottom-right corner represents the number of genes assigned to the profile.

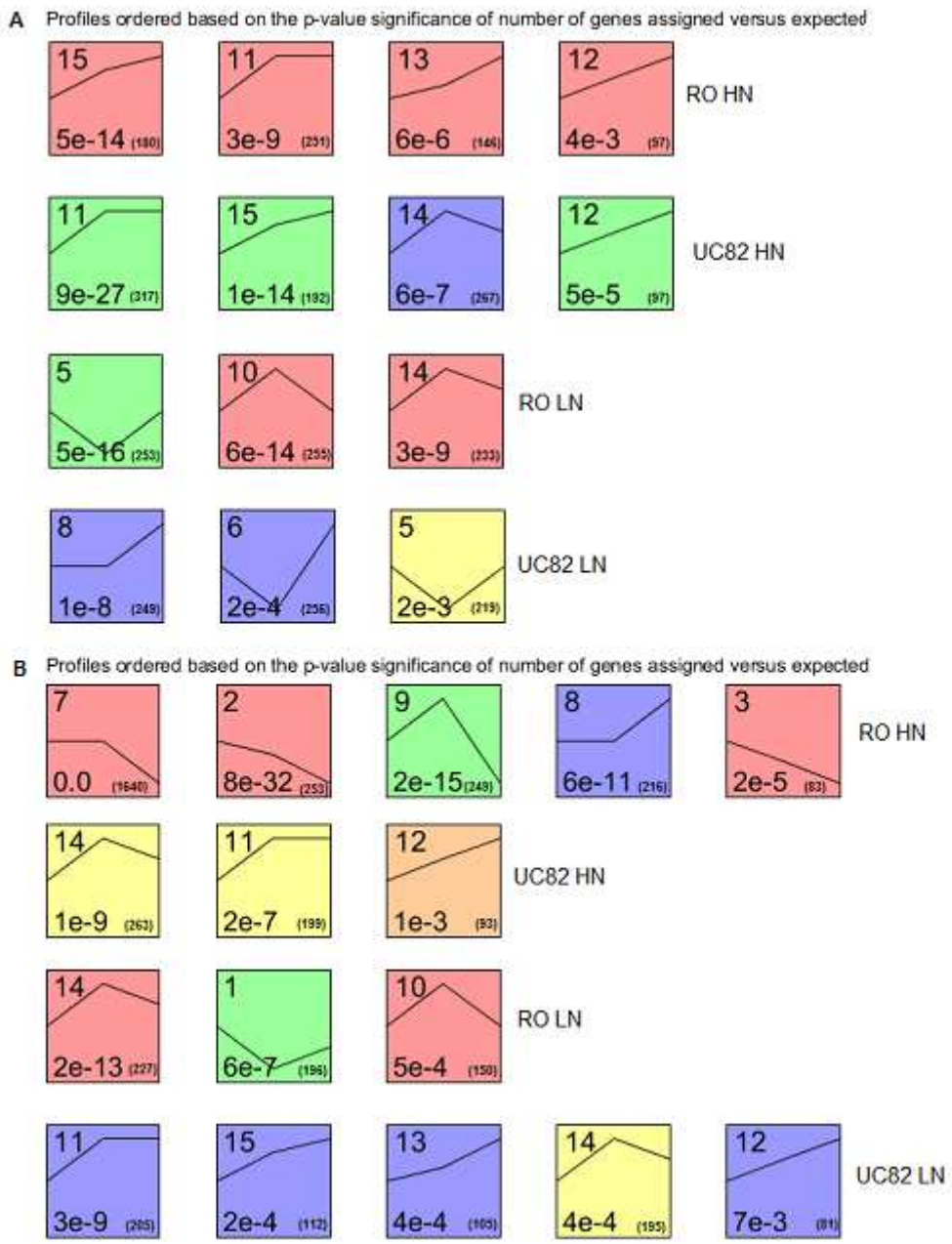

Figure 27. Significant temporal expression profiles of the DEGs identified between genotypes, times, N levels and their interactions in shoot (A) and root (B).

In shoot, in HN condition, DEGs of RO and UC82 were enriched into four significant profiles, including only up-regulated patterns (15, 11, 13, 12 in RO and 11, 15, 14, 12 in UC82). In LN condition, DEGs were enriched into 3 significant profiles for both genotypes including one down-regulated (5) and three up-regulated patterns (10, 14) in RO and one biphasic (6), one up-regulated (8) and one down-regulated (5) pattern in UC82 (Figure 27A).

In the root, in HN condition, DEGs were enriched into 5 and 3 significant profiles in RO and UC82, respectively, including 3 biphasic patterns (7, 9, 8) and two down-regulated patterns (2, 3) in RO, and 3 up-regulated patterns (14, 11, 12) in UC82. In LN condition, DEGs were

enriched into 3 and 5 significant profiles in RO and UC82, respectively, including two up-regulated (14, 10) and one down-regulated (1) patterns in RO, and 5 up-regulated patterns (11, 15, 13, 14, 12) in UC82 (Figure 27B). These results showed that all clustered genes were responsive to early N-treatment and were considered as the most important genes for the downstream analysis.

3.1.4.Differential gene expression analysis

In shoot, 395 DEGs including 275 up-regulated and 120 down-regulated were identified in RO*vs*UC82, while, in root, 482 DEGs, 223 up-regulated and 259 down-regulated, were identified. The DEGs increased overtime (from 0 to 24h) in both N conditions, except for the number of down-regulated genes in shoot (Figure 28). Moreover, after 24h, the number of significantly up- and down-regulated genes in RO*vs*UC82 increased in both tissues under LN treatment compared to HN (in shoot +25% and +17% of up- and down-regulated genes were observed, while in root +8% and +5%). These results indicated that both genotypes after 24h of N resupply were more responsive to LN compared HN, mainly in root (Figure 28).

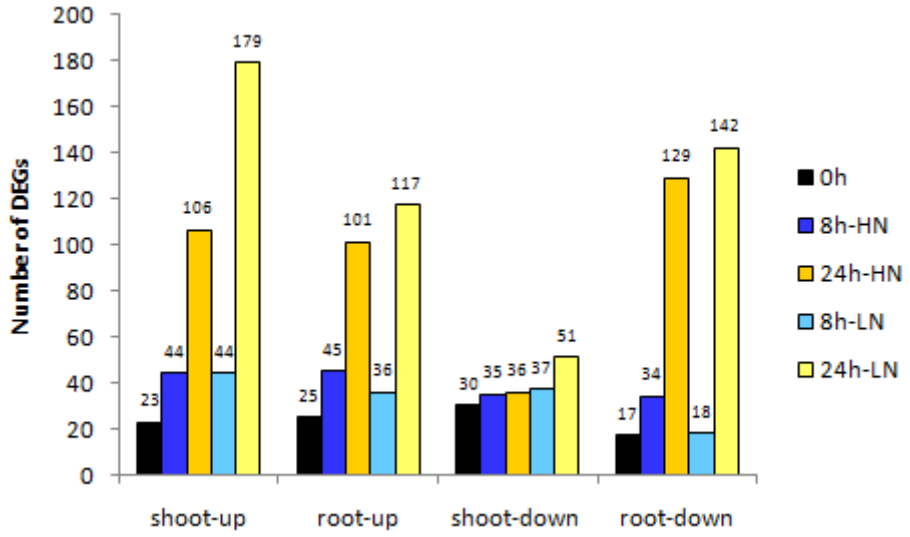

Figure 28. Number of up- and down-regulated genes for the comparison RO*vs*UC82 at different sampling-time and N level.

3.1.5.Gene Ontology (GO) and KEGG Enrichment analysis of N-responsive DEGs

To understand their function, the up- and down-regulated genes at starvation (0h) and after 8 and 24h N resupply in both tissues were functionally classified into biological process (BP), molecular function (MF) and cellular component (CC) (Figure 29, 30).

In BP, most of the up-regulated genes in RO*vs*UC8 were significantly enriched in "oxidation-reduction process", "response to stimulus", "response to stress" and "catabolic process", in both root and shoot at different times (Figure 29, 30). Interestingly, 7.2% of the up-regulated genes in shoot were enriched in "signaling" and "signal transduction" GO terms (Figure 29). The down-regulated genes in root were mainly involved into "response to stimulus", "localization" and "transport", while in shoot, they were associated to "protein metabolic process", "response to stimulus", "proteolysis" and "transmembrane transport" GO terms (Figure 29, 30).

Concerning MF, most of the up-regulated genes in root of RO*vs*UC8 were enriched in "oxidoreductase activity", "cation binding", "metal ion binding" and "cofactor binding" (Figure 29), whereas, in shoot, they were mainly enriched in "hydrolase activity", "catalytic activity acting on a protein" and "oxidoreductase activity" GO terms (Figure 30). The down-regulated genes in root were associated to "hydrolase activity", "transporter activity" and "transmembrane transporter activity" GO terms (Figure 29), while, in shoot, "cation binding", "metal ion binding" and "oxidoreductase activity" were the most enriched GO terms (Figure 30)

In CC, the up-regulated genes in root of RO*vs*UC8 were mainly enriched in the "extracellular region", "cell wall" and "external encapsulating structure" (Figure 29), while no CC GO term enrichment was observed in shoot (Figure 30). Finally, the down-regulated genes in root were enriched into the "cell periphery", "plasma membrane" and "Extracellular region" GO terms (Figure 29), while, in shoot, into the "cell periphery", "Chloroplast" and "plastid" GO terms (Figure 30).

The Kyoto Encyclopedia of Genes and Genomes orthologs (KEGG) analysis did not show any significant KEGG pathway enrichment of the down-regulated genes in both tissues of RO*vs*UC8. By contrast, the up-regulated genes were mainly enriched in the metabolic and MAPK (mitogen-activated protein kinases) signaling pathways as well as in plant hormone signal transduction KEGG pathways in shoot, and in the metabolic pathway, biosynthesis of secondary metabolites and phenylpropanoid biosynthesis KEGG pathways in root (Figure 31).

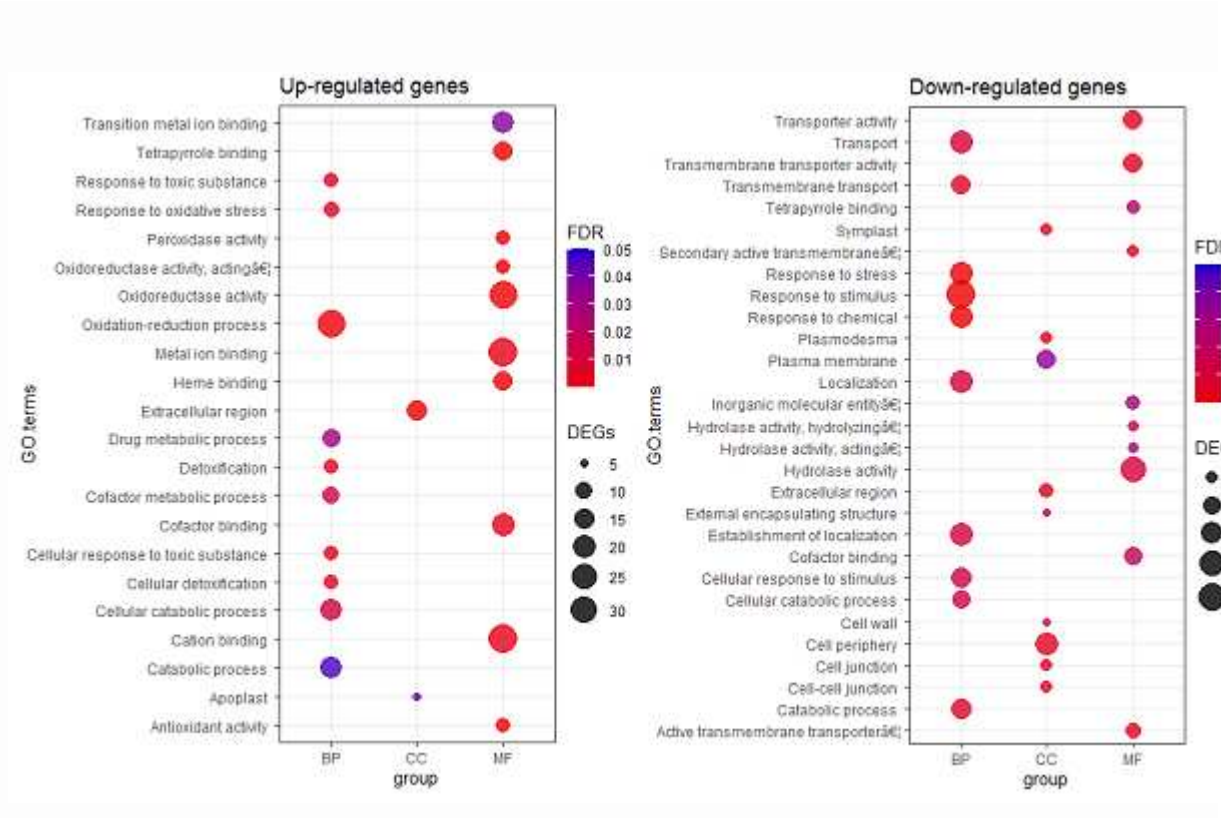

Figure 29.GO term enrichment analysis of the significant DEGs between RO and UC82 in root

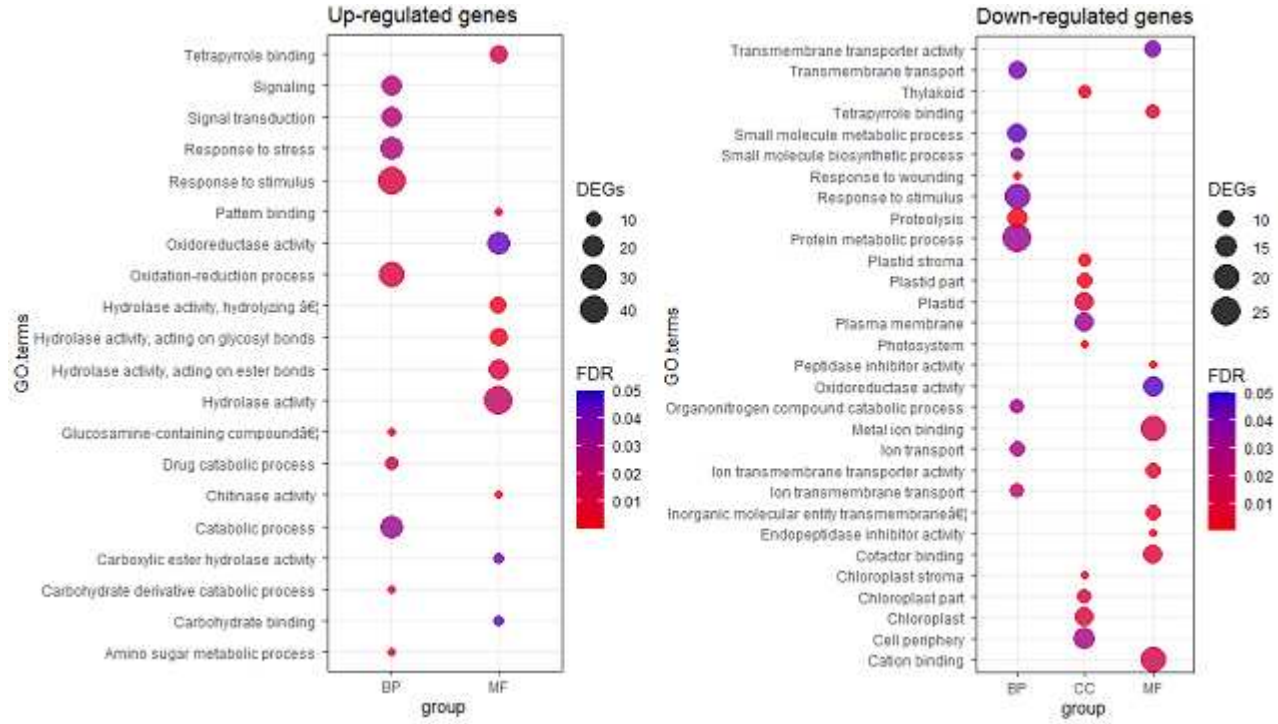

Figure 30.GO term enrichment analysis of the significant DEGs between RO and UC82 in shoot**.**

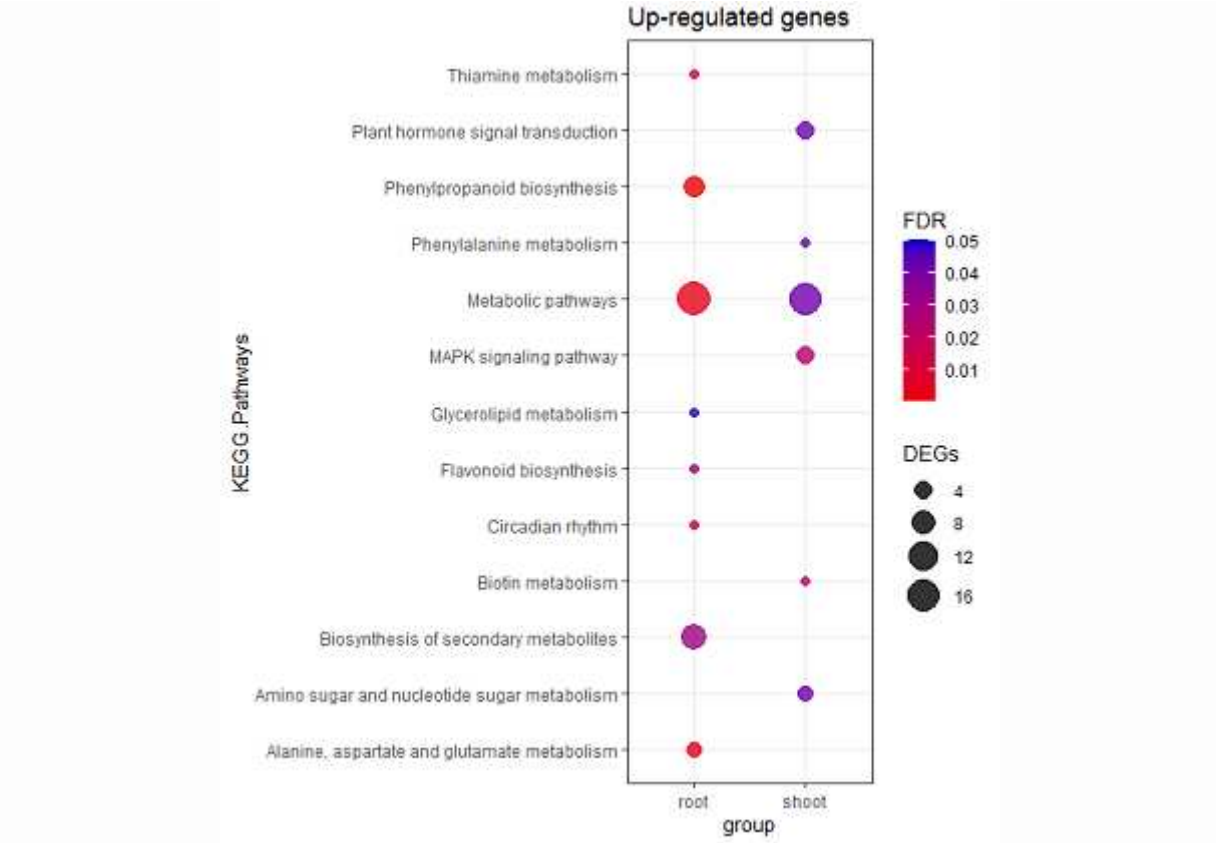

Figure 31. The KEGG pathway enrichment analysis of the up-regulated genes in RO*vs*UC82 in shoot and root.

3.1.6.DEGs involved in Plant Hormone Signal transduction, protein kinases signaling pathway, and N-transport in both shoot and root

3.1.6.1. DEGs involved in Plant Hormone Signal transduction

In our study, many hormones signaling-related transcripts were identified. In shoot, two auxin (auxin-regulated IAA17 and IAA-amido synthetase GH3.6), three ethylene (an ethylene response factor AP2/ERF4, and two ethylene-responsive transcription factor ERF1a and ERF2), an abscisic acid (ABA) signaling (protein STH-2-like), a Cytokinin activating enzyme encoding gene (cytokinin riboside 5'-monophosphate phosphoribohydrolase LOG8) and a Gibberellic Acid signaling (DELLA-GAI transcription factor) related genes were differentially expressed in RO*vs*UC82, after short-term N resupply (Figure 32A). In root, five auxin (an auxin responsive protein SAUR26, an auxin efflux carrier, two auxin response factor ARF, and the IAA-amido synthetase GH3.6), three ethylene-responsive transcription factors (ERF4, ERF1b and ERF2b), an abscisic acid (ABA) signaling (protein STH-2-like), a

jasmonic acid (JAZ3/TIFY6B) and a brassinosteroid (CURL3) related genes were differentially expressed (Figure 32B).

Most of the plant hormone related DEGs exhibited also a spatio-temporal specificity as shown in Figure 32. In shoot, *IAA17*, *GH3.6* and *ERF2* resulted up-regulated in RO*vs*UC8 only at 24h-LN (Figure 32A); in root, *GH3.6*, *ARF22-like* and *ERF1b* were up-regulated, and *SAUR26*, *ARF3*, *ERF4* and *STH-2-like* were down-regulated in the N-use efficient genotype (RO) at 24h-LN (Figure 32B).

3.1.6.2. DEGs involved in Protein kinase signaling pathways

The protein kinases (PKs) act as signal transducers or receptor proteins playing a crucial role in protein phosphorylation. In our study, many PK genes were found differentially expressed, in both tissues, between genotypes after the short-term LN-resupply, especially after 24h. In shoot, twenty-two PKs DEGs were identified including four receptor-like protein kinases (RLKs), four serine/threonine protein kinases (STPKs), four protein kinases family protein, three mitogen activated protein kinase kinase kinase (MAPKKKs), two CBL-interacting protein kinases (CIPK), two receptor-like protein kinases (RPKs), as well as a SNF1-related protein kinase, a protein NSP-interacting kinase 3-like and a CDPK (Figure 32A). Among the PKs, identified in shoot, *CIPK2* and *MAPK72* as well as a CDPK and a PK superfamily protein resulted up- and down-regulated in the N-use efficient genotype, respectively, at 8h, while two RLKs (of which 1 LRR-RLK), a RPK, a CIPK, two STPK, and a SNF1-related protein kinase appeared up-regulated in RO after 24h LN resupply (Figure 32A).

In root, fifteen (15) PKs were identified among which three STPKs, three MAPKs, three RPKs, three receptor-like kinase (LRR-RLK), as well as a histidine kinase (HK4), a calcium-dependent protein kinase (CDPK) and a protein kinase domain (Figure 32B). In root, the RO*vs*UC8 comparison highlighted a *MAPK14* and a *LRR-RLK* up-regulation as well as a *HK4*, *MKS1* and cysteine-rich RPK42 down-regulation, after 24h. Only an LRR-RLK gene appeared down-regulated at both 8h and 24h LN-resupply (Figure 32B).

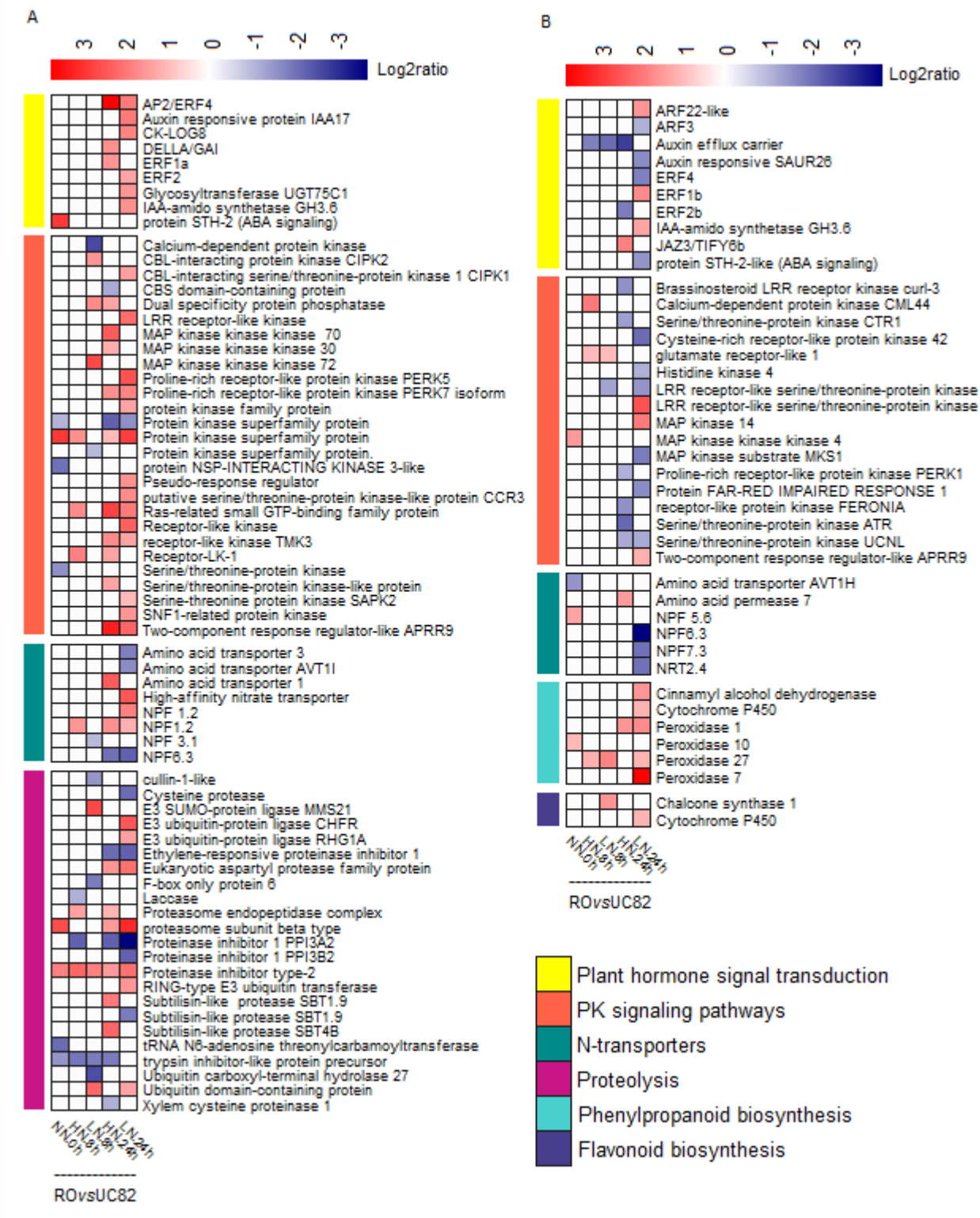

Figure 32. Heatmap of the main DEGs functional classes based on GO term and KEGG pathways enrichment analyses in root and shoot. (A) Heatmap of DEGs involved in Signal transduction and protein kinases signaling pathways, N-transport and proteolysis in shoot. (B) Heatmap of DEGs involved in Signal transduction and protein kinase signaling pathways, N-transport and phenylpropanoid and flavonoid biosynthesis in root. The color key indicates higher (red) or lower (navy) expression in RO*vs*UC82 at each sampling time and N level.

3.1.6.3. Differentially expressed N-transport related genes

In the early response to N resupply, eight and six N-transporters were found differentially expressed between genotypes in shoot and root, respectively (Figure 32). In shoot, three amino acid transporters (AATs), four nitrate/peptide transporters (two *NPF1.2*, *NPF3.1* and *NPF6.3*) and a high-affinity nitrate transporter were identified among the DEGs; while in root, an AAT (*AVT1H*), an amino acid permease, three nitrate/peptide transporters (*NPF5.6*, *NPF6.3*, and *NPF7.3*) and a high affinity nitrate transporter *NRT2.4* were detected. All the DEGs exhibited a spatio-temporal expression patterns, except *NPF6.3*, which was down-regulated in RO regardless the tissue and N-treatment after 24h, and *NPF1.2* that appeared up-regulated in RO shoot regardless of time and N-treatment (Figure 32A,B). Besides, a high-affinity nitrate transporter and *NPF1.2* were up-regulated in RO shoot compared to UC82 after 24h LN-resupply, while *NPF3.1*, *AAT3* and *AAT-AVT1I* were down-regulated in the N-use efficient genotype only at 8h and 24h in LN, respectively (Figure 32A). In root, *NRT2.4*, *NPF6.3* and *NPF7.3* were down-regulated in RO only at 24h-LN (Figure 32B).

3.1.7.Expression patterns of DEGs involved in proteolysis in shoot

In response to NO_3^- treatments, many DEGs identified in shoot were enriched in proteolysis, proteins degradation process, which regulates the availability of organic N for remobilization and allocation to N-demanding tissues. The ubiquitin-proteasome pathway is critical for plant protein degradation and mainly composed of ubiquitin-activating enzymes E1, ubiquitin-binding enzyme E2, ubiquitin-protein ligase E3, and 26S proteasome. In our results, genes encoding proteasome and E3 ubiquitin-protein ligase were more expressed in RO compared to UC82. In particular, the proteasome subunit beta type transcripts were more abundant in RO shoot after 24h LN resupply compared to the control (HN). In detail, an E3 SUMO-protein ligase *MMS21* as well as two E3 ubiquitin-protein ligases (*CHFR* and *RHG1A*) encoding genes were up-regulated after 8 and 24h LN resupply, respectively, and an E3 ubiquitin transferase transcripts were more abundant in RO compared to UC82 at 24h LN (Figure 32A). Moreover, since most plant proteases assume regulatory roles, their activity is strictly controlled by the presence of protease/proteinase inhibitors, which limits the proteolysis process. In our study, many protease/proteinase inhibitors related genes were down-regulated in RO shoot compared to UC82, among which an ethylene-responsive proteinase inhibitor, a proteinase inhibitor 1 *PPI3A2*, and a proteinase inhibitor 1 *PPI3B2*, which was down-

regulated only at 24h LN-resupply (Figure 32A). Overall, the variation in protease and protease inhibitor related gene expressions support the differences in organic N remobilization intensity between tomato genotypes (Figure 32A).

3.1.8. Expression patterns of DEGs involved in phenylpropanoids and flavonoids biosynthesis in root

Under abiotic stress, many plants increase the phenolic acids and flavonoids biosynthesis activting the phenylpropanoid biosynthesis pathway as an adaptive plant response to enhance stress tolerance. In our transcriptome data, the phenylpropanoid and flavonoid pathways enrichment was observed at LN condition. All the genes involved in these pathways were up-regulated in RO root compared to UC82, including a chalcon synthase (CHS1) (up-regulated in RO only after 8h form LN resupply), a cinnamyl alcohol dehydrogenase (CAD) and a cytochrome P450 (up-regulated in RO only after 24h LN) and 4 peroxydases, among which the peroxydase 7 was up-regulated in RO only after 24h LN (Figure 32B).

3.1.9. Differentially expressed transcription factors in response to early N-treatments

Our data revealed thirty-seven differentially expressed TFs between genotypes at the different times, in both shoot and root (Figure 33). Fourteen TFs encoding genes were found more expressed in RO shoot compared to UC82, including an ethylene response factor (*AP2/ERF4*), two basic helix-loop-helix (*bHLH*), a calmodulin-binding transcription activator (*CAMTA4*), a Gibberellic Acid Insensitive (*DELLA/GAI*), two ethylene responsive transcription factors (*ERF*), a Golden2-like 2 (*GLK2*), two MYBs and four zinc finger proteins (*ZF*).

In root, twenty-three differentially expressed TFs were identified: two auxin response factor (*ARF*), a *CAMTA4*, three *ERF*, a protein far-red impaired response 1 (*FAR1*), a GAGA-binding transcriptional activator (*GAF*), a Heat stress transcription factor A-5 *(HSF A-5*), a lateral organ boundaries (*LOB/LBD37*), a MADS-box transcription factor, two MYB, three nuclear factors Y (*NFYA6*, *B5* and *B10*), a protein indeterminate-domain (*IDD9*), a Teosinte branched1/Cincinnata/Proliferating cell factor (*TCP*), a TGACG motif-binding protein (*TGA*) and four ZF proteins (Figure 33). All the differentially expressed TFs were tissue-specific; by contrast, *CAMTA4* appeared down-regulated in both tissues regardless of time and N-condition. Moreover, 50% and 56.5% of TFs were differentially expressed only in LN

conditions in shoot and root, respectively. In detail, *MYB61* and *MYB-S3* were differentially expressed in shoot only after 8h LN-resupply, while *bHLH93-like*, *ERF2*, GLK2, *ZF-Constans-9-like* and *ZF-STOP1* were up-regulated in RO only after 24h from LN resupply. In root, all the LN-responsive TFs exhibited a differential expression between RO and UC82 only after 24h LN resupply (Figure 33).

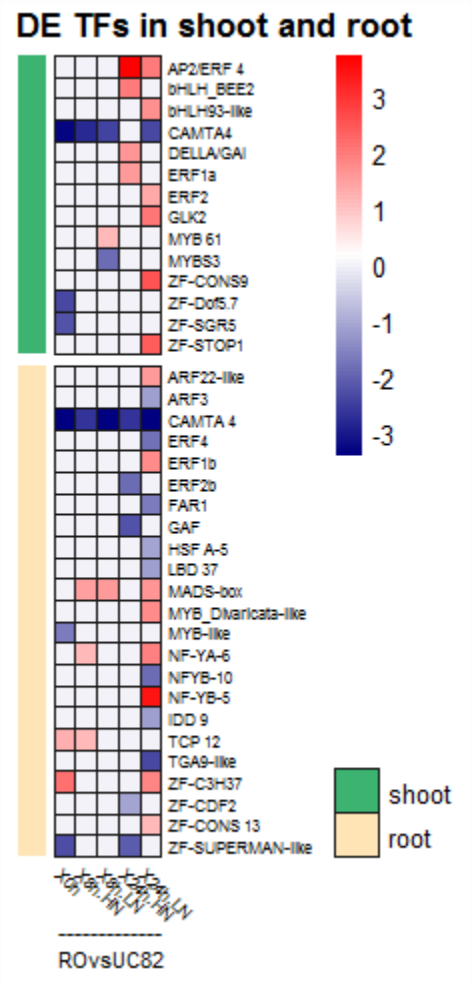

Figure 33. Heatmap of the differentially expressed TFs in shoot and root of RO and UC82 after 0h, 8h and 24h of N resupply.

3.3. Weighted Gene Co-expression network analysis

To identify co-expression modules and hub genes of tissue-specific transcriptional regulation networks associated to short-term LN supply, we conducted a weighted gene co-expression network analysis (WGCNA) including the 395 and 477 N-responsive DEGs identified in RO*vs*UC82 comparison in shoot and root, respectively. Our results revealed six co-expressed modules in both shoot and root including from 38 to 105 genes and from 30 to 159 genes, respectively (Figure 34B, C and 35B, C).

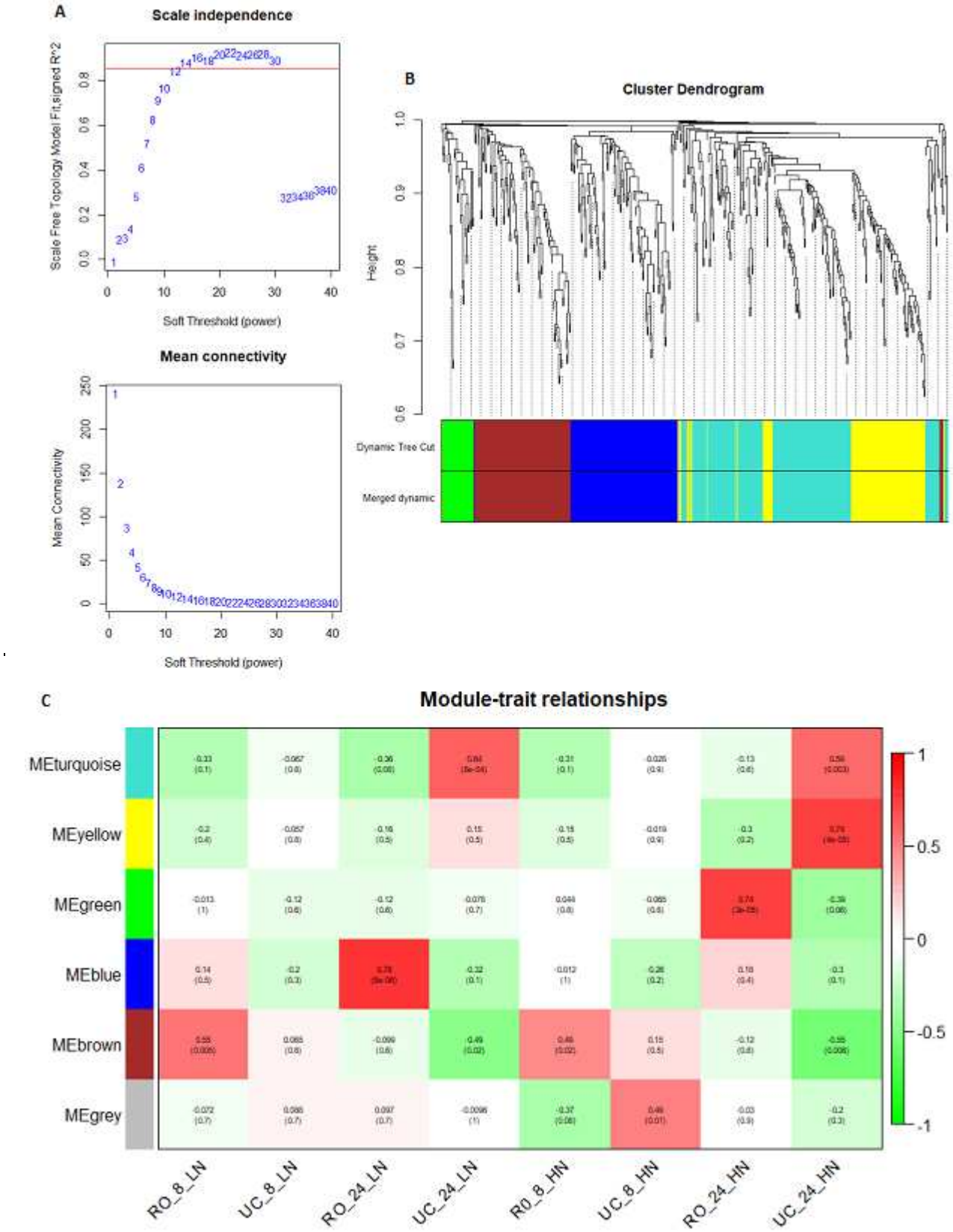

Figure 34. Scale independence and Mean Connectivity (A), Cluster dendrogram (B) and Module-trait relationship (C) of the 395 DEGs in tomato root exposed to low and high NO_3^- for 0, 8 or 24h (see Materials and Methods).

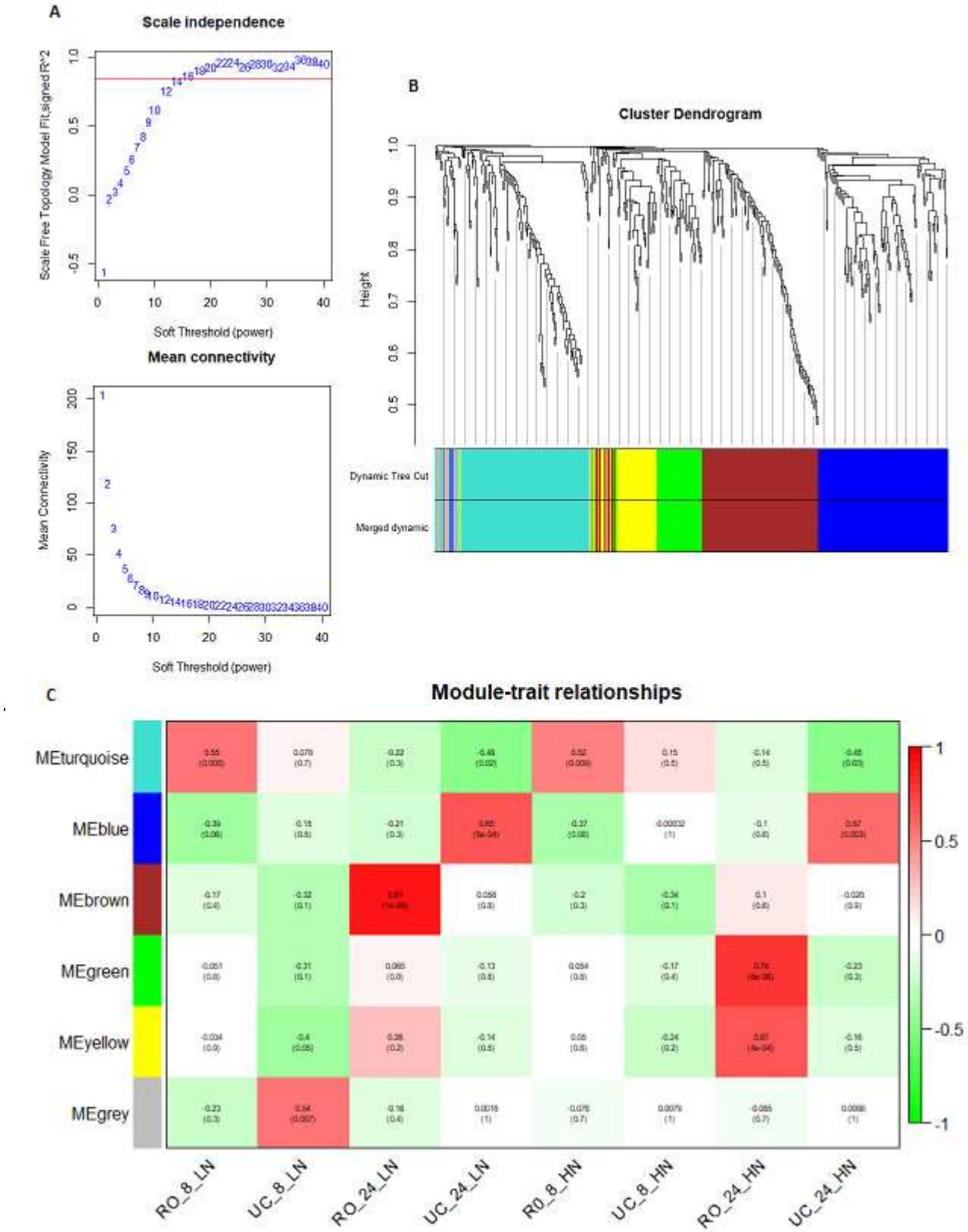

Figure 35.Scale independence and Mean Connectivity (A), Cluster dendrogram (B) and Module-trait relationship (C) of the 395 DEGs in tomato shoot exposed to low and high NO_3^- for 0, 8 or 24h (see Materials and Methods).

The analysis of the interaction between the co-expression and the sample treatments modules showed the expression levels of eigengenes (idealized representative genes) within each module for both shoot and root (Figures 34C and 35C). The results indicated that the brown module (ME= 0.91, P=1 × 10^{-9}) was the unique in shoot, exhibiting a significant correlation with LN treatment in the efficient genotype RO after 24h (Figure 34C), whereas in root the blue module (ME= 0.76, P= 6 × 10^{-6}) was significantly correlated to LN treatment in RO after 24h (Figure 35C). These results suggest that the DEGs belonging to these modules may play significant roles in the early response to LN-resupply in the efficient genotype compared to the inefficient ones.

3.3.1. LN-responsive modules analysis and identification of hub genes in shoot of the efficient genotypes

The identification of the LN-responsive modules were based on the ME absolute value > 0.75, while the hub genes, for each module, were selected using two scores: the Module Membership (MM) value, which emphasizes genes of importance to the module definition, and the Gene Trait Significance (GS), which pinpoints genes for which expression profiles are correlated with treatment sample.

3.3.1.1. Functional analysis of the brown module in shoot

The brown module, the unique highly correlated to LN treatment in shoot (ME= 0.91), grouped 98 genes induced only in RO. The GO term analysis of the eigengenes in this module showed a significant enrichment in Chlorophyll binding, Transferase activity and Anion binding molecular functions (Table S8). Here, 22 Hub genes related to RO-LN-24h were selected to meet the absolute value of the geneModuleMembership > 0.80 and geneTraitSignificance for RO-LN-24h > 0.80 (Figure 36A). The functional analysis of the hub genes revealed a significant enrichment in many BP GO terms such as Vegetative phase change, Carbohydrate mediated signaling, Response to nutrient and Cytokinin biosynthetic process. They were also significantly involved in Steroid, Zeatin, and secondary metabolites biosynthesis, and in Carbon fixation in photosynthetic organisms KEGG pathways (Table S9). Furthermore, the brown module regulatory network analysis revealed the 10 most connected genes (Figure 36B), among which an asparagine synthetase (*ASNS*, Solyc01g079880.3), a CBL-interacting serine/threonine-protein kinase 1 (*CIPK1*, Solyc05g053210.3), a Cytokinin riboside 5'-monophosphate phosphoribohydrolase (*LOG8*, Solyc06g075090.3), a Glycosyltransferase (*UGT73C4*, Solyc10g085870.1), a Sulfate

transporter 3.1 (*SULTR3.1*, Solyc09g082550.3), an Alternative oxidase 1 (*AOX1*, Solyc08g075540.3) and an Ethylen-responsive transcription factor 2 (*ERF2*, Solyc01g090340.2) (Figure 36B).

3.3.1.2. Functional analysis of the blue module in root

The blue module was the unique highly correlated to LN treatment in root (ME= 0.76), grouping 102 genes induced only in RO in response to 24h LN resupply. The functional analysis of these genes revealed any significant GO term or KEGG pathways enrichment. Filtering for geneModuleMembership > 0.75 and geneTraitSpecificity > 0.60, 16 hub genes were identified (Figure 37A). Even, these hub genes did not show any significant GO term or KEGG pathways enrichment. The blue module regulatory network analysis revealed the 10 most connected genes (Figure 37B), among them a Late embryogenesis abundant hydroxyproline-rich glycoprotein family (*LEA*, Solyc01g006320.3), a LRR receptor-like serine/threonine-protein kinase (*FEI1*, Solyc01g109650.3), a Nuclear transcription Factor YB5 (*NF-YB5*, Solyc01g067130.3), a Style cell-cycle inhibitor 1 (*SCI1*, Solyc05g008750.3) and an Annexin 5 (*AnnSl5*, Solyc01g097520.3) were identified (Figure 15B).

Finally, the expression patterns of the key genes identified for early LN response in RO, in brown and blue modules in shoot and root, respectively, are graphically presented in the heatmap (Figure 38).

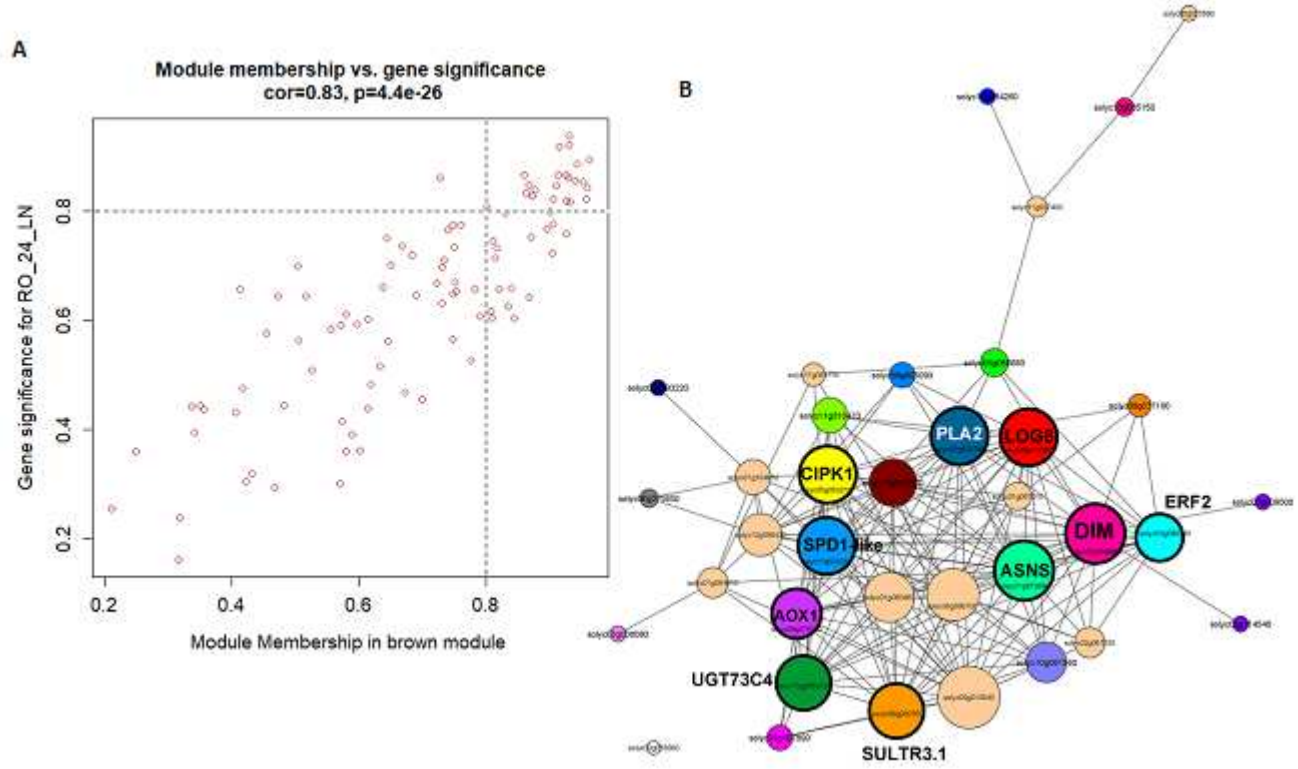

Figure 36. Module membership (MM) *vs*.gene significance (GS) for RO_24h_LN of the brown module in shoot (A), Network analysis of the selected genes by MM and GS (B).

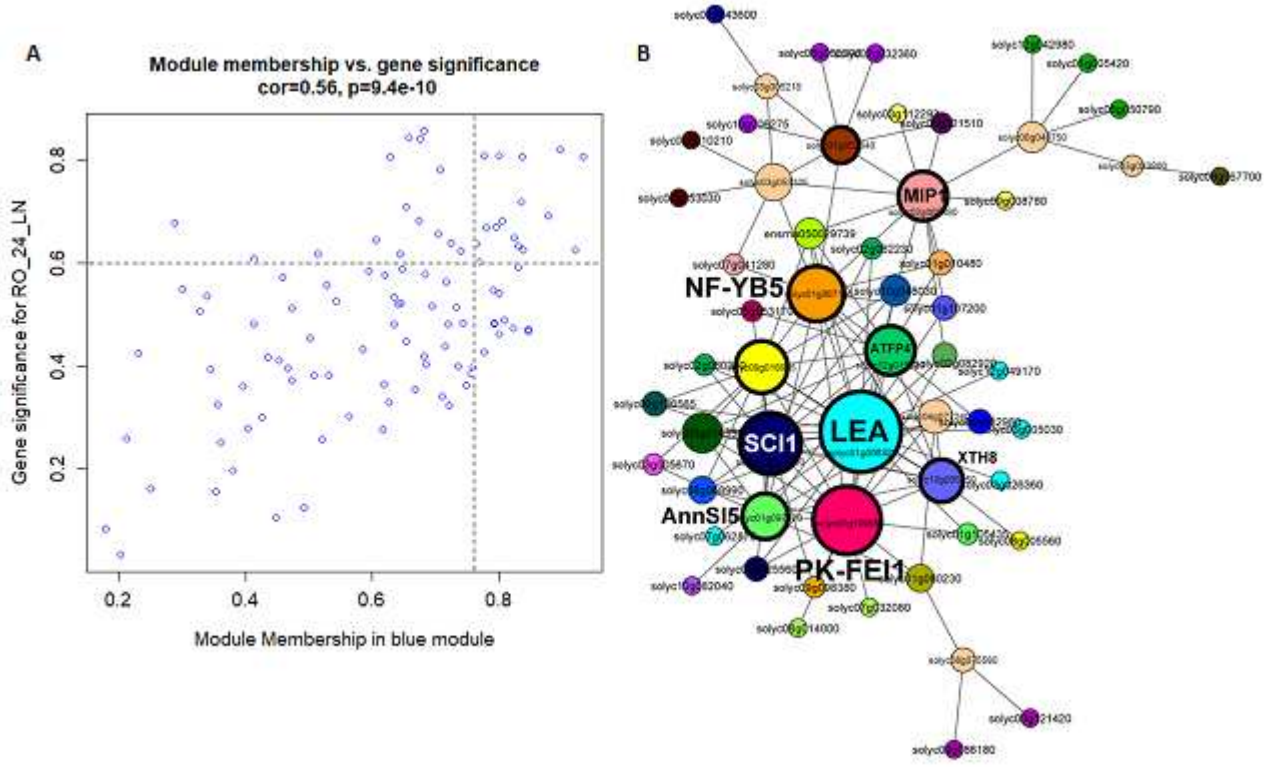

Figure 37. Module membership (MM) *vs*. gene significance (GS) for RO_24h_LN of the blue module in root (A), Network analysis of the selected genes by MM and GS (B).

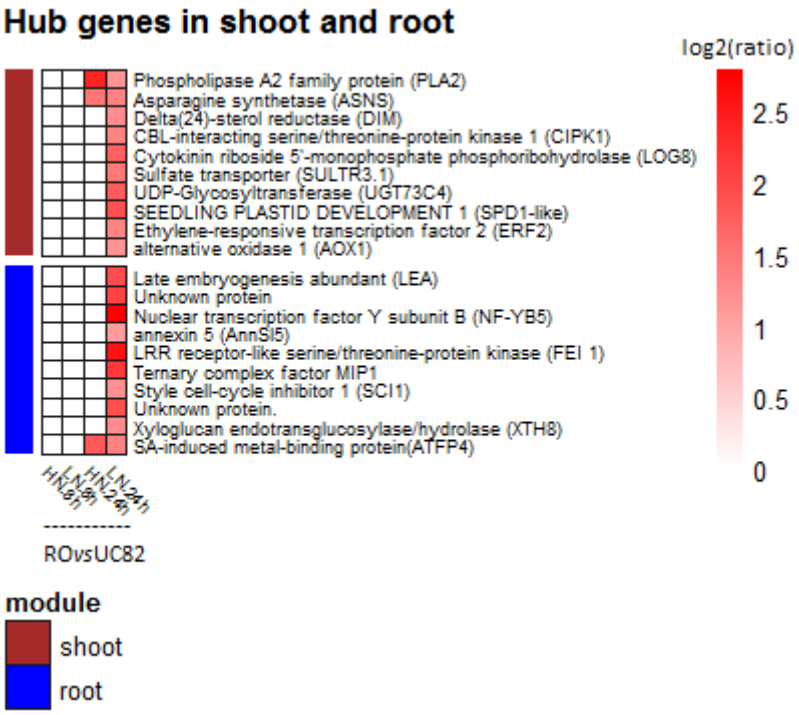

Figure 38. Heatmap of the expression level of the *hub* genes in shoot (brown module) and root (blue module) identified by Weighted Gene Co-expression Network Analysis (WGCNA).

4. Discussion

Improving crops nitrogen use efficiency (NUE) has become a significant challenge for a sustainable agriculture. To achieve this goal, a deep understanding of plant molecular responses to variable N conditions is crucial. Therefore, comparing the performances in response to N availability between high and low N-use efficient genotypes can effectively allow the dissection of the NUE complex regulatory networks. RNA-seq analysis has become the widely used approach to study the transcriptomic changes regulating crop responses to N availability as well as to identify key genes related to the N-stress tolerance between NUE-contrasting genotypes (Sinha *et al*., 2018; Goel *et al*., 2018; Subudhi *et al*., 2020; Sultana *et al*., 2020; Mauceri *et al*., 2021). In tomato, few transcriptomic analyses, using microarray or RNA-seq, have been applied to identify genes differentially regulated by NO_3^- (Wang *et al*., 2001; Renau-Morata *et al*., 2021), while a comparative transcriptome profiling between two NUE contrasting genotypes in response to LN supply have not been reported so far.

In this study, the early molecular response to low N (LN) was hypothesized to be crucial for determining the contrasting LN tolerance and NUE between the two tomato genotypes RO (NUE efficient) and UC82 (NUE inefficient) (Abenavoli *et al*., 2016, Aci *et al*., 2021). N-starved tomato plants exposed to LN and HN were monitored for transcriptomic changes, at starvation as well as after 8 and 24h of N resupply, in both shoot and root. An ANOVA multivariate model was adopted to identify the DEGs between N conditions and genotypes overtime. The analysis yielded more than two and three thousand N-responsive genes in both tissues, among which 398 and 477, in shoot and root, respectively, resulted differentially expressed between genotypes. Thus, tomato root transcriptome appeared more affected by NO_3^- resupply compared to shoot, confirming the already reported central role of roots in NUE (Sinha *et al*., 2018; Sun *et al*., 2020; Tiwari *et al*., 2020).

4.1. LN resupply triggers a spatio-temporal differential gene expression between the two NUE contrasting genotypes

The detailed analysis of the N-responsive DEGs expression patterns in the RO*vs*UC82 comparison, in both tissues, showed significant differences between LN and HN treatments overtime (0h, 8h and 24h), which were more marked after 24h LN-resupply. Our results suggested that the distinct transcriptional profiles between genotypes in an early response to LN treatment might govern NUE performances in tomato. Based on the GO and KEGG pathways enrichment analysis, tissue specific processes and pathways involving genes up-

regulated by LN treatment in RO*vs*UC82 were identified. In particular, “Plant hormone signal transduction” and “protein kinase signaling” as well as “phenylpropanoid and flavonoid biosynthesis” KEGG pathways were significantly enriched in shoot and root, respectively. Considering their important role in the early response to LN, we focused our analysis on the genes involved in these pathways.

4.1.1. Plant hormone signal transduction mediated LN signaling response

Phytohormones are key molecules in plant development and response to diverse environmental stimuli. Several studies demonstrated that NO_3^- availability regulates biosynthesis, degradation, transport, and signaling of phytohormones, which in turn play a critical role during the plant adaptation to low N (Kiba *et al.*, 2011; Krapp *et al.*, 2011; Sakakibara, 2006; Ristova *et al.*, 2016). For example, the auxin transport and signaling are critical for the root architecture modulation in response to N availability (Vanstraelen *et al.*, 2012). This relationship between NO_3^- availability and auxin metabolism has been reported in *Arabidopsis*, maize and rice (Krouk *et al.*, 2010; Wang *et al*, 2019). In our experiment, among the DEGs involved in plant hormone signal transduction, two and five auxin-related encoding genes were identified in shoot and root, respectively. Among them, an IAA amido-synthetase *GH3.6*, which regulates auxin excess in plant (Nakazawa *et al.*, 2001; Staswick *et al.*, 2005), was up-regulated in both shoot and root of RO*vs*UC82 only after 24h LN, indicating a synergic regulation of shoot and root auxin contents in the N-use efficient genotype during the response to LN. In addition, the expression of two auxin response factors encoding genes (*SAUR26, ARF3*) was significantly down-regulated in RO*vs*UC82 in root after 24h under N-stress.

Cytokinins are critical signaling molecules indicating N status in plants (Sakakibara, 2003; Sakakibara, 2006). Besides their fundamental role in root-shoot-root signaling (Narcy *et al.*, 2013; Naulin *et al.*, 2020), cytokinins are reported to repress the high-affinity NO_3^- transporter genes (Ruffel *et al.*, 2011), as well as to induce N-metabolism related genes such as nitrate reductase (*NR*) (Gaudinova, 1990). In our study, a putative tomato cytokinin riboside 5'-monophosphate phosphoribohydrolase *LOG8* transcripts, the main enzyme converting inactive cytokinin nucleotides to the biologically active free-base form (Kuroha *et al.*, 2009), was more abundant in RO*vs*UC82 in shoot after 24h LN resupply, confirming a potential cross-talk between NO_3^- and cytokinin signaling in tomato.

Ethylene responsive transcription factors (ERFs) are involved in ethylene signaling pathways and regulate many stress-related gene expressions controlling plant growth and development (Kazan, 2015; Xiao *et al*., 2016). Many ERFs encoding genes (*AP2/ERF4* and *ERF2* in shoot as well as *ERF1b* in root) resulted up-regulated in RO*vs*UC82 after 24h LN. The role of ethylene in the regulation of *Arabidopsis* root hair elongation when exposed to low NH_4^+ supply was recently revealed (Zhu *et al*., 2016). In response to low NO_3^-, *ERFs* were differentially expressed in rice and spinach in response to LN (Xie *et al.*, 2019; Sun *et al*., 2020; Joshi *et al*., 2020), and comparative transcriptomics on barley and rice genotypes with contrasting responses to N-stress revealed differentially expressed *ERFs* in response to LN (Quan *et al*., 2016; Subudhi *et al*., 2020).

4.1.2. Signal transduction-related protein kinases differentially expressed between RO and UC82 in response to early LN-stress

Protein Kinases (PKs) play important roles in the development and differentiation of eukaryotic cells, helping the organisms to cope with environmental stresses by regulating transcription through TFs activation (Hunter and Karin, 1992).

Mitogen activated PKs (MAPKs), MAPKKs and MAPKKKs are involved in plant stress resistance signal transduction, NO_3^-sensing and metabolism in several plants (Hu *et al*., 2009; Hao *et al*., 2011). In this respect, nitrate reductase (NR2) is phosphorylated by MPK7 and important regulatory proteins involved in NO_3^-signaling such as LOB domain binding proteins (LDB37 and LDB39) are targeted by many MAPKs (Chardin *et al*., 2017). Furthermore, five *MAPKKK* genes have been identified as direct targets of NLP7 (NIN Like Protein 7) TF, a master regulator of early NO_3^- signaling in root (Marchive *et al*., 2013; Chardin *et al*., 2017). In response to LN, we identified in our data set three *MAKKKs* significantly upregulated in the RO*vs*UC82 shoot, among which *MAPKKK72* only after 8h LN. In the RO*vs*UC82 root, a *MAPK14* and a MPK substrate (*MKS1*) resulted up- and down-regulated, respectively, after 24h LN.

Many genes encoding different subfamilies of receptor-like kinase (RLKs) are regulated by NO_3^-, but their responses were found highly variable in different transcriptome datasets, suggesting a specialized RLKs role based on cell types, organs, developmental stages, and growth conditions (Liu *et al*., 2020). The leucine-rich repeat receptor-like kinases (LRR-RLKs) are the largest RLKs family genes, with more than 200 members identified in

Arabidopsis (Shiu and Bleecker, 2001; Dievart and Clark, 2004). In our transcriptome data, many *LRR-RLKs* were differentially expressed between genotypes in both tissues after 8h or 24h at LN only. Several well-characterized LRR-RLKs were involved in plant developmental processes such as the meristem size regulation, organ growth, inflorescence architecture, stomatal cell as well as the vascular differentiation (Clay and Nelson, 2002; Masle *et al*., 2005; Shpak *et al*., 2005). Therefore, we hypothesize that *LRR-RLK*s might be decisive for tomato adaptation to low-N.

4.1.2.1. Calcium signaling pathways-related proteins kinase

The cross-link between calcium and NO_3^- signaling and uptake regulations, that requires Ca^{2+} dependent PKs (CDPKs) and calcineurin N-like protein/ CBL-interaction PKs (CBL/CIPKs), has been well documented (Sakakibara, 2003; Hu *et al*., 2008). In our transcriptome dataset, a *CDPK* and two CIPKs (*CIPK1* and *CIPK2*) were upregulated in the RO*vs*UC82 shoot after 8 and 24h LN resupply. The CDPK family seems to take part in the downstream signaling mediated by Ca^{2+} (Harmon *et al*., 2000; Boudsocq and Sheen, 2013), while the CBL–CIPK complexes regulates the homeostasis of intracellular macro and microelements in stressed plants (Zhu, 2003; Luan, 2009; Mao *et al*., 2016; Bender *et al*., 2018). Interestingly, recent studies revealed that NO_3^- resupply stimulated a rapid CIPK2 phosphorylation, highlighting the significance of NO_3^--activated calcium-sensor protein kinases (CPKs), and the NO_3^-–CPK–NLP regulatory network (Linn *et al*., 2017; Liu *et al*., 2017; Liu *et al*., 2020).

4.1.3. Transcription factors differential expression between genotypes induced by LN-stress

Five to seven percent of coding sequences within a plant genome are TFs, important regulators of plant signal transduction pathways under nutritional stress (Canales *et al*., 2014, Hoang *et al*., 2017). Transcriptional regulation plays a pivotal role in the activation/suppression of gene expression, largely controlled by promoters and their contributing cis-acting regulatory elements (CREs), which are specific binding sites for proteins involved in the initiation and regulation of transcription such as the TFs (Hernandez-Garcia and Finer, 2014). Among them, many TF families such as MYB, bHLH, bZIP, DOF, ERF, FAR1, G2-like, NF-YA, NF-YB and LOB have been reported to be involved in plant response to N deficiency (Castaings *et al*., 2008; Hao *et al*., 2011; Goel *et al*., 2018; Subudhi *et al*., 2020). In our transcriptomic analysis, TFs belonging bHLH and G2-like families

resulted upregulated in the RO*vs*UC82 shoot in response to LN resupply after 24h. Interestingly, the TF GLK2 directly activates many downstream target genes encoding chloroplast-localized or photosynthesis-related proteins, including those required for chlorophyll (Chl) biosynthesis, light harvesting, and electron transport (Waters *et al*., 2009; Wang *et al*., 2013). In addition, *GLK2* is reported to regulate chloroplast development in many plants, promoting photosynthesis in previously non-green cells (Powell *et al*., 2012; Wang *et al*., 2013; Nguyen *et al*., 2014; Kobayashi *et al*., 2013). More recently, the *GLK2* over-expression increased photosynthetic capacity determining higher biomass and grain yield in rice (Li *et al*., 2020). This correlation suggested that the *GLK2* upregulation in RO shoot could be involved in the higher biomass production observed in RO under N limiting supply (Aci *et al.*, 2021), determining its higher N-use efficiency compared to UC82.

In addition, many LN-responsive TFs were found differentially expressed only in RO*vs*UC82 root such as *ARF, FAR1, HSF*, *LOB/LBD* and *NF-YA* and *NF-YB*. Lateral Organ Boundaries Domain TFs (*LBD/LOB37/38/39*) were reported to be up-regulated by NO_3^- and to lesser extent by NH_4^+ and glutamine supplies, but also directly involved in the down-regulation of *NIA1*, *NIA2* and other NO_3^--inducible genes (Rubin *et al*., 2009; Medici and Krouk, 2014). In our RNAseq analysis, *LOB37* transcripts were less abundant in RO root respect to UC82 after 24h LN resupply, suggesting a lower repression of NO_3^- assimilation-related genes in the N-use efficient genotype compared to the inefficient one. Forthermore, the nuclear transcription factors *NF-YA* and *NF-YB* are involved in many plant processes playing a role in N nutrition (A2, A3 and A5) (Zhao *et al*., 2011; Leyva-González *et al*., 2012), as well as in the primary root growth (A2, A10 and B2) (Ballif *et al*., 2011; Sorin *et al*., 2014). Noteworthy, three members of this TF family (*NF-YA6, B5 and B10*) were found upregulated in RO*vs*UC82 after 24h LN resupply.

4.1.4. LN-stress induces the phenylpropanoids and flavonoid biosynthesis in the N-use efficient genotype

LN stressed plants show a significant reduction in the photosynthetic capacity becoming more susceptible to oxidative stress due to the accumulation of reactive-oxygen species (ROS) under light excess (Diaz *et al*., 2006). The induction of phenylpropanoid biosynthesis pathway represents a plant adaptive strategy in response to LN resulting in the synthesis of photo-protective pigments such as anthocyanins and flavanols, well-known antioxidants protecting plants from oxidative stress (Peng *et al*., 2008). High expression of several genes involved in

phenylpropanoid pathway was observed in many plants exposed to N deficiency, such as cucumber, oilseed rape, *Arabidopsis* and barley (Zhao *et al*., 2015; Quan *et al*., 2016; Goel *et al*., 2018, Sun *et al*., 2020). Furthermore, other studies described flavonoids as signals molecules (Buer *et al*., 2007; 2010; Brunetti *et al*., 2013) and more interestingly, their key role in the signal transduction from root to shoot in the early LN plant response was highlighted (Sun *et al*., 2020). Interestingly, the N-use efficient genotype RO displayed higher transcriptional levels of genes related to phenylpropanoid and flavonoid biosynthesis pathways compared to UC82, in root at LN resupply. In detail, a Chalcone Synthase 1 (*CHS1*) encoding gene, key enzyme in the flavonoids and anthocyanins synthesis (Dao *et al*., 2011) and a Cinnamyl alcohol dehydrogenase (*CAD*) encoding gene, enzyme involved in the biosynthesis of phenylpropanoid compounds (Tobias and Chow, 2005) were upregulated in RO after 8 and 24h LN resupply, respectively.

4.2. Co-expression network analysis reveals significant low N regulatory modules

NO_3^- regulates more than one thousand genes in both roots and shoots, and a significant percentage of these respond to NO_3^- itself, sustaining the complexity of its regulatory network in plant being coordinated with many other processes (Vidal *et al*., 2015). Our co-expression network analysis identified NO_3^- regulatory modules (one for each tissue) that were significantly up-regulated in response to LN in the N-use efficient genotype RO, after 24h N-resupply (brown and blue modules in shoot and root, respectively). Further, we identified the hubs genes with the maximum number of connections in the LN-regulatory networks, which might play key roles in the gene network. In shoot, the brown module included a Cytokinin riboside 5'-monophosphate phosphoribohydrolase (*LOG8*, Solyc06g075090.3) up-regulated in RO compared to UC82, among the most connected genes in the regulatory network. LOG8 is an activator of cytokinins, directly involved in NO_3^- signaling and N-metabolism regulation (Ruffel *et al*., 2011; Naulin *et al*., 2020). More interestingly, in the same module, the *ERF2* TF (Solyc01g090340.2), belonging to AP2/ERF family in tomato and homolog of Cytokinin Response Factor 5 encoding gene (*CRF5*) in *Arabidopsis*, was also identified as hub gene. The analysis of tomato knockout mutants revealed that *CRF5* homolog regulates leaves and flowers development but appeared also up-regulated in response to cytokinins, involved in the regulation of many abiotic stresses such as cold, drought and oxidative stresses in both

root and shoot (Shi *et al*., 2012; Gupta and Rashotte, 2014). These results might suggest an important regulatory role played by cytokinins in the differential early plant response to LN between the two N-contrasting tomato genotypes. Moreover, in the same module, an Asparagine synthetase (*ASNS*, Solyc01g079880.3) up-regulated in RO compared to UC82 at LN, was also identified as a hub gene. The ASNS is a key enzyme in the N-metabolism, which hydrolyzes glutamine to synthesize asparagine, the amino acid with the highest N/C ratio, used as the main N form stored and transported through the vascular tissues in many plants (Lea *et al*. 2007; Gaufichon *et al*. 2010). The *ASNS* over-expression in *Arabidopsis* revealed a higher asparagine levels in plant tissues together with an increased tolerance to N-deprivation (Lam *et al*., 2003; Igarashi *et al*., 2009), suggesting it as a good and viable strategy for improving NUE. Accordingly, our results suggested that RO is able to synthesize more asparagine in shoot compared to UC82, allowing to better withstand N-deficiency.

In root, the blue module included as hub genes a Late Embryogenesis Abundant protein (*LEA*, Solyc01g006320.3) and an Annexin 5 (*ANN5*, Solyc01g097520.3), both up-regulated in RO compared to UC82, after 24h LN-resupply. The LEA proteins are involved in plants adaptation to various abiotic stresses, acting as membrane stabilizers, ions chelators as well as antioxidants reducing cell damages (Tunnacliffe and Wise, 2007; Hirayama *et al*., 2010; Debnath *et al*., 2011). In the root apical meristem, Reactive Oxygen Species (ROS) production is regulated by the soil nutrient availability and is induced under NO_3^- deficiency (Wany *et al*., 2018). The antioxidant effect of LEA protein could attenuate ROS damages in RO root cells at LN. The Annexins are also stress induced proteins, among them *OsANN1* and *OsANN10* confer resistance to abiotic stress in rice by modulating ROS and/or lipid peroxidation levels (Qiao *et al*., 2015; Gao *et al*., 2020). Besides, *AtANN1* showed a peroxidase activity in response to drought stress by regulating ROS production (Goreka *et al*., 2005; Konopka-Postupolska *et al*., 2009). Our results highlighted the importance of ROS balancing under N-limiting condition, and the *LEA* and *ANN5* higher expressions in RO respect to UC82 could justify its higher tolerance to LN compared to UC82.

Finally, a model scheme, highlighting the high-NUE genotype (RO) responses to short-term LN stress, the main N-stress regulated pathways and the hub genes supposed to play a central role in the regulatory networks, has been proposed to sumup our results (Figure 39).

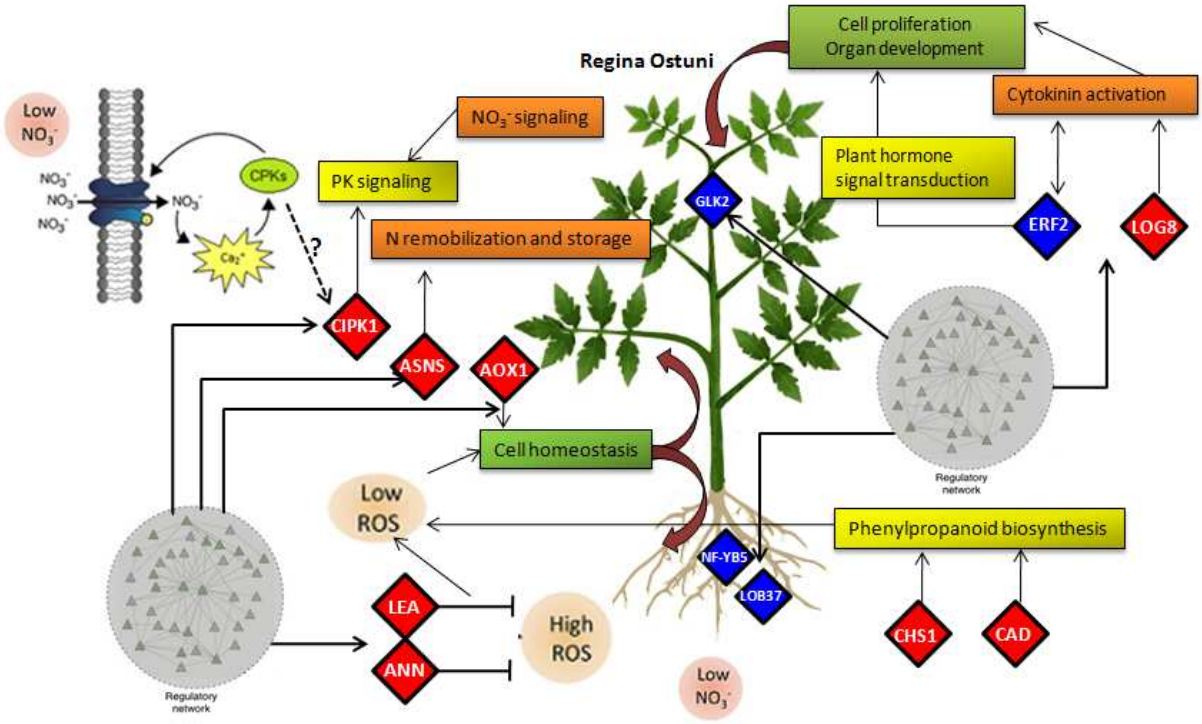

Figure 39.Model scheme showing the multilevel regulation of the short-term low NO_3^- stress in Regina Ostuni. Low NO_3^- (LN) induced an upregulation of the phenylpropanoid biosynthesis pathway, which contributes to reduce ROS production together with a higher expression of stress induced genes, such as Late Embriogenesis Abundente protein *(LEA)* and Annexine (*ANN*) in root, and Alternative Oxidase *(AOX1)* in shoot, which were among the central genes in both tissues regulatory networks. The antioxidant and scavenging activities of the encoded proteins might lead to shoot and root cell homestasis sustaining cell development and growth under LN stress. In shoot, plant hormone signal transduction and protein kinases (PK) signaling pathways were upregulated. Among the genes involved in these pathways a CBL-interacting PK (*CIPK1*), an Ethylen Responsive Transcription Factor (*ERF2*) and a cytokinin activating enzyme encoding gene (*LOG8*) were central genes in the regulatory network. *CIPK1* might be involved in primary NO_3^- response (PNR), whereas *ERF2* and *LOG8* are supposed to play a pivotal role in nitrate-cytokinin signaling cross-talk. The LN-induced cytokinins activation, suppose a subsequent cell proliferation and plant tissues growth. The Asparagine synthetase (*ASNS*), identified as hub gene in the shoot regulatory network, was upregulated suggesting a better management of the absorbed NO_3^- compared to low NUE genotype. The induced metabolic pathways and the function of the encoded protein are represented in yellow and orange, respectively. The putative responses resulting from the gene expressions, genes of interest, and transcription factors (TFs) are presented in green, red and blue colors, respectively.

5. Conclusion

This chapter represents the first transcriptional approach to deeply understand the tomato early responses (within 24 h) to LN, in both shoot and root. In our experimental setup, the potential mechanism underlying the nitrate regulation in two NUE-contrasting genotypes allowed us to formulate hypotheses for explaining RO higher NUE. In shoot, we provide a new scenario in which hormones and protein kinases signaling were probably involved in high NUE. So far, our results elucidated the nitrate, hormones and protein kinases interactions, furnishing novel insights in these combined signals, which have been unexplored in tomato. Thus, an interesting focus on future researches could be

the dissection of nitrate, hormone-protein kinase cross-talk interactions between N-contrasting genotypes in different tissues.

In root, the “phenylpropanoid and flavonoid biosynthesis” pathways were more enriched in the high-NUE genotype. In this regard, integrative transcriptomic and metabolomic analysis will be essential to provide a holistic understanding of N-nutrient/metabolite sensing and responses in tomato in order to plan future tomato breeding for NUE.

Finally, WGCNA decoded the dynamic regulatory network related to LN, pointing out an important role played by cytokinins and ROS balancing in early LN-tolerance mechanisms adopted by the efficient genotypes RO.

Chapter III

Weighted Gene Co-expression Network Analysis at tissue scale reveals candidate regulatory genes involved in long-term N-deficiency tolerance and high-NUE in tomato

1. Introduction

Nitrogen (N) deficiency has a significant impact on several plant physiological processes (Zhao *et al*., 2005). It directly affects the rate of photosynthesis since approximately 75% of N is allocated into chloroplasts and about 27% of it is utilized for the ribulose bisphosphate carboxylase/oxygenase (Rubisco) to ensure high photosynthetic activity (Evans, 1989, Makino, 2011). Nitrogen also influences stomatal opening (Evans, 1989) affecting CO_2 assimilation and sugar partitioning and consequently biomass production and crop yield (Foyer *et al*., 2011; Ishikawa-Sakurai *et al*., 2014; Jin *et al*., 2015). Besides, the plant responses to low N, at the molecular level, involve several transcriptome modulations inducing changes in different molecular functions and biological process mainly related to plant development (Zhang *et al*., 2006; Kant *et al*., 2011, Xu *et al*., 2012).

The identification of key genes to improve stress tolerance to low N conditions is a feasible way to improve NUE. Firstly, the identification of NUE-contrasting genotypes for a comparative understanding of gene expression and regulation in response to N stress condition is decisive (Hirel *et al*., 2007; Kant *et al*., 2010). Moreover, the manipulation of a single gene encoding an enzyme or transporter associated with N use often fails to improve NUE (Good *et al*., 2004), thus targeting transcription factors that concurrently regulate many N-use related genes could represent a promising approach to improve this trait (Ueda & Yanagisawa, 2018).

Transcriptome modulation and changes in the expression levels of N use-associated genes in tomato in response to N availability have been well documented (Wang *et al*., 2001, Ruzicka *et al*., 2010). Recently, the regulation of N-use related genes by a complex transcriptional network including several transcription factors has been revealed (Reneau-Morata *et al*., 2021). Although, the transcriptional network associated with N use was mostly analyzed in the model plant *Arabidopsis*, focusing on the plant response upon exposure to N limiting supply (Gaudinier *et al*., 2018; Varala *et al*., 2018; Brooks *et al*., 2019), less attention has been paid to the transcriptional networks underlying NUE. Even though different sets of genes has been suggested in barley, in rice and tobacco (Coneva *et al*., 2014, Yang *et al*., 2020, Sultana *et al*., 2020), key regulatory pathways and central transcription factors that regulate NUE have been hardly identified.

Gene co-expression network (GCN) analysis is a powerful system biology approach to identify modules of highly co-expressed or connected genes, providing a meaningful strategy to examine gene expression correlations from complex RNA-seq datasets across

developmental stages, treatments, tissues and time courses. A GCN is a set of relationships between genes where a node is defined as a gene connected to other genes by edges based on pairwise similarities (Gehan *et al*., 2015). Instead, a weighted gene co-expression network approach (WGCNA) assigns weights to the edges based on the strength of the correlation and can be used for finding modules of highly correlated genes, for summarizing clusters using the module eigengene or an intra-modular hub gene (Steve and Peter, 2008). A network analysis aims to connect gene expression profiles to phenotypic traits related to a treatment response. Hub nodes have been found to play vital roles in many networks; these highly connected genes are expected to play an important role in biological processes albeit not always significantly related to the trait of interest (Peter *et al*., 2013). However, intra-modular hub genes highly connected within a module are more likely to be biologically significant if the module is associated to the trait of interest (Horvath et Dong, 2008; Peter *et al*., 2013).

Studying plant responses to early low N is necessary to understand the differential regulatory mechanisms between the NUE-contrasting genotypes, but examining the differential adaptive responses to a longer low N stress between them is crucial to identify the key molecular factors leading to contrasting NUE. In this respect, this chapter investigate the molecular responses of two NUE contrasting tomato genotypes, RO (high-NUE genotype) and UC82 (low-NUE genotype), grown at LN for 7-days. Since the gene expression in plant is tissue specific, the present study aims to furnish a broad transcriptome profiling at tissue scale on tomato genotypes grown under different N supply to identify novel candidate regulatory genes related to N-limiting tolerance and high-NUE in tomato under long-term stress, combining a transcriptomic co-expression network approach with morpho-physiological traits.

2. Material and methods

2.1. Growth conditions under long-term N treatment

Seedlings of RO and UC82 (10-d old) were grown for 10 days under non-limiting NO_3^- conditions. Plantlets (20-d old) were starved for 5 days into an N-free solution, and then resupplied with low (LN; 0.5 mM) and high NO_3^- (HN; 10 mM) for 7 days. Then, shoot and root of each genotype were separately harvested and three biological replicates were used for the transcriptome analysis, each consisting of a pool of three plants (Figure 40).

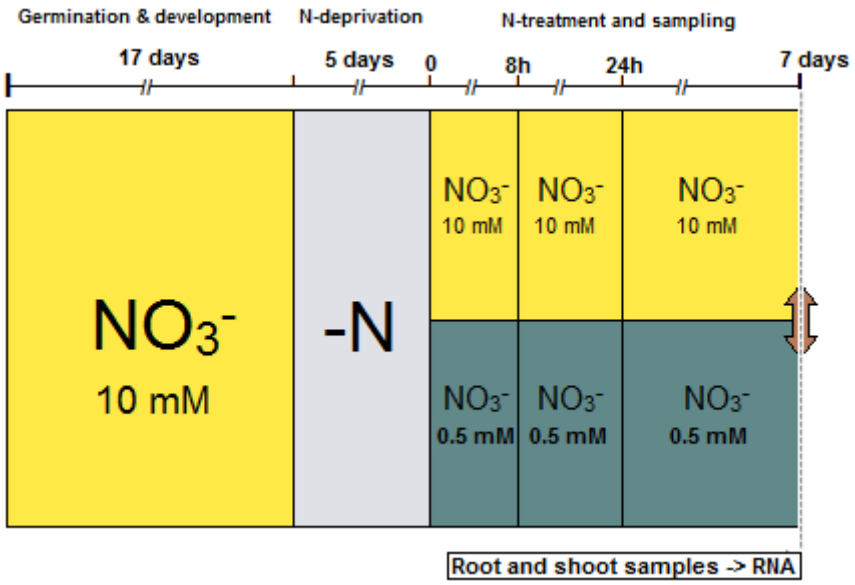

Figure 40. Experimental setup adopted for the long-term RNA-seq analysis.

2.2. RNA-seq analysis and data processing

Total RNA was extracted and purified using RNeasy Plant Mini Kit (Qiagen, Milano, Italy) following the manufacturer's protocol. RNA integrity was monitored on 1% denaturing RNA agarose gels and its purity checked using a NanoDrop 2000 (ThermoFisher Scientific, Wilmington, Delaware USA). Separate RNA-seq single-end sequencing libraries were prepared for each genotype (RO and UC82), treatment (HN and LN) and tissue (shoot and root) following the Transeq approach (Tzfadia *et al*., 2018). The 24 Libraries were sequenced on six lanes HiSeq 2500 System (Illumina), using the SR60 protocol. The raw data were processed to obtain high quality clean reads, removing adapter sequences, reads with unknown nucleotides "N" larger than 5%, and low-quality sequences. Clean reads were mapped to the tomato genome (SL3.0) from Ensembl Plants (http://plants.ensembl.org/Solanum_lycopersicum/Info/Index) using TopHat v2.0.12 (http://ccb.jhu.edu/software/tophat/index.html) (Kim *et al*., 2013). Reads per kilobase of transcript per million mapped reads (RPKM) were used to calculate genes expression levels.

2.2.1. Differentially expressed genes in response to long term N-limiting resupply

The gene expression profiles of both genotypes after 7 days HN and LN resupplies were analyzed to identify DEGs for the following pairwise comparisons: LN*vs*HN in RO and UC82 to evaluate the N effect, and RO*vs*UC82 at HN and LN for the genotypic effect in both shoot

and root. In detail, the normalized counts were compared for each comparison, employing the DESeq2 R package and for a false discovery rate (FDR) of 5% (Benjamini and Hochberg, 1995). The transcripts with an absolute adjusted $\log^2$ (fold change) ≥ 1 and FDR < 0.05 were considered. The DEGs and Venn diagrams were defined by the online tool https://bioinfogp.cnb.csic.es/tools/venny/index.html. Gene ontology (GO) enrichment analysis of DEGs was then performed using topGO R package version 2.14.0 (Pearce *et al*., 2014). In addition, pathway enrichment analysis was conducted by using kobas (v3.0) online tool (http://kobas.cbi.pku.edu.cn/), based on the Kyoto Encyclopedia of Genes and Genomes (KEGG) database (http://www.genome.ad.jp/kegg/).

2.3. Weighted Gene Coexpression Network Analysis (WGCNA)

The RPKM values of the identified DEGs were used for the gene co-expression network analysis performed using the WGCNA R package v1.51 (Langfelder and Horvath, 2008). The correlation between genes was performed by Pearson correlation coefficient (PCC) and used to calculate the distance matrix. The matrix was then used for the dynamic hierarchical clustering and to build the edges (connections) between nodes (genes) in the network.

2.3.1.Co-expression Networks Construction

Nine morpho-physiological traits related to both shoot and root and previously identified (Aci *et al*., 2021) were included in the WCGNA. In particular, NUE and its components NUtE and NUpE were considered for both tissues, shoot dry weight (SDW), SPAD values, shoot length (SL), leaf area (LA), leaf number (LN) and shoot N content (SNC) were also included into the shoot co-expression analysis, while root dry weight (RDW), root fineness (RF), root tissue density (TD), root length ratio (RLR), root mass ratio (RMR) and root N-content (R-Ncont) were included into the root co-expression analysis. The WCGNA was performed as already described in Chapter II except for the threshold powers, which were 14 and 26 to identify modules in shoot and root, respectively (Figure 51A and 52A).

2.3.2. Identification of Significant Modules and Functional Annotation

After the integration of the morpho-physiological data into the network, the module eigengene (ME), module membership (MM), and gene significance (GS) were then calculated. The functional analysis of relevant modules was performed to identify the potential processes and pathways involved in the traits. Gene ontology (GO) functional annotation and the KEGG were analyzed by Shiny and KOBAS 3.0, respectively.

2.3.3. Identification and visualization of hub genes

The hub genes were filtered for the geneModuleMembership and the geneTraitSignificance. After identifying the hub genes highly associated to NUE or NUE-related traits, a network visualization and analysis were carried out on Cytoscape v3.8.2 software (Shannon, 2003), allowing the identification of the highly connected genes.

2.4. Quantitative real-time PCR

Quantitative real-time PCR (RT-qPCR) was performed to validate the transcriptomic results on 10 genes associated with N-metabolism. Total RNA was extracted and purified using TRIzol™ reagent (Qiagen, Milano, Italy) according to the instructions provided by the manufacturer. The Maxima First Stand cDNA Synthesis Kit (Thermo Fisher Scientific Baltics UBA) was used to produce cDNA samples via reverse transcription according to the manufacturer instructions. Primer specificity of candidate genes was verified by melting curve using the mixed cDNA as template, and by 2% agarose gel electrophoresis analysis. The PowerUp SYBR Green master mix (Applied Biosystems by Thermo Fisher Scientific) and the StepOne™ Real-Time PCR System (Applied Biosystems, foster, CA, USA) were employed to perform qPCR with gene specific primers. Three biological and three technical replicates were adopted and the means of the relative gene expression (Ct) were normalized to the reference genes Actin and Ef1-α (Lovdal and Lillo, 2009). Primers were designed using Primer3 (v0.4.0) and listed in Table S4. Results of the Pearson correlation between RNAseq data and qRT-PCR were plotted in a scatter plot, which revealed a good and significant correlation ($r = 0.81$, $P < 0.0001$) (Figure S6).

3. Results

3.1. Transcriptome modulation in response to long-term N-limiting stress

3.1.1. RNA-seq analysis

Twenty-four libraries were construted to study the transcriptomic changes occurring in both shoot and root of RO and UC82 in response to long-term low (LN) and high N (HN) resupply (7 days) (Figure 40). Up to one hundred thirteen million clean reads were obtained and mapped to the tomato genome (SL3.0). Almost ninety-one million reads were aligned to the reference genome yielding an overall mapping percentage of 77.12% (Table S10), and about thirty-five thousand (35,845) transcripts were identified after assembly.

3.1.2. Differential gene expression analysis

To identify the differentially expressed genes (DEGs) after 7 days N-resupply, RO and UC82 transcriptome profiles were analyzed by the following pairwise comparisons: LN*vs*HN in RO and UC82 for evaluating the N effect and RO*vs*UC82 at HN and LN for the G effect in both tissues. About three thousand two hundred (3203) and two thousand (2031) DEGs were identified in the four comparisons in shoot and root, respectively (Figure 41A,B), and five hundred fifty-three (553) DEGs were shared between tissues (Figure 41C). To identify the common and specific DEGs for each treatment and genotype, Venn diagrams were plotted (Figure 42).

In shoot, in the LN*vs*HN comparison, two thousand two hundred twenty (2220) DEGs were found in RO, among which 1021 and 1119 up- and down-regulated, respectively. One thousand six hundred twenty-eight (1628) DEGs, 849 and 779 up- and down-regulated, respectively were found in UC82, nine hundred two (902) DEGs were shared between genotypes (Figure 42A,C). Furthermore, three hundred forty-one (341) DEGs, 166 and 175 up- and down-regulated, respectively, were found in the RO*vs*UC82 comparison at LN, while three hundred and ten (310) DEGs, among which 177 up- and 133 down-regulated, were identified at HN, and finally, eighty-three (83) DEGs were shared between N-treatments (Figure 42A,C). In root, nine hundred fifty-five (955) DEGs were identified in the LN*vs*HN comparison in RO, among which 407 up- and 548 down-regulated, respectively; one thousand three hundred thirty-four (1334) DEGs were found in UC82, 562 up- and 772 down-regulated, and five hundred thirty-one (531) DEGs were shared between genotypes (Figure 42B,D).

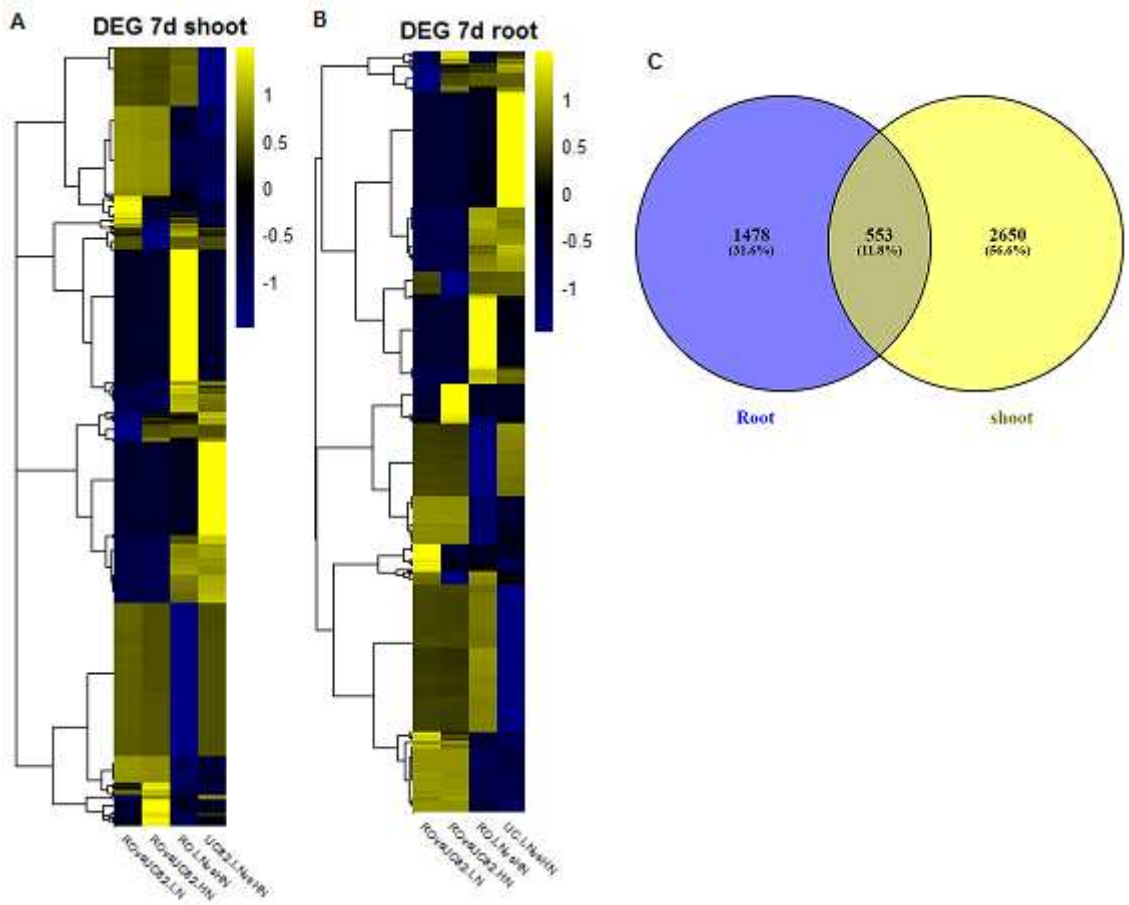

Figure 41. Heatmap of the expression profiles of all the identified DEGs from the four pairwise comparisons for N (RO-LN*vs*.HN and UC82-LN*vs*.HN) and G effect (RO*vs*.UC82-LN and RO*vs*.UC82-HN) in shoot (A) and root (B) The values are expressed as $\log^2$FC. Venn diagram of the DEGs identified in shoot and root (C).

In addition, two hundred five (205) DEGs were identified comparing RO*vs*UC82 at LN, among which 113 up- and 92 down-regulated, while three hundred fifteen (315) were found at HN, including 178 up- and 137 down-regulated, respectively (Figure 42B,D).

3.1.2.1. Genotype-specific LN-responsive DEGs

To study the genotype-specific LN responses, we focused on the DEGs identified exclusively in the LN*vs*HN comparison for each genotype in both shoot and root (Figures 43A, 44A). Interestingly, the LN-responsive DEGs in RO shoot were significantly enriched in photosynthesis, small molecule and organic acid metabolic processes GO terms, and in metabolic pathways, biosynthesis of secondary metabolites, aminoacyl-tRNA biosynthesis and carbon metabolism KEGG pathways (Figure 43B,C). By contrast, the UC82-specific LN-responsive DEGs were significantly enriched in negative regulation of proteolysis, of endopeptidase activity and of hydrolase activity GO terms, while any KEGG pathway was significantly enriched (Figure 43B,C).

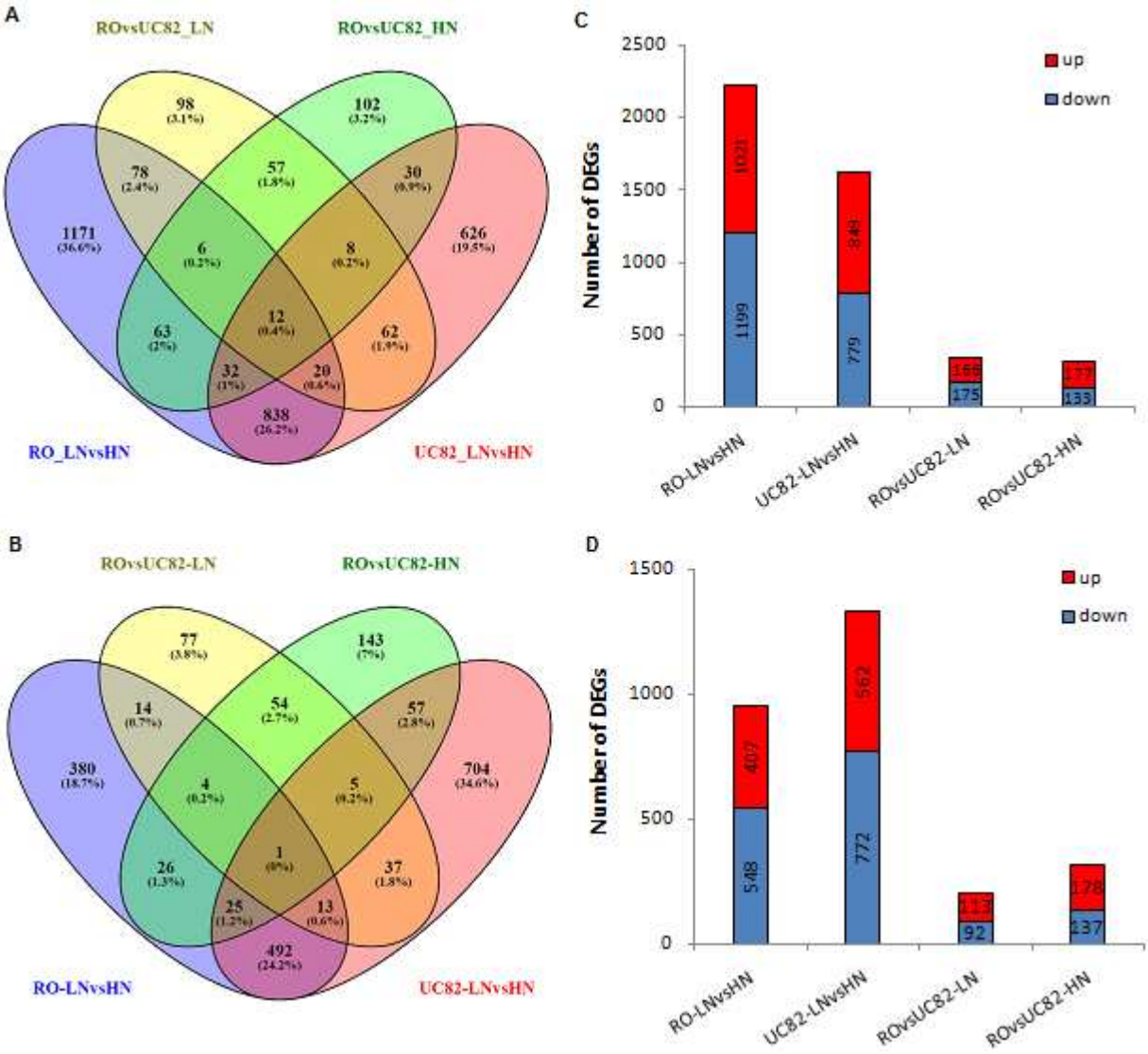

Figure 42. Venn diagrams of differentially expressed genes (DEGs) between the four comparisons in shoot (A) and root (B). The number of up and downregulated genes in shoot (C) and root (D).

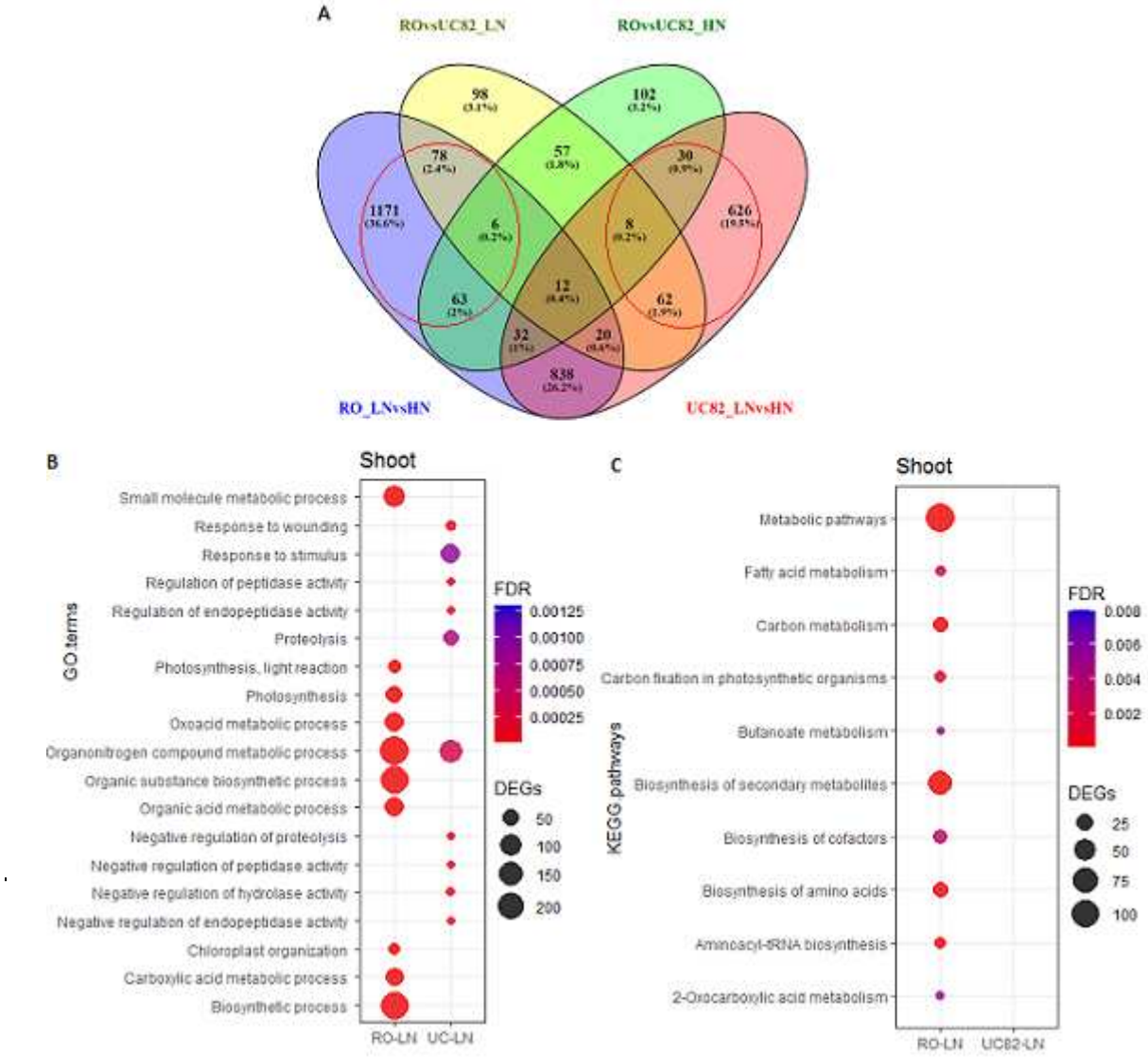

Figure 43. Functional enrichment analysis of genotype specific DEGs in response to LN in shoot: Venn diagram (A). Top 10 Biological process GO terms (B), KEGG pathways enrichment (C).

In root, the RO-specific LN-responsive DEGs were not significantly enriched in any GO term or KEGG pathway, while the UC82-specific DEGs were significantly enriched in oxidation-reduction and catabolic processes GO term, as well as in phenylpropanoid biosynthesis, metabolic pathway and the biosynthesis of secondary metabolites KEGG pathways (Figure 44B, C). In addition, under LN stress, nine hundred two (902) and five hundred thirty-one (531) DEGs were shared between genotypes in shoot and root, respectively. These last were significantly enriched in photosynthesis, generation of precursor metabolites energy and oxidation-reduction process GO terms, and in photosynthesis, carbon metabolism and carbon fixation in photosynthetic organism, as well as biosynthesis of amino acids and nitrogen metabolism KEGG pathways (Table S11).

3.1.4. LN-specific DEGs

We considered as "LN-specific", the DEGs found in the RO*vs*UC82 comparisons at LN condition excluding those shared with HN condition (Figure 45A, B). Thus, two hundred fifty-eight (258) and one hundred forty-one (141) LN-specific DEGs between genotypes were identified, in shoot and root, respectively (Table S12, S13). In shoot, photosynthesis, photosynthetic electron transport chain, and photosynthesis, light reaction were the three most significantly enriched biological process GO terms (Figure 45C). Furthermore, fatty acid degradation and tyrosine metabolism were the most significantly enriched KEGG pathways (Figure 45D). By contrast, any significant GO terms or KEGG pathways were enriched in root (Figure 45C, D).

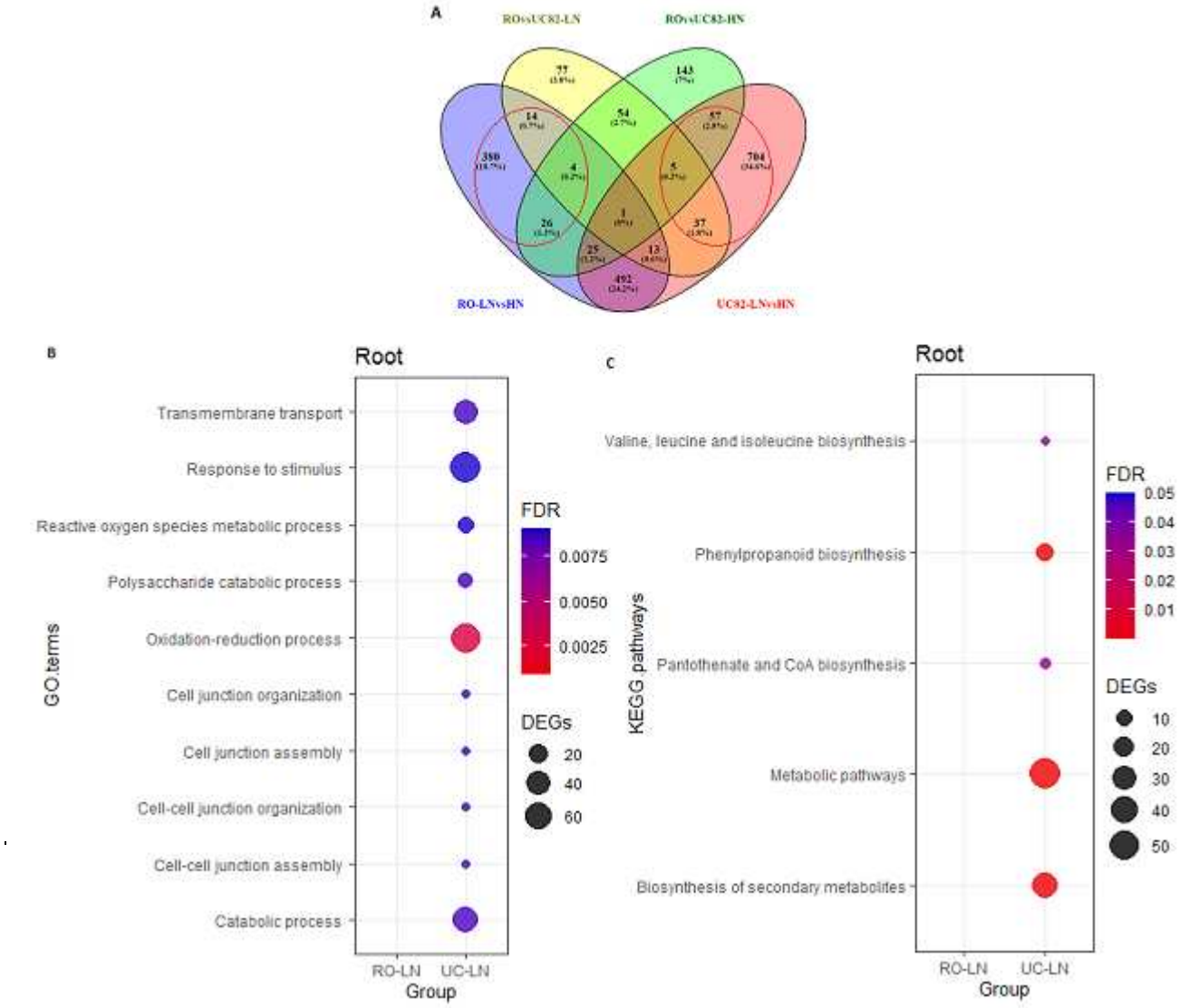

Figure 44. Functional enrichment analysis of genotypes specific DEGs in response to LN in root: Venn diagram (A), Top 10 Biological process GO terms (B), KEGG pathways enrichment (C).

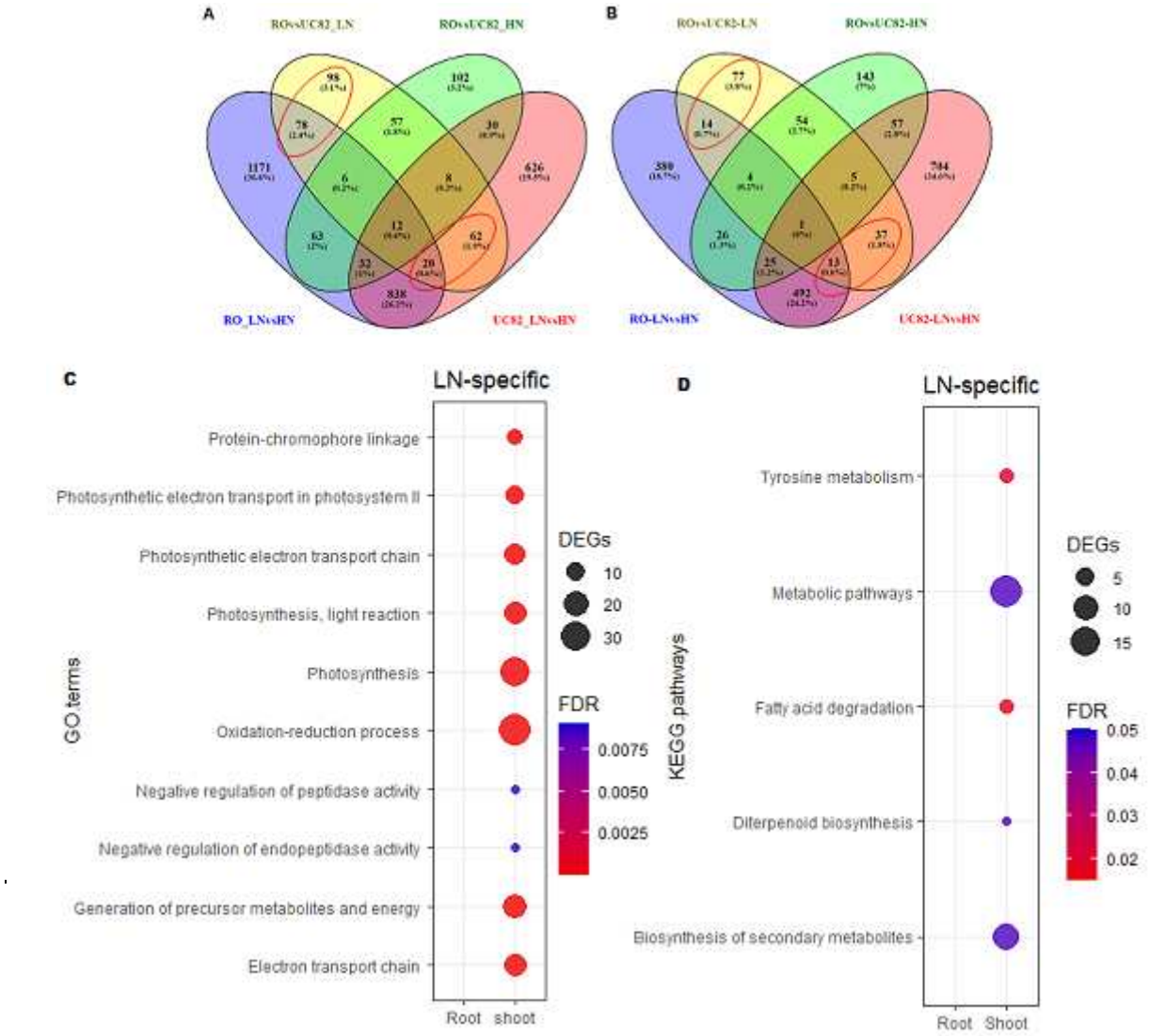

Figure 45. Functional enrichment analysis of the LN-specific DEGs identified by Venn diagrams for RO*vs*.UC82-LN comparison in shoot (A) and root (B), Top 10 Biological process terms (C), KEGG pathways enrichment (D).

3.1.4.1. Differentially expressed genes involved in photosynthesis

Among the two hundred fifty-eight (258) DEGs identified in shoot, thirty-four (34), involved in photosynthesis, were analyzed to better understand the relationship between NUE and C fixation and assimilation. Twenty-six DEGs were related to the light reaction, three to the Calvin cycle and one involved in photorespiration (Figure 46). Moreover, most of these DEGs were almost more expressed in RO compared to UC82 only at LN. In the primary photochemistry of the photosynthesis (light reaction), the transcript abundances of thirteen genes encoding protein related to the photosystem I reaction center (PSI RC), including nine P700 chlorophyll A apoprotein A1 and A2, were significantly higher in RO shoot (Figure 46). In the photosystem II reaction center (PSII RC), twelve genes were significantly more expressed in RO shoot compared to UC82, including D1 and D2 proteins as well as PSII reaction center CP43, Z proteins and two genes encoding the cytochrome b6/f complex subunits, which mediates electron transfer between PSI and PSII (Figure 46).

Three genes encoding the Rubisco large subunits, primary enzyme in C fixation and assimilation in the Calvin cycle were significantly more expressed in RO compared to UC82 shoot (Figure 46), indicating that RO channels more N into the photosynthetic apparatus, leading to a higher N utilization for C fixation under LN condition.

Furthermore, among the LN-specific DEGs, two chloroplast localized protein encoding genes *Ycf2* (Solyc04g024540.2) and *TIC214* (Solyc11g021260.1), involved in chloroplast protein import across the inner membrane, were found. The expression of *Ycf2* was significantly up-regulated in RO while *TIC214* appeared significantly down-regulated in UC82 in response to LN, as consequence, transcript abundances of both genes were significantly higher in RO compared to UC82 shoot only under LN condition. These results suggest the possible involvement of chloroplast protein import process in the differential LN response between genotypes.

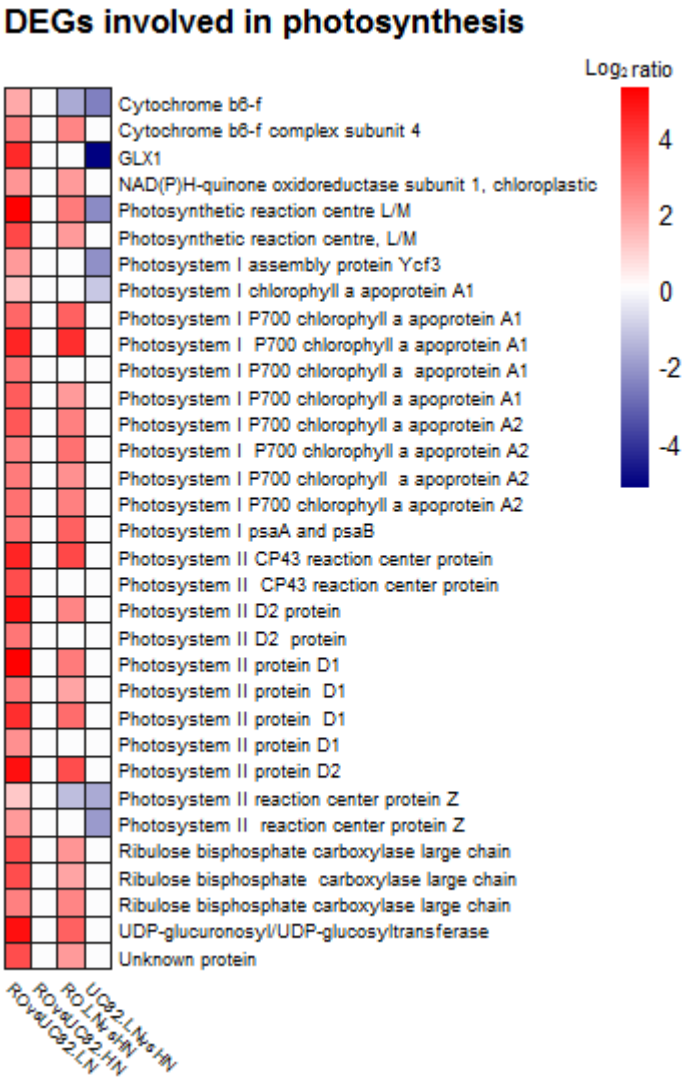

Figure 46. Heatmap of the DEGs involved in the photosynthesis process GO term. The values are expressed in log^2FC

3.1.5. Differentially expressed transcription factors

Interestingly, one hundred seventy-nine (179) and eighty-five (91) identified DEGs were TF coding genes in shoot and root, respectively, and only 32 were shared between tissues (Figure 47A). They belonged to 31 and 24 families in which bHLH and WRKY were the most represented TF families in shoot and root, respectively (Figure 47B,C). Venn diagrams were distinctly plotted for both tissues (Figure 47D,E) and their $log_2(FC)$ for the four comparisons are reported in Table S14, S15.

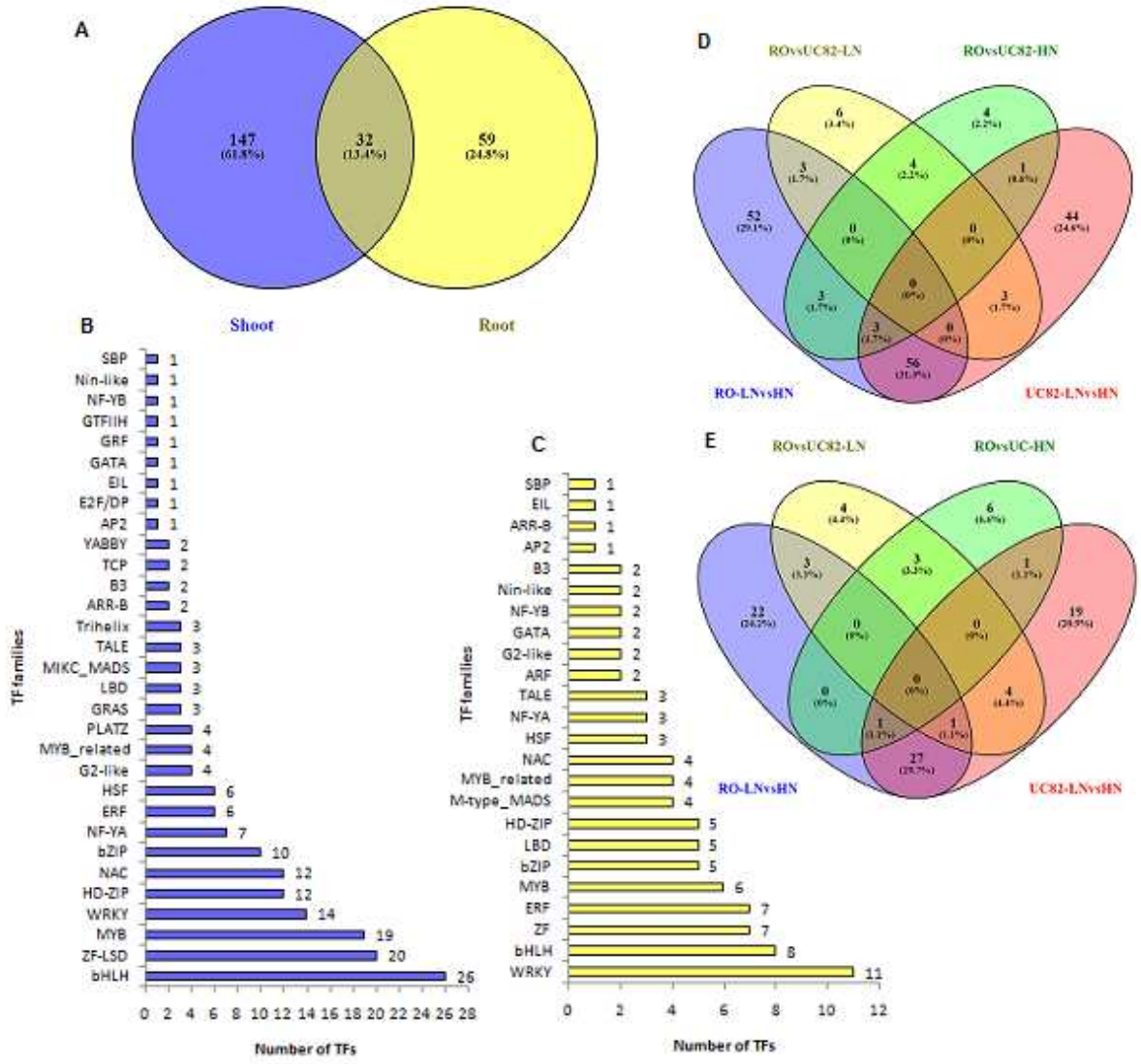

Figure 47. Distribution of DEGs encoding for different transcription factors families in shoot and root. Venn diagram for TFs total number in shoot and root (A), distribution for each TF family in shoot (B) and root (C), Venn diagrams for TFs identified in each comparison in shoot (D) and root (E).

In the LN*vs*HN comparisons, one hundred seventeen (117) genes encoding TFs, were differentially expressed in RO (84 up-regulated and 33 down-regulated) and one hundred seven (107) in UC82 (80 up-regulated and 27 down-regulated) in shoot (Figure 47D). In root, fifty-four genes encoding TFs were differentially expressed in RO (36 up-regulated and 18 down-regulated), and fifty-three in UC82 (36 up-regulated and 17 down-regulated) (Figure 47E). However, in the RO*vs*UC82 comparisons, the TFs differentially expressed were less than in the previous comparisons. In shoot, sixteen and fifteen were differentially expressed at LN and HN, respectively, while 4 TFs were shared between the N conditions (Figure 47D); in root, fifteen and eleven TFs were differentially expressed at LN and HN, respectively, and only 3 were shared (Figure 47E).

3.1.5.1. Genotype-specific LN-responsive TFs

We focused the analyses on the TF encoding genes that were differentially expressed in response to LN compared to HN supply within each genotype. Thirteen TF families encoded by 58 genes were LN-responsive only in RO shoot, including 40 up- and 18 down-regulated TFs (Figure 47D). The TF families bHLH (13), ZF (9), WRKY (8) and MYB (6) were the most represented (Figure 48A, Table 5). By contrast, forty-eight (48) DEGs encoding TFs belonging to twenty-four families were LN-responsive only in UC82 shoot , counting 36 up- and 12 down-regulated TFs (Figure 47D). The MYB (7), HD-ZIP (5), bHLH (4) and WRKY (4) TF families were mostly represented (Figure 48B, Table 5). In addition, fifty-nine (59) DEGs encoding TFs belonging twenty-one families were regulated by LN regardless of genotype (Figure 47D). All these TFs exhibited the same expression patterns in both genotypes shoot, in response to LN compared to HN, 44 up- and 15 down-regulated (Table 6). In detail, TF encoding genes belonging to NAC, MYB, NF-YA and HD-ZIP families were up-regulated by LN treatment, whereas LBD/LOB and G2-like TFs resulted down-regulated in both genotypes (Table 6).

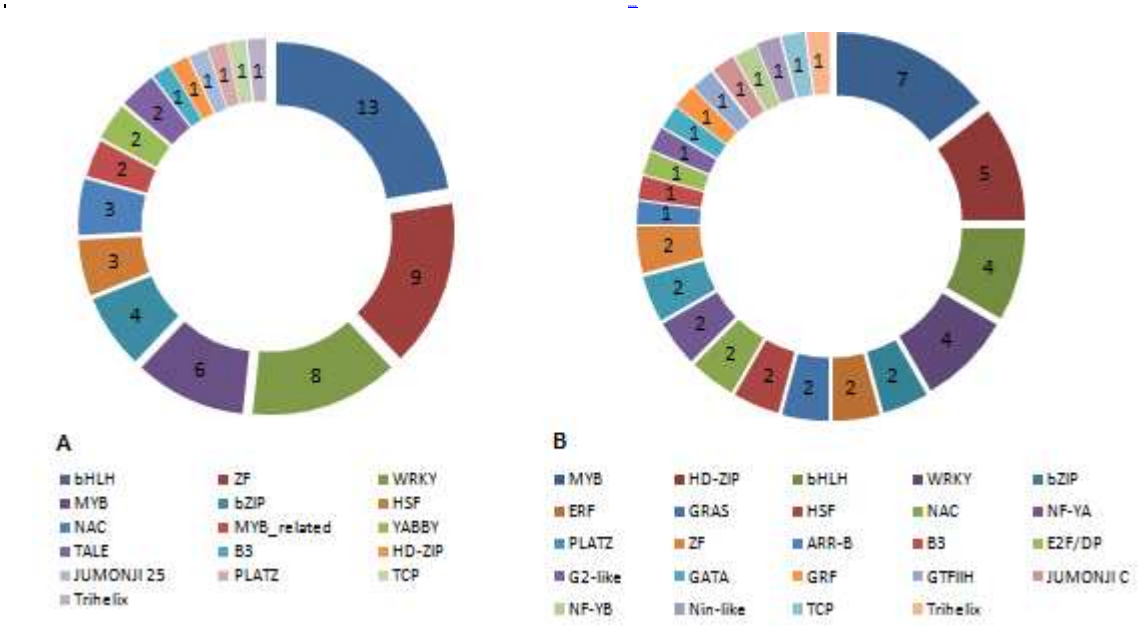

Figure 48.Genotype-specific LN responsive DEGs encoding transcription factors and their distribution in shoot of RO (A) and UC82 (B).

Table 5. Genotype-specific LN-responsive TFs in shoot of RO (A) and UC82 (B)

Genotype-specific							
RO	RO-LN*vs*.HN			**UC82**	UC82-LN*vs*.HN		
TFs families	Total	Up-regulated	Down-regulated	TFs families	Total	Up-regulated	Down-regulated
bHLH	13	10	3	MYB	7	7	0
ZF	9	3	6	HD-ZIP	5	4	1
WRKY	8	8	0	bHLH	4	2	2
MYB	6	3	3	WRKY	4	4	0
bZIP	4	3	1	bZIP	2	2	0
HSF	3	3	0	ERF	2	2	0
NAC	3	3	0	GRAS	2	1	1
MYB_related	2	2	0	HSF	2	2	0
YABBY	2	0	2	NAC	2	2	0
TALE	2	2	0	NF-YA	2	2	0
B3	1	0	1	PLATZ	2	1	1
HD-ZIP	1	1	0	ZF	2	2	0
JUMONJI 25	1	1	0	ARR-B	1	1	0
PLATZ	1	1	0	B3	1	1	0
TCP	1	0	1	E2F/DP	1	0	1
Trihelix	1	0	1	G2-like	1	0	1
-	-	-	-	GATA	1	0	1
-	-	-	-	GRF	1	1	0
-	-	-	-	GTFIIH	1	1	0
	-	-	-	JUMONJI C	1	0	1
	-	-	-	NF-YB	1	0	1
	-	-	-	Nin-like	1	0	1
	-	-	-	TCP	1	0	1
	-	-	-	Trihelix	1	1	0
Total	58	40	18	Total	48	36	12

Table 6. Shared LN-responsive TFs in shoots of RO and UC82 after 7days of N-resupply.

		RO-LN*vs*.HN		UC82-LN*vs*.HN	
TF families	Totale	Up-regulated	Down-regulated	Up-regulated	Down-regulated
NAC	7	7	0	7	0
ZF-CO-like	7	5	2	5	2
bHLH	6	2	4	2	4
MYB	5	5	0	5	0
NF-YA	5	5	0	5	0
HD-ZIP	4	4	0	4	0
bZIP	3	2	1	2	1
LBD	3	0	3	0	3
WRKY	3	3	0	3	0
ERF	2	2	0	2	0
G2-like	2	0	2	0	2
MIKC_MADS	2	2	0	2	0
MYB_related	2	2	0	2	0
AP2	1	0	1	0	1
ARR-B	1	1	0	1	0
EIL	1	1	0	1	0
GRAS	1	0	1	0	1
HSF	1	1	0	1	0
PLATZ	1	1	0	1	0
SBP	1	0	1	0	1
TALE	1	1	0	1	0
Total	59	44	15	44	15

Fourteen and sixteen DEGs encoding TFs, belonging to 25 and 24 families, were LN-responsive in root of RO and UC82, respectively (Figure 47E). In RO, 14 and 11 TFs were up and down-regulated, respectively, with WRKY (6) and ZF (4) as the most represented families (Figure 49A, Table 7). In UC82, 13 and 11 TFs were up and down-regulated, respectively, in response to LN with bHLH (4) and MYB (3) as the most represented families (Figure 49B, Table 7). Twenty-nine DEGs, encoding 17 TF families, were shared between genotypes at LN, showing the same expression patterns (up- and down-regulated) in both genotypes (Table 8).

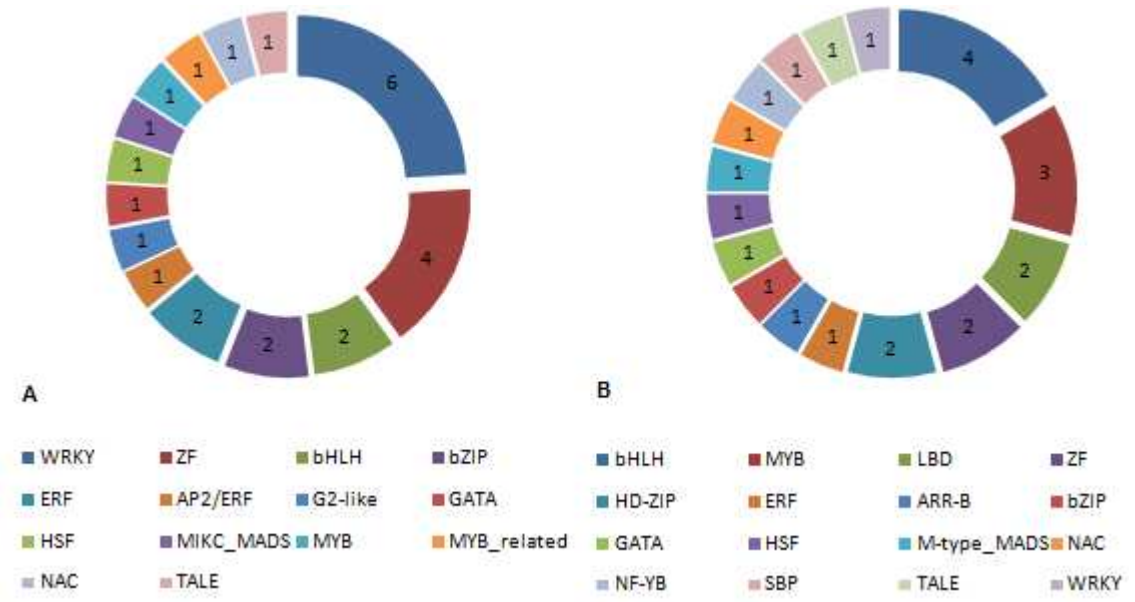

Figure 49. Genotype-specific LN responsive DEGs encoding transcription factors and their distribution in root of RO (A) and UC82 (B).

Table 7. Genotype-specific LN-responsive TFs in root of RO and UC82 after 7 days N-resupply.

Genotypic-specific							
RO	RO-LN*vs*.HN			**UC82**	UC82-LN*vs*.HN		
TFs families	Total	Up-regulated	Down-regulated	TFs families	Total	Up-regulated	Down-regulated
WRKY	6	6	0	bHLH	4	2	2
ZF	4	2	2	MYB	3	2	1
bHLH	2	2	0	LBD	2	1	1
bZIP	2	0	2	ZF	2	1	1
ERF	2	0	2	ARR-B	1	1	0
AP2/ERF	1	0	1	bZIP	1	1	0
G2-like	1	0	1	HD-ZIP	2	1	1
GATA	1	1	0	GATA	1	0	1
HSF	1	1	0	HSF	1	1	0
MIKC_MADS	1	0	1	M-type_MADS	1	0	1
MYB	1	0	1	NAC	1	1	0
MYB_related	1	1	0	NF-YB	1	0	1
NAC	1	0	1	SBP	1	0	1
TALE	1	1	0	TALE	1	1	0
-	-	-	-	WRKY	1	1	0
-	-	-	-	ERF	1	0	1
Total	25	14	11	Total	24	13	11

Table 8.LN-responsive TFs shared between RO and UC82 in root after 7days N-resupply.

	LN-responsive				
		RO-LN*vs*.HN		UC82-LN*vs*.HN	
TFs families	Total	Up-regulated	Down-regulated	Up-regulated	Down-regulated
ARF	2	2	0	2	0
bHLH	2	1	1	1	1
bZIP	2	1	1	1	1
ZF	1	1	0	1	0
ERF	3	3	0	3	0
G2-like	1	0	1	0	1
HD-ZIP	1	1	0	1	0
LBD	3	0	3	0	3
MIKC_MADS	1	1	0	1	0
MYB	2	2	0	2	0
MYB_related	1	1	0	1	0
NAC	2	2	0	2	0
NF-YA	3	3	0	3	0
NF-YB	1	1	0	1	0
Nin-like (NLP)	2	2	0	2	0
TALE	1	1	0	1	0
WRKY	1	0	1	0	1
Total	29	22	7	22	7

3.1.5.2. LN-specific DEGs encoding TFs

To identify the LN-regulated TFs probably involved in N-use efficiency, we firstly examined the expression profiles of the differentially expressed TFs in the genotype-specific LN-response (RO-LN*vs*HN or UC82-LN*vs*HN), in the LN-specific response between genotypes (RO*vs*UC82-LN), and those in common between these comparisons. We excluded from the analysis all the TFs differentially expressed between RO and UC82 regardless N-level (DEGs shared between RO*vs*UC82-LN and RO*vs*UC82-HN) and those specifically regulated at HN (RO*vs*UC82-HN) (Figure 50).

So, twenty-five DEGs encoding TFs, LN and tissue-specific, were identified. Twelve (12) TFs, belonging to 9 TF families, were identified in shoot, including 3 bHLH, 2 NAC, and one member each for HD-ZIP, NLP, HSF, MYB, TGA, G2-like and ZF, while 13, belonged to 9 TF families, were identified in root, including 3 ERF, 2 WRKY, 2 ZF and one member each for MYB, NAC, LOB, B3, HD-ZIP and TGA (Figure 50). The heatmap showed that *bHLH style2.1 (PRE2), bHLH 013* and *NAC2* TF encoding genes were up-regulated only in RO shoot in the LN*vs*HN as well as RO*vs*UC82 comparisons only at LN. By contrast, a *NAC* and *HSF8* TF encoding genes were up-regulated only in UC82 shoot in LN*vs*HN comparison and only at LN for RO*vs*UC82 comparison. More interestingly, a *NLP1* (Nin-like TF) resulted

significantly down-regulated in UC82 shoot in response to LN resupply respect to HN, but was up-regulated in RO compared to UC82 only under LN condition. Finally, the remaining LN-specific TFs were differentially expressed only between genotypes (RO*vs*UC82) at LN. In detail, *G2-like* and *TGA2* were up-regulated while the others were down-regulated in RO shoot compared to UC82 (Figure 50).

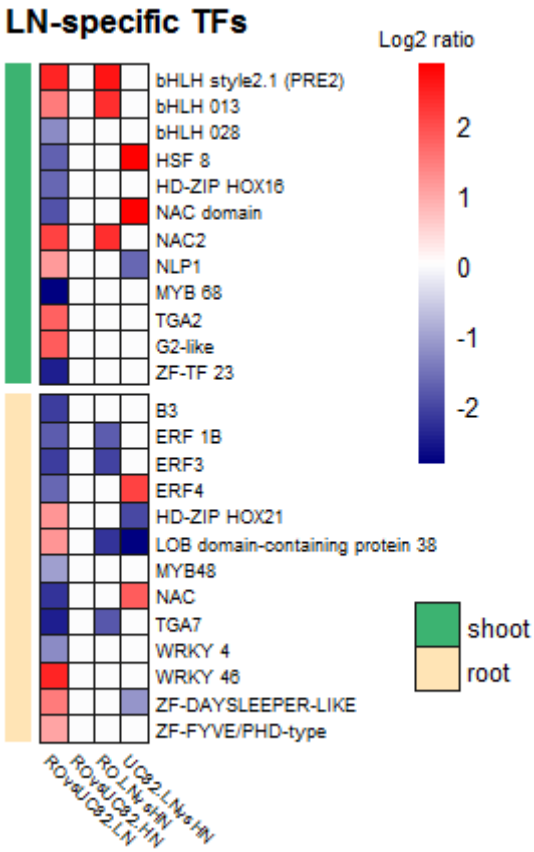

Figure 50. Heatmap of LN-specific transcription factors in tomato shoot and root. The values are expressed in log^2FC

By contrast, the LN-specific TFs in root showed different expression patterns. In detail, 3 TFs namely *ERF1B*, *ERF3* and *TGA7* appeared down-regulated only in RO in LN*vs*HN as well as in RO*vs*UC82 comparisons at LN (Figure 50). Furthermore, 4 TFs namely *ERF4*, *NAC*, *HD-ZIP HOX21*, and *ZF-Daysleeper-like*, were differentially expressed in the LN*vs*HN comparison only in UC82. The first two were up-regulated in the LN*vs*HN comparison but down-regulated in RO compared to UC82 only at LN, while the last two exhibited an opposite trend. Moreover, a *LOB38* was down-regulated in the LN*vs*HN regardless of genotypes but significantly up-regulated in RO compared to UC82. Finally, 5 TFs were differentially expressed only in RO*vs*.UC82 at LN, *WRKY46* and *ZF-FYVE/PHD-type* were up-regulated, while *WRKY4*, *MYB48* and *B3* down-regulated in RO compared to UC82 (Figure 50).

3.2. Weighted Gene Co-expression Network analysis

To identify hub genes, in the transcriptional regulation networks, associated with a long-term LN-stress in both tissues, we conducted a weighted gene correlation network analysis (WGCNA), including 3203 and 2031 DEGs identified in shoot and root, respectively. We tagged seventeen and fifteen co-expressed modules including from 39 to 1136 and from 37 to 510 genes in shoot and root, respectively (Figure 51B, C and 52B, C).

The interactions between the co-expression and the morpho-physiological traits modules were then analyzed and the expression levels of eigengenes (idealized representative genes) within each module in both tissues were reported (Figures 51D, 52D). The module-trait relationships were determined for ME value > 0.75. The identification of the hub genes for each module was carried out by using the Module Membership (MM) value, which emphasizes genes of importance into the module, and the Gene Trait Significance (GS), which pinpoints genes whose expression profiles are correlated with a physiological trait.

The results showed the lightgreen (ME= 0.97, P= 1×10^{-7}) and greenyellow (ME= 0.87, P= 2×10^{-4}) modules as the most significantly correlated with NUE, and the turquoise module to SDW (ME = 0.88, P = 2×10^{-4}) and SNC (ME = 0.93, P = 5×10^{-5}) in shoot (Figure 51D).

In root, the turquoise module appeared significantly correlated to NUpE (ME = 0.96, P= 6×10^{-7}) and R-Ncont (ME= 0.82, P= 1×10^{-3}) (Figure 52D).

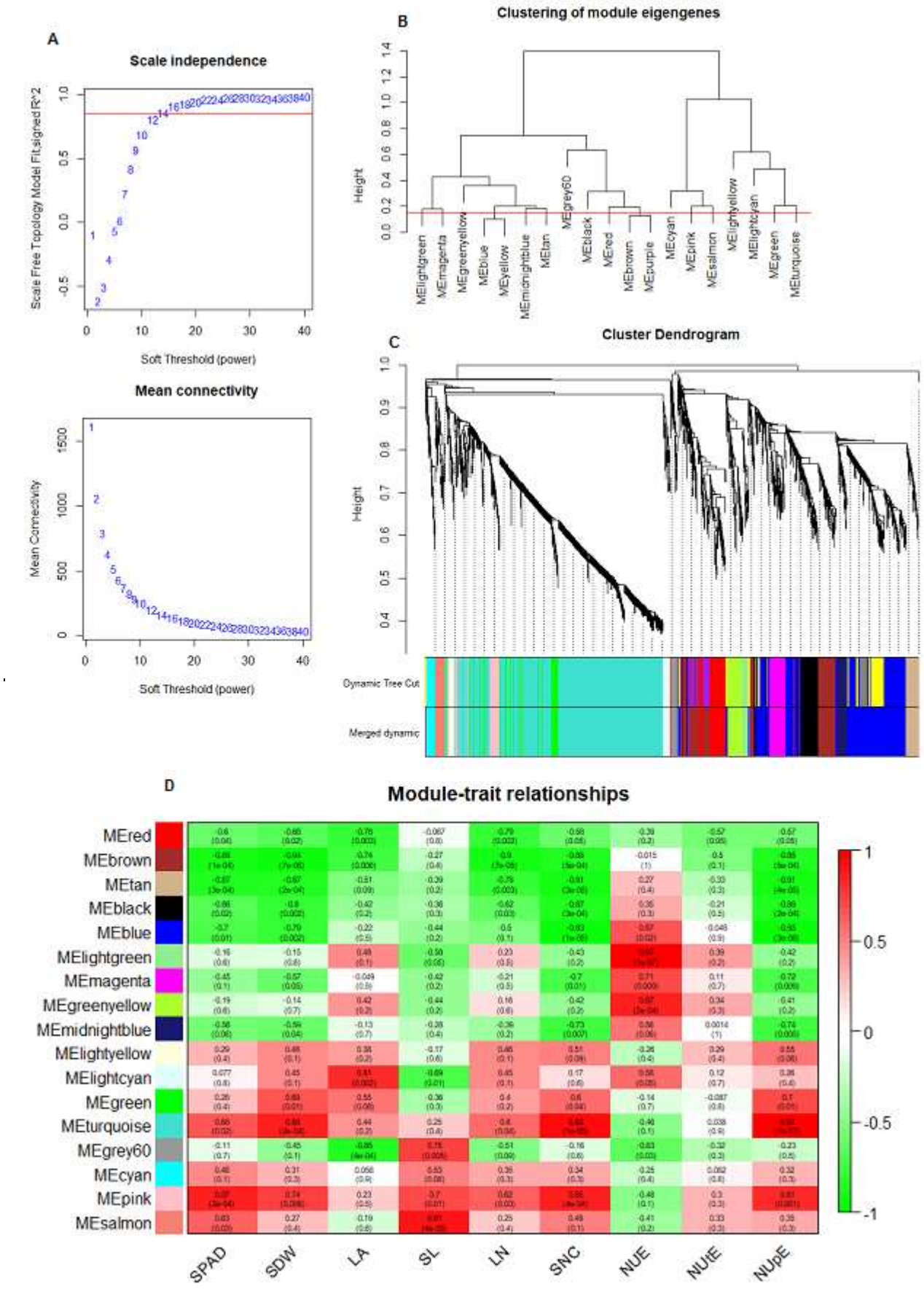

Figure 51. Scale independence and Mean Connectivity (A), Clustering of module eingengenes (B), Cluster dendrogram (C) and Module-trait relationship (D) of the 3203 DEGs in the tomato shoot (see Materials and Methods).

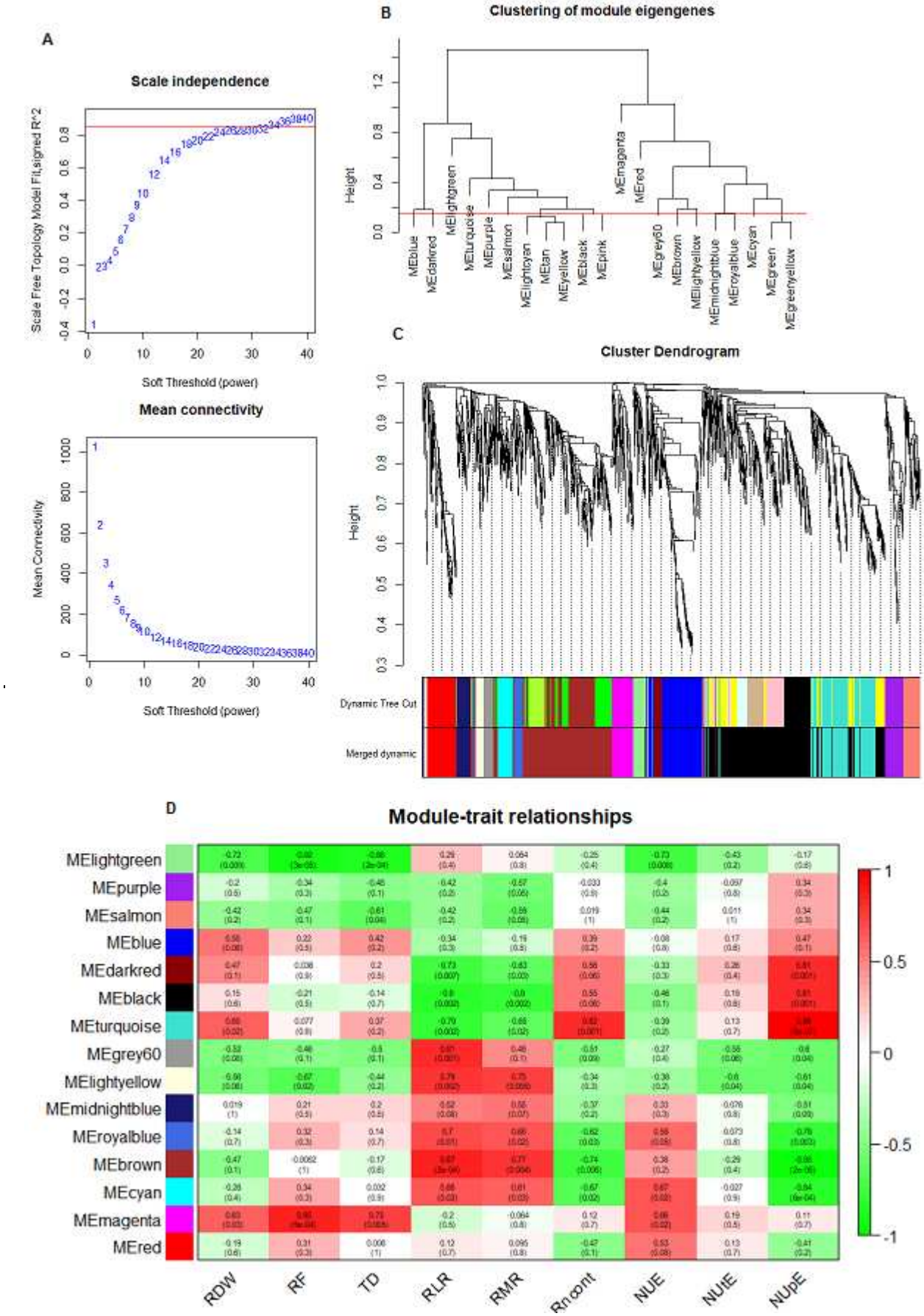

Figure 52. Scale independence and Mean Connectivity (A), Clustering of module eingengenes (B), Cluster dendrogram (C) and Module-trait relationship (D) of the 3203 DEGs in the tomato root (see Materials and Methods).

3.2.1. NUE-related modules in shoot and identification of novel candidate genes for LN-tolerance and NUE improvement

3.2.1.1. Functional analysis of the lightgreen module in shoot

In shoot, the lightgreen co-expression module was the most correlated to NUE (ME= 0.97) and its co-expressed genes were up-regulated in RO respect to UC82 in LN condition. GO term analysis of the eigengenes included in this module showed a significant enrichment in the photosynthesis and regulation of translational elongation BP (Table S16). The NUE-related hub genes in the lightgreen module were selected for a geneModuleMembership > 0.85 and a geneTraitSignificance for NUE > 0.80 (Figure 53A). Twenty-four genes satisfied this condition among which seven potential key genes related to NUE: three TFs, Solyc06g008590.3 (Auxin-regulated *IAA17*), Solyc05g024230.2 (*ERF/CRF2-like*) and Solyc12g009050.2 (Nuclear transcription factor *NFY-A6*), and four genes, Solyc12g033060.2 (Photosystem I P700 chlorophyll a apoprotein A2), Solyc01g105350.2 (Glycosyltransferase), Solyc05g045670.3 (Glucose-6-phosphate/phosphate-translocator) and Solyc03g115650.3 (Eukaryotic translation initiation factor 5A-1) (Figure 53B).

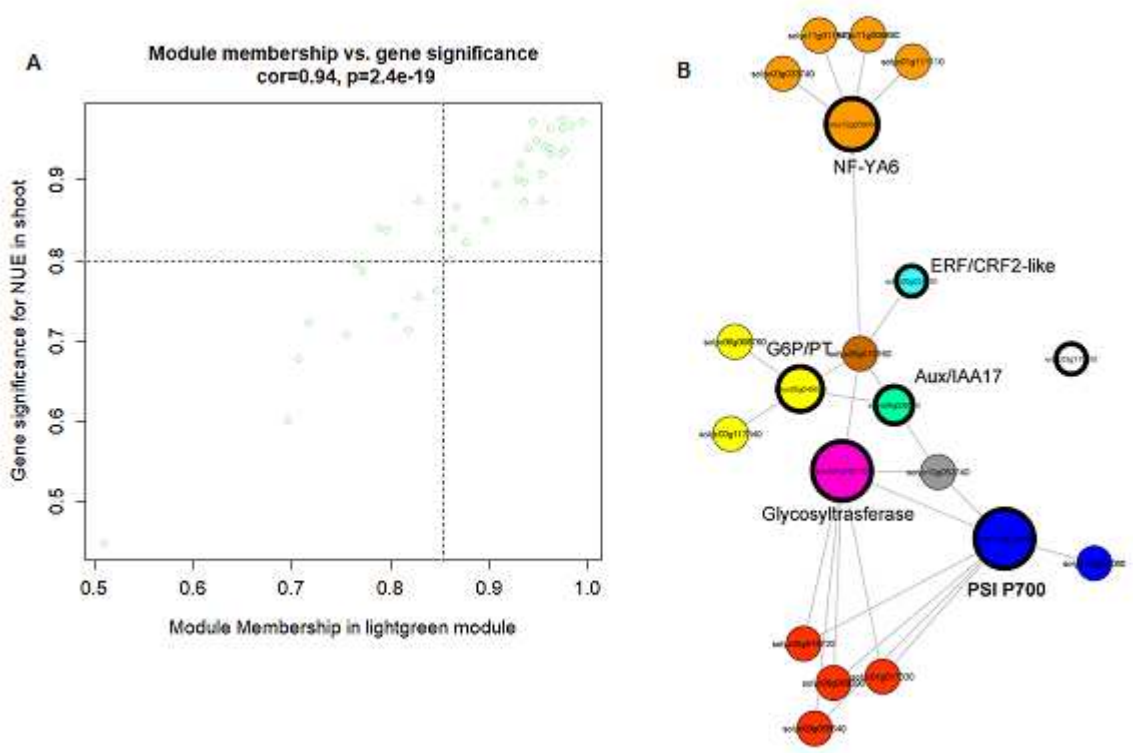

Figure 53. Module membership (MM) *vs.* gene significance (GS) for NUE in the lightgreen module in shoot (A), Network analysis of the hub genes in the same module (B). Node size represents the connectivity degree of genes.

3.2.1.2. Functional analysis of the greenyellow module in shoot

The greenyellow module was also induced by LN and positively correlated to NUE (ME= 0.87). The eigengenes were significantly enriched in photosynthesis, photosynthetic electron transportchain, photosynthetic electron transport in photosystem II and photosynthetic light reaction BP GO term (Table S16). Filtering for a geneModuleMembership > 0.80 and a geneTraitSignificance for NUE > 0.75, we identified fifty-two hub genes (Figure 54A). The network analysis identified six key genes in the module including three TFs, Solyc02g067380.3 (*bHLH style2.1 (PRE2)*), Solyc02g088180.3 (*NAC2*), and four genes namely Solyc04g024540.2 (*Ycf2*), Solyc01g081310.3 (Glutathione S-transferase T3), Solyc11g012130.2 (Early nodulin-like protein 2-like) and Solyc05g016120.2 (PSII protein D1) (Figure 54B).

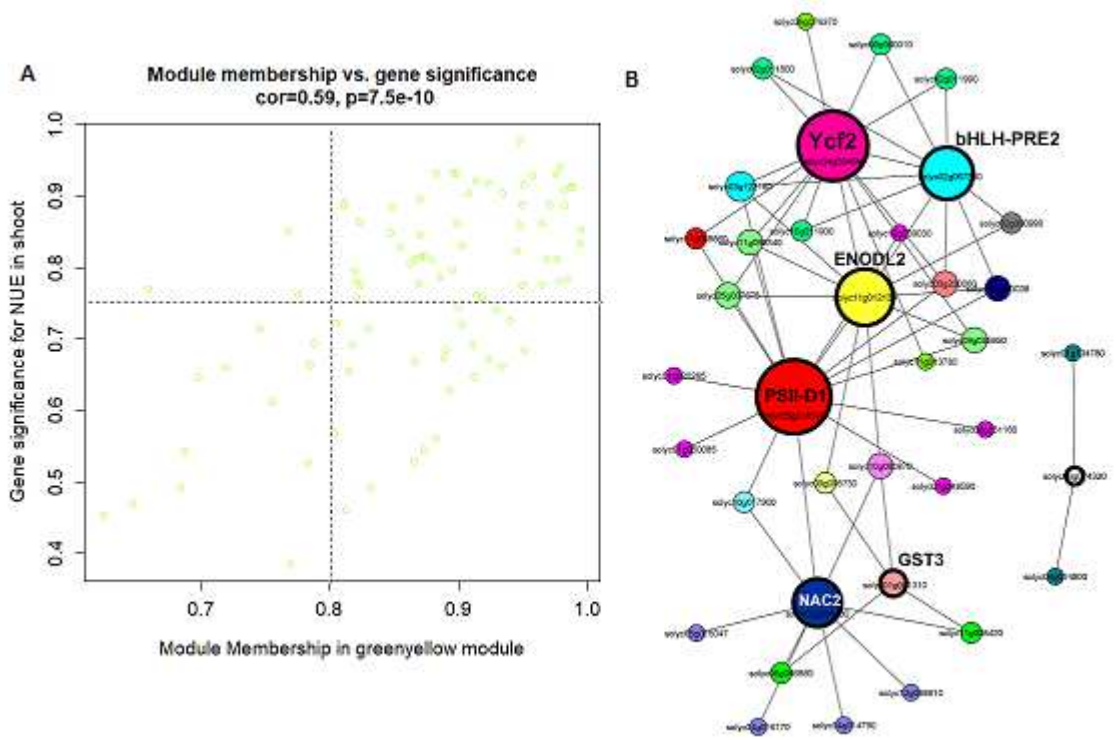

Figure 54. Module membership (MM) *vs.* gene significance (GS) for NUE in the greenyellow module in shoot (A), Network analysis of the hub genes in the same module (B). Node size represents the connectivity degree of genes.

3.2.1.3. Functional analysis of the turquoise module in shoot

The turquoise module was the largest one with 1136 eigengenes, including genes generally down-regulated in response to N-deficiency as the N-assimilation related enzymes encoded by Solyc01g080280.3 (Chloroplast glutamine synthase), Solyc01g108630.3 (Nitrite reductase), Solyc02g086820.3 (Chloroplast carbonic anhydrase) and Solyc03g063560.3 (Glutamate synthase). This module was significantly correlated to SNC (ME= 0.93), SDW (ME= 0.88), and chlorophyll content (SPAD) (ME= 0.66) (Figure 51D). Since high NUE definition was based on a high biomass production (SDW) (see chapter I), the turquoise is the most suitable module to investigate the regulatory network governing LN-response in tomato.

GO term analysis of the eigengenes in this module showed significant enrichment for photosynthesis, organonitrogen compound biosynthetic process, small molecule metabolic process and photosynthesis, light reaction biological process (Table S16). KEGG pathway analysis showed a significant enrichment in photosynthesis, biosynthesis of secondary metabolites and carbon metabolism pathways. More interestingly, the eigengenes in this module were also significantly enriched in carbon fixation in photosynthetic organisms, as well as biosynthesis of amino acids and nitrogen metabolism pathways (Table S17).

One hundred sixty-three hub genes were identified in this module for a geneModuleMembership > 0.95 and a geneTraitSignificance for SDW > 0.85 (Figure 55A). The network analysis revealed 8 key genes related to SDW with the highest connectivity, including Solyc01g009990.3 (Peptidyl-prolyl cis-trans isomerase), Solyc08g006930.3 (photosystem I reaction center subunit psaK, chloroplastic), Solyc02g063150.3 (RuBP carboxylase small subunit), Solyc04g076870.3 (Glutamyl-tRNA reductase), Solyc08g014340.3 (Cysteine synthase), Solyc02g083810.3 (Ferredoxin--NADP reductase, chloroplastic), Solyc04g009030.3 (Glyceraldehyde-3-phosphate dehydrogenase) and Solyc10g018300.2 (Transketolase). The regulatory network showed the highly correlated genes to the identified key genes in turquoise module (PCC > 0.99) (Figure 55B).

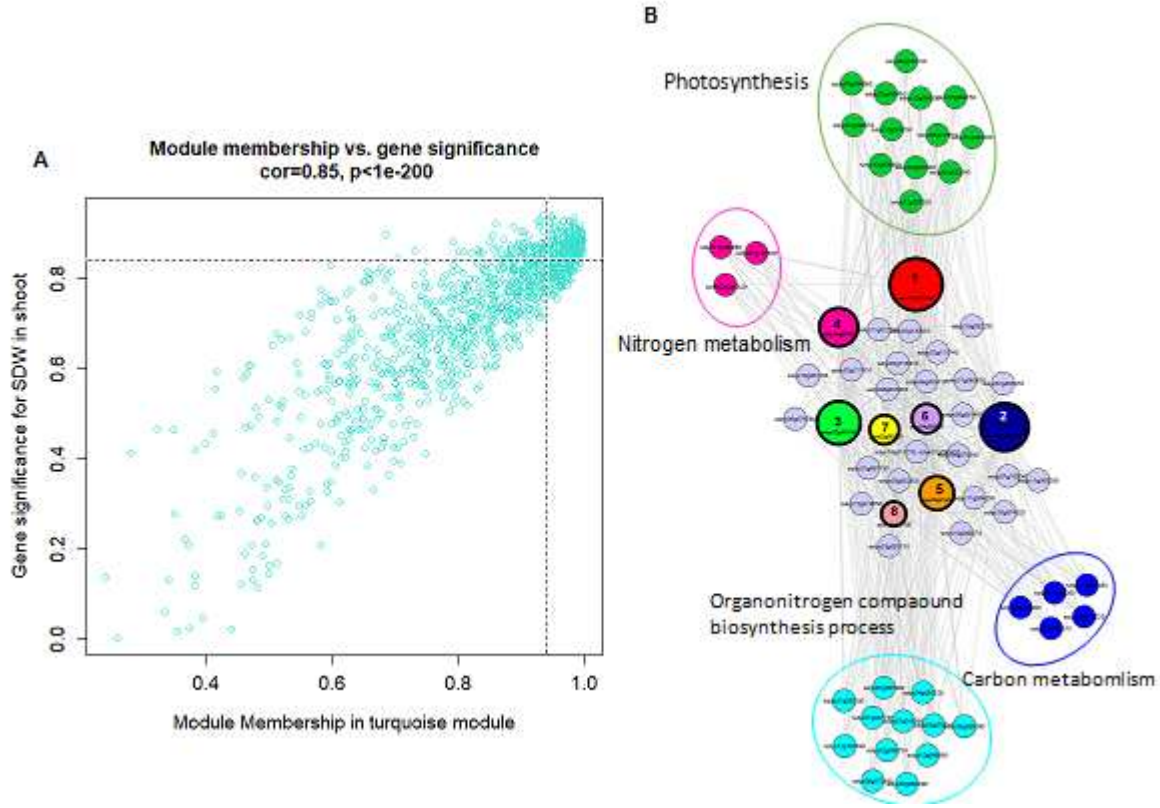

Figure 55. Module membership (MM) *vs.* gene significance (GS) for SDW in the turquoise module in shoot (A), Network analysis of the hub genes in the same module (B). Node size represents the connectivity degree of genes.

3.2.2. NUpE-related modules analysis and identification of hub genes in root

3.2.2.1. Functional analysis of the turquoise module in root

In root, the turquoise module included 235 genes mainly downregulated by LN w.r.t HN in both genotypes. This module was significantly related to NUpE (ME= 0.96) and RN-content (ME= 0.82). GO term analysis of the eigengenes showed significant enrichment in response to stimulus, to inorganic substance and stress, as well as transmembrane transport and response to nitrate biological processes (Table S18). The NUpE-related hub genes in the turquoise module were selected for a geneModuleMembership > 0.85 and a geneTraitSignificance for NUpE > 0.85 (Figure 56A).

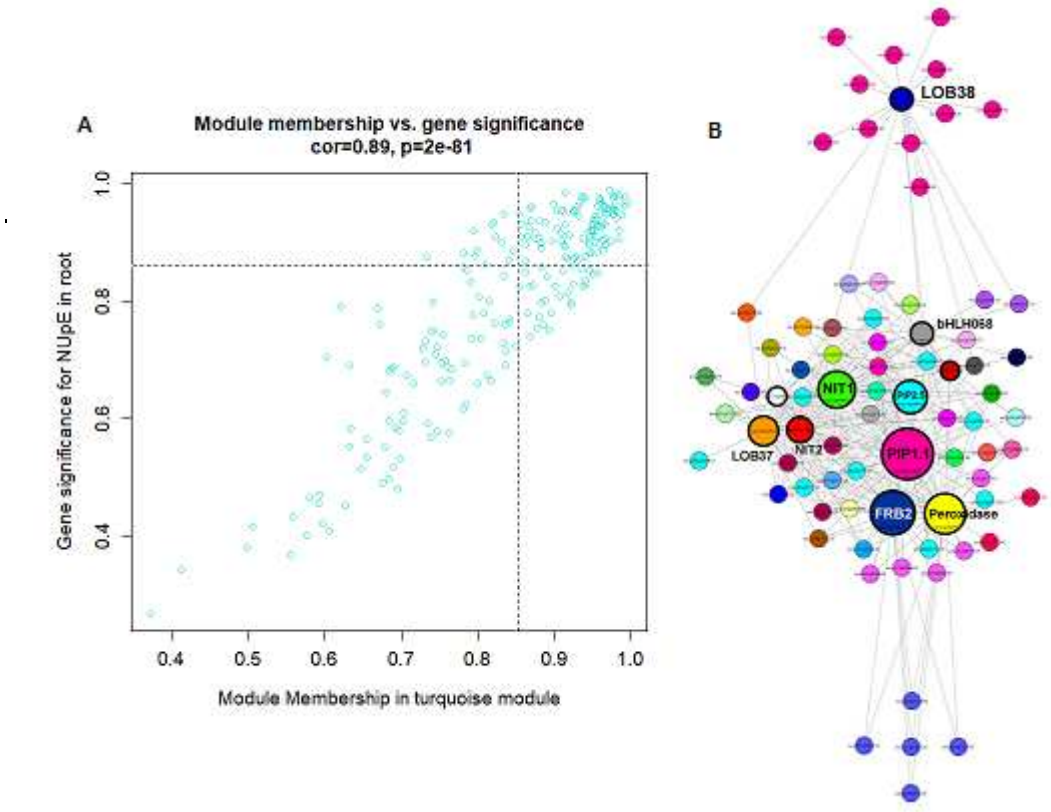

Figure 56. Module membership (MM) *vs*.gene significance (GS) for NUpE in the turquoise module in roots (A), Network analysis of the hub genes in the same module (B). Node size represents the connectivity degree of genes.

One hundred fourteen hub genes were identified and they were significantly enriched in establishment of localization, transport, localization and transmembrane transport BP GO terms. Network analysis allowed the identification of 11 key genes related to NUpE among the most connected genes in the turquoise module, including three N-transporters:

Solyc08g007430.2 (*NIT2*), Solyc08g078950.3 (*NIT1*), and Solyc11g069760.1 (*NRT2.4*); three TFs: Solyc02g092550.3 (*LOB37*), Solyc01g107190.3 (*LOB38*) and Solyc10g079680.2 (*bHLH 068*) and two aquaporins (plasma membrane intrinsic protein): Solyc08g008050.3 (*PIP1.1*) and Solyc10g084120.2 (*PIP2.5*). Furthermore, Solyc12g017910.2 a potassium transporter, Solyc02g090450.3 a Peroxidase 10 and Solyc11g006910.2 a Ferredoxin R-B2 were also identified (Figure 56B).

The heatmaps show the expression patterns of key genes identified for NUE, SDW and NUpE in the different comparisons for N and G effect in lightgreen, greenyellow and turquoise modules in shoot (A), and turquoise in root (B) (Figure 57A,B).

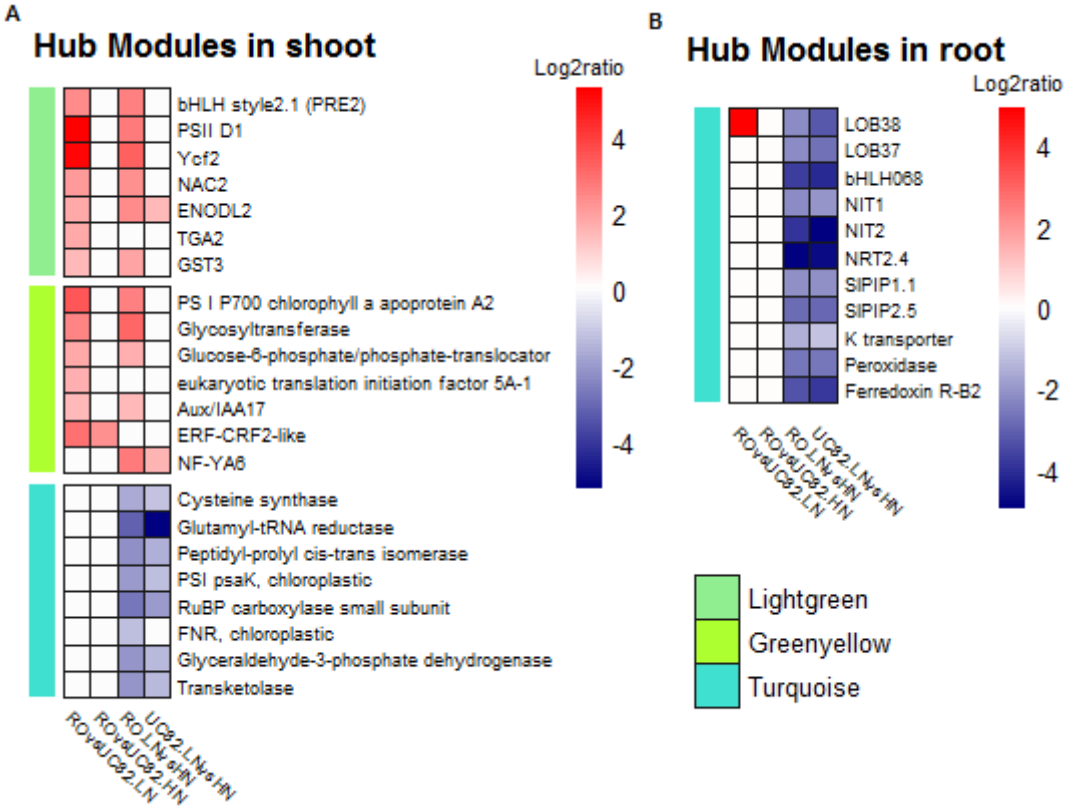

Figure 57. Heatmaps of the expression patterns of the key genes identified for NUE, SDW and NUpE in the different comparisons for N and G effects in modules lightgreen, greenyellow and turquoise in shoot (A), and turquoise in root (B). The values are expressed in log^2FC.

4. Discussion

The identification of key genes involved in the plant adaptation to low N availability has become strategic for improving NUE, especially when NUE-contrasting genotypes are compared (Hirel *et al*., 2007; Kant *et al*., 2010). Recently, through comparative transcriptomic approach, key genes regulating NUE have been identified in several species (Goel *et al*., 2018; Subudhi *et al*., 2020, Mauceri *et al*., 2021). To deepen the knowledge on the molecular mechanisms mediating the long term (7 days) N-deficiency responses leading to high-NUE in tomato, we performed a transcriptomic analysis between two NUE-contrasting genotypes, RO and UC82, which yielded 3,203 and 2,031 DEGs in shoot and root, respectively, taking into account both nitrate (N) and genotype (G) variables.

4.1. LN-stress positively affects photosynthesis in the N-use efficient genotype

A high photosynthesis capacity is mainly dependent on the chloroplasts N content in leaf (Evans, 1989; Evans and Poorter, 2001; Ripullone *et al*., 2003), therefore, N availability affects significantly this vital physiological process (Wei *et al*., 2016; Lin *et al*., 2017). The cross-talk between photosynthesis and N assimilation has been underlined by a significant correlation between the leaf N content and CO_2 assimilation rate (Makino, 2011). Indeed, photosynthesis provides energy and carbon skeletons required for N assimilation, but in this mutual interplay, N promotes the expression of photosynthesis-related genes (Martin *et al*. 2002), and soluble sugars promote the expression of NO_3^- assimilation-related genes (Faure *et al*. 1994; Melo-Oliveira *et al*. 1996). Thus, the interaction between C and N metabolisms is the reason for which N nutrition is crucial for biomass production and crop yield.

De Groot *et al*., (2003) demonstrated that the abundance of PSI and PSII related proteins and their activities were negatively affected by N deficiency in tomato. Recently, the down-regulation of genes encoding components of the photosynthesis light and dark reactions in two rapeseed NUE-contrasting genotypes in response to LN-stress, with less extent in the high-NUE genotype, was reported, suggesting that the photosynthesis process might be inhibited under long-term LN-stress (Yang *et al*., 2020; Li *et al*., 2020). Conversely, in our study, thirty (30) genes were significantly enriched in the photosynthesis process, including photosynthesis light reaction, photosynthetic electron transport chain, and C fixation in Calvin-Benson cycle, and specifically up-regulated by LN-stress in RO compared to UC82.

These results also appeared in agreement with our previous hypothesis, where we supposed that RO at LN was able to allocate more N into the shoot compared to UC82 (Aci *et al*., 2021), which in turn positively affected its photosynthetic process as well as C fixation and assimilation. Recent studies on *Arabidopsis* mutants, *aap2*, with enhanced N partitioning to leaves respect to wild-type, revealed an increase of the electron transport rate as well as chlorophyll and Rubisco contents, which in turn promoted leaf growth, C fixation rate and delay in leaf senescence and overall higher NUE (Perchlik and Tegeder, 2018). The pivotal role of these genes in photosynthesis efficiency and plant growth, among which PSI and II subunits, cytochrome B6/f complex, FNRs and Rubisco, has been previously demonstrated (Carmo-Silva *et al*., 2015; Ermakova *et al*., 2019). Taken together, the up-regulation of the genes involved in photosynthesis in RO shoot compared to UC82 might sustain the different NUE performances between genotypes at long-term LN-stress.

4.2. Co-expression network analysis reveals a synergic effect of root and shoots enriched functions essential for LN-adaptation and NUE enhancement

The co-expression network analysis allows the identification of gene clusters with similar expression pattern, and is useful to assess how genes expression is relevant to a specific phenotype. Here, the WGCNA was applied for the first time, to identify co-expression modules and hub genes correlated to the high-NUE phenotype in tomato. The analysis was able to classify shoot and root N-responsive DEGs in 17 and 15 co-expression modules, respectively. In shoot, the most significant modules (lightgreen and greenyellow) were positively correlated to NUE and SDW, and the functional analysis of the co-expressed genes highlighted their significant involvement in photosynthesis process, C and N metabolism pathways. In root, the most significant co-expression module (turquoise) was correlated to NUpE including genes involved in transmembrane transport activity and response to nitrate biological processes.

In the lightgreen and greenyellow module regulatory networks identified in shoot, three and two hub TF genes were found, respectively. The TFs are known to play a central role in many abiotic stress adaptations including N-deficiency stress (Canales *et al*., 2014). Among them, *bHLH style2.1* and *NAC2* were specifically up-regulated in the N-use efficient genotype under LN. The tomato *bHLH style2.1* or *PRE2* over-expression was reported to promote cell elongation and affect plant morphogenesis (Chen *et al*. 2007, Zhu *et al*., 2017). The *NAC2*

over expression resulted in drought and salt stress tolerant phenotype in tobacco and *Arabidopsis*, by maintaining high chlorophyll content and positively affecting photosynthesis and other biological processes (Borgohain *et al*., 2019; van Beek *et al*., 2021). Interestingly, in the greenyellow module, these hub TF genes were co-expressed with two central hub nodes, the chloroplast protein encoding genes *PSII-D1* and *Ycf2*. In particular, the D1 protein, a key PSII subunit, is dynamically regulated by environmental signals and its decrease results in the photosynthesis inhibition (Nishiyama and Murata, 2014; Watkins *et al*., 2020). In addition, the chloroplastic protein Ycf2 has been recently described as a fundamental component of the chloroplast proteins import complex. This complex, responsible for the protein import from cytosol into the chloroplast, has a crucial role from which rely other plant essential biological processes such as C and N-metabolism (Paila *et al*., 2015; Sjuts *et al*., 2017; Nakai, 2018). Thus, the up-regulation of these genes involved in the photosynthesis machinery regulation in RO respect to UC82 further confirm the RO high potential to adapt to a long-term LN stress.

In root, the module correlated to NUpE was enriched in transmembrane transport and nitrate response. Interestingly, two nitrate transporters *NIT1* and *NIT2* and two aquaporins *PIP1.1* and *PIP2.5* were identified as hub genes in this regulatory network. The two NIT genes are homologs of the *Arabidopsis NPF6.3* encoding gene, a nitrate transporter which coordinates root branching beyond nitrate transport (Liu and Tsay, 2003; Léran *et al*., 2013; Maghiaoui *et al*, 2020; Wang *et al*., 2020). More recently, the over-expression of the *OsNPF6.5* and *VvNPF6.5* homologs from rice and grape resulted in a significantly NUE improvement in rice and *Arabidopsis*, respectively (Hu *et al*., 2015; Wang *et al*., 2018; He *et al*., 2020).

Furthermore, the identification of two plasma membrane-type (PIPs) aquaporins (*PIP1.1* and *PIP2.5*) as central genes in the regulatory network of a NUpE correlated module agreed with their role in water and nutrients transport in the root xylem-mesophyll (Shatil-Cohen *et al*., 2011; Vandeleur *et al*., 2014). Notably, the aquaporins (AQPs) role in plant N uptake and transport is largely regulated by water flow, and this cross-talk has been widely investigated, showing that AQPs over-expression positively affects total N uptake (Tanguilig *et al*., 1987; Aharon *et al*., 2003; Sadok and Sinclair., 2010). Moreover, root aquaporin genes were significantly up-regulated in rice after 24h N-resupply, including *OsPIP1.1*, *OsPIP2.2*, *OsPIP2.3*, *OsPIP2.4* and *OsPIP2.5* (Wang *et al*., 2001). By contrast, *AtPIP2.1*, *AtPIP2.2*, *AtPIP2.4*, *AtPIP1.2*, and *AtPIP1.3* gene expressions significantly decreased in response to 6 days nitrogen starvation (Di Pietro *et al*., 2013). Accordingly, in our transcriptome data, *NIT* and *PIP* genes were key regulator genes in the turquoise module network. Exhibiting a strong

GS for NUpE, they represent significant molecular markers, which over-expression might improve tomato NUpE and by the way NUE in N-deficient condition. Finally, the results of the analyses performed in this chapter allowed us to depict a model scheme of the long-term LN stress regulation in RO (Figure 58).

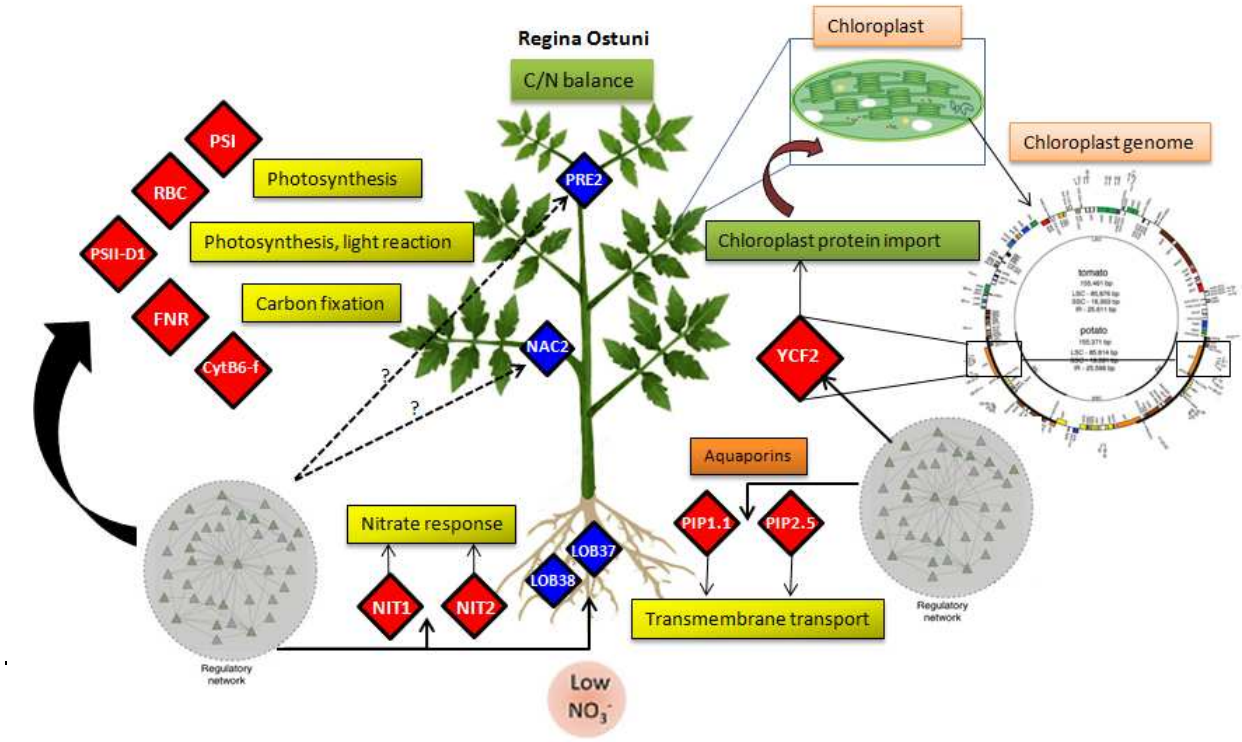

Figure 58. Model scheme showing the multilevel regulation of the long-term low NO_3^- stress in Regina Ostuni. In shoot, the photosynthesis is the main biological process upregulated by stress, including genes involved in photosynthesis light reaction (*PSI*, *PSII*, *CytB6-f*, *FNR*) as well as C fixation (Rubisco, *RBC*) which are central genes in the regulatory networks correlated to NUE. These results suggest the C/N balance as a potential target for NUE improvement. The results also suggest the central role played by the chloroplast in high NUE genotype, since *YCF2* in chloroplast genome is strongly upregulated. Recently reported to be involved in chloroplast protein import, *YCF2* is among the central genes in shoot regulatory network correlated to NUE, suggesting an ongoing and improved activity of chloroplast stroma proteins leading to a higher plant adaptation to NO_3^- stress. In root, the central genes identified in the regulatory networks correlated to NUpE are involved in Nitrate response and transmembrane transport activity biological processes, including two NO_3^- transporters (*NIT1* and *NIT2)* and two aquaporins (*PIP1.1* and *PIP2.5*). The overexpression of these genes should improve solute/ NO_3^- transport and distribution in the plant to sustain plant adaptation to long-term low NO_3^- stress. The induced metabolic pathways and the function of the encoded protein are presented in yellow and orange, respectively. The putative responses resulting from the gene expressions, genes of interest and transcription factors (TFs) are indicated in green, red and blue colors, respectively**.** Tomato chloroplast genome (Daniell *et al.*, 2006).

5. Conclusion

In the present study, we performed a transcriptome comparative analysis of two tomato genotypes in response to low nitrate treatments for 7 days (long-term). Our data provided deeper knowledge on LN-stress adaptive molecular mechanism in tomato and allowed us to identifyspecific gene networks that might confer high NUE. So, we can sustain that the contrasting genotypes adopt different strategies in response to long-term low nitrate

conditions. In shoot, the efficient genotype (RO) compared to the inefficient one (UC82) showed a higher expression of genes related to photosynthesis light and dark reactions. In this respect, future research should focus on the role of chloroplast in plant LN-adaptive responses. The weighted gene co-expression network analysis (WGCNA) in both tissues revealed several nitrate regulatory modules and the main biological functions correlated to NUE and NUpE in tomato. In shoot, the general mechanisms regulating NUE appeared mainly related to photosynthesis process and the interaction between N and C metabolisms. Whereas, in root, the main processes regulating NUpE were related to transmembrane transport activity. The significance of these analyses indicated that in shoot (NUtE) and root (NUpE) the regulated functions might synergistically contribute to the high-NUE phenotype, combining N-transport (root) and photosynthetic (shoot) activities. Thus, our data-mining approach, correlating the morpho-physiological traits to the gene expression profiles, was able to identify new candidate genes and TFs as key regulators for improving tomato NUE, and provided further insight on the LN-stress effect on the biological processes in tomato.

General conclusions and future perspectives

The present PhD thesis aimed to investigate the main differences between two NUE contrasting tomato genotypes, at morpho-physiological and molecular levels, underlying the NUE complex trait. Our comprehensive analyses confirmed the complexity of the physiological and molecular events leading to an efficient N-use in the plant system, as well as the functional regulations taking place in both shoot and root to achieve a high-NUE. They resulted highly controlled at the transcriptional level involving different key genes and regulators that operated in a time and tissue dependent manner.

The analysis on the NUE contrasting genotypes corroborated our previous results confirming a first hypothesis on the major role played by NUtE in the determination of high-NUE phenotype in tomato (Chapter I). Relative expression of genes such as *SlCLCa* and *SlNRT1.5* highlighted two different strategies adopted by the N-use efficient genotype (RO), which placed in order nitrate transport/allocation to shoot for assimilation instead of its storage into root vacuoles as observed in the N-use inefficient ones (UC82). Although the data furnished by this first analysis on the genotype pair were consistent, they were considered as the tip of the iceberg. Thus, to reach a general framework on the molecular mechanisms underlying the LN-deficiency tolerance and the high-NUE in tomato, an RNAseq approach was adopted. Firstly, we dissected and compared the transcriptomic responses between genotypes at short term to study the N-induced responses within 24h N resupply, later, the same experimental setup was adopted under long-term (7 days) LN-stress to detect genotype specific adaptive responses.

Taking into accounts the variables genotype (G), nitrogen supply (N) and sampling time (T) and their interactions, the analysis of differentially expressed genes (DEGs) revealed a time-dependent differential response between genotypes. Two DEG panels were identified: the LN-stress responsive DEGs (identified after short-term LN-resupply) and the LN-stress adaptive DEGs (resulting from the long-term or adaptive responses to LN-stress). Moreover, besides the time effect on the LN-stress responses, we emphasized the specific responses in both tissues at short-term, which roles became synergic at the long-term LN-stress to achieve high-NUE. At short-term (Chapter 2), in shoots, NUE-contrasting genotypes showed a differential regulation of plant hormone signal transduction and protein kinases signaling pathways, in which important genes involved in primary nitrate response such as CIPKs and CDPKs were up-regulated in the NUE-efficient genotype. In root, the same genotype exhibited higher expression of a cinnamyl alcohol dehydrogenase (*CAD*) and a chalcone

synthase 1 (*CHS1*) encoding genes, which are two important enzymes involved in phenylpropanoids and flavonoids biosynthesis, pathways highly induced in the plant stress-adaptive responses. Besides, the differential expression of several TFs such as *GLK2* in shoot and *LOB37* in root could be correlated with a higher LN-tolerance given their involvement in the regulation of chloroplasts development processes and N-assimilation enzyme encoding genes (*NIA* and *NIR*), respectively. These results suggested that the early molecular events in response to LN-stress are pivotal for determining the future adaptive responses.

As a complementary tool to the differential expression analysis, the co-expression network analysis offers the advantage to capture more relevant transcriptomics information using the gene co-expression modules and the analysis of their regulatory networks (Chapter 2 and 3). A set of co-expressed modules associated to LN-stress response in tomato by the weighted gene co-expression network analysis (WGCNA) was identified, providing insights into the biological processes and regulation of the early responses to low N.

The functional analysis of the co-expressed modules correlated to LN-treatment at short-term indicated the putative genes regulating LN-stress responses in the N-use efficient genotype. In detail, a cytokinin riboside 5'-monophosphate phosphoribohydrolase (*LOG8*, Solyc06g075090.3), an ethylene responsive transcription factor (*ERF2*, Solyc01g090340.2) and an asparagine synthetase (*ASNS*, Solyc01g079880.3), as well as a late embryogenesis abundant protein (*LEA*, Solyc01g006320.3) and an annexin5 (*ANN5*, Solyc01g097520.3) were the key regulatory genes in shoot and root, respectively. These results decoded the dynamic regulatory networks of the early responses adopted by the high NUE genotypes (RO) to face LN-stress, in which cytokinin metabolism (*LOG8* and *ERF2*) and ROS balancing *(LEA* and *ANN5)* appeared to be the main regulators.

At long-term (Chapter 3), the genotypes exhibited a differential regulation of the photosynthesis processes, in which most of the related DEGs were up-regulated in the efficient genotype. Among them, we identified both light and dark reaction related genes leading to an unquestionable C/N balancing helpful for growth optimization under low nitrate stress. The WGCNA emphasized the co-expressed modules significantly correlated to NUE and its component NUpE, as well as the main biological functions and key genes in the regulatory networks controlling these complex traits. In shoot, the general mechanisms regulating NUE were related to photosynthesis and the interaction between N and C metabolisms, while those regulating NUpE in root were related to transmembrane transport activity. In shoot, two TFs, *bHLH style2.1* (Solyc02g067380.3) and *NAC2* (Solyc02g088180.3), as well as two chloroplastic protein encoding genes, *Ycf2*

(Solyc04g024540.2), and the photosystem II subunit D1 *psbA* (Solyc05g016120.2) were identified as the key genes in the regulatory network of the NUE-associated module. In root, two nitrate transporters *NIT1* and *NIT2* and two aquaporins *PIP1.1* and *PIP2.5* as key genes in the regulatory network of the NUpE-associated module were identified. These analyses highlighted a possible synergic action of shoot (NUtE) and root (NUpE), combining the photosynthetic and solute transport activities, respectively, to achieve the low nitrate stress adaptation and high-NUE.

The molecular mechanisms and functional features of the genes responsible for NUE in tomato have not been determined so far, but the information obtained from chapter 2 and 3 represent a valuable source of data that will guide our future researches. For instance, the identification of a cytokinin-activating encoding gene as a hub gene in the short-term LN resupply regulatory network suggests the key role of this hormone in sustaining NO_3^--stress and high NUE in tomato. These findings are in agreement with previous studies which highlighted the high correlation between nitrogen nutrition and cytokinin content observed in several crops such as tobacco, barley and maize, as well as the role played by cytokinin in the partial restoration of the morphological adaptation to nutritional stress. Accordingly, future researches might focus on the comparative evaluation of the endogen cytokinin level in response to short- and long-term NO_3^- stress between RO and UC82 to elucidate the effective role of cytokinin in high NUE. In addition, *Ycf2* as hub gene in the NUE regulatory network attracted our attention on the potential role that chloroplast might play in the regulation of NO_3^- stress and NUE improvement. Thus, further researches should focus on the comparative analysis of the chloroplast protein import between RO and UC82 to highlight the chloroplast proteome modulation in response to N stress.

Likewise, increasing knowledge on the *Arabidopsis* genes and their transcripts has produced a large number of mutants for specific genes. Thus, the identified tomato NUE key regulatory genes, such as *NIT1* and *NIT2,* as well as *bHLH style 2.1* and *NAC2* were found to be *AtNPF6.3, AtBNQ3* and *AtORE1* homologs, respectively. The incorporation of such genes in targeted studies would complement our findings by validating their effective implication in NUE and NUpE. In addition, to date most of the genetic studies focused on over-expressing gene of interest to improve NUE, but the advances in genome sequencing and high-throughput approaches have enabled the researchers to use genome editing tools for the functional characterization of many genes useful for crop improvement. Hence, the use of CRISPR/Cas9 to down-regulate or knockdown the identified key genes would be a more specific approach to improve NUE in tomato. Finally, the study of the proteome and

metabolome changes beside the transcriptome response and estimate their correlations is another important objective. The combination of different “omics” studies will provide a more detailed view on the tomato response to low nitrate stress, and will allow us to have a complete framework on NUE mechanisms to better guide future breeding programs in the frame of sustainable agriculture.

Acknowledgements

Many times I thought about the moment to write these words of appreciation for the moments that I lived during the PhD. One of the great things of my PhD is that I had to interact with many people, before COVID pandemic has come and restricted everything. I hope to not forget some people. If I do, I apologize in advance.

I would like to acknowledge my tutor Professor Francesco Sunseri and my co-tutor Professor Maria Rosa Abenavoli for giving me the opportunity to perform this research. I appreciate all your support, your precious time and help, and your humble commitment during these 3 years.

I would like to thank Dr. Antonio Lupini for the encouragement, the precious time and the long scientific discussions that we shared. You solved many problems very quickly and I will always thank you for your kind availability and humble commitment.

Also, I would like to thank the Professor Antonio Gelsomino, Professor Agostino Sorgonà, Dr. Francesco Mercati and Dr. Guglielmo Puccio that allowed and helped me to achieve diverse analyses.

All my acknowledgments go to my Lab colleagues Antonio Mauceri, Rossana Sidari, Antonio Calvi, Emilio Lopresti, Giuseppe Badaglicca, Rosa Vescio, Antonino Zumbo and Ciro Caldiero, each one of you brought me strength and joy and I spend a great time with you during lab work and outside.

Thanks to all my PhD colleagues, the friends with whom I shared the best and the worst of this journey (and more): Gianmarco Carrà, Valentina Librizzi, Enrica Alicandri, Valeria Imeneo, Maria Rosaria Tassone, Antonella Nucera and Rosa Rao.

A special thank goes to all my Italian and Algerian friends for their support and love: Anna Rocca, Soraya Belalia, Bea, Mina, Anna Caputo, Nawel Malek, Rossana Sidari, Rosa Vescio, Gaetano Messina, Nino, Tomasso, Luigi, all boys and girls of Residenza Universitaria di Merito via Roma as well as Rocco Sicari, Professors Catanoso and Professor Bagnato for giving me the opportunity to live 3 years in a beautiful and peaceful context.

Many thanks to Dr.ssa Angela Crucitti for her continuous availability and kind help during these 3 academic years.

References

- Abenavoli MR, Longo C, Lupini A, Miller AJ, Araniti, F, Mercati F, et al. (2016) Phenotyping two tomato genotypes with different nitrogen use efficiency. *Plant Physiol. Biochem.* **107**: 21-32.
- Aci MM, Lupini A, Mauceri A, Sunseri F, Abenavoli MR (2021) New insights into N-utilization efficiency in tomato (*Solanum lycopersicum* L.) under N limiting condition. *Plant Physiol. Biochem* **166**: 634–644.
- Aharon R, Shahak Y, Wininger S, Bendov R, Kapulnik Y, Galili G (2003) Overexpression of a plasma membrane aquaporin in transgenic tobacco improves plant vigor under favorable growth conditions but not under drought or salt stress. *Plant Cell.* **15**: 439-447.
- Alfatih A, Wu J, Zhang ZS, Xia JQ, Jan SU, Yu LH, Xiang CB (2020) Rice NIN-LIKE PROTEIN 1 rapidly responds to nitrogen deficiency and improves yield and nitrogen use efficiency. *J. Exp. Bot.* **71**: 6032–6042.
- Almagro A, Lin SH, Tsay YF (2008) Characterization of the Arabidopsis nitrate transporter NRT1.6 reveals a role of nitrate in early embryo development. *Plant Cell* **20**: 3289-3299
- Alvarez JM, Vidal EA, Gutiérrez RA (2012) Integration of local and systemic signaling pathways for plant N responses. *Current Opinion in Plant Biology* **15**:185-191.
- Anas M, Liao F, Verma KK, Sarwar MA, Mahmood A, Chen ZL, et al. (2020) Fate of nitrogen in agriculture and environment: agronomic, eco-physiological and molecular approaches to improve nitrogen use efficiency. *Biological Research* **53**: 47-66.
- Andrews M (1986) The partitioning of nitrate assimilation between root and shoot of higher plants. *Plant Cell Environ*. **9**: 511-519.
- Andrews M, Lea PJ (2013) Our nitrogen 'footprint': the need for increased crop nitrogen use efficiency. *Annals of Applied Biology* **163**: 165– 169.
- Antonacci S, Maggiore T, Ferrante A (2007) Nitrate Metabolism in Plants under Hypoxic and Anoxic Conditions. *Plant Stress* **1(2)**: 136-141
- Austin AT, Bustamante MMC, Nardoto GB, Mitre SK, Pérez T, Ometto JPHB, et al. (2013) Latin America's nitrogen challenge. *Science* **340**: 149.

- Ballif J, Endo S, Kotani M, MacAdam J, Wu Y (2011) Over-expression of HAP3b enhances primary root elongation in *Arabidopsis*. *Plant Physiol. Biochem.* **49**: 579–583.
- Barbier-Brygoo H, De Angeli A, Filleur S, Frachisse JM, Gambale F, Thomine S, et al. (2011) Anion channels/transporters in plants: from molecular bases to regulatory networks. *Annu. Rev. Plant Biol.* **62**: 25–51.
- Barone A, Chiusano ML, Ercolano MR, Giuliano G, Grandillo S, Frusciante L (2008) Structural and functional genomics of tomato. *Int. J. Plant Genom.* **2008**:1-12.
- Bender KW, Zielinski RE, Huber SC (2018) Revisiting paradigms of Ca^{2+} signaling protein kinase regulation in plants. *Biochemical J.* **475**: 207–223.
- Berendse F, Aerts R (1987) Nitrogen-use-efficiency: a biologically meaningful definition? *Functional Ecology* **1**: 293–296.
- Bernard SM, Habash DZ (2009) The importance of cytosolic glutamine synthetase in nitrogen assimilation and recycling. *New Phytol*. **182**: 608–620.
- Bi YM, Wang RL, Zhu T, Rothstein SJ (2007) Global transcription profiling reveals differential responses to chronic nitrogen stress and putative nitrogen regulatory components in Arabidopsis. *BMC Genomics* **8**: 281.
- Bigot J, Lefevre J and Boucaud J (1991) Changes in the amide and amino acid composition of xylem exudates from perennial ryegrass (*Lolium Perenne* L.) during regrowth after defoliation. *Plant and Soil* **136**: 59-64.
- Bloom AJ (2015) Photorespiration and nitrate assimilation: a major intersection between plant carbon and nitrogen. *Photosynth Res* **123**: 117–128
- Borgohain P, Saha B, Agrahari R, Chowardhara B, Sahoo S, van der Vyver C, Panda SK (2019) SlNAC2 overexpression in Arabidopsis results in enhanced abiotic stress tolerance with alteration in glutathione metabolism. *Protoplasma* **256**: 1065-1077.
- Boudsocq M, Sheen J (2013) CDPKs in immune and stress signaling. *Trends Plant Sci* 18: 30–40.
- Bouguyon E, Brun F, Meynard D, Kubes M, Pervent M, Léran S, et al. (2015). Multiple mechanisms of nitrate sensing by Arabidopsis nitrate transceptor NRT1.1. *Nature Plants* **1**: 15015.
- Brooks C, Nekrasov V, Lippman ZB, Van Eck J (2014) Efficient gene editing in tomato in the first generation using the clustered regularly interspaced short palindromic repeats/CRISPR-associated9 system. *Plant Physiol*. **166**: 1292-7.

- Brooks MD, Cirrone J, Pasquino AV, et al. (2019) Network Walking charts transcriptional dynamics of nitrogen signaling by integrating validated and predicted genome-wide interactions. *Nature Communications* **10**: 1569.
- Brunetti C, Di Ferdinando M, Fini A, Pollastri S, Tattini M (2013) Flavonoids as Antioxidants and Developmental Regulators: Relative Significance in Plants and Humans. *Int. J. Mol. Sci*. **14**: 3540-3555.
- Buer CS, Imin N, Djordjevic MA (2010) Flavonoids: New roles for old molecules. *J. Integ. Plant. Biol.* **52**: 98–111.
- Buer CS, Muday GK, Djordjevic MA (2007) Flavonoids are differentially taken up and transported long distances in Arabidopsis. *Plant Physiol*. **145**: 478–490.
- Butterbach-Bahl K, Gundersen P, Ambus P, Augustin J, Beier C, Boeckx P, et al. (2011) Nitrogen processes in terrestrial ecosystems. In Sutton MA, Howard CM, Erisman JW (Eds) *The European nitrogen assessment: sources, effects and policy perspectives*, Cambridge University Press.
- Campbell WH (1999) Nitrate reductase structure, function and regulation: bridging the gap between biochemistry and physiology. *Annu. Rev. Plant Phys*. **50**: 277-303.
- Canales J, Contreras-López O, Álvarez JM, Gutiérrez RA (2017) Nitrate induction of root hair density is mediated by TGA1/TGA4 and CPC transcription factors in *Arabidopsis thaliana*. *Plant J*. **92**: 305-316.
- Canales J, Moyano TC, Villarroel E, Gutiérrez RA (2014) Systems analysis of transcriptome data provides new hypotheses about Arabidopsis root response to nitrate treatments. *Front Plant Sci*. **5**: 22.
- Cantarella H, Otto R, Soares RJ, Gomes de Brito Silva A (2018) Agronomic efficiency of NBPT as a urease inhibitor: a review. *J Adv Res* **13**: 19–27.
- Carmo-Silva E, Scales JC, Madgwick PJ, Parry MA. (2015) Optimizing Rubisco and its regulation for greater resource use efficiency. *Plant, Cell & Environment* **38**: 1817-1832.
- Carrari F, Baxter C, Usadel B, Urbanczyk-Wochniak E, Zanor M-I, Nunes-Nesi A, et al. (2006) Integrated Analysis of Metabolite and Transcript Levels Reveals the Metabolic Shifts That Underlie Tomato Fruit Development and Highlight Regulatory Aspects of Metabolic Network Behavior. *Plant Physiology* **142**: 1380-1396.
- Castaings L, Camargo A, Pocholle D, Gaudon V, Texier Y, Boutet-Mercey S, et al. (2009) The nodule inception-like protein 7 modulates nitrate sensing and metabolism in Arabidopsis. *Plant J*. **57**: 426-435.

- Ceccarelli S (1996) Adaptation to low/high input cultivation. *Euphytica* **92**: 203-214.
- Cerezo M, Tillard P, Filleur S, Munos S, Daniel-Vedele F, Gojon A (2001) Major alterations of the regulation of root NO_3^- uptake are associated with the mutation of *Nrt2.1* and *Nrt2.2* genes in Arabidopsis. *Plant Physiol*. **127**: 262– 271.
- Chamizo-Ampudia A, Sanz-Luque E, Llamas A, Galvan A, Fernandez E, (2017) Nitrate Reductase Regulates Plant Nitric Oxide Homeostasis. *Trends Plant Sci*. **22(2)**:163-174.
- Chardin C, Schenk ST, Hirt H, Colcombet J, Krapp A (2017) Mitogen-Activated Protein Kinases in nutritional signaling in Arabidopsis. *Plant Sci*. **260**: 101-108.
- Chardon F, Barthélémy J, Daniel-Vedele F, Masclaux-Daubresse C (2010) Natural variation of nitrate uptake and nitrogen use efficiency in Arabidopsis thaliana cultivated with limiting and ample nitrogen supply. *J. Exp. Bot*. **61**: 2293-2302.
- Chatzav M, Peleg Z, Ozturk L, Yazici A, Fahima T, Cakmak I, Saranga Y (2010) Genetic diversity for grain nutrients in wild emmer wheat: potential for wheat improvement. *Ann Bot* **105**: 1211–1220.
- Chen K, Chen H, Tseng C, Tsay Y (2020) Improving nitrogen use efficiency by manipulating nitrate remobilization in plants. *Nature Plants* **6**: 1126-1135.
- Chen KY, Cong B, Wing R, Vrebalov J, Tanksley SD (2007) Changes in regulation of a transcription factor lead to autogamy in cultivated tomatoes. *Science* **318**: 643–645.
- Chen Z, Liu C, Wang Y, He T, Gao R, Xu H, et al. (2018) Expression Analysis of Nitrogen Metabolism-Related Genes Reveals Differences in Adaptation to Low-Nitrogen Stress between Two Different Barley Cultivars at Seedling Stage. *Int. J. Genomics* **2018**: 1-10.
- Chopin F, Orsel M, Dorbe MF, Chardon F, Truong HN, Miller AJ, et al. (2007) The *Arabidopsis* AtNRT2.7 nitrate transporter controls nitrate content in seeds. *Plant Cell* 19: 1590-1602.
- Clay NK, Nelson T (2002) VH1, a provascular-specific receptor kinase that influences leaf cell patterns in Arabidopsis. *Plant Cell* **14**: 2707–2722.
- Congreves KA, Otchere O, Ferland D, Farzadfar S, Williams S, Arcand MM (2021) Nitrogen Use Efficiency Definitions of Today and Tomorrow. *Front. Plant Sci*. **12**:637108.
- Coque M, Galleis A (2007) Genetic variation for Nitrogen Remobilization and Postsilking Nitrogen Uptake in Maize Recombinant Inbred Lines: Heritabilities and Correlations among Traits. *Crop Science* **47**: 1787-1796.

- Cormier F, Foulkes J, Hirel B, Gouache D, Moenne-Loccoz Y, Le Gouis J (2016) Breeding for increased nitrogen-use efficiency: a review for wheat (*T. aestivum* L.). *Plant Breed*. **135**: 255–278.
- Crawford N, Glass A (1998) Molecular and physiological aspects of nitrate uptake in plants. *Trends Plant Sci*. **3**: 389-395.
- Crawford NM (1995) Nitrate: nutrient and signal for plant growth. *Plant Cell* **7**: 859–868.
- Crawford NM, Forde BG (2002) Molecular and developmental biology of inorganic nitrogen nutrition. In Meyerowitz E, Somerville C (Eds) *The Arabidopsis Book*. American Society of Plant Biologists, Rockville, MD.
- Crews TE, Peoples MB (2004) Legume versus fertilizer sources of nitrogen: ecological tradeoffs and human needs. *Agric. Ecosyst. Environ*. **102**: 279–297.
- Dan Y, Yan H, Munyikwa T, Dong J, Zhang Y, Armstrong CL (2006) MicoTom-a high-throughput model transformation system for functional genomics. *Plant Cell Rep* **25**: 432–441.
- Daniell H, Lee SB, Grevich J, Saski C, Quesada-Vargas T, Guda C et al. (2006) Complete chloroplast genome sequences of Solanum bulbocastanum, Solanum lycopersicum and comparative analyses with other Solanaceae genomes. *Theor Appl Genet.* **112(8)**: 1503-1518.
- Dao TT, Linthorst HJ, Verpoorte R (2011) Chalcone synthase and its functions in plant resistance. *Phytochemistry reviews* **10**: 397–412.
- De Angeli A, Monachello D, Ephritikhine G, Frachisse JM, Thomine S, Gambale F, Barbier-Brygoo H (2006) The nitrate/proton antiporter *AtCLCa* mediates nitrate accumulation in plant vacuoles. *Nature* **442**: 939-942.
- De Groot CC, Marcelis LFM, Van den Boogaard R, Kaiser WM, Lambers H (2003). Interaction of nitrogen on phosphorus nutrition in determining growth. *Plant Soil* **248**: 257-268.
- Debaeke P, Rouet P, Justes E (2006) Relationship between the normalized SPAD index and the nitrogen nutrition index: Application to durum wheat. *J. Plant Nutrition* **29**: 75-92.
- Debnath M, Pandey M, Bisen PS (2011) An omics approach to understand the plant abiotic stress. *Omics* **15**: 739–762.

- Di Pietro M, Vialaret J, Li GW, Hem S, Prado K, Rossignol M, et al. (2013) Coordinated post-translational responses of aquaporins to abiotic and nutritional stimuli in *Arabidopsis* roots. *Mol. Cell. Proteom.* **12**: 3886–3897.
- Diaz C, Lemaitre T, Christ C, et al. (2008) Nitrogen recycling and remobilization are differentially controlled by leaf senescence and development stage in Arabidopsis under low nitrogen nutrition. *Plant Physiology* **147**: 1437–1449.
- Diaz C, Saliba-Colombani V, Loudet O, Belluomo P, Moreau L, Daniel-Vedele F, et al. (2006) Leaf yellowing and anthocyanin accumulation are two genetically independent strategies in response to nitrogen limitation in Arabidopsis thaliana. *Plant Cell Physiol*. **47**: 74–83.
- Dievart A, Clark SE (2004) LRR-containing receptors regulating plant development and defense. *Development* **131**: 251–261.
- Dimkpa CO, Andrews J, Sanabria J, Bindraban PS, Singh Upendra Elmer, WH, Gardeatorresdey JL, White JC (2020) Interactive effects of drought, organic fertilizer, and zinc oxide nanoscale and bulk particles on wheat performance and grain nutrient accumulation. *Sci. Total Envir*. **722**: 137808
- Doorenbos J, Kassam AH (1986) Yield response to water. FAO Irrigation and Drainage Paper 33. Rome, FAO.
- Ermakova M, Lopez-Calcagno PE, Raines CA, Furbank RT, Von Caemmerer S (2019) Overexpression of the Rieske FeS protein of the Cytochrome b6f complex increases C4 photosynthesis in *Setaria viridis*. *Commun Biol* **2**: 314
- Ernst J, Bar-Joseph Z (2006) STEM: a tool for the analysis of short time series gene expression data. *BMC Bioinformatics* **7**: 191.
- Ernst OR, Kemanian AR, Mazzilli S, Siri-Prieto G, Dogliotti S (2020) The dos and don'ts of no-till continuous cropping: evidence from wheat yield and nitrogen use efficiency. *Field Crops Res*. **257**:107934.
- Esteban R, Ariz I, Cruz C, Moran JF (2016) Mechanisms of ammonium toxicity and the quest for tolerance. *Plant Science* **248**: 92–101.
- Evans JR (1989) Photosynthesis and nitrogen relationships in leaves of C3 plants. *Oecologia* **78**: 9-19
- Evans JR and Poorter H (2001) Photosynthetic acclimation of plants to growth irradiance: the relative importance of specific leaf area and nitrogen partitioning in maximizing carbon gain. *Plant, Cell & Environment* **24**: 755-767.

- Fageria NK, Baligar VC (2005) Enhancing nitrogen use efficiency in crop plants. In Sparks DL (Eds) *Advances in Agronomy*, San Diego, FL: Elsevier Academic Press Inc.
- Fan SC, Lin CS, Hsu PK, Lin SH, Tsay YF (2009) The Arabidopsis nitrate transporter NRT1.7, expressed in phloem, is responsible for source-to-sink remobilization of nitrate. *Plant Cell* **21**: 2750-2761.
- Fan X, Naz M, Fan X, Xuan W, Miller AJ, Xu G (2017) Plant nitrate transporters: from gene function to application. *J. Exp. Bot*. **68**: 2463–2475.
- Faure JD, Jullien M, Caboche M (1994) Zea3: a pleiotropic mutation affecting cotyledon development, cytokinin resistance and carbon-nitrogen metabolism. *Plant J.* **5**: 481–491.
- Filleur S, Daniel-Vedele F (1999) Expression analysis of a high-affinity nitrate transporter isolated from Arabidopsis thaliana by differential display. *Planta* **207**: 461–469.
- Fisher KA, Meisinger JJ, James BR (2016) Urea hydrolysis rate in soil toposequences as influenced by pH, carbon, nitrogen, and soluble metals. *J. Environ. Qual*. **45**: 349–359.
- Food and Agriculture Organization of the United Nations, 2020. FAOstat Database. Rome, Italy: FAO. Retrieved May 20, 2020 from http://faostat3.fao.org/home
- Forde BG (2014) Nitrogen signaling pathways shaping root system architecture: an update. *Curr. Opin. Plant Biol*. **21**: 30–36.
- Forde BG, Clarkson DT (1999) Nitrate and ammonium nutrition of plants: Physiological and molecular perspectives. *Adv. Bot. Res.* 301: 1-90.
- Forde BG, Lea PJ (2007) Glutamate in plants: metabolism, regulation, and signaling. J. *Exp. Bot.* **58**: 2339– 2358.
- Fox AR, Maistriaux LC, Chaumont F (2017) Toward understanding of the high number of plant aquaporin isoforms and multiple regulation mechanisms. *Plant Science* **264**: 179–187.
- Foyer CH, Shigeoka S (2011) Understanding oxidative stress and antioxidant functions to enhance photosynthesis. *Plant Physiol*. **155**: 93–100.
- Frary A, Nesbitt TC, Frary A, Grandillo S, Van Der Knaap E, Cong B, et al. (2000) A quantitative trait locus key to the evolution of tomato fruit size. *Science* **289**: 85–88.
- Fredes I, Moreno S, Diaz FP, Gutierrez RA (2019) Nitrate signaling and the control of Arabidopsis growth and development. *Current Opinion in Plant Biology* **47**: 112-118

- Gallais A, Coque M (2005) Genetic variation and selection for nitrogen use efficiency in maize, a synthesis. *Maydica* **50**: 531–547.
- Gao S, Song T, Han J, He M, Zhang Q, Zhu Y, Zhu Z (2020) A calcium-dependent lipid binding protein, OsANN10, is a negative regulator of osmotic stress tolerance in rice; *Plant Sci.* **293**: 11
- Gaudinier A, Rodriguez-Medina J, Zhang L, Olson A, Liseron-Monfils C, Bågman AM, et al. (2018) Transcriptional regulation of nitrogen-associated metabolism and growth. *Nature* **563**: 259–264.
- Gaudinova A (1990) The Effect of Cytokinins on Nitrate Reductase Activity. *Bioogia Plantarum (PRAHA)* 32 (2): 89-96.
- Geelen D, Lurin C, Bouchez D, Frachisse JM, Lelievre F, Courtial B, et al. (2000) Disruption of putative anion channel gene AtCLC-a in Arabidopsis suggests a role in the regulation of nitrate content. *Plant J.* **21**: 259-267.
- Gehan MA, Greenham K, Mockler TC, McClung CR (2015) Transcriptional networks-crops, clocks, and abiotic stress. *Current Opinion in Plant Biology* **24**: 39–46.
- Geiger D, Maierhofer T, AL-Rasheid KAS, Scherzer S, Mumm P, Liese A, et al. (2011) Stomatal closure by fast abscisic acid signaling is mediated by the guard cell anion channel SLAH3 and the receptor RCAR1. *Sci. Signal*. **4**: ra32
- Gelli M, Duo Y, Konda AR, Zhang C, Holding DR, Dweikat IM (2014) Identification of differentially expressed genes between sorghum genotypes with contrasting nitrogen stress tolerance by genome-wide transcriptional profiling. *BMC Genomics* **15**: 179.
- Glass AD, Britto DT, Kaiser BN, Kinghorn JR, Kronzucker HJ, Kumar A, et al. (2002) The regulation of nitrate and ammonium transport systems in plants. *J. Exp. Bot*. **53**: 855–864.
- Glass ADM, Shaff JE, Kochian LV (1992) Studies of the uptake of nitrate in barley. IV. Electrophysiology. *Plant Physiol*. **99**: 456–463.
- Goel P, Sharma NK, Bhuria M, Sharma V, Chauhan R, Pathania S, et al. (2018) Transcriptome and Co-Expression Network Analyses Identify Key Genes Regulating Nitrogen Use Efficiency in *Brassica juncea* L. *Sci. Rep.* **8**: 7451.
- Gojon A, Krouk G, Perrine-Walker F, Laugier E (2011) Nitrate transceptor(s) in plants. *J. Exp. Bot*. **62**: 2299–2308.

- Good AG, Johnson SJ, De Pauw M, Carroll RT, Savidov N, Vidmar J, et al. (2007). Engineering nitrogen use efficiency with alanine aminotransferase. *Botany* **85**: 252–262.
- Good AG, Shrawat AK, Muench DG (2004) Can less yield more? Is reducing nutrient input into the environment compatible with maintaining crop production? *Trends Plant Sci*. **9**: 597-605.
- Granato ISC, Bermudez FP, Reis GG, Dovale JC, Miranda GV, Fritsche-Neto R (2014) Index selection of tropical maize genotypes for nitrogen use efficiency. *Bragantia* **73**: 153-159.
- Guan P (2017) Dancing with Hormones: A Current Perspective of Nitrate Signaling and Regulation in Arabidopsis. *Front. Plant Sci.* **8**:1697.
- Guo FQ, Wang R, Crawford NM (2002) The Arabidopsis dual-affinity nitrate transporter gene AtNRT1.1 (CHL1) is regulated by auxin in both shoots and roots. *J. Exp. Bot*. **53**: 835–844.
- Guo JH, Liu XJ, Zhang Y, Shen JL, Han WX, Zhang WF, et al. (2010). Significant acidification in major Chinese croplands. *Science* **327**: 1008–1010.
- Gupta S, Rashotte AM (2014) Expression patterns and regulation of SlCRF3 and SlCRF5 in response to cytokinin and abiotic stresses in tomato (*Solanum lycopersicum*)**.** *J. Plant Physiol*. **171**: 349-358.
- Gutiérrez RA (2012) Systems biology for enhanced plant nitrogen nutrition. *Science* **336**: 1673-1675.
- Hachiya T, Sakakibara H (2017) Interactions between nitrate and ammonium in their uptake, allocation, assimilation, and signaling in plants. *J. Exp. Bot*. **68**: 2501-2512.
- Halvorson AD, Reule CA (2007) Irrigated, no-till corn and barley response to nitrogen in northern Colorado. *Agronomy Journal* **99**: 1521-1529.
- Han YL, Liao Q, Yu Y, Song HX, Liu Q, Rong XM, et al. (2015) Nitrate reutilization mechanisms in the tonoplast of two Brassica napus genotypes with different nitrogen use efficiency. *Acta Physiol. Plant*. **37**: 42.
- Han YL, Song HX, Liao Q, Yu Y, Jian SF, Lepo JE, Liu Q, et al. (2016) Nitrogen use efficiency is mediated by vacuolar nitrate sequestration capacity in roots of *Brassica napus*. *Plant Physiol.* 170: 1684-1698.
- Hannon GJ (2002) RNA interference. *Nature* **418**: 244–251.

- Hao QN, Zhou XA, Sha AH, Wang C, Zhou R, Chen SL (2011) Identification of genes associated with nitrogen-use efficiency by genome-wide transcriptional analysis of two soybean genotypes. *BMC Genomics* **12**: 525-536.
- Harmon AC, Gribskov M, Harper JF (2000) CDPKs - a kinase for every Ca^{2+} signal? *Trends Plant Sci.* **4:**154-159.
- Hawkesford MJ, Horst W, Kichey T, Lambers H, Schjoerring J, Møller IS, White P (2012) Functions of Macronutrients. In Marschner P (Eds) *Mineral Nutrition of Higher Plants*, San Diego: Academic Press, pp. 135–189.
- Hawkesford MJ, Riche AB (2020) Impacts of G x E x M on nitrogen use efficiency in wheat and future prospects. *Front. Plant Sci*. **11**: 1157.
- He Y, Xi X, Zha Q, Lu Y, Jiang A (2020) Ectopic expression of a grape nitrate transporter VvNPF6.5 improves nitrate content and nitrogen use efficiency in Arabidopsis. *BMC Plant Biol* **20**: 549.
- Hernandez-Garcia CM, Finer JJ (2014) Identification and validation of promoters and cis-acting regulatory elements. *Plant Sci.* **217**: 109–119.
- Herridge DF, Peoples MB, Boddey RM (2008) Global inputs of biological nitrogen fixation in agricultural systems. *Plant Soil* **311**: 1–18.
- Hirayama T, Shinozaki K (2010) Research on plant abiotic stress responses in the post-genome era: past, present and future. *Plant J.* **61**: 1041–1052.
- Hirel B, Le Gouis J, Ney B, Gallais A (2007) The challenge of improving nitrogen use efficiency in crop plants: towards a more central role for genetic variability and quantitative genetics within integrated approaches. *J. Exp. Bot*. **58**: 2369– 2387.
- Hirel B, Tétu T, Lea PJ, Dubois F (2011) Improving nitrogen use efficiency in crops for sustainable agriculture. *Sustainability* **3**: 1452–1485.
- Hirose T, Bazzaz FA (1998) Trade-off between light-and nitrogen-use efficiency in canopy photosynthesis. *Ann. Bot*. **82**: 195-202.
- Ho CH, Lin SH, Hu HC, Tsay YF (2009) CHL1 functions as a nitrate sensor in plants. *Cell* **138**: 1184–1194.
- Hoang XLT, Nhi DNH, Thu NBA, Thao NP, Tran LP (2017) Transcription Factors and Their Roles in Signal Transduction in Plants under Abiotic Stresses. *Curr Genomics.***18(6)**: 483-497.
- Hodge A (2004) The plastic plant: root responses to heterogeneous supplies of nutrients. *New Phytologist* **162**: 9–24.

- Hodge A, Stewart J, Robinson D, Griffiths BS, Fitter AH (2000). Plant N capture and microfaunal dynamics from decomping grass and earthworm residues in soil. *Soil Biology and Biochemistry* **32**: 1763–1772.
- Horvath S, Dong J (2008) Geometric interpretation of gene coexpression network analysis. *PLoS Comput Biol* **4**: e1000117.
- Hsu PK, Tsay YF (2013) Two phloem nitrate transporters, NRT1.11 and NRT1.12, are important for redistributing xylem-borne nitrate to enhance plant growth. *Plant Physiol*. **163**: 844–856.
- Hu B, Wang W, Ou S, Tang J, Li H, Che R, et al. (2015) Variation in NRT1.1B contributes to nitrate-use divergence between rice subspecies. *Nat Genet* **47**: 834–838.
- Hu HC, Wang YY, Tsay YF (2009) AtCIPK8, a CBL-interacting protein kinase, regulates the low-affinity phase of the primary nitrate response. *Plant J*. **57**: 264–278.
- Hu J, Rampitsch C, Bykova NV (2015) Advances in plant proteomics toward improvement of crop productivity and stress resistance. *Front. Plant Sci*. **6**: 209.
- Hunter T, Karin M (1992) The regulation of transcription by phosphorylation. *Cell* **70**: 375-387.
- Igarashi D, Ishizaki T, Totsuka K, Ohsumi C (2009) ASN2 is a key enzyme in asparagine biosynthesis under ammonium sufficient conditions. Plant Biotechnol. 26: 153-159.
- Iqbal A, Qiang D, Zhun W, Xiangru W, Huiping G, Zhang H, et al. (2020) Growth and nitrogen metabolism are associated with nitrogen-use efficiency in cotton genotypes, *Plant Physiology and Biochemistry* **149**: 61-74.
- Ishikawa-Sakurai J, Hayashi H, Murai-Hatano M (2014) Nitrogen availability affects hydraulic conductivity of rice roots, possibly through changes in aquaporin gene expression. *Plant Soil* **379**: 289–300.
- Jackson LE, Burger M, Cavagnaro TR (2008) Roots, nitrogen transformations, and ecosystem services. *Annual Review of Plant Biology* **59**: 341-363.
- Jämtgård S, Näsholm T, Huss-Danell K (2010) Nitrogen compounds in soil solutions of agricultural land. *Soil Biol. Biochem*. **42**: 2325–2330.
- Jin X, Yang G, Tan C, Zhao C (2015) Effects of nitrogen stress on the photosynthetic CO2 assimilation, chlorophyll fluorescence, and sugar-nitrogen ratio in corn. *Sci. Rep*. **5**: 9311.

- Jones DL, Owen AG, Farrar JF (2002) Simple method to enable the high resolution determination of total free amino acids in soil solutions and soil extracts. *Soil Biol. Biochem*. **34**: 1893–1902.
- Joshi V, Joshi M, Penalosa A (2020) Comparative analysis of tissue-specific transcriptomic responses to nitrogen stress in spinach (*Spinacia oleracea*). *PLOS ONE* **15**: e0232011
- Kant S (2017) Understanding nitrate uptake, signaling and remobilization for improving plant nitrogen use efficiency. *Seminars in Cell & Developmental Biology* **74**: 89-96.
- Kant S, Bi YM, Weretilnyk E, Barak S, Rothstein SJ (2008) The Arabidopsis halophytic relative *Thellungiella halophila* tolerates nitrogen-limiting conditions by maintaining growth, nitrogen uptake, and assimilation. *Plant Physiology* **147**: 1168-1180.
- Kant S., Bi YM, Rothstein SJ (2011) Understanding plant response to nitrogen limitation for the improvement of crop nitrogen use efficiency. *J. Exp. Bot*. **62**: 1499–1509.
- Kazan K (2015) Diverse roles of jasmonates and ethylene in abiotic stress tolerance. *Trends Plant Sci*. **20**: 219–229.
- Kiba T, Feria-Bourrellier AB, Lafouge F, et al. (2012) The Arabidopsis nitrate transporter NRT2.4 plays a double role in roots and shoots of nitrogen-starved plants. *Plant Cell* **24**: 245–258.
- Kiba T, Inaba J, Kudo T, Ueda N, Konishi M, Mitsuda N, et al. (2018) Repression of nitrogen-starvation responses by members of the Arabidopsis GARP-Type transcription factor NIGT1/HRS1 subfamily. *Plant Cell* **30**: 925–945.
- Kiba T, Krapp A (2016) Plant nitrogen acquisition under low availability: regulation of uptake and root architecture. *Plant & Cell Physiology* **57**: 707–714.
- Kiba T, Kudo T, Kojima M, Sakakibara H (2011) Hormonal control of nitrogen acquisition: roles of auxin, abscisic acid, and cytokinin. *J. Exp. Bot*. **62**: 1399–1409.
- Kilambi HV, Manda K, Sanivarapu H, Maurya VK, Sharma R, Sreelakshmi Y (2016) Shotgun proteomics of tomato fruits: evaluation, optimization and validation of sample preparation methods and mass spectrometric parameters. *Front. Plant Sci*. **7**: 1-14.

- Kim D, Pertea G, Trapnell C, Pimentel H, Kelley R, Salzberg SL (2013) TopHat2: accurate alignment of transcriptomes in the presence of insertions, deletions and gene fusions. *Genome Biol*. **14**: R36.
- Kobayashi K, Sasaki D, Noguchi K, Fujinuma D, Komatsu H, Kobayashi M, et al. (2013) Photosynthesis of root chloroplasts developed in *Arabidopsis* lines overexpressing *GOLDEN2-LIKE* transcription factors. *Plant Cell Physiol.* **54**: 1365–1377.
- Kojima S, Bohner A, Gassert B, Yuan L, von Wiren N (2007) AtDUR3 represents the major transporter for high-affinity urea transport across the plasma membrane of nitrogen-deficient Arabidopsis roots. *Plant J.* **52**: 30–40.
- Kollaricsné Horváth M, Hoffmann B, Cernák I, Baráth S, Polgár Z, Taller J (2019) Nitrogen utilization of potato genotypes and expression analysis of genes controlling nitrogen assimilation. *Biol. Fut.* **70**: 25-37.
- Konishi M, Yanagisawa S (2010). Identification of a nitrate-responsive cis-element in the Arabidopsis NIR1 promoter defines the presence of multiple cis-regulatory elements for nitrogen response. *Plant J*. **63**: 269–282.
- Konopka-Postupolska D, Clark G, Goch G, Debski J, Floras K, Cantero A, et al. (2009) The role of annexin 1 in drought stress in *Arabidopsis*. *Plant Physiol*. **150**: 1394–410.
- Konozy EHE, Rogniaux H, Causse M, Faurobert M (2013) Proteomic analysis of tomato (*Solanum lycopersicum*) secretome. *J. Plant Res*. **126**: 251-266.
- Kotur Z, Mackenzie N, Ramesh S, Tyerman SD, Kaiser BN, Glass AD (2012) Nitrate transport capacity of the *Arabidopsis thaliana* NRT2 family members and their interactions with AtNAR2.1. *New Phytol*. **194**: 724–731.
- Krapp A, Berthomé R, Orsel M, Mercey-Boutet S, Yu A, Castaings L, et al. (2011) Arabidopsis roots and shoots show distinct temporal adaptation pattern towards N starvation. *Plant Physiology* **157**: 1255–1258.
- Krapp A, David LC, Chardin C, Girin T, Marmagne A, Leprince AS, et al. (2014) Nitrate transport and signalling in Arabidopsis. *J. Exp Bot*. **65**: 789–798.
- Krause C, Richter S, Knöll C, Jürgens G (2013) Plant secretome - from cellular process to biological activity. *Biochim. Biophys. Acta* **1834**: 2429-2441.
- Kronzucker HJ, Glass ADM, Siddiqi MY, Kirk GJ (2000) Comparative kinetic analysis of ammonium and nitrate acquisition by tropical lowland rice, implications for rice cultivation and yield potential. *New Phytol*. **145**: 471–476.

- Krouk G (2016) Hormones and nitrate: a two-way connection. *Plant Mol. Biol.* **91**: 599–606.
- Krouk G, Lacombe B, Bielach A, Perrine-Walker F, Malinska K, Mounier E, et al. (2010) Nitrate-regulated auxin transport by NRT1. 1 defines a mechanism for nutrient sensing in plants. *Developmental Cell* **18**: 927–37.
- Kuroha T, Tokunaga H, Kojima M, Ueda N, Ishida T, Nagawa S, et al. (2009) Functional analyses of LONELY GUY cytokinin-activating enzymes reveal the importance of the direct activation pathway in Arabidopsis. *Plant Cell* **21**: 3152-69.
- Kushibiki T, Tabata Y (2005) Preparation of poly(ethylene glycol) introduced cationized gelatin as a non-viral gene carrier. *J Biomater Sci Polym Ed* **16**: 1447–1461.
- Lam HM, Coschigano KT, Oliveira IC, Melo-Oliveira R and Coruzzi GM (1996) The molecular-genetics of nitrogen assimilation into amino acids in higher plants. *Annu Rev Plant Physiol Plant Mol Biol* **47**: 569-93.
- Lam HM, Wong P, Chan HK, Yam KM, Chen L, Chow CM, Coruzzi GM (2003) Overexpression of the ASN1 gene enhances nitrogen status in seeds of Arabidopsis. *Plant Physiol*. **132:** 926–35.
- Lammerts van Bueren ET, Struik P (2017) Diverse concepts of breeding for nitrogen use efficiency. A review. *Agron. Sustain. Dev.* **37**: 1-24.
- Langfelder P, Horvath S. (2008) WGCNA: an R package for weighted correlation network analysis. *BMC Bioinformatics* **9**: 559.
- Langfelder P, Mischel PS, Horvath S. (2013) When is hub gene selection better than standard meta-analysis? *PLoS One* **8**: e61505.
- Le Gouis J, Béghin D, Heumez E, Pluchard P (2000) Genetic differences for nitrogen uptake and nitrogen utilization efficiencies in winter wheat. *European Journal of Agronomy* **12**: 163-173.
- Lea PJ, Forde BG (1994) The use of mutants and transgenic plants to study amino acid metabolism. *Plant Cell Environ*. **17**: 541–556.
- Lea PJ, Miflin BJ (1974) An alternative route for nitrogen assimilation in higher plants. *Nature* **251**: 614.
- Lea PJ, Sodek L, Parry PR, Shewry PR, Halford NG (2007) Asparagine in plants *Ann. Appl. Biol.* **150**: 1-26

- Léran S, Edel KH, Pervent M, Hashimoto K, Corratgé-Faillie C, Offenborn JN, et al. (2015) Nitrate sensing and uptake in Arabidopsis are enhanced by ABI2, a phosphatase inactivated by the stress hormone abscisic acid. *Science Signaling* **8**: ra43.
- Léran S, Muños S, Brachet C, Tillard P, Gojon A, Lacombe B (2013) *Arabidopsis* NRT1.1 is a bidirectional transporter involved in root-to-shoot nitrate translocation. *Mol. Plant*.**6(6)**: 1984-1987.
- Léran S, Varala K, Boyer JC, Chiurazzi M, Crawford N, DanielVedele F, et al. (2014) A unified nomenclature of NITRATE TRANSPORTER 1/PEPTIDE TRANSPORTER family members in plants. *Trends Plant Sci*. **19**: 5–9.
- Leyva-González MA, Ibarra-Laclette E, Cruz-Ramirez A, Herrera-Estrella L (2012) Functional and transcriptome analysis reveals an acclimatization strategy for abiotic stress tolerance mediated by *Arabidopsis* NF-YA family members. *PLoS ONE* **7**: e48138.
- Lezhneva L, Kiba T, Feria-Bourrellier AB, Lafouge F, Boutet-Mercey S, Zoufan P, et al. (2014) The Arabidopsis nitrate transporter NRT2.5 plays a role in nitrate acquisition and remobilization in nitrogen-starved plants. *Plant J*. **80**: 230–241.
- Li G, Tillard P, Gojon A, Maurel C (2016) Dual regulation of root hydraulic conductivity and plasma membrane aquaporins by plant nitrate accumulation and high-affinity nitrate transporter NRT2.1. *Plant Cell Physiol*. **57**: 733–742.
- Li JY, Fu YL, Pike SM, Bao J, Tian W, Zhang Y, et al. (2010) The Arabidopsis nitrate transporter NRT1.8 functions in nitrate removal from the xylem sap and mediates cadmium tolerance. *Plant Cell* **22**: 1633-1646.
- Li W, Wang Y, Okamoto M, Crawford NM, Siddiqi MY, Glass AD (2007) Dissection of the AtNRT2.1: AtNRT2.2 inducible high-affinity nitrate transporter gene cluster. *Plant Physiol*. **143:** 425–433.
- Li X, Wang P, Li J., Wei S, Yan Y, Yang J, et al. (2020) Maize *GOLDEN2-LIKE* genes enhance biomass and grain yields in rice by improving photosynthesis and reducing photoinhibition. *Commun Biol.* **3**: 151
- Li X, Wang Y, Chen S, Tian H, Fu D, Zhu B, Luo Y, Zhu H (2018) Lycopene Is Enriched in Tomato Fruit by CRISPR/Cas9-Mediated Multiplex Genome Editing. *Front. Plant Sci.* **9**: 559.
- Li XQ, Sveshnikov D, Zebarth BJ, Tai H, Koeyer DD, Millard P, et al. (2010) Detection of nitrogen sufficiency in potato plants using gene expression markers. *Am. J. Potato Res*. **87**: 50-59.

- Lian XM, Xing YZ, Yan H, Xu CG, Li XH, Zhang QF (2005) QTLs for low nitrogen tolerance at seedling stage identified using a recombinant inbred line population derived from an elite rice hybrid. *Theor. Appl. Genet.* 112: 85-96.
- Liang G, He H, Yu D (2012) Identification of nitrogen starvation-responsive microRNAs in *Arabidopsis thaliana*. *PLoS One* **7**: e48951.
- Lin SH, Kuo HF, Canivenc G, Lin CS, Lepetit M, Hsu PK, et al. (2008) Mutation of the Arabidopsis NRT1.5 nitrate transporter causes defective root-to-shoot nitrate transport. *Plant Cell* **20**: 2514-2528.
- Linn J, Ren M, Berkowitz O, Ding W, van der Merwe MJ, Whelan J, Jost R (2017) Root cell-specific regulators of phosphate-dependent growth. *Plant Physiology* **174**: 1969–1989.
- Liu J, An X, Cheng L, Chen F, Bao J, Yuan L, et al. (2010) Auxin transport in maize roots in response to localized nitrate supply. *Annals of Botany* **106**: 1019–1026.
- Liu KH, Diener A, Lin Z, Liu C, Sheen J (2020) Primary nitrate responses mediated by calcium signalling and diverse protein phosphorylation. *J. Exp. Bot.* **71***:* 4428–4441.
- Liu KH, Huang CY, Tsay YF (1999) CHL1 is a dual-affinity nitrate transporter of Arabidopsis involved in multiple phases of nitrate uptake. *Plant Cell* **11**: 865–874.
- Liu KH, Niu Y, Konishi M, Wu Y, Du H, Chung HS, et al. (2017) Discovery of nitrate–CPK–NLP signalling in central nutrient–growth networks. *Nature* **545**: 311–316.
- Liu KH, Tsay YF (2003) Switching between the two action modes of the dual-affinity nitrate transporter CHL1 by phosphorylation. *EMBO J.* **22**: 1005–1013.
- Liu LH, Ludewig U, Frommer WB, von Wiren N (2003) AtDUR3 encodes a new type of high-affinity urea/H+ symporter in *Arabidopsis. Plant Cell* **15**: 790–800.
- Livak KJ, Schmittgen TD (2001) Analysis of relative gene expression data using Real-Time Quantitative PCR and the $2^{-\Delta\Delta Ct}$ method. *Methods* **25**: 402-408.
- Loqué D, Tillard P, Gojon A, Lepetit M (2003) Gene expression of the NO3- transporter NRT1.1 and the nitrate reductase NIA1 is repressed in Arabidopsis roots by NO2-, the product of NO3- reduction. *Plant Physiol*. **132**: 958–967.
- Løvdal T, Lillo C (2009) Reference gene selection for quantitative real-time PCR normalization in tomato subjected to nitrogen, cold, and light stress. *Anal. Biochem*. **387**: 238–242.

- Lu XK, Mao QG, Gilliam FS, Luo YQ, Mo JM (2014) Nitrogen deposition contributes to soil acidification in tropical ecosystems. *Global Change Biol* **20**: 3790–3801.
- Luan S (2009) The CBL-CIPK network in plant calcium signaling. *Trends Plant Sci*. **14**: 37-42.
- Luo J (2015) Metabolite-based genome-wide association studies in plants. *Current Opinion in Plant Biology* **24**: 31-38.
- Lupini A, Mercati F, Araniti F, Miller AJ, Sunseri F, Abenavoli MR (2016) NAR2.1/NRT2.1 functional interaction with NO_3^- and H^+ fluxes in high-affinity nitrate transport in maize root regions. *Plant Physiol. Biochem*. **102**: 107-114.
- Lupini A, Princi MP, Araniti F, Miller AJ, Sunseri F, Abenavoli MR (2017) Physiological and molecular responses in tomato under different forms of N nutrition. *J. Plant Physiol.* **216**: 17-25.
- Lynch JP (2013) Steep, cheap and deep: an ideotype to optimize water and N acquisition by maize root systems. *Ann Bot* **112**: 347–357.
- Ma W, Li J, Qu B, He X, Zhao X, Li B, et al. (2014) Auxin biosynthetic gene TAR2 is involved in low nitrogen-mediated reprogramming of root architecture in Arabidopsis. *Plant J* **78**: 70–79.
- Maghiaoui A, Bouguyon E, Moliner CC, Perrine-Walker F, Alcon C, Krouk G, et al. (2020) The Arabidopsis NRT1.1 transceptor coordinately controls auxin biosynthesis and transport for regulating root branching in response to nitrate. *J. Exp. Bot*. **71**: 4480–4494.
- Mahjourimajd S, Kuchel H, Langridge P, Okamoto M (2016) Evaluation of Australian wheat genotypes for response to variable nitrogen application. *Plant Soil* **399**: 247–253.
- Mahler RL, Harder RW (1984) The influence of tillage methods, cropping sequence and N rates on the acidification of a northern Idaho soil. *Soil Sci*. **137**: 52– 60.
- Makino A (2011) Photosynthesis, grain yield, and nitrogen utilization in rice and wheat. *Plant Physiol*. **155**: 125–129.
- Mao J, Nuruzzaman Manik SM, Shi S, Chao J, Jin Y, Wang Q, Liu H (2016) Mechanisms and physiological roles of the CBL-CIPK networking system in *Arabidopsis thaliana*. *Genes* 7: 62.

- Marchive C, Roudier F, Castaings L, Brehaut L, Blondet E, Colot V (2013) Nuclear retention of the transcription factor NLP7 orchestrates the early response to nitrate in plants *Nat. Commun*. **4**: 1713.
- Marschner H (2012) Marschner's Mineral Nutrition of Higher Plants, 3rd Edn London: Academic Press
- Marschner H, Kirkby EABC, Engels C (1997) Importance of cycling and recycling of mineral nutrients within plants for growth and development. *Bot. Acta* **110**: 265-273.
- Martin T, Oswald O, Graham IA (2002) Arabidopsis seedling growth, storage lipid mobilization, and photosynthetic gene expression are regulated by carbon:nitrogen availability. *Plant Physiol*. **128(2)**: 472-481.
- Martinez-Feria RA, Castellano MJ, Dietzel RN, Helmers MJ, Liebman M, Huber I, et al. (2018) Linking crop-and soil-based approaches to evaluate system nitrogen-use efficiency and tradeoffs. *Agric. Ecosyst. Environ*. **256**: 131–143.
- Masclaux-Daubresse C, Daniel-Vedele F, Dechorgnat J, Chardon F, Gaufichon L, Suzuki A (2010) Nitrogen uptake, assimilation and remobilisation in plants: challenges for sustainable and productive agriculture, *Annals Bot*. **105**: 1141-1157.
- Masclaux-Daubresse C, Reisdorf-Cren M, Orsel M (2008) Leaf nitrogen remobilisation for plant development and grain filling. *Plant Biol*. **10:** 23-36.
- Masle J, Gilmore SR, Farquhar GD (2005) The ERECTA gene regulates plant transpiration efficiency in Arabidopsis. *Nature* **436**: 866–870.
- Mauceri A, Abenavoli MR, Toppino L, Panda S, Mercati F, Aci MM, et al. (2021) Transcriptomic analysis revealed WRKY33 potential involvement in eggplant NUE under low N supply. *J. Exp. Bot*. **72**: 4237-4253.
- Mauceri A, Bassolino L, Lupini A, Badeck F, Rizza F, Schiavi M, et al. (2020) Genetic variation in eggplant (*Solanum melongena* L.) for nitrogen use efficiency (NUE) under contrasting NO_3^- supply. *J. Integr. Plant Biol*. **62**: 487-508.
- McAllister CH, Beatty PH, Good AG (2012) Engineering nitrogen use efficient crop plants: the current status. *Plant Biotechnol. J.* **10**: 1011–1025.
- Medici A, Krouk G (2014) The Primary Nitrate Response: a multifaceted signalling pathway. *J. Exp. Bot*. **65**: 5567–5576.
- Melo-Oliveira R, Oliveira IC, Coruzzi GM (1996) Arabidopsis mutant analysis and gene regulation define a nonredundant role for glutamate dehydrogenase in nitrogen assimilation. *Proc. Natl. Acad. Sci. USA*. **93**: 4718-4723.

- Meyer C, Stitt M (2001) Nitrate reductase and signalling. In Lea PJ, Morot-GaudryJF (Eds) *Plant nitrogen*. New York: Springer, pp. 37–59.
- Meyer RC, Gryczka C, Neitsch C, Müller M, Bräutigam A, Schlereth A, et al. (2019) Genetic diversity for nitrogen use efficiency in *Arabidopsis thaliana*. *Planta* **250**: 41-57.
- Mickelson S, See D, Meyer FD, Garner JP, Foster CR, Blake TK, Fischer AM (2003) Mapping of QTL associated with nitrogen storage and remobilization in barley (*Hordeum vulgare* L.) leaves. *J. Exp. Bot.* **54**: 801-812.
- Miller AJ, Cramer MD (2004) Root nitrogen acquisition and assimilation. *Plant Soil* **274**: 1–36.
- Miller AJ, Fan X, Orsel M, Smith SJ, Wells DM (2007) Nitrate transport and signalling. *J. Exp. Bot*. **58**: 2297–2306.
- Miller AJ, Smith SJ (2008) Cytosolic nitrate ion homeostasis: could it have a role in sensing nitrogen status? *Ann. Bot*. **101**: 485–489.
- Miller C, White MM (1980) A voltage-dependent chloride conductance channel from Torpedo electroplax membrane. *Ann. N. Y. Acad. Sci*. **341**: 534–551.
- Moll RH, Kamprath EJ, Jackson WA (1982) Analysis and interpretation of factors which contribute to efficiency to nitrogen utilization. *Agron. J.* **74**: 562-564.
- Monachello D, Allot M, Oliva S, Krapp A, Daniel-Vedele F, BarbierBrygoo H, et al . (2009) Two anion transporters AtClCa and AtClCe fulfil interconnecting but not redundant roles in nitrate assimilation pathways. *New Phytol*. **183**: 88-94.
- Moose S, Below F.E. (2009) Biotechnology Approaches to Improving Maize Nitrogen Use Efficiency. In Kriz AL, Larkins BA (Eds) *Molecular Genetic Approaches to Maize Improvement*. Biotechnology in Agriculture and Forestry, vol 63. Springer, Berlin, Heidelberg
- Moreno S, Canales J, Hong L, Robinson D, Roeder AH, Gutiérrez RA (2020) Nitrate Defines Shoot Size through Compensatory Roles for Endoreplication and Cell Division in *Arabidopsis thaliana*. *Curr. Biol*. **30**: 1988–2000.
- Müller D, Waldie T, Miyawaki K, To JP, Melnyk CW, Kieber JJ, et al. (2015) Cytokinin is required for escape but not release from auxin mediated apical dominance. Plant J 82:874–886
- Mulvaney RL, Khan SA, Ellsworth TR (2009) Synthetic nitrogen fertilizers deplete soil nitrogen: a global dilemma for sustainable cereal production. *J. Environ. Qual*. **38**: 2295–2314.

- Munos S, Cazettes C, Fizames C, Gaymard F, Tillard P, Lepetit M, et al. (2004) Transcript profiling in the chl1-5 mutant of Arabidopsis reveals a role of the nitrate transporter NRT1.1 in the regulation of another nitrate transporter, NRT2.1. *Plant Cell* **16**: 2433–2447.
- Nakai M (2018) New perspectives on chloroplast protein import. *Plant Cell Physiol*. **59**: 1111–1119.
- Nakazawa M, Yabe N, Ichikawa T, Yamamoto YY, Yoshizumi T, Hasunuma K, Matsui M (2001) DFL1, an auxin-responsive GH3 gene homologue, negatively regulates shoot cell elongation and lateral root formation, and positively regulates the light response of hypocotyl length. *Plant J.* **25**: 213-221.
- Narcy P, Bouguyon E, Gojon A (2013) Nitrogen acquisition by roots: physiological and developmental mechanisms ensuring plant adaptation to a fluctuating resource. *Plant Soil* **370**: 1–29
- Naulin PA, Armijo GI, Vega AS, Tamayo KP, Gras DE, de la Cruz J, Gutiérrez RA (2020) Nitrate Induction of Primary Root Growth Requires Cytokinin Signaling in *Arabidopsis thaliana*. *Plant Cell Physiol*. **61**: 342-352.
- Nedelyaeva OI, Shuvalov AV, Balnokin Y (2020) Chlorid channels and transporters of the CLC family in plant. *Russian Journal of Plant Physiology* **67(5)**:767-784
- Negi J, Matsuda O, Nagasawa T, Oba Y, Takahashi H, Kawai-Yamada M, et al. (2008) CO_2 regulator SLAC1 and its homologues are essential for anion homeostasis in plant cells. *Nature* **452**: 483–486.
- Nguyen CV, Vrebalov JT, Gapper NE, Zheng Y, Zhong S, Fei Z, Giovannoni JJ (2014) Tomato *GOLDEN2-LIKE* transcription factors reveal molecular gradients that function during fruit development and ripening. *Plant Cell* **26**: 585–601.
- Nguyen GN, Joshi S, Kant S (2017) Water availability and nitrogen use in plants: effects, interaction, and underlying molecular mechanisms. In Kamiya MA, Hossain TDJ, Burritt LP, Tran T Fujiwara (Eds) *Plant Macronutrient Use Efficiency*, San Diego, CA: Academic Press, pp 233–243.
- Nguyen GN, Kant S (2018) Improving nitrogen use efficiency in plants: effective phenotyping in conjunction with agronomic and genetic approaches. *Funct. Plant Biol*. **45**: 606–619.
- Nishiyama Y, Murata N (2014) Revised scheme for the mechanism of photoinhibition and its application to enhance the abiotic stress tolerance of the photosynthetic machinery. *Appl Microbiol Biotechnol*. **98(21):** 8777-8796.

- Noguero M, Lacombe B. (2016) Transporters Involved in Root Nitrate Uptake and Sensing by Arabidopsis. *Front. Plant Science* **7**: 1391.
- O'Brien JA, Vega A, Bouguyon E, Krouk G, Gojon A, Coruzzi G, et al. (2016) Nitrate transport, sensing, and responses in plants. *Mol. Plant* **9**: 837–856.
- Okamoto M, Vidmar JJ, Glass ADM (2003) Regulation of NRT1 and NRT2 gene families of Arabidopsis thaliana: responses to nitrate provision. *Plant Cell Physiol* **44**: 304–317.
- Okumoto S, Pilot G (2011) Amino acid export in plants: A missing link in nitrogen cycling. *Mol Plant* **4**:453–463
- Orsel M, Chopin F, Leleu O, Smith SJ, Krapp A, Daniel-Vedele F, Miller AJ (2006) Characterization of a two-component high-affinity nitrate uptake system in Arabidopsis. Physiology and protein-protein interaction. *Plant Physiol*. **142**: 1304–1317.
- Orsel M, Filleur S, Fraisier V, Daniel-Vedele F, (2002) Nitrate transport in plants: which gene and which control? *J. Exp. Bot*. **53**: 825-833.
- Orzaez D, Medina A, Torrez S, Fernandez-Moreno JP, Rambla JL, Fernandez-Del-Carmen A, et al. (2009) A visual reporter system for virus-induced gene silencing in tomato fruit based on anthocyanin accumulation. *Plant Physiol* **150**: 1122–1134.
- Overvoorde P, Fukaki H, Beeckman T (2010) Auxin control of root development. *Cold Spring Harb. Perspect. Biol*. **2**: a001537.
- Paila YD, Richardson LGL, Schnell DJ (2015) New insights into the mechanism of chloroplast protein import and its integration with protein quality control, organelle biogenesis and development. *J. Mol. Biol*. **427**: 1038–1060.
- Park OK (2004) Proteomic studies in plants. *J. Biochem. Mol. Biol*. **37**: 133-138.
- Parker JL, Newstead S (2014) Molecular basis of nitrate uptake by the plant nitrate transporter NRT1.1. *Nature* **507**: 68–72.
- Pathak RR, Lochab S, Raghuram N (2011) Plant systems | improving plant nitrogen-use efficiency. In Moo-Young M. (Eds) *Comprehensive Biotechnology*, 2nd ed,, New York: NY: Elsevier, pp 209–218
- Peña PA, Quach T, Sato S, Ge Z, Nersesian N, Dweikat IM, et al. (2017) Molecular and phenotypic characterization of transgenic wheat and sorghum events expressing the barley alanine aminotransferase. *Planta* **246**: 1097–1107.

- Peng B, Guan K, Tang J, Ainsworth EA, Asseng S, Bernacchi CJ, et al. (2020) Towards a multiscale crop modelling framework for climate change adaptation assessment. *Nat. Plants* **6**: 338–348.
- Peng M, Bi Y-M, Zhu T, Rothstein SJ (2007) Genome-wide analysis of Arabidopsis responsive transcriptome to nitrogen limitation and its regulation by the ubiquitin ligase gene NLA. *Plant Molecular Biology* **65**: 775–797.
- Peng M, Hudson D, Schofield A, Tsao R, Yang R, Gu H, et al. (2008) Adaptation of Arabidopsis to nitrogen limitation involves induction of anthocyanin synthesis which is controlled by the NLA gene. *J Exp Bot*. **59**: 2933–44.
- Perchlik M, Tegeder M (2017) Improving plant nitrogen use efficiency through alteration of amino acid transport processes. *Plant Physiol.* **175**: 235–247.
- Plett DC, Holtham LR, Okamoto M, Garnett TP (2018) Nitrate uptake and its regulation in relation to improving nitrogen use efficiency in cereals. In Seminars in Cell & Developmental Biology **74**: 97-104. Academic Press.
- Plett DC, Ranathunge K, Melino VJ, Kuya N, Uga Y, Kronzucker HJ (2020) The intersection of nitrogen nutrition and water use in plants: new paths toward improved crop productivity. *J. Exp. Bot*. **71**: 4452–4468.
- Poitout A, Crabos A, Petřík I, Novák O, Krouk G, Lacombe B, Ruffel S (2018) Responses to Systemic Nitrogen Signaling in Arabidopsis Roots Involve trans-Zeatin in Shoots. *Plant Cell* **30**: 1243–1257.
- Powell ALT, Nguyen CV, Hill T, Cheng KL, Figueroa-Balderas R, Aktas H, et al. (2012) Uniform ripening encodes a golden 2-like transcription factor regulating tomato fruit chloroplast development. *Science* **336**: 1711–1715.
- Poza-Carrión C, Paz-Ares J (2019) When nitrate and phosphate sensors meet. *Nature Plants* **5**: 339–340.
- Qiao B, Zhang Q, Liu DL, Wang HQ, Yin JY, Wang R, et al. (2015) A calcium-binding protein, rice annexin OsANN1, enhances heat stress tolerance by modulating the production of H_2O_2. *J Exp Bot*. **66**: 5853–5866.
- Quan X, Zeng J, Ye L, Chen G, Han Z, Shah JM, Zhang G (2016) Transcriptome profiling analysis for two Tibetan wild barley genotypes in responses to low nitrogen. *BMC Plant Biol.* **16**: 30.
- Quraishi UM, Abrouk M, Murat F, Pont C, Foucrier S, Desmaizieres G, et al. (2011) Cross-genome map based dissection of a nitrogen use efficiency ortho-metaQTL in bread wheat unravels concerted cereal genome evolution. *Plant J.* **65**: 745-756.

- Rahayu YS, Walch-Liu P, Neumann G, Römheld V, von Wirén N, Bangerth F (2005) Root-derived cytokinins as long-distance signals for NO_3^- induced stimulation of leaf growth. *J. Exp. Bot.* **56**: 1143–1152.
- Rashid M, Bera S, Medvinsky AB, Sun GQ, Li BL. Chakraborty A (2018) Adaptive regulation of nitrate transceptor NRT1.1 in fluctuating soil nitrate conditions. i*Science* **2**: 41–50.
- Ravasz E, Somera A, Mongru D, Oltvai Z, Barabasi A (2002) Hierarchical organization of modularity in metabolic networks. *Science* **297**: 1551–1555.
- Reay D, Davidson E, Smith K et al. (2012) Global agriculture and nitrous oxide emissions. *Nature Clim. Change* **2**: 410–416.
- Reis AR, Favarin JL, Malavolta E, Júnior JL, Moraes MF (2009) Photosynthesis, chlorophylls, and SPAD readings in coffee leaves in relation to nitrogen supply. *Commun. Soil Sci. Plant Anal*. **40**: 1512-1528.
- Remans T, Nacry P, Pervent M, Girin T, Tillard P, Lepetit M, et al. (2006). A central role for the nitrate transporter NRT2.1 in the integrated morphological and physiological responses of the root system to nitrogen limitation in Arabidopsis. *Plant Physiol.* **140**: 909–921
- Renau-Morata B, Molina RV, Minguet EG, Cebolla-Cornejo J, Carrillo L, Martí R, et al. (2021) Integrative Transcriptomic and Metabolomic Analysis at Organ Scale Reveals Gene Modules Involved in the Responses to Suboptimal Nitrogen Supply in Tomato. *Agronomy* **11**: 1320.
- Ripullone F, Grassi G, Lauteri M, Borghetti M. (2003) Photosynthesis–nitrogen relationships: interpretation of different patterns between Pseudotsuga menziesii and Populus × euroamericana in a mini-stand experiment. *Tree Physiol.* **23**:137-144.
- Ristova D, Carré C, Pervent M, Medici A, Kim GJ, Scalia D, et al. (2016) Combinatorial interaction network of transcriptomic and phenotypic responses to nitrogen and hormones in the Arabidopsis thaliana root. *Sci Signal*. **451**:rs13.
- Robertson GP, Vitousek PM (2009) Nitrogen in agriculture: balancing the cost of an essential resource. *Annu. Rev. Environ. Resour*. **34**: 97-125.
- Rodgers CO, Barneix AJ (1988) Cultivar differences in the rate of nitrate uptake by intact wheat plants as related to growth rate. *Physiologia Plantarum* **72**: 121-126.
- Rodríguez-Leal D, Lemmon ZH, Man J, Bartlett ME, Lippman ZB (2017) Engineering Quantitative Trait Variation for Crop Improvement by Genome Editing. *Cell* **171**: 470-480.

- Rossato L, Laine P, Ourry A (2001) Nitrogen storage and remobilization in Brassica napus L. during the growth cycle: Nitrogen fluxes within the plant and changes in soluble protein patterns. *J. Exp. Bot*. **52**: 1655-1663.
- Rubin G, Tohge T, Matsuda F, Saito K., Scheible WR (2009) Members of the LBD family of transcription factors repress anthocyanin synthesis and affect additional nitrogen responses in Arabidopsis. *Plant Cell* **21**: 3567-3584
- Ruffel S, Gojon A, Lejay L (2014) Signal interactions in the regulation of root nitrate uptake. *J. Exp. Bot*. **65**: 5509–5517.
- Ruffel S, Krouk G, Ristova D, Shasha D, Birnbaum KD, Coruzzi GM (2011) Nitrogen economics of root foraging: transitive closure of the nitrate-cytokinin relay and distinct systemic signaling for N supply vs. demand. *PNAS* **108**: 18524–18529.
- Ruzicka K, Strader LC, Bailly A, Yang H, Blakeslee J, Langowski L, et al. (2010) Arabidopsis PIS1 encodes the ABCG37 transporter of auxinic compounds including the auxin precursor indole-3-butyric acid. *PNAS* **107**: 10749–10753.
- Sadok W, Sinclair TR (2010) Transpiration response of 'slow-wilting' and commercial soybean (*Glycine max* (L.) Merr.) genotypes to three aquaporin inhibitors. *J Exp Bot*. **61**: 821-9.
- Sakakibara H (2006) Cytokinins: activity, biosynthesis, and translocation. *Annu. Rev Plant Biol*. **57**: 431–449.
- Sakakibara H (2003) Nitrate-specific and cytokinin-mediated nitrogen signaling pathways in plants. *J Plant Res*. **116 (3)**: 253-257.
- Salon C, Munier-Jolain NG, Duc G, Voisin AS, Grandgirard D, Larmure A, et al. (2001) Grain legume seed filling in relation to nitrogen acquisition: A review and prospects with particular reference to pea. *Agronomie* **21**: 539–552.
- Santi S, Locci G, Monte R, Pinton R, Varanini Z (2003) Induction of nitrate uptake in maize roots: expression of a putative high-affinity nitrate transporter and plasma membrane H^+-ATPase isoforms. *J. Exp. Bot*. **54**: 1851– 1864.
- Santi S, Locci G, Pinton R, Cesco S, Varanini Z (1995) Plasma membrane H^+-ATPase in maize roots induced for NO_3^- uptake. *Plant Physiol*. **109**: 1277–1283.
- Scheible WR, Morcuende R, Czechowski T, Fritz C, Osuna D, Palacios-Rojas N, et al. (2004) Genome-wide reprogramming of primary and secondary metabolism, protein synthesis, cellular growth processes, and the regulatory infrastructure of Arabidopsis in response to nitrogen. *Plant Physiol.* **136**: 2483–2499

- Schiltz S, Munier-Jolain N, Jeudy C, Burstin J, Salon C (2005) Dynamics of exogenous nitrogen partitioning and nitrogen remobilization from vegetative organs in pea revealed by ^{15}N in vivo labeling throughout seed filling. *Plant Physiol*. **137**: 1463-1473.
- Schmidt C, Schroeder JI (1994). Anion selectivity of slow anion channels in the plasma membrane of guard cells. *Plant Physiol*. **106**: 383–391.
- Schmitz G, Theres K (1999) Genetic control of branching in *Arabidopsis* and tomato. *Curr. Opin. Plant Biol*. **2**: 51-55.
- Scholberg J, McNeal BL, Boote KJ, Jones JW, Locascio SJ, Olson SM (2000) Nitrogen stress effects on growth and nitrogen accumulation by field-grown tomato. *Agron. J*. **92**: 159-167.
- Schroeder JI, Delhaize E, Frommer WB, Guerinot ML, Harrison MJ, Herrera-Estrella L, et al. (2013) Using membrane transporters to improve crops for sustainable food production. *Nature* **497**: 60–66.
- Schroeder JI, Keller BU (1992) Two types of anion channel currents in guard cells with distinct voltage regulation. *PNAS* **89**: 5025–5029.
- Schumaker KS, Sze H (1987) Decrease of pH gradients in tonoplast vesicles by NO and C: evidence for H+-coupled anion transport. *Plant Physiol*. **83**: 490–496.
- Sechley KA, Yamaya T, Oaks A (1992) Compartmentation of nitrogen assimilation in higher plants. *Int. Rev. Cytol*. **134**: 85–163.
- Shannon P (2003) Cytoscape: a software environment for integrated models of biomolecular interaction networks. *Genome Res*. **13**: 2498–2504
- Shatil-Cohen A, Attia Z, Moshelion M (2011) Bundle-sheath cell regulation of xylem-mesophyll water transport via aquaporins under drought stress: A target of xylem-borne aba? *Plant J*. **67**: 72–80.
- Shi X, Gupta S, Rashotte AM (2012) *Solanum lycopersicum* cytokinin response factor (SlCRF) genes: characterization of CRF domain-containing ERF genes in tomato. *J. Exp. Bot*. **63**: 973-982.
- Shiu SH, Bleecker AB (2001) Receptor-like kinases from Arabidopsis form a monophyletic gene family related to animal receptor kinases. *PNAS* **98**: 10763–10768.
- Shpak ED, McAbee JM, Pillitteri LJ, Torii KU (2005) Stomatal patterning and differentiation by synergistic interactions of receptor kinases. *Science* **309**: 290–293.

- Siddiqi MY, Glass ADM (1981) Utilization index: A modified approach to the estimation and comparison of nutrient utilization efficiency in plants. *J. Plant Nutr*. **4**: 289-302.
- Siddiqi MY, Glass ADM, Ruth TJ, Rufty T (1990) Studies of the uptake of nitrate in barley: I. Kinetics of $13NO_3^-$ influx. *Plant Physiol*. **93**: 1426–1432.
- Sinha SK, Kumar A, Tyagi A, Venkatesh K, Paul D, Singh NK, Mandal PK (2020) Root architecture traits variation and nitrate-influx responses in diverse wheat genotypes under different external nitrogen concentrations, *Plant Physiology and Biochemi*stry **148**: 246-259.
- Sinha VB, Jangam AP, Raghuram N (2018) Biological determinants of crop use efficiency and biotechnological avenues for improvement. In Sutton M. (Eds) *Proceeding of the N2013*, Berlin: Springer.
- Sjuts I, Soll J, Bölter B (2017) Import of soluble proteins into chloroplasts and potential regulatory mechanisms. *Front. Plant Sci*. **8:** 168.
- Smirnoff N, Stewart G (1985). Nitrate assimilation and translocation by higher plants: Comparative physiology and ecological consequences. *Physiol. Plant*. **64**: 133-140.
- Socolow RH (1999) Nitrogen management and the future of food: Lessons from the management of energy and carbon. *PNAS* **96**: 6001-6008.
- Sorgonà A, Cacco G, Di Dio L, Schmidt W, Perry PJ, Abenavoli MR (2010) Spatial and temporal patterns of net nitrate uptake regulation and kinetics along the tap root of Citrus aurantium. *Acta Physiologiae Plantarum* **32**: 683-694.
- Sorgonà A, Lupini A, Mercati F, Di Dio L, Sunseri F, Abenavoli MR (2011) Nitrate uptake along the maize primary root: an integrated physiological and molecular approach. *Plant Cell Environ*. **34**:1127–1140.
- Sorin C, Declerck M, Christ A, Blein T, Ma L, Lelandais-Briere C, et al. (2014) A miR169 isoform regulates specific NF-YA targets and root architecture in *Arabidopsis*. *New Phytol.* **202**: 1197–1211.
- Staswick PE, Serban B, Rowe M, Tiryaki I, Maldonado MT, Maldonado MC, Suza W (2005) Characterization of an Arabidopsis enzyme family that conjugates amino acids to indole-3-acetic acid. *Plant Cell* **17**:616-627.
- Stitt M (1999) Nitrate and the regulation of primary metabolism, allocation and growth. *Curr. Opin. Plant Sci*. **2**: 178–186
- Subudhi PK, Garcia RS, Coronejo S, Tapia R (2020) Comparative Transcriptomics of Rice Genotypes with Contrasting Responses to Nitrogen Stress Reveals Genes

Influencing Nitrogen Uptake through the Regulation of Root Architecture. *Int J Mol Sci*. **21**: 5759.

- Sultana N, Islam S, Juhasz A, Yang R, She M, Alhabbar Z, et al. (2020) Transcriptomic Study for Identification of Major Nitrogen Stress Responsive Genes in Australian Bread Wheat Cultivars. *Front. Genet*. **11**: 583785.
- Sun C-H, Yu J-Q, Hu D-G (2017) Nitrate: A Crucial Signal during Lateral Roots Development. *Front. Plant Sci*. **8**: 485.
- Sun J, Bankston JR, Payandeh J, Hinds TR, Zagotta WN, Zheng, N (2014) Crystal structure of the plant dual-affinity nitrate transporter NRT1.1. *Nature* **507**: 73–77.
- Sun L, Di DW, Li G, Li Y, Kronzucker HJ, Shi W (2020) Transcriptome analysis of rice (*Oryza sativa* L.) in response to ammonium resupply reveals the involvement of phytohormone signaling and the transcription factor OsJAZ9 in reprogramming of nitrogen uptake and metabolism. *J. Plant Physiol*. **246-247**:153137.
- Suresh BV, Roy R, Sahu K, Misra G, Chattopadhyay D (2014) Tomato Genomic Resources Database: An Integrated Repository of Useful Tomato Genomic Information for Basic and Applied Research. *PLOS ONE* **9**: e86387.
- Sutton MA, Bleeker A, Howard CM, Bekunda M, Grizzetti B, de Vries W, et al. (2013) Our Nutrient World: The challenge to produce more food and energy with less pollution. Global Overview of Nutrient Management. Centre for Ecology and Hydrology, Edinburgh on behalf of the Global Partnership on Nutrient Management and the International Nitrogen Initiative114
- Suzuki A, Vidal J, Gadal P (1982) Glutamate synthase isoforms in rice immunological studies of enzymes in green leaf, etiolated leaf, and root tissues. *Plant Physiol*. **70**: 827-832.
- Swarbreck SM, Wang M, Wang Y, Kindred D, Sylvester-Bradley R, Shi M, et al. (2019) A roadmap for lowering crop nitrogen requirement. *Trends Plant Sci*. **24**: 892–904.
- Takei K, Ueda N, Aoki K, Kuromori T, Hirayama T, Shinozaki K, Yamaya T, Sakakibara H (2004) AtIPT3 is a key determinant of nitrate-dependent cytokinin biosynthesis in Arabidopsis. *Plant Cell Physiol*. **45**: 1053–1062.
- Tang Y, Sun X, Hu C, Tan Q, Zhao X (2013) Genotypic differences in nitrate uptake, translocation and assimilation of two Chinese cabbage cultivars (*Brassica campestris* L. ssp. Chinensis (L.)). *Plant Physiol. Biochem*. **70**: 14-20.

- Tang Z, Fan X, Li Q, Feng H, Miller AJ, Shen Q, Xu G (2012) Knockdown of a rice stelar nitrate transporter alters long-distance translocation but not root influx. *Plant Physiol*. **160**: 2052-2063.
- Tanguilig VC, Yambao EB, O'toole JC, De Datta SK (1987) Water stress effects on leaf elongation, leaf water potential, transpiration, and nutrient uptake of rice, maize, and soybean. *Plant Soil.* **103**: 155–168.
- Taochy C, Gaillard I, Ipotesi E, et al. (2015) The Arabidopsis root stele transporter NPF2.3 contributes to nitrate translocation to shoots under salt stress. *Plant J*. **83**: 466–479.
- The Tomato Genome Consortium (2012) The tomato genome sequence provides insights into fleshy fruit evolution. *Nature* **485**: 635–641.
- Tian H, De Smet I, Ding Z (2014) Shaping a root system: regulating lateral versus primary root growth. *Trends Plant Sci*. **19**: 426–431.
- Tian Z, Li Y, Liang Z, Guo H, Cai J, Jiang D, Cao W, Dai T (2016) Genetic improvement of nitrogen uptake and utilization of winter wheat in the Yangtze River Basin of China. *Field Crops Research* **196**: 251–260.
- Tieman D, Zhu G, Lin T, Nguyen C, Bies D, Rambla JL, et al. (2017) A chemical genetic roadmap to improved tomato flavor. *Science* **355**: 391-394.
- Tilman D, Cassman KG, Matson PA, Naylor R, Polasky S (2002) Agricultural sustainability and intensive production practices. *Nature* **418**: 671–677.
- Tiwari JK, Buckseth T, Zinta R, Saraswati A, Singh RK, Rawat S, Dua VK, Chakrabarti SK (2020) Transcriptome analysis of potato shoots, roots and stolons under nitrogen stress. *Sci. Rep*. **10**: 4.
- Tobias CM, Chow EK (2005) Structure of the cinnamyl-alcohol dehydrogenase gene family in rice and promoter activity of a member associated with lignification. *Planta* **220**: 678-88.
- Tobin AK, Ridley SM, Stewart GR (1985) Changes in the activities of chloroplast and cytosolic isoenzymes of glutamine synthetase normal leaf growth and plastid development in wheat. *Planta* **163**: 544-548.
- Tong Y, Zhou JJ, Li Z, Miller AJ (2005) A two-component high-affinity nitrate uptake system in barley. *Plant J*. **41**: 442–450.
- Townsley BT, Sinha NR (2012) A new development: evolving concepts in leaf ontogeny. *Annu. Rev. Plant Biol*. **63**: 535-562.

- Tran MT, Doan DTH, Kim J, Song YJ, Sung YW, Das S, et al. (2021) CRISPR/Cas9-based precise excision of SlHyPRP1 domain(s) to obtain salt stress-tolerant tomato. *Plant Cell Rep*. **40**: 999–1011.
- Tsay YF, Ho CH, Chen HY, Lin SH (2011) Integration of Nitrogen and Potassium Signaling. *Ann. Rev. Plant Biol.* **62**: 207-226.
- Tsay YF, Schroeder JI, Feldmann KA, Crawford NM (1993) The herbicide sensitivity gene CHL1 of Arabidopsis encodes a nitrate-inducible nitrate transporter. *Cell* **72**: 705– 713.
- Tunnacliffe A, Wise M (2007) The contining conundrum of the LEA proteins. *Naturwissenschaften* **94**: 791-812.
- Turpin DH, Elrifi IR, Birch DG, Weger HG, Holmes JJ (1988) Interactions between photosynthesis, respiration, and nitrogen assimilation in microalgae. *Can J Bot* **66**: 2083-2097.
- Tzfadia O, Bocobza S, Defoort J, Almekias-Siegl E, Panda S, Levy M, et al. (2018) The 'TranSeq' 3´-end sequencing method for high-throughput transcriptomics and gene space refinement in plant genomes. *Plant J*. **96**: 223–232.
- Ueda Y, Kiba T, Yanagisawa S (2020) Nitrate-inducible NIGT1 proteins modulate phosphate uptake and starvation signalling via transcriptional regulation of SPX genes. *Plant J*. **102**: 448– 466.
- Ueda Y, Yanagisawa S (2018) Transcription factor-based genetic engineering to increase nitrogen use efficiency. In Shrawat AK, Zayed A, Lightfoot DA (Eds) *Engineering nitrogen utilization in crop plants*, Cham, Switzerland: Springer Nature, pp 37–55.
- Undurraga SF, Ibarra-Henríquez C, Fredes I, Miguel-Álvarez JM, Gutiérrez RA (2017) Nitrate signaling and early responses in Arabidopsis roots. *J. Exp. Bot*. **68:** 2541-2551.
- Vahisalu T, Kollist H, Wang YF, Nishimura N, Chan WY, Valerio G, et al. (2008) SLAC1 is required for plant guard cell S-type anion channel function in stomatal signalling. *Nature* **452**: 487–491.
- van Beek CR, Guzha T, Kopana N, van der Westhuizen CS, Panda SK, van der Vyver C (2021) The *SlNAC2* transcription factor from tomato confers tolerance to drought stress in transgenic tobacco plants. *Physiol Mol Biol Plants* **27**: 907-921.
- Van der Hoeven R, Ronning C, Giovannoni J, Martin G, Tanksley S (2002) Deductions about the number, organization, and evolution of genes in the tomato

genome based on analysis of a large expressed sequence tag collection and selective genomic sequencing. *Plant Cell* **14**: 1441-1456.

- Vandeleur RK, Sullivan W, Athman A, Jordans C, Gilliham M, Kaiser BN, Tyerman SD (2014) Rapid shoot-to-root signalling regulates root hydraulic conductance via aquaporins. *Plant Cell Environ.***37**: 520–538.
- Vanstraelen M, Benková E (2012) Hormonal interactions in the regulation of plant development. *Ann. Rev. Cell Develop. Biol.* **28**: 463–87.
- Varala K, Marshall-Colón A, Cirrone J, Brooks MD, Pasquino AV, Léran S, et al. (2018) Temporal transcriptional logic of dynamic regulatory networks underlying nitrogen signaling and use in plants. *PNAS* **115**: 6494–6499.
- Velthof GL, Barot S, Bloem J, Butterbach-Bahl K, de Vries W, Kros J, et al. (2011) Nitrogen as a threat to European soil quality. In Sutton MA, Howard CM, Erisman JW, Billen G, Bleeker A, Grennfelt P, van Grinsven H, Grizzetti B (Eds) *The European nitrogen assessment*. Cambridge, UK: Cambridge University Press, pp 494-509
- Vidal EA, Alvarez JM, Moyano TC, Gutiérrez RA (2015) Transcriptional networks in the nitrate response of *Arabidopsis thaliana*. *Curr. Opin. Plant Biol* **27:** 125–132.
- Vidal EA, Araus V, Lu C, Parry G, Green PJ, Coruzzi GM, Gutiérrez RA (2010) Nitrate-responsive miR393/AFB3 regulatory module controls root system architecture in *Arabidopsis thaliana*. *PNAS* **107**:4477–4482.
- Vidal EA, Gutiérrez RA (2008) A systems view of nitrogen nutrient and metabolite responses in Arabidopsis. *Current Opinion in Plant Biology* **11**: 521–529.
- Vidal EA, Moyano TC, Canales J, Gutiérrez RA (2014) Nitrogen control of developmental phase transitions in *Arabidopsis thaliana*. *J. Exp. Bot.* **65**: 5611–5618.
- Vijayalakshmi P, Kiran TV, Rao YV, Srikanth B, Rao IS, Sailaja B et al. (2013) Physiological approaches for increasing nitrogen use efficiency in rice. *Indian J. Plant Physiol.* **18**: 208–222.
- Vitousek PM, Naylor R, Crews T, David MB, Drinkwater LE, Holland E, et al (2009) Nutrient imbalances in agricultural development. *Science* **324:** 1519–1520.
- Von der Fecht-Bartenbach J, Bogner M, Krebs M, Stierhof Y-D, Schumacher K, Ludewig U (2007) Function of the anion transporter AtCLC-d in the trans-Golgi network. *Plant J.* **50**:466–474.
- Von Mutius E (2000) Current review of allergy and immunology. *J Allergy Clin Immun* **105**: 9-19.

- Walch-Liu P, Forde BG (2008) Nitrate signaling mediated by the NRT1.1 nitrate transporter antagonises L-glutamate-induced changes in root architecture. *Plant J.* **54**: 820– 828.
- Waldie T, Leyser O (2018) Cytokinin targets auxin transport to promote shoot branching. *Plant Physiol*. **177**: 803– 818.
- Walker L, Boddington C, Jenkins D, Wang Y, Grønlund JT, Hulsmans J, et al. (2017) Changes in gene expression in space and time orchestrate environmentally mediated shaping of root architecture. *Plant Cell* **29**: 2393–2412.
- Wang D, Samsulrizal NH, Yan C, Allcock NS, Craigon J, Blanco-Ulate B, et al. (2019) Characterization of CRISPR mutants targeting genes modulating pectin degradation in ripening tomato. *Plant Physiol*. **179**: 544-557.
- Wang P, Fouracre J, Kelly S, Karki S, Gowik U, Aubry S, et al. (2013) Evolution of GOLDEN2-LIKE gene function in C(3) and C (4) plants. *Planta* **237**: 481-495.
- Wang P, Wang Z, Pan Q, Sun X, Chen H, Chen F, et al. (2019) Increased biomass accumulation in maize grown in mixed nitrogen supply is mediated by auxin synthesis. J. *Exp. Bot.* **70**: 1859-1873.
- Wang R, Guegler K, LaBrie ST, Crawford NM (2000) Genomic analysis of a nutrient response in Arabidopsis reveals diverse expression patterns and novel metabolic and potential regulatory genes induced by nitrate. *Plant Cell* **12**: 1491–1509.
- Wang R, Tischner R, Gutierrez RA, Hoffman M, Xing X, Chen M, et al. (2004) Genomic analysis of the nitrate response using a nitrate reductase-null mutant of Arabidopsis. *Plant Physiol*. **136**: 2512–2522.
- Wang R, Xing X, Wang Y, Tran A, Crawford NM (2009) A genetic screen for nitrate regulatory mutants captures the nitrate transporter gene NRT1.1. *Plant Physiol*. **151**: 472–478.
- Wang T, Zhang H, Zhu H (2019) CRISPR technology is revolutionizing the improvement of tomato and other fruit crops. *Hortic. Res*. **6**: 77.
- Wang W, Hu B, Li A, Chu C (2020) NRT1.1s in plants: functions beyond nitrate transport. *J Exp Bot*. **71(15)**: 4373-4379.
- Wang W, Hu B, Yuan D, Liu Y, Che R, Hu Y, Ou S, Liu Y (2018). Expression of the nitrate transporter gene OsNRT1.1A/OsNPF6.3 confers high yield and early maturation in rice. *Plant Cell* **30**: 638–651.

- Wang YH, Garvin DF, Kochian LV (2001) Nitrate-induced genes in tomato roots. Array analysis reveals novel genes that may play a role in nitrogen nutrition. *Plant Physiol*. **127**: 345-359.
- Wang YY, Cheng YH, Chen KE, Tsay YF (2018) Nitrate transport, signaling, and use efficiency. *Ann. Rev. Plant Biol*. **69**: 85–122.
- Wang YY, Hsu PK, Tsay YF (2012) Uptake, allocation and signaling of nitrate. *Trends Plant Sci*. **17**: 458–467.
- Wang ZH, Li SX, Malhi S (2008) Effects of fertilization and other agronomic measures on nutritional quality of crops. *J. Sci. Food Agricul.* **88**: 7-23.
- Wany CH, Foyer KJ, Gupta S (2018) Nitrate, NO and ROS signaling in stem cell homeostasis. *Trends Plant Sci*. **23**: 1041-1044
- Warren CR (2006) Potential organic and inorganic N uptake by six Eucalyptus species. *Funct. Plant Biol*. **3**: 653–660.
- Waters MT, Wang P, Korkaric M, Capper RG, Saunders NJ, Langdale JA (2009) GLK transcription factors coordinate expression of the photosynthetic apparatus in *Arabidopsis*. *Plant Cell* **21**: 1109-1128.
- Watkins KP, Williams-Carrier R, Chotewutmontri P, Friso G, Teubner M, Belcher S, et al. (2020) Exploring the proteome associated with the mRNA encoding the D1 reaction center protein of Photosystem II in plant chloroplasts. *Plant J*, **102**: 369-382.
- Wedlich KV, Rintoul N, Peacock S, Cape JN, Coyle M, Toet S, Barnes J, Ashmore M (2012) Effects of ozone on species composition in an upland grassland. *Oecologia* **168**: 1137-1146.
- Wege S, De Angeli A, Droillard MJ, Kroniewicz L, Merlot S, Cornu D, et al. (2014) Phosphorylation of the vacuolar anion exchanger AtCLCa is required for the stomatal response to abscisic acid. *Sci. Signal*. **7**: ra65.
- Wei X, Su X, Cao P, Liu X, Chang W, Li M. (2016) Spinach Photosystem II-LHCII supercomplex at 3.2 Å resolution. *Nature* **534**: 69–74.
- Wirth J, Chopin F, Santoni V, Viennois G, Tillard P, Krapp A (2007) Regulation of root nitrate uptake at the NRT2.1 protein level in Arabidopsis thaliana. *J. Biol. Chem*. **282**: 23541–23552.
- Xia X, Cheng X, Li R, Yao J, Li Z, Cheng Y (2021) Advances in application of genome editing in tomato and recent development of genome editing technology. *Theor Appl Genet* **134**: 2727–2747.

- Xiao G, Qin H, Zhou J, Quan R, Lu X, Huang R, Zhang H (2016) OsERF2 controls rice root growth and hormone responses through tuning expression of key genes involved in hormone signaling and sucrose metabolism. *Plant Mol. Biol*. **90**: 293–302. doi: 10.1007/s11103-015-0416-9
- Xie Z, Nolan TM, Jiang H, Yin Y (2019) AP2/ERF Transcription Factor Regulatory Networks in Hormone and Abiotic Stress Responses in *Arabidopsis*. *Front Plant Sci*. **10**: 228.
- Xu G, Fan X, Miller AJ (2012) Plant nitrogen assimilation and use efficiency. *Ann. Rev. Plant Biol*. **63**: 153-182.
- Xu H, Liu C, Lu R, Guo G, Chen Z, He T, et al. (2016) The difference in responses to nitrogen deprivation and re-supply at seedling stage between two barley genotypes differing nitrogen use efficiency. *Plant growth regulation* **79**: 119-126.
- Yang F, Cao X, Gao B, Zhao L, Li F (2015) Short-term effects of rice straw biochar on sorption, emission, and transformation of soil NH_4^+-N. *Environ. Sci. Pollut. R*. **22**: 9184-9192.
- Yang XH, Xia XZ, Zeng Y, Nong BX, Zhang ZQ, Wu YY, et al. (2020) Genome-wide identification of the peptide transporter family in rice and analysis of the PTR expression modulation in two near-isogenic lines with different nitrogen use efficiency. *BMC Plant Biol*. **20**: 193.
- Yang XS, Wu J, Ziegler TE, Yang X, Zayed A, Rajani MS, et al. (2011) Gene expression biomarkers provide sensitive indicators of in planta nitrogen status in maize. *Plant Physiol.* **157**: 1841-1852.
- Yao X, Nie J, Bai R, Sui X (2020) Amino Acid Transporters in Plants: Identification and Function. *Plants* **9**: 972.
- Yip A, Horvath S (2007) Gene network interconnectedness and the generalized topological overlap measure. *BMC Bioinform.* **8**: 22
- Yip Delormel T, Boudsocq M (2019) Properties and functions of calcium-dependent protein kinases and their relatives in *Arabidopsis thaliana*. *New Phytol*. **224**: 585–604.
- Yu C, Liu Y, Zhang A, Su S, Yan A, Huang L, et al. (2015) MADS-box transcription factor OsMADS25 regulates root development through affection of nitrate accumulation in rice. *PLoS One* **10**: e0135196.
- Yu LH, Miao ZQ, Qi GF, Wu J, Cai XT, Mao JL, et al. (2014) MADS-Box transcription factor AGL21 regulates lateral root development and responds to multiple external and physiological signals. *Mol. Plant* **7**: 1653–1669.

- Yu Y, Liu J, Li F, Zhang X, Zhang C, Xiang J (2017) Gene set based association analyses for the WSSV resistance of pacific white shrimp *Litopenaeus vannamei*. *Sci. Rep*. **7**: 40549.
- Yuan S, Zhang ZW, Zheng C, Zhao ZY, Wang Y, Feng LY, et al. (2016) Arabidopsis cryptochrome 1 functions in nitrogen regulation of flowering. *PNAS* **113:** 7661–7666.
- Zandalinas SI, Rivero RM, Martínez V, Gómez-Cadenas A, Arbona V (2016) Tolerance of citrus plants to the combination of high temperatures and drought is associated to the increase in transpiration modulated by a reduction in abscisic acid levels. *BMC Plant Biol*. **16**: 105.
- Zanin L, Tomasi N, Wirdnam C, Meier S, Komarova NY, Mimmo T, et al. (2014) Isolation and functional characterization of a high affinity urea transporter from roots of *Zea mays*. *BMC Plant Biol.* **14**: 222.
- Zhang D, Zhang Y, Yang W, Miao G (2006) Biological response of roots in different spring wheat genotypes to low nitrogen stress. *Acta Agron. Sin*. **32**: 1349–1354.
- Zhang X, Davidson EA, Mauzerall DL, Searchinger TD, Dumas P, Shen Y (2015) Managing nitrogen for sustainable development. *Nature* **528**: 51-9
- Zhang Z, Xiong S, Wei Y, Meng X, Wang X, Ma X (2017) The role of glutamine synthetase isozymes in enhancing nitrogen use efficiency of N-efficient winter wheat. *Sci Rep* **7**, 1000.
- Zhang Q, Song T, Guan C, Gao Y, Ma J, Gu X et al. (2021) OsANN4 modulates ROS production and mediates Ca2+ influx in response to ABA. *BMC Plant Biol*. **21**, 474
- Zhao D, Reddy KR, Kakani VG, Reddy VR (2005) Nitrogen deficiency effects on plant growth, leaf photosynthesis, and hyperspectral reflectance properties of sorghum. *Europ. J. Agron.* **22**: 391–403.
- Zhao J, Sauvage C, Zhao J, Bitton F, Bauchet G, Liu D, et al. (2019) Meta-analysis of genome-wide association studies provides insights into genetic control of tomato flavor. *Nature Communications* **10**:1-12.
- Zhao M, Ding H, Zhu JK, Zhang F, Li WX (2011) Involvement of miR169 in the nitrogen-starvation responses in *Arabidopsis*. *New Phytol.* **190**: 906–915.
- Zhao W, Yang X, Yu H, Jiang W, Sun N, Liu X et al. (2015) RNA-Seq-Based Transcriptome Profiling of Early Nitrogen Deficiency Response in Cucumber Seedlings Provides New Insight into the Putative Nitrogen Regulatory Network, *Plant and Cell Physiology* **56 (3)**: 455–467.

- Zhu C, Yang N, Guo Z, Qian M, Gan L (2016) An ethylene and ROS-dependent pathway is involved in low ammonium-induced root hair elongation in Arabidopsis seedlings. *Plant Physiol Biochem.* **105**: 37-44.
- Zhu G, Peng S, Huang J, Cui K, Nie L, Wang F (2016) Genetic improvements in rice yield and concomitant increases in radiation- and nitrogen-use efficiency in Middle Reaches of Yangtze River. *Sci. Rep*. **6**: 21049.
- Zhu G, Wang S, Huang Z, Zhang S, Liao Q, Zhang C, et al (2018) Rewiring of the Fruit Metabolome in Tomato Breeding. *Cell* **172**: 249-261.
- Zhu JK (2003) Regulation of ion homeostasis under salt stress. *Curr. Opin. Plant Biol*. **6**: 441–445.
- Zhu Z, Chen G, Guo X, Yin W, Yu X, Hu J, et al. (2017) Overexpression of *SlPRE2*, an atypical bHLH transcription factor, affects plant morphology and fruit pigment accumulation in tomato. *Sci Rep*. **7**: 5786.
- Zifarelli G, Pusch M (2010) CLC transport proteins in plants. *FEBS Letters* **584**: 2122–2127.

Appendix

Table S1. ANOVA of root and shoot N content

N-content	Shoot	Root
G	***	**
[N]	***	***
G*[N]	***	ns

* $0.01 < p \leq 0.05$; ** $0.001 < p < 0.01$; *** $p < 0.001$

Table S2. ANOVA of relative gene expression ($2^{-\Delta Ct}$) in shoot and root of RO and UC82 at T0

T0	Shoot							Root			
	NR	**NIR**	**GS2**	**GOGAT**	**NRT1.7**	**NRT2.7**	**CLCa**	**NR**	**CLCa**	**NRT1.5**	**NRT1.8**
G	*	ns	**	ns	ns	ns	ns	**	**	*	***

* $0.01 < p \leq 0.05$; ** $0.001 < p < 0.01$; *** $p < 0.001$

Table S3: ANOVA of relative gene expression ($2^{-\Delta\Delta Ct}$) in shoot and root of RO and UC82 within each time point (8h, 24h and 7 days)

Time	**Shoot**							**Root**			
8h	**NR**	**NIR**	**GS2**	**GOGAT**	**NRT1.7**	**NRT2.7**	**CLCa**	**NR**	**CLCa**	**NRT1.5**	**NRT1.8**
G	ns	*	ns	*	**	ns	***	***	*	***	*
N	**	ns	ns	***	***	ns	**	**	ns	ns	**
G*N	ns	**	ns	*	**	ns	***	*	***	ns	*
24h	**NR**	**NIR**	**GS2**	**GOGAT**	**NRT1.7**	**NRT2.7**	**CLCa**	**NR**	**CLCa**	**NRT1.5**	**NRT1.8**
G	**	ns	***	***	***	***	***	***	***	***	**
N	ns	ns	***	***	*	**	***	***	***	***	***
G*N	ns	ns	***	**	ns	***	***	ns	*	***	**
7d	**NR**	**NIR**	**GS2**	**GOGAT**	**NRT1.7**	**NRT2.7**	**CLCa**	**NR**	**CLCa**	**NRT1.5**	**NRT1.8**
G	**	***	ns	***	ns	***	***	ns	**	**	***
N	**	***	ns	***	***	***	***	***	***	***	ns
G*N	ns	***	ns	**	ns	***	***	ns	*	**	ns

* $0.01 < p \leq 0.05$; ** $0.001 < p < 0.01$; *** $p < 0.001$

Table S4. Primers designed for qRT-PCR

Gene	Accession ID	Primer Sequences (5' to 3')		Amplicon length
NR	NM_001328498.1	Forward	5'-GGTGGATGGATGGCAAAGGA-3'	127
		Reverse	5'-TCCTCACCTCGGACATGGAA-3'	
GOGAT	XM_004234907.4	Forward	5'-GTGGTTTGGGCCATCTCTGA-3'	83
		Reverse	5'-CACGACTGTTGGCTGCTTTT-3'	
GS2	NM_001323669.1	Forward	5´-TGGAGTTGAGGTGTAATTGTTGG-3´	105
		Reverse	5´-CATTCGGAAAGAGCACACCA-3´	
Nir2	XM_004248688.4	Forward	5´-GGACAGGTTGCCCAAATACA-3´	67
		Reverse	5´-GTCAGGCATCCCATGAATCCG-3´	
NRT1.7	XM_004238712.2	Forward	5'- TCCCCGAAAACATGAGCAGT -3'	117
		Reverse	5'- GCCCATTTCCTCCCGTAGTG -3'	
CLC-a	XM_004231738	Forward	5´-CGTCTCCCTTTTCACCTCCA-3´	93
		Reverse	5´-CCAGGACAGGACCCTTGAAT-3´	
NRT1.5	XM_004244498.4	Forward	5´-TCCTTAGTGTAGCAGGCGTC-3´	127
		Reverse	5´-ACCAGTCCAATACCCATCCG-3´	
NRT1.8	XM_010328990.3	Forward	5´-GCCTTTGTGCAGTGTCTCAA-3´	141
		Reverse	5´-CTGTTTTCATTGCAGCCCCT-3´	
SlNITR2.1	XM_004236138.3	Forward	5'-AGTCAAGTGGATGCATTTCGG-3'	70
		Reverse	5'-CAGTTTCTGGGTTGAATGAGAA-3'	
ERF1a	NM_001247912.2	Forward	5'- AGGGGTCCTTGGTCTCTACT-3'	147
		Reverse	5'- ACTTCTCTTGTGCTTGACTCTTC-3'	
Actin*	NM_001330119.1	Forward	5´AGGTATTGTGTTGGACTCTGGTGAT-3´	81
		Reverse	5´-ACGAGAATGGCATGTGGAA-3´	
EF1-α*	NM_001247106.2	Forward	5´-GGAACTTGAGAAGGAGCCTAAG-3´	165
		Reverse	5´-TTCTTGACAACACCGACAGC-3´	

*) Reference genes used as internal standards.

Table S5. Number of clean reads generated from each sample sequenced (Transeq) and mapped to the tomato genome using TopHat for RO and UC82, at 0h (T0), 8h (T1) and 24h (T2), in HN and LN conditions, in shoot (S) and root (R)

Sample	clean_reads	Mapped-reads	Mapping %
ROT0S	1906022	1280489	67,18
ROT0S	2133203	1306173	61,23
ROT0S	1465065	838270	57,22
ROT0R	3401261	2491873	73,26
ROT0R	2049678	1239176	60,46
ROT0R	3571786	2426064	67,92
UCT0S	1509414	864869	57,3
UCT0S	5178363	3810513	73,59
UCT0S	1419839	821282	57,84
UCT0R	1332848	729165	54,71
UCT0R	3469504	2555943	73,67
UCT0R	3395649	2474260	72,87
ROT1SH	5152158	3748111	72,75
ROT1SH	3586413	2757065	76,88
ROT1SH	2583650	1911254	73,97
ROT1SL	2335660	1642635	70,33
ROT1SL	3559648	2755046	77,4
ROT1SL	1416171	738684	52,16
ROT1RH	3366388	2520089	74,86
ROT1RH	3365036	2451567	72,85
ROT1RH	6093885	4594774	75,4
ROT1RL	14533866	11489361	79,05
ROT1RL	3604946	2615165	72,54
ROT1RL	1367049	795828	58,22
UCT1SH	6217803	4958484	79,75
UCT1SH	3540802	2692242	76,03
UCT1SH	3697532	2856704	77,26
UCT1SL	2299919	1646243	71,58
UCT1SL	2672861	1957243	73,23
UCT1SL	917008	467909	51,03
UCT1RH	3712470	2661288	71,69
UCT1RH	7124110	5830217	81,84
UCT1RH	9329400	7622436	81,7
UCT1RL	9992107	8028419	80,35
UCT1RL	7291868	5863890	80,42
UCT1RL	2092043	1424449	68,09
ROT2SH	2489830	2024078	81,29
ROT2SH	3852398	2955460	76,72
ROT2SH	585464	304249	51,97
ROT2SL	3980049	3077826	77,33
ROT2SL	2159429	1561060	72,29
ROT2SL	15326609	11696417	76,31
ROT2RH	1106165	657169	59,41
ROT2RH	5605041	4289862	76,54
ROT2RH	3174546	2100201	66,16
ROT2RL	11723454	9089555	77,53
ROT2RL	3629206	2626764	72,38
ROT2RL	928381	364513	39,26
UCT2SH	10635783	9125540	85,8
UCT2SH	4703095	3840046	81,65
UCT2SH	5861620	4710523	80,36
UCT2SL	5974063	4979620	83,35
UCT2SL	5595378	4441595	79,38
UCT2SL	9453256	7711955	81,58

Table S5. Number of clean reads generated from each sample which were sequenced (Transeq) and mapped to the tomato genome using TopHat (continue)

UCT2RH	**8205400**	**6643086**	**80,96**
UCT2RH	1070968	798855	74,59
UCT2RH	6337623	5259622	82,99
UCT2RL	6768783	5638612	83,3
UCT2RL	2656735	2079494	78,27
UCT2RL	6317154	5227071	82,74
Total	268825855	206070353	72,14

Table S6. Differentially expressed genes ($p<0.05$) detected by multivariate linear model in shoot and root including Genotype (RO and UC82), Time (0h, 8h, 24h), Nitrate (Low N, and High N) and their interactions.

Fitted model	No. of Gene in Shoot	No. of Gene in Root
Genotype (G)	**3387**	**3357**
N level (N)	912	2123
Time (T)	8281	7329
G*N	**1084**	**1272**
G*T	2133	2418
N*T	1417	1300
G*N*T	**1190**	**886**
Total unique genes	**4812**	**4802**

Table S7. Number of significantly clustered genes in shoot and root after 0h, 8h and 24h of N treatment

N level	Shoot	Root
HN	1160	2754
LN	1315	1104
Total unique genes	2041	3119

Table S8. Molecular function GO term enrichment of the co-expressed genes in the brown module in shoot.

	Enrichment FDR	Genes in list	Total genes	Functional Category
MF	0.0384	3	42	Chlorophyll binding
MF	0.0477	2	15	Secondary active sulfate transmembrane transporter activity
MF	0.0477	2	16	Sulfate transmembrane transporter activity
MF	0.0477	2	20	Anion:anion antiporter activity
MF	0.0477	2	20	Solute:anion antiporter activity
MF	0.0484	2	27	Peptide:proton symporter activity
MF	0.0484	2	26	Oxidoreductase activity. acting on the CH-CH group of donors. NAD or NADP as acceptor
MF	0.0484	4	198	Active ion transmembrane transporter activity
MF	0.0484	2	24	Sulfur compound transmembrane transporter activity
MF	0.0485	1	2	Abscisic acid glucosyltransferase activity
MF	0.0485	4	229	Secondary active transmembrane transporter activity
MF	0.0485	1	2	12-oxophytodienoate reductase activity
MF	0.0485	18	3298	Transferase activity
MF	0.0485	2	35	Thiolester hydrolase activity
MF	0.0485	2	31	Oligopeptide transmembrane transporter activity
MF	0.0485	18	3216	Anion binding
MF	0.0485	1	2	Delta24-sterol reductase activity
MF	0.0485	2	39	Quercetin 3-O-glucosyltransferase activity
MF	0.0485	2	39	Quercetin 7-O-glucosyltransferase activity

Table S9. Biological process GO term enrichment of the brown module hub genes

	Enrichment FDR	Genes in list	Total genes	Functional Category
BP	0.0229	1	3	Vegetative phase change
BP	0.0229	1	2	Carbohydrate mediated signaling
BP	0.0269	1	4	Response to nutrient
BP	0.0380	1	10	Cytokinin biosynthetic process
BP	0.0315	1	6	Regulation of autophagy
BP	0.0315	1	8	Monocarboxylic acid transport
BP	0.0315	1	8	Response to monosaccharide
BP	0.0315	1	5	Response to decreased oxygen levels
BP	0.0315	1	6	Response to oxygen levels
BP	0.0315	1	6	Cellular response to carbohydrate stimulus
BP	0.0315	1	7	Positive regulation of response to alcohol
BP	0.0315	1	7	Positive regulation of cellular response to alcohol
BP	0.0315	1	8	Detection of chemical stimulus
BP	0.0315	1	8	Response to hexose
BP	0.0315	1	8	Response to glucose
BP	0.0315	1	7	Positive regulation of abscisic acid-activated signaling pathway

Table S10. Number of clean reads generated from each sample sequenced (Transeq) and mapped to the tomato genome using TopHat for RO and UC82, at 7 days (T3), in HN and LN conditions, in shoot (S) and root (R)

Sample	clean_reads	Mapped-reads	Mapping %
ROT3SH	3107845	2398164	77,16
ROT3SH	4494375	3578928	79,63
ROT3SH	4600766	3616028	78,6
ROT3SL	3836049	3042013	79,3
ROT3SL	3716852	2845552	76,56
ROT3SL	2353197	1571870	66,8
ROT3RH	5264489	4263259	80,98
ROT3RH	11056404	9034300	81,71
ROT3RH	481448	249179	51,76
ROT3RL	2308771	1356120	58,74
ROT3RL	6908084	5381598	77,9
ROT3RL	3181312	2497200	78,5
UCT3SH	1930357	1488231	77,1
UCT3SH	4470751	3439242	76,93
UCT3SH	6078711	4862125	79,99
UCT3SL	5283474	4377207	82,85
UCT3SL	4109698	3317847	80,73
UCT3SL	4741566	3911465	82,49
UCT3RH	5233669	4278101	81,74
UCT3RH	5714540	4662286	81,59
UCT3RH	6880676	5909860	85,89
UCT3RL	5040767	4051984	80,38
UCT3RL	6434248	5036824	78,28
UCT3RL	6642419	5000646	75,28
Total	113870468	90170029	77,12

Table S11. Top 10 Biological process GO terms and KEGG pathways enrichment of the common DEGs between RO-LNvsHN and UC82-LNvsHN comparisons

	Enrichment FDR	Genes in list	Total genes	Functional Category
BP	1,63E-38	59	225	Photosynthesis
BP	1,76E-21	33	122	Photosynthesis, light reaction
BP	7,92E-18	17	28	Photosynthesis, light harvesting
BP	1,36E-17	50	396	Generation of precursor metabolites and energy
BP	6,47E-16	109	1679	Oxidation-reduction process
BP	1,01E-12	11	15	Photosynthesis, light harvesting in photosystem I
BP	3,87E-12	175	3757	Biosynthetic process
BP	1,89E-11	169	3652	Organic substance biosynthetic process
BP	6,46E-11	80	1265	Organonitrogen compound biosynthetic process
BP	8,07E-10	160	3559	Cellular biosynthetic process
KEGG	9,54E-09	122	1630	Metabolic pathways
KEGG	1,07E-08	76	831	Biosynthesis of secondary metabolites
KEGG	1,70E-06	20	102	Photosynthesis
KEGG	2,65E-06	27	190	Carbon metabolism
KEGG	3,13E-06	10	21	Photosynthesis - antenna proteins
KEGG	3,64E-05	13	56	Carbon fixation in photosynthetic organisms
KEGG	4,68E-05	11	40	Porphyrin and chlorophyll metabolism
KEGG	1,15E-04	12	55	Glyoxylate and dicarboxylate metabolism
KEGG	3,50E-04	10	43	Glycine serine and threonine metabolism
KEGG	1,85E-02	16	166	Biosynthesis of amino acids

Table S12. List of the LN-specific DEGs in ROvsUC82 comparison in shoot

Gene ID	Gene annotation	LFC	LFC	LFC	LFC	padjs	padjs	padjs	padjs
		ROvsUC82-LN	ROvsUC82-HN	RO-LNvsHN	UC82-LNvsHN	ROvsUC82-LN	ROvsUC82-HN	RO-LNvsHN	UC82-LNvsHN
ENSRNA050029895		2,452	0	0,000	0,000	0,003	*	*	*
ENSRNA050030006		3,756	0	0,000	-2,507	0,000	*	*	0,000
Solyc00g174330.3	Pathogenesis-related protein 1	-2,397	0	0,000	1,989	0,008	*	*	0,013
Solyc00g174340.2	Pathogenesis-related protein 1b	-2,715	0	0,000	2,674	0,002	*	*	0,000
Solyc00g230080.1	Photosystem II protein D2	4,904	0	3,657	0,000	0,000	*	1,4E-06	*
Solyc01g005770.3	Unknown protein	1,635	0	0,000	0,000	0,012	*	*	*
Solyc01g006300.3	LECEVI1A	-1,280	0	1,755	2,411	0,000	*	4,7E-10	0,000
Solyc01g006400.3	Pistil extensin like protein, partial CDS only	-2,178	0	0,000	1,623	0,000	*	*	0,000
Solyc01g006560.3	Lipoxygenase	-1,015	0	0,000	1,649	0,046	*	*	0,000
Solyc01g017330.2	Photosystem I P700 chlorophyll a apoprotein A1	3,165	0	3,180	0,000	0,002	*	1,9E-04	*
Solyc01g017600.3	transmembrane protein 45B-like	-1,458	0	0,000	0,000	0,000	*	*	*
Solyc01g020285.1	Unknown protein	4,748	0	2,370	0,000	0,000	*	1,0E-04	*
Solyc01g048590.2	Photosynthetic reaction centre, L/M	5,191	0	2,750	-2,328	0,000	*	8,4E-04	0,012
Solyc01g057000.3	Universal stress protein	-3,470	0	0,000	3,279	0,000	*	*	0,000
Solyc01g057760.3	RNA helicase DEAD2	-2,049	0	-2,581	0,000	0,029	*	2,4E-04	*
Solyc01g060085.1	Ribulose bisphosphate carboxylase large chain	3,632	0	1,867	0,000	0,000	*	2,4E-03	*
Solyc01g073680.3	Bifunctional inhibitor/lipid-transfer protein/seed storage 2S albumin superfamily protein	-1,214	0	0,000	0,000	0,000	*	*	*
Solyc01g073720.2	Transmembrane protein	-1,450	0	0,000	1,337	0,016	*	*	0,009
Solyc01g079300.3	Stachyose synthase	-3,052	0	0,000	0,000	0,002	*	*	*
Solyc01g081310.3	glutathione S-transferase T3	1,466	0	1,817	0,000	0,002	*	5,0E-06	*
Solyc01g087780.2	serine protease SBT4A	-1,654	0	-1,758	0,000	0,010	*	9,2E-04	*
Solyc01g095960.3	O-acyltransferase WSD1-like	-3,238	0	0,000	0,000	0,001	*	*	*
Solyc01g102770.1	Photosystem II reaction center protein Z	2,125	0	0,000	-2,058	0,000	*	*	0,000
Solyc01g105120.3	protein LNK1	1,212	0	0,000	0,000	0,000	*	*	*
Solyc01g105350.2	Glycosyltransferase	2,512	0	3,111	0,000	0,000	*	9,1E-09	*
Solyc01g105450.3	ABC transporter G family member 11	-1,640	0	1,886	3,070	0,005	*	1,3E-04	0,000
Solyc01g108020.3	Thioredoxin M3, chloroplastic	-3,210	0	0,000	0,000	0,001	*	*	*

Solyc01g110340.3	Endoglucanase	-1,761	0	-1,771	0,000	0,005	*	1,0E-03	*
Solyc01g111110.3	transmembrane protein	1,007	0	1,763	0,000	0,000	*	3,3E-29	*
Solyc01g112010.3	RNA-binding (RRM/RBD/RNP motifs) family protein	2,294	0	0,000	0,000	0,015	*	*	*
Solyc01g112190.3	NIN-like	1,146	0	0,000	-1,639	0,048	*	*	0,000
Solyc02g011800.1	NAD(P)H-quinone oxidoreductase subunit 1, chloroplastic	2,142	0	2,065	0,000	0,048	*	1,1E-02	*
Solyc02g011815.1	Unknown protein	2,508	0	0,000	0,000	0,027	*	*	*
Solyc02g011990.1	Photosystem II protein D1	2,338	0	0,000	0,000	0,048	*	*	*
Solyc02g020960.2	Photosystem I P700 chlorophyll a apoprotein A1	2,853	0	0,000	0,000	0,003	*	*	*
Solyc02g062390.3	abscisic acid and environmental stress-inducible protein TAS14	-2,679	0	0,000	3,948	0,005	*	*	0,000
Solyc02g062500.3	2-oxoglutarate (2OG) and Fe(II)-dependent oxygenase superfamily protein	-1,091	0	1,493	1,696	0,026	*	1,4E-04	0,000
Solyc02g062570.3	Phosphatidic acid phosphatase	1,817	0	0,000	0,000	0,013	*	*	*
Solyc02g062680.3	Anaphase-promoting complex subunit 10	-1,760	0	0,000	1,755	0,015	*	*	0,004
Solyc02g065060.3	Short-chain dehydrogenase/reductase SDR	1,248	0	0,000	0,000	0,005	*	*	*
Solyc02g066830.3	Nuclear transport factor 2 (NTF2) family protein with RNA binding (RRM-RBD-RNP motifs) domain-containing protein	1,880	0	0,000	0,000	0,032	*	*	*
Solyc02g067380.3	bHLH style2.1 (PRE2)	2,402	0	2,599	0,000	0,046	*	3,3E-03	*
Solyc02g067975.1	Unknown protein	-2,088	0	-2,241	0,000	0,025	*	2,0E-03	*
Solyc02g069910.2	Unknown protein	-2,069	0	-1,742	0,000	0,018	*	2,1E-02	*
Solyc02g076920.3	bHLH transcription factor 013	1,484	0	2,298	0,000	0,015	*	3,7E-06	*
Solyc02g077420.3	Phospholipase A1-II 1	-1,393	0	0,000	1,502	0,032	*	*	0,004
Solyc02g077860.1	Ribulose bisphosphate carboxylase large chain	2,568	0	2,473	0,000	0,013	*	2,7E-03	*
Solyc02g078610.3	Splicing factor 3B subunit 2	2,370	0	0,000	0,000	0,028	*	*	*
Solyc02g080635.1	Unknown protein	4,388	0	0,000	-3,321	0,000	*	*	0,000
Solyc02g081980.3	Apyrase	-1,095	0	-1,415	0,000	0,001	*	2,7E-07	*
Solyc02g083720.3	MLO-like protein	2,122	0	0,000	-2,162	0,050	*	*	0,011
Solyc02g084800.3	Peroxidase	2,326	0	1,569	0,000	0,000	*	2,6E-03	*
Solyc02g088180.3	NAC domain-containing protein	2,100	0	2,300	0,000	0,002	*	6,4E-05	*
Solyc02g088270.3	hypothetical protein (DUF1997)	-2,472	0	0,000	2,178	0,011	*	*	0,009
Solyc02g090070.3	BTB/POZ domain-containing protein	-1,023	0	-1,495	0,000	0,043	*	3,4E-05	*
Solyc02g090230.3	Nuclear pore complex protein NUP58	-1,418	0	-1,646	0,000	0,009	*	2,0E-04	*
Solyc02g093180.3	HXXXD-type acyl-transferase family protein	-2,941	0	1,702	3,223	0,000	*	2,4E-02	0,000
Solyc03g006110.3	Non-specific serine/threonine protein kinase	2,849	0	0,000	-1,725	0,000	*	*	0,034
Solyc03g006350.3	Zinc finger transcription factor 23	-2,467	0	0,000	0,000	0,019	*	*	*
Solyc03g006490.3	Stem-specific protein TSJT1	-1,058	0	0,000	0,000	0,041	*	*	*
Solyc03g006550.3	Terpene synthase	-4,394	0	-2,412	2,256	0,000	*	3,5E-04	0,000
Solyc03g013160.3	Amino acid transporter	-2,168	0	0,000	0,000	0,022	*	*	*

Solyc03g020060.3	Proteinase inhibitor type-2	-3,522	0	0,000	0,000	0,000	*	*	*
Solyc03g025830.3	Myosin heavy chain-related protein	-1,797	0	-1,557	0,000	0,038	*	3,0E-02	*
Solyc03g026120.3	S-adenosyl-L-methionine-dependent methyltransferases superfamily protein	1,760	0	0,000	-1,998	0,003	*	*	0,000
Solyc03g026260.3	TraB family protein	1,175	0	0,000	0,000	0,005	*	*	*
Solyc03g034240.3	Abscisic acid (Aba)-deficient 4	-2,495	0	0,000	0,000	0,028	*	*	*
Solyc03g044660.3	4-hydroxy-tetrahydrodipicolinate synthase	-1,057	0	-1,183	0,000	0,001	*	2,6E-05	*
Solyc03g095650.3	MLO-like protein	-1,708	0	0,000	2,597	0,030	*	*	0,000
Solyc03g096050.3	2-oxoglutarate (2OG) and Fe(II)-dependent oxygenase superfamily protein	-2,366	0	0,000	1,590	0,005	*	*	0,044
Solyc03g097930.3	Unknown protein	-1,117	0	0,000	0,000	0,049	*	*	*
Solyc03g098100.3	Methylecgonone reductase	-1,339	0	0,000	1,563	0,001	*	*	0,000
Solyc03g098710.1	Kunitz-like protease inhibitor	-3,302	0	0,000	0,000	0,001	*	*	*
Solyc03g098760.2	Serine protease inhibitor 1	-3,420	0	0,000	2,790	0,000	*	*	0,001
Solyc03g098790.2	cathepsin D inhibitor protein	-3,688	0	0,000	2,127	0,000	*	*	0,000
Solyc03g114020.3	D-ribose-binding periplasmic protein	-1,016	0	0,000	0,000	0,001	*	*	*
Solyc03g114100.1	hypothetical protein	-1,862	0	-1,887	0,000	0,009	*	1,2E-03	*
Solyc03g114970.3	Protein SPIRAL1	1,075	0	0,000	-1,177	0,005	*	*	0,000
Solyc03g115650.3	eukaryotic translation initiation factor 5A-1	1,660	0	0,000	0,000	0,000	*	*	*
Solyc03g116680.3	Methyl-CpG-binding domain-containing protein 11	-2,307	0	0,000	0,000	0,012	*	*	*
Solyc03g117640.1	MAP kinase kinase kinase 29	2,671	0	0,000	0,000	0,016	*	*	*
Solyc03g120090.1	Pyridoxal 5'-phosphate synthase pdxS subunit	-1,808	0	0,000	0,000	0,040	*	*	*
Solyc03g122000.3	Cytochrome b6-f complex subunit 4	2,633	0	2,469	0,000	0,018	*	5,6E-03	*
Solyc03g122180.3	Oligouridylate-binding protein 1A	3,295	0	4,060	0,000	0,000	*	1,6E-08	*
Solyc04g005280.3	bHLH transcription factor 028	-1,268	0	0,000	0,000	0,041	*	*	*
Solyc04g007820.3	Sn-1 protein	1,384	0	1,078	0,000	0,030	*	4,6E-02	*
Solyc04g007825.1	Kirola	1,231	0	0,000	0,000	0,020	*	*	*
Solyc04g010230.3	Pectate lyase	2,459	0	2,118	0,000	0,036	*	2,5E-02	*
Solyc04g015340.3	Carboxypeptidase	-1,195	0	0,000	0,000	0,004	*	*	*
Solyc04g016000.3	Heat shock transcription factor protein 8	-1,740	0	0,000	2,856	0,041	*	*	0,000
Solyc04g016170.2	Photosystem I P700 chlorophyll a apoprotein A2	2,934	0	2,557	0,000	0,005	*	4,3E-03	*
Solyc04g017620.3	Phosphatidylinositol 4-phosphate 5-kinase	-1,372	0	0,000	0,000	0,026	*	*	*
Solyc04g017720.3	Gibberellin regulated protein	-1,324	0	-2,846	-1,750	0,000	*	1,1E-33	0,000
Solyc04g024540.2	Protein Ycf2	5,121	0	3,200	0,000	0,000	*	1,8E-05	*
Solyc04g024885.1	Unknown protein	3,666	0	2,088	0,000	0,000	*	1,5E-02	*
Solyc04g025170.3	ABC transporter G family member 24	-1,605	0	0,000	0,000	0,039	*	*	*
Solyc04g025560.3	ADP-ribosylation factor	3,362	0	0,000	0,000	0,000	*	*	*

Solyc04g039840.1	Ribulose bisphosphate carboxylase large chain	3,650	0	2,194	0,000	0,000	*	1,7E-02	*
Solyc04g049150.2	Unknown protein	3,110	0	0,000	0,000	0,001	*	*	*
Solyc04g051280.3	nucleolin	-2,585	0	0,000	0,000	0,011	*	*	*
Solyc04g051670.3	RNA cytidine acetyltransferase	1,088	0	0,000	0,000	0,018	*	*	*
Solyc04g072375.1	Unknown protein	-4,003	0	0,000	3,119	0,000	*	*	0,000
Solyc04g074780.3	Plastid-targeted protein 3	2,670	0	0,000	0,000	0,008	*	*	*
Solyc04g081070.3	Protein ACCUMULATION AND REPLICATION OF CHLOROPLASTS 6, chloroplastic	-1,300	0	-1,533	0,000	0,010	*	1,7E-04	*
Solyc04g081650.3	Cyclin	-2,002	0	0,000	0,000	0,001	*	*	*
Solyc04g082980.2	Tetratricopeptide repeat protein SKI3	2,154	0	0,000	-2,962	0,015	*	*	0,000
Solyc05g006980.3	Homeobox-leucine zipper protein HOX16	-1,648	0	0,000	0,000	0,035	*	*	*
Solyc05g007240.1	zinc finger CCHC domain protein	1,062	0	0,000	0,000	0,001	*	*	*
Solyc05g007675.1	apyrase 6	2,495	0	2,304	0,000	0,031	*	1,1E-02	*
Solyc05g007770.3	NAC domain TF	-1,910	0	0,000	3,413	0,006	*	*	0,000
Solyc05g008190.3	Transducin/WD40 repeat-like superfamily protein	1,001	0	0,000	0,000	0,048	*	*	*
Solyc05g009990.3	Leucine-rich repeat	-1,329	0	-2,096	0,000	0,005	*	7,9E-09	*
Solyc05g010160.3	Importin-9	1,072	0	0,000	0,000	0,026	*	*	*
Solyc05g010420.2	S-adenosylmethionine decarboxylase	-1,076	0	0,000	0,000	0,000	*	*	*
Solyc05g010423.1	Unknown protein	-1,463	0	-1,234	0,000	0,000	*	1,4E-05	*
Solyc05g015415.1	Unknown protein	-2,367	0	0,000	0,000	0,048	*	*	*
Solyc05g016120.2	Photosystem II protein D1	5,276	0	2,715	0,000	0,000	*	3,0E-04	*
Solyc05g021190.2	Photosystem II D2 protein	2,858	0	0,000	0,000	0,007	*	*	*
Solyc05g021510.2	Unknown protein	3,367	0	0,000	0,000	0,000	*	*	*
Solyc05g023720.1	Cytochrome f	1,799	0	-1,662	-2,587	0,004	*	7,6E-04	0,000
Solyc05g026600.3	Terpene synthase	2,612	0	0,000	0,000	0,012	*	*	*
Solyc05g045670.3	Glucose-6-phosphate/phosphate-translocator	1,799	0	1,614	0,000	0,000	*	3,8E-09	*
Solyc05g051350.2	Rhamnogalacturonate lyase	-2,416	0	0,000	0,000	0,030	*	*	*
Solyc05g051530.3	ABC transporter G family member 11	1,623	0	1,366	0,000	0,017	*	2,0E-02	*
Solyc05g052890.3	Plant/protein	1,844	0	-1,410	-2,560	0,005	*	2,7E-03	0,000
Solyc05g053080.2	scarecrow-like protein 14	1,166	0	0,000	0,000	0,000	*	*	*
Solyc05g054560.3	CASP-like protein	-1,616	0	0,000	1,360	0,030	*	*	0,029
Solyc06g005890.3	DUF674 family protein	-2,128	0	0,000	0,000	0,000	*	*	*
Solyc06g006110.3	Vacuolar cation/proton exchanger	-1,125	0	0,000	0,000	0,000	*	*	*
Solyc06g008590.3	auxin-regulated IAA17	1,409	0	1,411	0,000	0,011	*	2,2E-03	*
Solyc06g009940.1	Photosystem I P700 chlorophyll a apoprotein A1	3,314	0	2,127	0,000	0,000	*	1,7E-02	*
Solyc06g043038.1	Unknown protein	3,896	0	3,150	0,000	0,000	*	2,5E-04	*

Solyc06g048930.3	two-component response regulator ARR17	-1,588	0	0,000	1,405	0,033	*	*	0,022
Solyc06g051080.3	UDP-glucose pyrophosphorylase 3	-1,098	0	-1,334	0,000	0,036	*	7,0E-04	*
Solyc06g060010.3	Terpene synthase	3,102	0	2,962	0,000	0,001	*	2,7E-04	*
Solyc06g062370.3	acid phosphatase 1-like	-1,835	0	0,000	1,757	0,005	*	*	0,002
Solyc06g066860.2	2-oxoglutarate (2OG) and Fe(II)-dependent oxygenase superfamily protein	1,612	0	0,000	0,000	0,018	*	*	*
Solyc06g068120.3	DUF4050 family protein	1,819	0	0,000	-1,073	0,000	*	*	0,039
Solyc06g069240.2	branched1b	3,310	0	0,000	0,000	0,000	*	*	*
Solyc06g071310.3	LIM domain-containing protein	-1,175	0	-1,204	0,000	0,035	*	6,4E-03	*
Solyc06g071670.1	S-adenosyl-L-methionine-dependent methyltransferases superfamily protein	1,384	0	0,000	-1,434	0,004	*	*	0,000
Solyc06g072160.3	Alcohol dehydrogenase 1	2,584	0	0,000	-2,233	0,016	*	*	0,017
Solyc06g072845.1	hypothetical protein	-2,784	0	0,000	3,832	0,000	*	*	0,000
Solyc06g074090.3	7-dehydrocholesterol reductase	1,272	0	1,946	1,023	0,000	*	4,5E-14	0,001
Solyc06g074320.3	Transcription factor TGA2	1,759	0	0,000	0,000	0,002	*	*	*
Solyc06g076370.3	low-temperature-induced protein	2,572	0	2,047	0,000	0,024	*	3,0E-02	*
Solyc06g076580.1	Unknown protein	-1,648	0	0,000	0,000	0,011	*	*	*
Solyc06g083030.3	Carboxypeptidase	-1,163	0	0,000	0,000	0,038	*	*	*
Solyc06g083070.3	Fimbrin-2	-2,345	0	0,000	0,000	0,041	*	*	*
Solyc07g006380.3	Defensin-like protein	-2,709	0	0,000	2,993	0,004	*	*	0,000
Solyc07g006500.3	trehalose-6-phosphate synthase 1	-1,822	0	0,000	1,139	0,001	*	*	0,027
Solyc07g006550.2	ribonuclease 3-like	-2,285	0	0,000	0,000	0,033	*	*	*
Solyc07g007250.3	Metallocarboxypeptidase inhibitor	-3,478	0	0,000	2,864	0,000	*	*	0,000
Solyc07g008610.2	(DB142) meloidogyne-induced giant cell protein	-2,021	0	-2,163	0	0,023	*	1,9E-03	*
Solyc07g014670.3	Cytochrome P450	-1,389	0	0,000	1,236	0,011	*	*	0,009
Solyc07g041720.1	Germin-like protein	-1,252	0	-3,447	-1,985	0,026	*	1,1E-19	0,000
Solyc07g051890.1	MAP kinase kinase kinase 53	-2,503	0	0,000	0,000	0,030	*	*	*
Solyc07g054280.1	Tyrosine/DOPA decarboxylase 3	2,542	0	0,000	0,000	0,026	*	*	*
Solyc08g005960.2	Bifunctional inhibitor/lipid-transfer protein/seed storage 2S albumin superfamily protein	1,115	0	0,000	-2,248	0,012	*	*	0,000
Solyc08g008420.3	Mitochondrial pyruvate carrier	1,183	0	0,000	0,000	0,005	*	*	*
Solyc08g013758.1	putative F-box protein At1g49610	-2,156	0	-1,413	0,000	0,002	*	4,3E-02	*
Solyc08g061160.2	Unknown protein	3,099	0	2,390	0,000	0,002	*	7,7E-03	*
Solyc08g066880.3	Nucleoside phosphorylase, family 1	-2,102	0	0,000	1,240	0,001	*	*	0,040
Solyc08g067520.2	Non-specific lipid-transfer protein	1,831	0	0,000	0,000	0,031	*	*	*
Solyc08g068330.3	Aspartate aminotransferase	-1,292	0	0,000	1,102	0,035	*	*	0,032
Solyc08g068390.3	Glyoxysomal fatty acid beta-oxidation multifunctional protein MFP-a	1,921	0	1,935	0,000	0,000	*	9,2E-11	*
Solyc08g074410.3	Tryptophan--tRNA ligase, cytoplasmic	-2,042	0	0,000	0,000	0,033	*	*	*

Solyc08g074680.2	partialpolyphenol oxidase A	-1,372	0	0,000	1,217	0,038	*	*	0,027
Solyc08g075490.3	9-cis-epoxycarotenoid dioxygenase	-1,164	0	-1,946	0,000	0,004	*	3,5E-10	*
Solyc08g075790.3	Vacuolar protein sorting-associated protein 62	-1,099	0	0,000	0,000	0,013	*	*	*
Solyc08g077100.3	RING/U-box superfamily protein	2,277	0	0,000	0,000	0,043	*	*	*
Solyc08g079200.1	Bifunctional inhibitor/lipid-transfer protein/seed storage 2S albumin superfamily protein	-1,623	0	0,000	0,000	0,000	*	*	*
Solyc08g079850.2	Subtilisin-like protease	-1,669	0	-1,695	0,000	0,020	*	3,8E-03	*
Solyc08g079870.2	subtilisin	-1,694	0	0,000	0,000	0,012	*	*	*
Solyc08g080730.3	Tetraspanin-10	1,597	0	0,000	-1,327	0,044	*	*	0,049
Solyc08g081620.3	LEU13054 endo-1,4-beta-glucanase precursor	-1,165	0	0,000	1,316	0,028	*	*	0,002
Solyc09g005730.3	Plant protein 1589 of Uncharacterized protein function	1,612	0	3,951	3,540	0,002	*	3,7E-16	0,000
Solyc09g006000.3	zinc/iron-chelating domain protein	-1,354	0	-1,279	0,000	0,018	*	6,7E-03	*
Solyc09g007020.2	Pathogenesis-related protein 1	-1,557	0	0,000	0,000	0,029	*	*	*
Solyc09g008670.3	threonine deaminase	-3,340	0	0,000	3,492	0,000	*	*	0,000
Solyc09g009690.3	Inosine/uridine-preferring nucleoside hydrolase domain-containing protein	-1,575	0	0,000	0,000	0,001	*	*	*
Solyc09g010860.3	expansin precursor 4	-1,007	0	-1,116	0,000	0,010	*	4,9E-04	*
Solyc09g011970.2	Laccase	-1,985	0	0,000	0,000	0,002	*	*	*
Solyc09g014480.2	Polygalacturonase inhibiting protein	-1,886	0	0,000	0,000	0,005	*	*	*
Solyc09g014860.3	Protein LURP-one-related 15	-2,422	0	0,000	0,000	0,018	*	*	*
Solyc09g015280.1	Photosystem I assembly protein Ycf3	2,069	0	0,000	-2,172	0,001	*	*	0,000
Solyc09g055950.1	Photosystem II D2 protein	4,891	0	2,447	0,000	0,000	*	3,1E-03	*
Solyc09g059240.3	Cytochrome P450	-2,246	0	-1,225	1,662	0,000	*	4,8E-03	0,000
Solyc09g059640.2	Photosystem I P700 chlorophyll a apoprotein A2	2,582	0	2,879	0,000	0,023	*	7,2E-04	*
Solyc09g065620.3	Chlorophyllase	-2,841	0	0,000	2,679	0,001	*	*	0,000
Solyc09g082760.3	Aspartic proteinase A1	-1,132	0	0,000	0,000	0,000	*	*	*
Solyc09g083440.3	Proteinase inhibitor I13, potato inhibitor I	-3,237	0	0,000	1,914	0,000	*	*	0,000
Solyc09g089490.3	Proteinase inhibitor	-2,768	0	0,000	2,583	0,011	*	*	0,005
Solyc09g089500.3	Proteinase inhibitor 1 PPI3B2	-3,737	0	0,000	2,991	0,000	*	*	0,001
Solyc09g089540.3	Proteinase inhibitor	-4,406	0	0,000	3,427	0,000	*	*	0,000
Solyc09g089580.3	2-oxoglutarate (2OG) and Fe(II)-dependent oxygenase superfamily protein	-1,845	0	1,598	3,196	0,023	*	3,2E-02	0,000
Solyc09g091800.3	glycine-rich protein 23-like	-2,348	0	0,000	0,000	0,017	*	*	*
Solyc09g092715.1	pupal cuticle protein Edg-91-like	1,340	0	0,000	0,000	0,003	*	*	*
Solyc10g005320.3	Tryptophan synthase beta chain	-3,036	0	0,000	1,976	0,003	*	*	0,049
Solyc10g008160.3	uniform ripening	1,793	0	0,000	0,000	0,035	*	*	*
Solyc10g009060.1	MAP kinase kinase kinase 72	-2,166	0	0,000	0,000	0,005	*	*	*
Solyc10g012370.3	Cysteine synthase	-1,631	0	0,000	0,000	0,026	*	*	*

Solyc10g017890.1	Photosystem I chlorophyll a apoprotein A1	1,231	0	0,000	-1,064	0,002	*	*	0,004
Solyc10g017900.1	Photosystem I P700 chlorophyll a apoprotein A1	4,517	0	4,288	0,000	0,000	*	9,8E-08	*
Solyc10g017910.2	Photosystem I P700 chlorophyll a apoprotein A2	2,715	0	2,294	0,000	0,010	*	8,9E-03	*
Solyc10g045640.2	Transmembrane emp24 domain-containing protein p24delta5	-1,549	0	0,000	0,000	0,036	*	*	*
Solyc10g050730.2	Cupredoxin	-2,823	0	0,000	2,516	0,007	*	*	0,006
Solyc10g052740.2	Photosystem I psaA and psaB	2,860	0	3,179	0,000	0,007	*	1,4E-04	*
Solyc10g055390.2	Major facilitator superfamily protein	1,845	0	0,000	-1,569	0,002	*	*	0,004
Solyc10g075110.2	Non-specific lipid-transfer protein	-1,782	0	1,910	2,912	0,000	*	5,0E-08	0,000
Solyc10g075160.1	Ferredoxin	-1,310	0	0,000	0,000	0,000	*	*	*
Solyc10g076670.2	2-oxoglutarate (2OG) and Fe(II)-dependent oxygenase superfamily protein	-2,602	0	0,000	0,000	0,022	*	*	*
Solyc10g076860.2	FH protein interacting protein FIP2	1,375	0	1,304	0,000	0,029	*	1,2E-02	*
Solyc10g078350.2	Transcription elongation factor	-3,031	0	0,000	2,505	0,001	*	*	0,002
Solyc10g078770.2	11 kDa late embryogenesis abundant protein	-2,618	0	0,000	2,288	0,018	*	*	0,017
Solyc10g079010.2	hypothetical protein	-1,862	0	-2,058	0,000	0,014	*	6,9E-04	*
Solyc10g079320.2	Glycosyltransferase	-2,736	0	0,000	0,000	0,009	*	*	*
Solyc10g080870.3	Cytochrome P450	2,393	0	0,000	-1,760	0,008	*	*	0,037
Solyc10g081540.2	2-(3-amino-3-carboxypropyl)histidine synthase subunit 2	1,412	0	0,000	0,000	0,007	*	*	*
Solyc10g084150.2	Cytokinin riboside 5'-monophosphate phosphoribohydrolase	-1,023	0	1,513	1,693	0,030	*	2,1E-05	0,000
Solyc10g085150.2	Alkyl transferase	-1,519	0	0,000	1,558	0,009	*	*	0,001
Solyc11g006070.2	Peptidyl-prolyl cis-trans isomerase	-1,686	0	0,000	0,000	0,001	*	*	*
Solyc11g006890.2	Unknown protein	1,323	0	0,000	0,000	0,000	*	*	*
Solyc11g007530.2	RING/U-box superfamily protein	1,869	0	0,000	0,000	0,037	*	*	*
Solyc11g008420.2	SKP1-like protein	2,654	0	0,000	0,000	0,017	*	*	*
Solyc11g010870.2	Unknown protein	-2,517	0	0,000	0,000	0,021	*	*	*
Solyc11g012130.2	Early nodulin-like protein 2-like	1,770	0	2,376	1,422	0,001	*	3,4E-07	0,012
Solyc11g012860.2	coiled-coil protein	-1,680	0	-1,837	0,000	0,005	*	2,1E-04	*
Solyc11g013780.1	Photosystem II protein D1	2,744	0	1,823	0,000	0,006	*	4,6E-02	*
Solyc11g021260.1	Protein TIC 214	2,425	0	0,000	-2,879	0,012	*	*	0,000
Solyc11g039860.2	Unknown protein	3,205	0	1,788	-1,266	0,000	*	4,0E-04	0,029
Solyc11g044638.1	Unknown protein	3,216	0	0,000	0,000	0,001	*	*	*
Solyc11g044910.2	Beta-D-xylosidase 4	-2,427	0	-1,416	1,632	0,000	*	1,3E-02	0,002
Solyc11g045260.1	Photosystem II CP43 reaction center protein	3,605	0	0,000	0,000	0,000	*	*	*
Solyc11g050770.1	Photosystem II reaction center protein Z	1,167	0	-1,293	-1,653	0,002	*	3,0E-05	0,000
Solyc11g056340.1	Photosynthetic reaction centre, L/M	3,703	0	2,103	0,000	0,000	*	1,4E-04	*
Solyc11g056680.1	Leucine-rich repeat receptor-like protein	1,406	0	0,000	0,000	0,004	*	*	*

Solyc11g071205.1	Unknown protein	1,495	0	1,171	0,000	0,008	*	2,0E-02	*
Solyc11g071290.2	Alcohol dehydrogenase-like protein	-3,352	0	-1,645	0,000	0,000	*	1,5E-02	*
Solyc12g005640.2	R2R3MYB transcription factor 68	-2,817	0	0,000	0,000	0,008	*	*	*
Solyc12g006260.1	Glycine rich protein-interacting protein	-1,623	0	0,000	1,665	0,018	*	*	0,003
Solyc12g007080.2	Unknown protein	-3,141	0	-2,908	0,000	0,001	*	3,0E-04	*
Solyc12g009270.1	Plant invertase/pectin methylesterase inhibitor superfamily protein	1,042	0	0,000	0,000	0,030	*	*	*
Solyc12g010020.2	Leucine aminopeptidase A1	-3,467	0	0,000	1,663	0,000	*	*	0,049
Solyc12g010980.2	HXXXD-type acyl-transferase family protein	-1,211	0	-1,889	0,000	0,002	*	1,6E-09	*
Solyc12g011370.2	Cationic amino acid transporter	-2,472	0	-2,045	0,000	0,033	*	3,2E-02	*
Solyc12g019110.2	Valine--tRNA ligase	-1,024	0	-1,855	0,000	0,046	*	1,1E-07	*
Solyc12g019320.2	Protein DETOXIFICATION	-1,100	0	-1,398	0,000	0,000	*	5,8E-10	*
Solyc12g032990.2	UDP-glucuronosyl/UDP-glucosyltransferase	4,907	0	3,237	0,000	0,000	*	3,4E-05	*
Solyc12g033060.2	Photosystem I P700 chlorophyll a apoprotein A2	3,455	0	2,600	0,000	0,000	*	1,8E-03	*
Solyc12g035670.2	SAC3/GANP/Nin1/mts3/eIF-3 p25	-1,592	0	-1,405	0,000	0,015	*	1,2E-02	*
Solyc12g036850.2	Unknown protein	2,594	0	2,387	0,000	0,017	*	7,5E-03	*
Solyc12g038080.1	Photosystem II CP43 reaction center protein	4,459	0	3,722	0,000	0,000	*	7,1E-06	*
Solyc12g039030.1	Photosystem II protein D1	4,324	0	3,025	0,000	0,000	*	1,9E-04	*
Solyc12g088640.2	Carbohydrate esterase, putative (DUF303)	2,618	0	0,000	0,000	0,010	*	*	*
Solyc12g094700.2	Xylem cysteine proteinase 1	-1,701	0	0,000	0,000	0,000	*	*	*
Solyc12g096770.1	HXXXD-type acyl-transferase family protein	-1,377	0	-1,386	0,000	0,000	*	1,7E-05	*
Solyc12g096900.2	Disease resistance protein (TIR-NBS-LRR class) family	-1,007	0	0,000	0,000	0,003	*	*	*

Table S13. List of the LN-specific DEGs in ROvsUC82 comparison in root

Gene ID	Gene annotation	Log2(FC)				FDR			
		ROvsUC82-LN	ROvsUC82-HN	RO-LNvsHN	UC82-LNvsHN	ROvsUC82-LN	ROvsUC82-HN	RO-LNvsHN	UC82-LNvsHN
ENSRNA050029895		-2,262	0	0,000	0,000	0,009	*	*	*
ENSRNA050029901		-2,301	0	0,000	2,384	0,009	*	*	0,001
ENSRNA050029911		-2,508	0	0,000	0,000	0,000	*	*	*
ENSRNA050030202		-3,046	0	0,000	2,083	0,000	*	*	0,001
ENSRNA050030523		-2,464	0	0,000	1,757	0,001	*	*	0,012
ENSRNA050030532		-3,313	0	0,000	0,000	0,000	*	*	*
Solyc00g007110.3		-1,135	0	0,000	0,000	0,043	*	*	*
Solyc00g020000.1	Unknown protein	-1,847	0	0,000	0,000	0,045	*	*	*
Solyc01g005730.3	NL0C	1,857	0	0,000	0,000	0,045	*	*	*
Solyc01g005860.2	Unknown protein	1,007	0	0,000	0,000	0,036	*	*	*
Solyc01g006950.3	syntaxin-121-like	1,067	0	0,000	0,000	0,016	*	*	*
Solyc01g067370.3	TSB	1,630	0	0,000	0,000	0,000	*	*	*
Solyc01g081310.3	glutathione S-transferase T3	2,427	0	1,784	0,000	0,000	*	0,000	*
Solyc01g087320.3	Zinc finger, FYVE/PHD-type	1,010	0	0,000	0,000	0,028	*	*	*
Solyc01g101120.3	Carbohydrate-binding X8 domain superfamily protein	-1,149	0	0,000	0,000	0,021	*	*	*
Solyc01g103230.3	Non-lysosomal glucosylceramidase	-2,062	0	0,000	0,000	0,025	*	*	*
Solyc01g103590.3	Lactoylglutathione lyase / glyoxalase	-1,086	0	0,000	0,000	0,005	*	*	*
Solyc01g105550.1	Acylsugar acetyltransferase	2,014	0	0,000	0,000	0,034	*	*	*
Solyc01g106810.3	short hypocotyl in white light1	-1,633	0	0,000	0,000	0,036	*	*	*
Solyc01g107190.3	LOB domain-containing protein 38	1,202	0	-2,248	-3,233	0,003	*	0,000	0,000
Solyc01g109470.3	BURP domain-containing protein	-1,141	0	0,000	1,365	0,000	*	*	0,000
Solyc01g111230.3	Dirigent protein	1,213	0	0,000	0,000	0,000	*	*	*
Solyc02g062500.3	2-oxoglutarate (2OG) and Fe(II)-dependent oxygenase superfamily protein	1,160	0	0,000	0,000	0,015	*	*	*
Solyc02g063420.3	Hydroxyproline-rich glycoprotein family protein	-2,192	0	0,000	0,000	0,005	*	*	*
Solyc02g064680.3	Calcium-transporting ATPase	2,133	0	1,886	-1,881	0,022	*	0,018	0,015
Solyc02g066830.3	Nuclear transport factor 2 (NTF2) family protein with RNA binding (RRM-RBD-RNP motifs) domain-containing protein	2,292	0	0,000	0,000	0,001	*	*	*
Solyc02g067410.2	Homeobox-leucine zipper protein HOX21	1,181	0	0,000	-2,000	0,028	*	*	0,000

Solyc02g069180.3	SBP (S-ribonuclease binding protein) family protein	-1,448	0	0,000	0,000	0,010	*	*	*
Solyc02g082130.2	Surfeit locus protein 6	-1,536	0	0,000	0,000	0,026	*	*	*
Solyc02g085120.3	Laccase	1,050	0	0,000	0,000	0,008	*	*	*
Solyc02g091050.3	Protein DETOXIFICATION	-1,888	0	0,000	0,000	0,049	*	*	*
Solyc02g092700.3	DUF1230 family protein (DUF1230)	1,177	0	0,000	0,000	0,043	*	*	*
Solyc03g007820.3	Unknown protein	1,381	0	0,000	-1,191	0,001	*	*	0,001
Solyc03g031590.3	S-type anion channel SLAH1	1,713	0	-2,709	-5,168	0,040	*	0,000	0,000
Solyc03g032050.3	Ras-related protein Rab-11A	-1,817	0	0,000	0,000	0,036	*	*	*
Solyc03g032080.3	Auxin efflux carrier	-1,596	0	0,000	0,000	0,029	*	*	*
Solyc03g083770.1	Plant invertase/pectin methylesterase inhibitor superfamily protein, putative	-1,828	0	0,000	2,948	0,031	*	*	0,000
Solyc03g090990.1	Bifunctional inhibitor/lipid-transfer protein/seed storage 2S albumin superfamily protein	-1,545	0	0,000	0,000	0,040	*	*	*
Solyc03g094060.3	Polyadenylate-binding protein 1	-2,405	0	0,000	0,000	0,003	*	*	*
Solyc03g097950.3	50S ribosomal protein L29, chloroplastic	1,638	0	0,000	0,000	0,036	*	*	*
Solyc03g113580.2	Germin	-1,743	0	-1,191	0,000	0,000	*	0,016	*
Solyc03g113610.3	Polynucleotide 5'-hydroxyl-kinase NOL9	1,444	0	0,000	0,000	0,007	*	*	*
Solyc03g114860.3	alpha-1,4-glucan-protein synthase [UDP-forming] 2-like	1,977	0	1,526	0,000	0,000	*	0,000	*
Solyc03g114940.3	Cytochrome P450	-2,288	0	1,041	3,333	0,000	*	0,006	0,000
Solyc03g114960.3	Galactose oxidase/kelch repeat superfamily protein	-1,076	0	0,000	0,000	0,009	*	*	*
Solyc03g118200.3	Calcium-dependent phospholipid-binding Copine family protein	-1,036	0	0,000	0,000	0,048	*	*	*
Solyc03g118530.3	Protein kinase domain	-1,143	0	0,000	0,000	0,030	*	*	*
Solyc03g119600.1	NIMIN2b protein	-1,744	0	-2,156	0,000	0,036	*	0,001	*
Solyc03g120600.3	Plant cadmium resistance protein	1,969	0	0,000	-2,986	0,030	*	*	0,000
Solyc04g007075.1	Unknown protein	1,962	0	0,000	-1,756	0,009	*	*	0,005
Solyc04g008075.1	Unknown protein	1,459	0	0,000	-2,199	0,019	*	*	0,000
Solyc04g009690.2	Disease resistance protein	1,872	0	0,000	-1,636	0,007	*	*	0,005
Solyc04g014310.1	Unknown protein	-2,265	0	0,000	0,000	0,007	*	*	*
Solyc04g015490.3	Mg-protoporphyrin IX chelatase	1,130	0	0,000	0,000	0,050	*	*	*
Solyc04g015610.3	DUF642 domain-containing protein	1,332	0	-1,246	-2,177	0,009	*	0,004	0,000
Solyc04g049670.3	Pseudo-response regulator	1,080	0	0,000	0,000	0,010	*	*	*
Solyc04g050220.2	Unknown protein	-1,929	0	0,000	0,000	0,041	*	*	*

Solyc04g051100.3	Unknown protein	2,835	0	0,000	0,000	0,000	*	*	*
Solyc04g056507.1	Unknown protein	-2,305	0	0,000	0,000	0,003	*	*	*
Solyc04g063245.1	Cytochrome	-2,490	0	0,000	0,000	0,002	*	*	*
Solyc04g071615.1	Unknown protein	-1,892	0	0,000	2,779	0,030	*	*	0,000
Solyc04g072460.3	Transcription factor TGA7	-2,471	0	-1,823	0,000	0,002	*	0,022	*
Solyc04g074950.3	Dihydrofolate reductase	1,790	0	0,000	0,000	0,029	*	*	*
Solyc04g077860.3	Sigma-B regulation protein RsbQ	-1,195	0	-1,677	-1,297	0,039	*	0,000	0,000
Solyc05g012770.3	WRKY transcription factor 4	-1,281	0	0,000	0,000	0,000	*	*	*
Solyc05g014275.1	DUF659 domain-containing protein/Dimer_Tnp_hAT domain-containing protein	1,088	0	0,000	-1,026	0,031	*	*	0,010
Solyc05g024415.1	Unknown protein	-1,078	0	-1,461	0,000	0,000	*	0,000	*
Solyc05g046020.3	Peroxidase	1,106	0	0,000	0,000	0,000	*	*	*
Solyc05g050490.3	ATPase	2,166	0	0,000	0,000	0,003	*	*	*
Solyc05g050500.1	ATP synthase delta chain chloroplastic-like	-1,646	0	0,000	0,000	0,013	*	*	*
Solyc05g051030.3	Protein cornichon-like protein 4	-1,419	0	0,000	0,000	0,000	*	*	*
Solyc05g051480.2	Unknown protein	2,389	0	0,000	0,000	0,001	*	*	*
Solyc05g051530.3	ABC transporter G family member 11	1,090	0	-1,181	-1,528	0,046	*	0,006	0,000
Solyc05g052030.1	ethylene response factor 4	-1,681	0	0,000	2,105	0,010	*	*	0,000
Solyc05g052420.2	Abscisic acid receptor PYL6	-1,374	0	0,000	1,526	0,006	*	*	0,000
Solyc05g052870.3	Glycosyltransferase	1,042	0	0,000	-1,269	0,035	*	*	0,000
Solyc06g005310.3	Transcription factor MYB48	-1,052	0	0,000	0,000	0,000	*	*	*
Solyc06g005470.3	Unknown protein	-1,421	0	-2,236	-1,339	0,000	*	0,000	0,000
Solyc06g007760.3	Ycf54-like protein	1,514	0	0,000	0,000	0,010	*	*	*
Solyc06g064970.3	GDSL esterase/lipase 5-like	1,421	0	0,000	0,000	0,030	*	*	*
Solyc06g066750.3	To encode a PR protein, Belongs to the plant thionin family with the following members:, putative	1,316	0	0,000	-1,564	0,003	*	*	0,000
Solyc06g066820.3	Le3OH-13b-hydroxylase	-1,786	0	0,000	0,000	0,000	*	*	*
Solyc06g082070.3	Protein trichome birefringence-like 45	1,375	0	0,000	0,000	0,035	*	*	*
Solyc07g008980.3	defensin-like protein 19	-2,141	0	0,000	1,758	0,000	*	*	0,000
Solyc07g009020.2	defensin-like protein 19	-1,063	0	-1,165	0,000	0,000	*	0,000	*
Solyc07g009070.3	defensin-like protein 19	-1,529	0	-1,440	0,000	0,003	*	0,003	*
Solyc07g009080.3	defensin-like protein 19	-1,039	0	-1,321	0,000	0,030	*	0,000	*

Solyc07g009090.3	defensin-like protein 19	-1,063	0	-1,741	0,000	0,000	*	0,000	*
Solyc07g009310.3	Unknown protein	-1,337	0	0,000	2,123	0,002	*	*	0,000
Solyc07g014590.3	Isoamylase 1, chloroplastic	-1,431	0	0,000	1,110	0,035	*	*	0,038
Solyc07g017880.3	Peroxidase	1,291	0	0,000	-1,368	0,000	*	*	0,000
Solyc07g049550.3	1-aminocyclopropane-1-carboxylate oxidase 2	-1,366	0	1,200	2,890	0,000	*	0,000	0,000
Solyc07g052660.1	Early nodulin-like protein 1-like	1,086	0	0,000	-1,282	0,001	*	*	0,000
Solyc07g053560.3	phosphorelay protein	2,052	0	0,000	0,000	0,025	*	*	*
Solyc07g056170.3	Subtilisin-like protease	2,046	0	0,000	-1,920	0,002	*	*	0,001
Solyc08g006280.2	Transcriptional factor B3 family protein	-2,097	0	0,000	0,000	0,023	*	*	*
Solyc08g013940.3	Protein kinase family protein	1,687	0	0,000	-1,529	0,018	*	*	0,008
Solyc08g066310.2	Receptor-like protein kinase	1,829	0	0,000	-2,034	0,041	*	*	0,002
Solyc08g067340.3	WRKY transcription factor 46	2,426	0	0,000	0,000	0,004	*	*	*
Solyc08g067690.2	Unknown protein	-1,402	0	-2,895	-1,421	0,000	*	0,000	0,000
Solyc08g067740.3	Unknown protein	-1,166	0	0,000	0,000	0,017	*	*	*
Solyc08g068380.3	Unknown protein	-2,252	0	0,000	1,820	0,001	*	*	0,002
Solyc08g078460.3	Oxidoreductase family protein	1,031	0	0,000	-1,184	0,042	*	*	0,001
Solyc08g080310.1	Protein DETOXIFICATION	1,318	0	-2,400	-3,868	0,026	*	0,000	0,000
Solyc08g083370.3	Soluble inorganic pyrophosphatase	1,365	0	0,000	-1,104	0,010	*	*	0,016
Solyc09g005480.3	F-box associated interaction domain-containing protein	-1,407	0	0,000	0,000	0,001	*	*	*
Solyc09g009420.1	hypothetical protein	1,559	0	0,000	0,000	0,015	*	*	*
Solyc09g082210.3	DUF581 domain-containing protein	-1,170	0	0,000	1,011	0,040	*	*	0,026
Solyc09g082280.3	Lipid transfer protein	-1,972	0	0,000	2,348	0,001	*	*	0,000
Solyc09g083090.3	Non-specific serine/threonine protein kinase	-1,744	0	0,000	0,000	0,036	*	*	*
Solyc09g091200.3	Serinc-domain containing serine and sphingolipid biosynthesis protein	1,019	0	-1,113	-1,454	0,001	*	0,000	0,000
Solyc09g098500.3	Got1/Sft2-like vescicle transport protein family	1,498	0	0,000	0,000	0,001	*	*	*
Solyc10g007280.3	P-loop containing nucleoside triphosphate hydrolases superfamily protein	1,656	0	0,000	0,000	0,036	*	*	*
Solyc10g008350.3	hypothetical protein	1,021	0	0,000	-1,460	0,037	*	*	0,000
Solyc10g018200.2	Ankyrin repeat/KH domain protein (DUF1442)	-1,149	0	-1,163	0,000	0,000	*	0,000	*
Solyc10g045240.2	Beta-glucosidase	1,475	0	0,000	-1,030	0,005	*	*	0,034
Solyc10g054850.2	Er lumen protein retaining receptor-like protein	1,172	0	0,000	0,000	0,047	*	*	*

Solyc10g078410.2	F-box protein	1,883	0	0,000	0,000	0,029	*	*	*
Solyc10g079010.2	hypothetical protein	-1,500	0	0,000	0,000	0,025	*	*	*
Solyc10g080010.2	Glycosyltransferase family 61 protein	1,399	0	0,000	-1,188	0,014	*	*	0,012
Solyc10g080090.2	zinc finger BED domain-containing protein DAYSLEEPER-like	1,466	0	0,000	-1,163	0,018	*	*	0,028
Solyc10g083290.2	invertase 6	2,481	0	0,000	0,000	0,000	*	*	*
Solyc10g084070.1	Unknown protein	-2,267	0	0,000	1,823	0,009	*	*	0,016
Solyc10g085160.2	S-adenosyl-L-methionine-dependent methyltransferases superfamily protein	1,123	0	0,000	0,000	0,026	*	*	*
Solyc10g085830.2	O-methyltransferase, putative	1,174	0	0,000	0,000	0,005	*	*	*
Solyc11g011225.1	Unknown protein	-1,126	0	0,000	0,000	0,042	*	*	*
Solyc11g011750.2	Ethylene-responsive transcription factor 1B	-1,760	0	-1,768	0,000	0,010	*	0,003	*
Solyc11g039950.2	Splicing factor 3B subunit 4	1,040	0	0,000	0,000	0,050	*	*	*
Solyc11g045240.2	Unknown protein	2,009	0	0,000	0,000	0,017	*	*	*
Solyc11g061720.1	Serine/threonine-protein kinase UCNL	-1,561	0	-1,587	0,000	0,014	*	0,004	*
Solyc11g069750.2	High-affinity nitrate transporter 2	-1,960	0	0,000	0,000	0,002	*	*	*
Solyc11g072930.2	Leucine-rich repeat protein kinase family protein	1,095	0	0,000	-1,515	0,034	*	*	0,000
Solyc12g005360.2	MAP kinase kinase kinase 83	1,190	0	0,000	0,000	0,000	*	*	*
Solyc12g005960.2	Ethylene-responsive transcription factor 4	-2,146	0	-2,041	0,000	0,001	*	0,001	*
Solyc12g006997.1	Heavy metal transport/detoxification superfamily protein	-1,640	0	-2,214	-1,118	0,000	*	0,000	0,000
Solyc12g008910.2	Translation machinery-associated protein 22	-1,359	0	0,000	0,000	0,021	*	*	*
Solyc12g036415.1	Unknown protein	-2,289	0	0,000	0,000	0,005	*	*	*
Solyc12g037950.2	protein PLANT CADMIUM RESISTANCE 2-like	1,463	0	0,000	-1,413	0,000	*	*	0,000
Solyc12g077630.1	Unknown protein	2,021	0	0,000	0,000	0,032	*	*	*
Solyc12g088020.1	Farnesylcysteine lyase	-2,375	0	0,000	0,000	0,004	*	*	*
Solyc12g088410.2	Glycosyl hydrolase family 35 protein	1,946	0	0,000	0,000	0,042	*	*	*

Table S14. List of the TF encoding genes differentially expressed in the four comparisons in shoot: ROvsUC82-LN, ROvsUC82-HN, RO-LNvsHN and UC82-LNvsHN

Gene ID	Gene annotation	Log2(FC)				
		ROvsUC82-LN	ROvsUC82-HN	RO-LNvsHN	UC82-LNvsHN	Family
Solyc04g049800.3	AP2-like ethylene-responsive transcription factor	0,000	0,000	-1,170	-1,338	AP2
Solyc05g014260.3	Two-component response regulator	0,000	0,000	1,845	1,697	ARR-B
Solyc07g005140.3	Two-component response regulator	0,000	0,000	0,000	1,759	ARR-B
Solyc01g108120.3	B3 domain-containing protein	0,000	0,000	0,000	1,641	B3
Solyc03g111500.3	B3 domain-containing protein	0,000	0,000	-2,023	0,000	B3
Solyc01g102300.3	bHLH transcription factor 006	0,000	-2,552	3,641	0,000	bHLH
Solyc01g109700.3	bHLH transcription factor 010	0,000	0,000	-1,623	-2,390	bHLH
Solyc02g062690.3	bHLH transcription factor 012	0,000	0,000	-1,197	0,000	bHLH
Solyc02g067380.3	bHLH style2.1 (PRE2)	2,402	0,000	2,599	0,000	bHLH
Solyc02g076920.3	bHLH transcription factor 013	1,484	0,000	2,298	0,000	bHLH
Solyc02g078130.3	bHLH transcription factor 079	0,000	0,000	1,422	0,000	bHLH
Solyc02g079760.3	Basic helix-loop-helix (BHLH) DNA-binding superfamily protein	0,000	0,000	1,040	0,000	bHLH
Solyc02g084880.3	Basic helix-loop-helix (BHLH) DNA-binding superfamily protein	0,000	0,000	1,659	0,000	bHLH
Solyc03g007410.3	Basic helix-loop-helix (BHLH) DNA-binding superfamily protein	0,000	0,000	-2,697	0,000	bHLH
Solyc03g095980.3	bHLH transcription factor 021	0,000	0,000	0,000	-2,590	bHLH
Solyc03g097820.2	bHLH transcription factor 022	0,000	0,000	0,000	1,267	bHLH
Solyc03g114230.2	bHLH transcription factor 082	-2,504	-2,347	0,000	0,000	bHLH
Solyc03g114720.3	bHLH transcription factor 023	0,000	-1,071	0,000	0,000	bHLH
Solyc03g118310.3	bHLH transcription factor 083	0,000	0,000	-3,913	-2,766	bHLH
Solyc03g119390.3	bHLH transcription factor 026	0,000	0,000	1,915	0,000	bHLH
Solyc04g005280.3	bHLH transcription factor 028	-1,268	0,000	0,000	0,000	bHLH
Solyc04g005660.3	transcription factor PRE6-like	0,000	0,000	-2,645	0,000	bHLH
Solyc06g050840.3	bHLH transcription factor135	0,000	0,000	-1,781	-1,422	bHLH
Solyc06g051260.3	bHLH transcription factor 043	0,000	-1,173	1,660	0,000	bHLH
Solyc06g065040.3	bHLH transcription factor 086	0,000	0,000	1,062	1,404	bHLH
Solyc06g072520.2	bHLH transcription factor GBOF-1	0,000	0,000	2,286	2,072	bHLH
Solyc07g063830.3	bHLH transcription factor142	0,000	0,000	1,744	0,000	bHLH
Solyc08g081140.3	bHLH transcription factor 090	0,000	0,000	1,280	0,000	bHLH
Solyc09g097870.3	bHLH transcription factor 062	0,000	0,000	-1,095	-1,122	bHLH
Solyc10g006640.3	bHLH transcription factor153	0,000	0,000	0,000	-1,879	bHLH
Solyc11g056650.2	bHLH transcription factor 096	0,000	0,000	0,000	1,325	bHLH
Solyc01g109880.3	BZIP transcription factor	0,000	0,000	1,763	0,000	bZIP
Solyc02g061990.3	BZIP transcription factor FD	0,000	0,000	3,796	2,427	bZIP
Solyc04g054320.3	leucine-zipper transcription factor	0,000	0,000	0,000	1,112	bZIP
Solyc04g071160.3	Basic-leucine zipper (BZIP) transcription factor family protein	0,000	0,000	0,000	1,349	bZIP
Solyc04g078840.3	AREB	0,000	0,000	1,885	0,000	bZIP
Solyc06g049040.3	Basic-leucine zipper (BZIP) transcription factor family protein	0,000	0,000	-1,169	-2,098	bZIP
Solyc06g074320.3	Transcription factor TGA2	1,759	0,000	0,000	0,000	bZIP
Solyc09g005610.3	BZIP transcription factor	0,000	0,000	3,401	2,172	bZIP
Solyc09g009490.3	ABSCISIC ACID-INSENSITIVE 5-like protein 4	0,000	0,000	2,209	0,000	bZIP
Solyc12g010800.2	Basic-leucine zipper (BZIP) transcription factor family protein	0,000	0,000	-1,096	0,000	bZIP
Solyc01g007760.3	Transcription factor E2FA	0,000	0,000	0,000	-1,355	E2F/DP
Solyc01g096810.3	EIL3	0,000	0,000	2,341	1,134	EIL
Solyc01g065980.3	Ethylene Response Factor E	0,000	0,000	1,624	1,123	ERF
Solyc01g090560.3	Ethylene-responsive transcription factor	0,000	0,000	1,528	1,833	ERF
Solyc04g078640.2	Ethylene-responsive transcription factor RAP2-1	0,000	0,000	0,000	1,076	ERF
Solyc05g024230.2	ethylene-responsive transcription factor CRF2-like	2,911	2,262	0,000	0,000	ERF
Solyc06g009810.3	ethylene-responsive transcription factor CRF1	0,000	2,491	0,000	0,000	ERF
Solyc06g066540.1	Ethylene-responsive transcription factor	0,000	0,000	0,000	2,203	ERF
Solyc02g090400.3	Myb family transcription factor	0,000	0,000	0,000	-1,427	G2-like
Solyc05g009720.3	Myb-like transcription factor family protein	0,000	2,431	-3,285	-1,304	G2-like
Solyc07g053630.3	Two-component response regulator	0,000	0,000	-1,815	-1,462	G2-like
Solyc10g008160.3	uniform ripening	1,793	0,000	0,000	0,000	G2-like
Solyc09g075600.2	GATA transcription factor-like protein	0,000	0,000	0,000	-2,001	GATA
Solyc02g092570.1	Transcription factor GRAS	0,000	0,000	-2,088	-1,742	GRAS
Solyc05g054170.3	Scarecrow-like protein 5	0,000	0,000	0,000	1,347	GRAS
Solyc09g090830.3	BolA protein	0,000	0,000	0,000	-1,685	GRAS

Solyc04g077510.3	Growth-regulating factor 8	0,000	0,000	0,000	1,684	GRF
Solyc04g054700.3	General transcription factor IIH subunit	0,000	0,000	0,000	1,168	GTFIIH
Solyc01g090460.3	HD-ZIP	0,000	0,000	0,000	1,400	HD-ZIP
Solyc01g096320.3	Homeobox-leucine zipper protein HOX6	0,000	0,000	2,739	3,091	HD-ZIP
Solyc02g062960.3	Homeobox-leucine zipper protein HOX14	0,000	0,000	1,764	2,057	HD-ZIP
Solyc02g063520.3	Homeobox-leucine zipper protein HAT22	0,000	0,000	3,457	2,351	HD-ZIP
Solyc02g091930.3	Homeobox-leucine zipper protein HOX27	0,000	0,000	0,000	1,058	HD-ZIP
Solyc03g082550.3	Homeobox-leucine zipper protein HOX6	0,000	0,000	0,000	3,188	HD-ZIP
Solyc03g113270.3	LEVAHOX1G L	0,000	0,000	1,244	1,052	HD-ZIP
Solyc04g077220.3	Homeobox-leucine zipper protein HAT22	0,000	0,000	0,000	1,965	HD-ZIP
Solyc05g006980.3	Homeobox-leucine zipper protein HOX16	-1,648	0,000	0,000	0,000	HD-ZIP
Solyc05g007180.3	jasmonic acid 1	0,000	0,000	0,000	-1,162	HD-ZIP
Solyc05g051460.3	Homeobox-leucine zipper protein HOX4	0,000	0,000	1,403	0,000	HD-ZIP
Solyc06g035940.3	Homeobox-leucine zipper protein ROC5	4,661	3,443	0,000	0,000	HD-ZIP
Solyc02g072000.3	Heat shock transcription factor	0,000	0,000	1,532	0,000	HSF
Solyc04g016000.3	Heat shock transcription factor protein 8	-1,740	0,000	0,000	2,856	HSF
Solyc06g053950.2	Heat stress transcription factor A-2e	0,000	0,000	2,202	1,875	HSF
Solyc08g080540.3	Heat stress transcription factor B-2b	0,000	0,000	0,000	1,756	HSF
Solyc12g007070.2	Heat shock transcription factor	0,000	0,000	1,416	0,000	HSF
Solyc12g098520.2	Heat stress transcription factor A-5	0,000	0,000	1,244	0,000	HSF
Solyc02g082400.3	lysine-specific demethylase TF-JMJ25	0,000	0,000	1,697	0,000	JUMONJI 25
Solyc03g083240.3	Transcription factor jumonji (JmjC)	0,000	0,000	0,000	-2,181	JUMONJI C
Solyc01g107190.3	LOB domain-containing protein 38	0,000	0,000	-1,485	-1,701	LBD
Solyc02g092550.3	LOB domain-containing protein 38	0,000	0,000	-1,927	-2,450	LBD
Solyc03g119530.3	LOB domain-containing protein 41	0,000	0,000	-1,658	-1,482	LBD
Solyc12g087830.2	MADS-box transcription factor	2,209	2,239	0,000	0,000	MADS
Solyc06g069430.3	FRUITFULL-like MADS-box 1	0,000	0,000	2,459	2,432	MIKC_MADS
Solyc08g080100.3	MADS box transcription factor AGAMOUS	0,000	0,000	3,174	3,223	MIKC_MADS
Solyc01g079620.3	colorless fruit epidermis	0,000	-1,498	2,949	1,351	MYB
Solyc02g067340.3	R2R3MYB transcription factor 96	0,000	0,000	-2,589	0,000	MYB
Solyc02g079280.3	MYB transcription factor	0,000	0,000	2,143	0,000	MYB
Solyc03g112390.3	R2R3MYB transcription factor 86	0,000	0,000	1,335	1,197	MYB
Solyc04g064540.3	R2R3MYB transcription factor 115	0,000	0,000	2,261	0,000	MYB
Solyc04g078420.1	R2R3MYB transcription factor 70	0,000	0,000	0,000	2,190	MYB
Solyc05g053150.2	R2R3MYB transcription factor 71	0,000	0,000	0,000	3,889	MYB
Solyc05g053330.3	Transcription factor	0,000	0,000	0,000	2,283	MYB
Solyc06g005330.3	R2R3MYB transcription factor 59	0,000	0,000	1,364	1,756	MYB
Solyc06g065100.3	R2R3MYB transcription factor 3	0,000	0,000	1,228	0,000	MYB
Solyc06g071690.3	R2R3MYB transcription factor 50	0,000	0,000	0,000	1,544	MYB
Solyc09g008250.3	blind-like1	0,000	0,000	-1,127	0,000	MYB
Solyc09g090790.3	R2R3MYB transcription factor 79	0,000	0,000	-1,974	0,000	MYB
Solyc10g005460.3	MYB transcription factor	0,000	0,000	0,000	2,469	MYB
Solyc10g086250.2	R2R3MYB transcription factor 75	0,000	0,000	2,961	2,142	MYB
Solyc10g086270.2	R2R3MYB transcription factor 28	0,000	0,000	0,000	2,321	MYB
Solyc12g005640.2	R2R3MYB transcription factor 68	-2,817	0,000	0,000	0,000	MYB
Solyc12g006800.2	myb family transcription factor EFM-like	0,000	0,000	0,000	2,419	MYB
Solyc12g049350.2	R2R3MYB transcription factor 11	0,000	-1,617	3,883	2,233	MYB
Solyc04g005100.3	transcription factor MYB1R1-like	0,000	0,000	1,563	0,000	MYB_related
Solyc04g080500.3	Protein RADIALIS-like 6	0,000	0,000	2,328	2,546	MYB_related
Solyc06g005310.3	Transcription factor MYB48	0,000	0,000	1,974	2,049	MYB_related
Solyc06g076270.3	Telomere repeat-binding protein 2	0,000	0,000	2,135	0,000	MYB_related
Solyc01g009860.3	NAC domain-containing protein	0,000	0,000	1,438	1,012	NAC
Solyc02g088180.3	NAC domain-containing protein	2,100	0,000	2,300	0,000	NAC
Solyc03g115850.3	NAC domain-containing protein	0,000	0,000	1,994	0,000	NAC
Solyc04g005610.3	NAC domain-containing protein 2	0,000	0,000	2,609	2,815	NAC
Solyc04g079940.3	NAC domain-containing protein	0,000	0,000	1,729	1,247	NAC
Solyc05g007770.3	NAC domain TF	-1,910	0,000	0,000	3,413	NAC
Solyc05g055470.3	NAC domain-containing protein 13	0,000	0,000	0,000	1,518	NAC
Solyc06g060230.3	NAC domain-containing protein	0,000	0,000	1,750	1,827	NAC
Solyc06g069710.3	NAC domain-containing protein	0,000	0,000	1,910	0,000	NAC
Solyc07g063410.3	NAC domain protein	0,000	0,000	2,337	3,830	NAC
Solyc07g066330.3	NAC domain-containing protein	0,000	0,000	2,491	1,866	NAC

Solyc10g005010.3	NAC domain-containing protein	0,000	0,000	2,102	2,095	NAC
Solyc10g079150.2	Nuclear transcription factor Y subunit A-7	0,000	0,000	2,119	2,015	NFYA
Solyc10g081840.2	Nuclear transcription factor Y subunit A	0,000	0,000	0,000	2,167	NFYA
Solyc12g009050.2	Nuclear transcription factor Y subunit A-6	0,000	0,000	2,667	1,572	NFYA
Solyc01g006930.3	Nuclear transcription factor Y subunit A-4	0,000	0,000	2,947	2,558	NF-YA
Solyc01g008490.3	Nuclear transcription factor Y subunit A-7	0,000	0,000	0,000	1,177	NF-YA
Solyc01g087240.3	Nuclear transcription factor Y subunit A-9	0,000	0,000	2,429	1,463	NF-YA
Solyc08g062210.3	Nuclear transcription factor Y subunit A-1	0,000	0,000	2,409	1,763	NF-YA
Solyc01g067130.3	Nuclear transcription factor Y subunit B	0,000	0,000	0,000	-2,538	NF-YB
Solyc01g112190.3	NLP1	1,146	0,000	0,000	-1,639	Nin-like
Solyc01g091000.3	PLATZ transcription factor family protein	0,000	0,000	0,000	1,958	PLATZ
Solyc03g044625.1	PLATZ transcription factor family protein	0,000	0,000	1,929	0,000	PLATZ
Solyc04g008090.3	PLATZ transcription factor family protein	0,000	0,000	0,000	-1,814	PLATZ
Solyc08g076860.3	PLATZ transcription factor family protein	0,000	0,000	2,314	2,099	PLATZ
Solyc10g009080.3	Squamosa promoter binding protein 3	0,000	0,000	-1,922	-2,285	SBP
Solyc01g007070.3	BEL1-like homeodomain protein 3	0,000	0,000	1,446	0,000	TALE
Solyc01g100510.3	knotted 4	0,000	0,000	2,173	0,000	TALE
Solyc04g077210.3	Knotted 1	0,000	0,000	2,432	1,456	TALE
Solyc01g008230.3	TCP transcription factor 15	0,000	0,000	-2,118	0,000	TCP
Solyc03g119770.3	branched1a	0,000	0,000	0,000	-2,168	TCP
Solyc03g122030.1	Trihelix transcription factor ASIL2	0,000	2,876	0,000	2,189	Trihelix
Solyc04g071360.3	Trihelix transcription factor GTL1	0,000	-2,139	0,000	0,000	Trihelix
Solyc08g061910.3	trihelix transcription factor GTL1-like	0,000	0,000	-1,663	0,000	Trihelix
Solyc01g079260.3	WRKY transcription factor 23	0,000	0,000	1,314	0,000	WRKY
Solyc01g095630.3	WRKY transcription factor 41	0,000	0,000	1,097	1,167	WRKY
Solyc02g032950.3	WRKY transcription factor 16	0,000	0,000	0,000	1,559	WRKY
Solyc02g071130.3	WRKY transcription factor 71	0,000	0,000	0,000	2,282	WRKY
Solyc05g012500.3	WRKY transcription factor 57	0,000	0,000	1,172	0,000	WRKY
Solyc05g015850.3	WRKY transcription factor 75	0,000	0,000	0,000	1,961	WRKY
Solyc06g066370.3	WRKY transcription factor 31	0,000	0,000	1,135	1,174	WRKY
Solyc07g005650.3	WRKY transcription factor 32	0,000	0,000	1,557	0,000	WRKY
Solyc07g056280.3	WRKY transcription factor 30	0,000	0,000	0,000	1,998	WRKY
Solyc08g006320.3	WRKY transcription factor 11	0,000	0,000	1,309	0,000	WRKY
Solyc08g067340.3	WRKY transcription factor 46	0,000	0,000	3,276	3,204	WRKY
Solyc09g015770.3	WRKY transcription factor 81	0,000	0,000	1,627	0,000	WRKY
Solyc10g009550.3	WRKY transcription factor 42	0,000	0,000	1,587	0,000	WRKY
Solyc12g014610.2	WRKY transcription factor 20	0,000	0,000	1,508	0,000	WRKY
Solyc12g096350.2	WRKY transcription factor 10	0,000	0,000	1,724	0,000	WRKY
Solyc01g091010.3	CRABS CLAW-like protein1a	0,000	0,000	-2,369	0,000	YABBY
Solyc06g073920.3	CRABS CLAW-like protein 2a	0,000	0,000	-1,968	0,000	YABBY
Solyc05g052570.3	Zinc finger transcription factor 39	0,000	0,000	1,113	0,000	ZF
Solyc06g009070.3	Zinc finger transcription factor 41	0,000	0,000	0,000	1,424	ZF
Solyc07g047940.3	Zinc finger transcription factor 49	0,000	0,000	-3,480	-2,248	ZF
Solyc10g080260.2	Zinc finger transcription factor 62	0,000	0,000	-1,516	0,000	ZF
Solyc01g107170.2	Zinc finger protein	0,000	0,000	1,110	1,592	ZF-C2H2
Solyc02g085580.3	Protein indeterminate-domain 1	0,000	0,000	1,105	1,572	ZF-C2H2
Solyc03g098070.3	C2H2-like zinc finger protein	0,000	-1,401	1,760	0,000	ZF-C2H2
Solyc06g072360.3	Zinc finger protein	0,000	-1,106	0,000	0,000	ZF-C2H2
Solyc06g074360.3	Zinc finger protein WIP3	0,000	0,000	2,233	0,000	ZF-C2H2
Solyc07g063970.3	C2H2 zinc finger protein	0,000	0,000	-2,512	-1,792	ZF-C2H2
Solyc02g086430.3	Zinc finger transcription factor 21	0,000	0,000	0,000	1,733	ZF-C3H
Solyc03g006350.3	Zinc finger transcription factor 23	-2,467	0,000	0,000	0,000	ZF-C3H
Solyc05g008670.3	Zinc finger transcription factor 36	0,000	0,000	2,287	2,520	ZF-C3H
Solyc06g082010.3	Zinc finger transcription factor 48	0,000	0,000	2,090	1,670	ZF-C3H
Solyc03g119540.3	Zinc finger protein	0,000	0,000	-2,027	0,000	ZF-CO-like
Solyc04g007210.3	Zinc finger protein CONSTANS-LIKE 7	0,000	0,000	-1,912	0,000	ZF-CO-like
Solyc05g024010.3	Zinc finger protein CONSTANS-LIKE 15	0,000	0,000	-1,571	0,000	ZF-CO-like
Solyc09g074560.3	Zinc finger protein CONSTANS-LIKE 15	0,000	0,000	2,029	1,226	ZF-CO-like
Solyc04g074990.3	Zinc-finger homeodomain protein 1	0,000	0,000	-1,236	0,000	ZF-HD
Solyc08g077060.3	Zinc finger, LSD1-type	0,000	0,000	-1,169	0,000	ZF-LSD

Table S15. List of the TF encoding genes differentially expressed in the four comparisons in shoot: ROvsUC82-LN, ROvsUC82-HN, RO-LNvsHN and UC82-LNvsHN

Gene ID	Gene annotation	Log2(FC)				
		ROvsUC82-LN	ROvsUC82-HN	RO-LNvsHN	UC82-LNvsHN	Family
Solyc07g018290.3	AP2-like ethylene-responsive transcription factor	0,000	0,000	-1,335	0,000	AP2
Solyc08g008380.3	Auxin Response Factor 9B	0,000	0,000	2,031	2,036	ARF
Solyc01g096070.3	Auxin Response Factor 18	0,000	0,000	1,546	1,607	ARF
Solyc06g061030.3	Two-component response regulator APRR2-like protein	0,000	1,269	0,000	1,247	ARR-B
Solyc03g111410.3	B3 domain-containing protein	0,000	1,340	0,000	0,000	B3
Solyc08g006280.2	Transcriptional factor B3 family protein	-2,097	0,000	0,000	0,000	B3
Solyc01g106460.3	bHLH transcription factor 007	0,000	0,000	1,445	1,626	bHLH
Solyc01g096370.3	transcription factor MYC2	0,000	0,000	0,000	1,534	bHLH
Solyc02g076920.3	bHLH transcription factor 013	0,000	0,000	0,000	1,378	bHLH
Solyc01g102300.3	bHLH transcription factor 006	0,000	0,000	1,360	0,000	bHLH
Solyc01g111130.3	bHLH transcription factor 011	0,000	0,000	1,048	0,000	bHLH
Solyc04g078690.3	bHLH transcription factor 035	0,000	0,000	0,000	-1,133	bHLH
Solyc02g078130.3	bHLH transcription factor 079	0,000	0,000	0,000	-1,201	bHLH
Solyc03g031450.3	Basic helix-loop-helix (BHLH) DNA-binding superfamily protein	0,000	0,000	-1,895	-2,648	bHLH
Solyc05g050220.3	Common plant regulatory factor 1	0,000	0,000	1,688	1,751	bZIP
Solyc01g109880.3	BZIP transcription factor	0,000	0,000	0,000	1,350	bZIP
Solyc07g053450.3	Basic-leucine zipper (BZIP) transcription factor family protein	0,000	0,000	-1,074	0,000	bZIP
Solyc04g072460.3	Transcription factor TGA7	-2,471	0,000	-1,823	0,000	bZIP
Solyc08g006110.3	Basic leucine zipper 9-like transcription factor	0,000	0,000	-1,212	-1,010	bZIP
Solyc06g008740.3	Zinc finger transcription factor 40	0,000	0,000	0,000	1,140	C3H
Solyc06g082010.3	Zinc finger transcription factor 48	0,000	0,000	1,198	0,000	C3H
Solyc02g086430.3	Zinc finger transcription factor 21	0,000	0,000	-1,067	0,000	C3H
Solyc09g074560.3	Zinc finger protein CONSTANS-LIKE 15	0,000	1,442	1,303	2,709	CO-like
Solyc05g024010.3	Zinc finger protein CONSTANS-LIKE 15	0,000	0,000	1,627	0,000	CO-like
Solyc03g112930.3	Dof zinc finger protein	0,000	0,000	-1,132	0,000	Dof
Solyc01g009170.3	EIL-EIN3/EIL	0,000	-1,875	0,000	0,000	EIL
Solyc05g052030.1	ethylene response factor 4	-1,681	0,000	0,000	2,105	ERF
Solyc01g091760.2	Ethylene-responsive transcription factor 1	0,000	0,000	1,866	2,021	ERF
Solyc01g065980.3	Ethylene Response Factor E	0,000	0,000	1,518	1,949	ERF
Solyc01g090340.2	Ethylene-responsive transcription factor 2	0,000	0,000	1,146	1,340	ERF
Solyc09g075420.3	ethylene response factor E	0,000	-1,083	0,000	0,000	ERF
Solyc11g011750.2	Ethylene-responsive transcription factor 1B	-1,760	0,000	-1,768	0,000	ERF
Solyc12g005960.2	Ethylene-responsive transcription factor 4	-2,146	0,000	-2,041	0,000	ERF
Solyc05g051060.3	Homeodomain-like superfamily protein	0,000	0,000	-1,513	0,000	G2-like
Solyc05g009720.3	Myb-like transcription factor family protein	0,000	0,000	-3,710	-4,108	G2-like
Solyc04g015360.3	GATA transcription factor	0,000	0,000	1,165	0,000	GATA
Solyc01g090760.3	GATA transcription factor	0,000	0,000	0,000	-1,412	GATA
Solyc01g096320.3	Homeobox-leucine zipper protein HOX6	0,000	0,000	1,253	2,042	HD-ZIP
Solyc03g034120.3	Homeobox-leucine zipper protein HOX14	0,000	0,000	0,000	1,595	HD-ZIP
Solyc06g035940.3	Homeobox-leucine zipper protein ROC5	4,339	4,766	0,000	0,000	HD-ZIP
Solyc02g062960.3	Homeobox-leucine zipper protein HOX14	-1,499	-1,595	0,000	0,000	HD-ZIP
Solyc02g067410.2	Homeobox-leucine zipper protein HOX21	1,181	0,000	0,000	-2,000	HD-zip
Solyc04g016000.3	Heat shock transcription factor protein 8	0,000	0,000	0,000	1,222	HSF
Solyc09g009100.3	Heat stress transcription factor A3	0,000	0,000	1,254	0,000	HSF
Solyc03g026020.3	Heat shock transcription factor	0,000	-1,432	0,000	0,000	HSF
Solyc05g009320.3	LOB domain-containing protein 40	0,000	0,000	0,000	1,660	LBD
Solyc03g119530.3	LOB domain-containing protein 41	0,000	0,000	-1,035	-1,384	LBD
Solyc06g082770.3	LOB domain-containing protein 4	0,000	0,000	0,000	-1,668	LBD
Solyc02g092550.3	LOB domain-containing protein 38	0,000	0,000	-2,245	-2,794	LBD
Solyc01g107190.3	LOB domain-containing protein 38	1,202	0,000	-2,248	-3,233	LBD
Solyc08g080100.3	MADS box transcription factor AGAMOUS	0,000	0,000	1,210	1,582	MIKC_MADS
Solyc02g084630.3	TDR6 transcription factor	0,000	0,000	-1,739	0,000	MIKC_MADS

Solyc07g052700.3	MADS-box transcription factor	-2,121	-2,362	0,000	0,000	M-type_MADS
Solyc01g106170.3	MADS box transcription factor AGAMOUS	0,000	0,000	0,000	-1,718	M-type_MADS
Solyc04g056310.3	MYB transcription factor	0,000	0,000	2,895	2,527	MYB
Solyc09g090790.3	R2R3MYB transcription factor 79	0,000	0,000	0,000	1,808	MYB
Solyc01g057910.3	R2R3MYB transcription factor 2	0,000	0,000	1,689	1,321	MYB
Solyc06g005330.3	R2R3MYB transcription factor 59	0,000	0,000	0,000	1,243	MYB
Solyc01g111500.3	R2R3MYB transcription factor 7	0,000	0,000	-1,064	0,000	MYB
Solyc01g102340.3	R2R3MYB transcription factor 61	0,000	0,000	0,000	-1,012	MYB
Solyc04g005100.3	transcription factor MYB1R1-like	0,000	0,000	1,596	2,018	MYB_related
Solyc08g065380.3	Transcription factor MYB1R1	0,000	0,000	2,136	0,000	MYB_related
Solyc02g036370.3	Protein REVEILLE 7-like	0,000	-1,083	0,000	0,000	MYB_related
Solyc06g005310.3	Transcription factor MYB48	-1,052	0,000	0,000	0,000	MYB_related
Solyc04g005610.3	NAC domain-containing protein 2	0,000	0,000	2,980	2,039	NAC
Solyc01g104900.3	NAC domain-containing protein	0,000	0,000	1,659	2,004	NAC
Solyc08g068380.3	NAC trascription factor	-2,252	0,000	0,000	1,820	NAC
Solyc03g097650.3	NAC domain	0,000	0,000	-1,087	0,000	NAC
Solyc08g062210.3	Nuclear transcription factor Y subunit A-1	0,000	0,000	2,495	2,852	NF-YA
Solyc01g006930.3	Nuclear transcription factor Y subunit A-4	0,000	0,000	2,133	2,466	NF-YA
Solyc01g087240.3	Nuclear transcription factor Y subunit A-9	0,000	0,000	1,923	1,503	NF-YA
Solyc01g067130.3	Nuclear transcription factor Y subunit B	0,000	0,000	3,387	3,157	NF-YB
Solyc01g099320.3	Nuclear transcription factor Y subunit B-4	0,000	0,000	0,000	-1,627	NF-YB
Solyc01g112190.3	NLP1	0,000	0,000	2,205	3,623	Nin-like
Solyc08g013900.3	NLP4	0,000	0,000	2,580	3,453	Nin-like
Solyc05g012040.3	Squamosa promoter binding protein 6b	0,000	0,000	0,000	-1,512	SBP
Solyc04g079830.2	Homeobox protein BEL1-like protein	0,000	0,000	1,322	2,058	TALE
Solyc09g011380.3	BEL1-like homeodomain protein 9	0,000	0,000	0,000	1,336	TALE
Solyc01g007070.3	BEL1-like homeodomain protein 3	0,000	0,000	1,275	0,000	TALE
Solyc07g055280.3	WRKY transcription factor 78	0,000	0,000	0,000	1,146	WRKY
Solyc08g008280.3	WRKY transcription factor 53	0,000	0,000	2,045	0,000	WRKY
Solyc10g009550.3	WRKY transcription factor 42	0,000	0,000	2,025	0,000	WRKY
Solyc03g116890.3	WRKY transcription factor 39	0,000	0,000	2,023	0,000	WRKY
Solyc06g068460.3	WRKY transcription factor 40	0,000	0,000	1,735	0,000	WRKY
Solyc03g095770.3	WRKY transcription factor 80	0,000	0,000	1,600	0,000	WRKY
Solyc06g066370.3	WRKY transcription factor 31	0,000	0,000	1,550	0,000	WRKY
Solyc08g067340.3	WRKY transcription factor 46	2,426	0,000	0,000	0,000	WRKY
Solyc05g007110.2	WRKY transcription factor 76	0,000	1,173	0,000	0,000	WRKY
Solyc05g012770.3	WRKY transcription factor 4	-1,281	0,000	0,000	0,000	WRKY
Solyc03g113120.3	WRKY transcription factor 73	0,000	0,000	-1,287	-2,128	WRKY
Solyc10g080090.2	zinc finger BED domain-containing protein DAYSLEEPER-like	1,466	0,000	0,000	-1,163	ZF

Table S16. Biological process GO term enrichment of the co-expressed genes in lightgreen, greenyellow and turquoise module in shoot

Module	Enrichment FDR	Genes in list	Total genes	Functional Category
Lightgreen	4.77E-08	8	225	Photosynthesis
Lightgreen	1.29E-02	2	13	Regulation of translational elongation
Greenyellow	9.20E-18	17	225	Photosynthesis
Greenyellow	5.62E-14	10	58	Photosynthetic electron transport chain
Greenyellow	5.62E-14	8	22	Photosynthetic electron transport in photosystem II
Greenyellow	2.03E-12	11	122	Photosynthesis. light reaction
Greenyellow	2.51E-09	10	175	Electron transport chain
Greenyellow	4.40E-07	11	396	Generation of precursor metabolites and energy
Greenyellow	3.18E-04	4	48	Protein-chromophore linkage
Greenyellow	3.18E-04	16	1679	Oxidation-reduction process
Turquoise	7.19E-57	80	225	Photosynthesis
Turquoise	7.50E-34	140	1265	Organonitrogen compound biosynthetic process
Turquoise	5.11E-33	132	1164	Small molecule metabolic process
Turquoise	8.48E-29	42	122	Photosynthesis. light reaction
Turquoise	2.63E-24	65	396	Generation of precursor metabolites and energy
Turquoise	2.57E-21	85	736	Oxoacid metabolic process
Turquoise	2.64E-21	85	738	Organic acid metabolic process
Turquoise	1.76E-20	82	714	Carboxylic acid metabolic process
Turquoise	5.40E-20	19	28	Photosynthesis. light harvesting
Turquoise	2.73E-19	78	685	Amide biosynthetic process

Table S17. KEGG pathway enrichment of the co-expressed genes in turquoise module in shoot

Enrichment FDR	Genes in list	Total genes	Functional Category
1.893e-31	130	1194	Metabolic pathways
6.590e-22	21	33	Photosynthesis
3.063e-20	79	695	Biosynthesis of secondary metabolites
5.659e-17	33	149	Carbon metabolism
3.358e-13	16	38	Carbon fixation in photosynthetic organisms
4.520e-11	14	36	Porphyrin and chlorophyll metabolism
2.096e-10	23	124	Biosynthesis of amino acids
3.818e-10	25	152	Biosynthesis of cofactors
1.421e-08	8	13	Photosynthesis
1.049e-07	12	44	Glyoxylate and dicarboxylate metabolism
2.472e-07	23	180	Ribosome
1.217e-05	8	27	Aminoacyl-tRNA biosynthesis
4.599e-05	8	32	Fatty acid metabolism
0.000339	8	42	Glycine, serine and threonine metabolism
0.000339	5	14	Nitrogen metabolism
0.000415	11	82	Glycolysis / Gluconeogenesis
0.000508	6	24	Fatty acid biosynthesis
0.001082	5	18	Sulfur metabolism
0.001357	6	29	Pentose phosphate pathway
0.001357	4	11	Biosynthesis of unsaturated fatty acids

Table S18. Top 10 Biological process GO terms and KEGG pathways enrichment of the co-expressed genes in turquoise module in root

	Enrichment FDR	Genes in list	Total genes	Functional Category
BP	1,71E-08	45	2184	Response to stimulus
BP	2,93E-07	13	192	Response to inorganic substance
BP	3,13E-07	29	1142	Response to stress
BP	1,70E-06	26	1033	Transmembrane transport
BP	5,19E-05	4	12	Response to nitrate
BP	2,60E-06	5	14	Fluid transport
BP	2,60E-06	5	14	Water transport
BP	5,24E-06	36	1960	Transport
BP	5,59E-06	37	2074	Localization
BP	5,59E-06	36	1981	Establishment of localization
KEGG	0,0082	20	1194	Metabolic pathways
KEGG	0,0739	2	14	Nitrogen metabolism
KEGG	0,0800	2	18	Zeatin biosynthesis
KEGG	0,0800	11	695	Biosynthesis of secondary metabolites
KEGG	0,1022	2	30	Alanine, aspartate and glutamate metabolism
KEGG	0,1022	3	83	Amino sugar and nucleotide sugar metabolism
KEGG	0,1022	4	149	Carbon metabolism
KEGG	0,1484	3	101	Phenylpropanoid biosynthesis
KEGG	0,17587	2	51	Pentose and glucuronate interconversions
KEGG	0,17587	1	7	Brassinosteroid biosynthesis

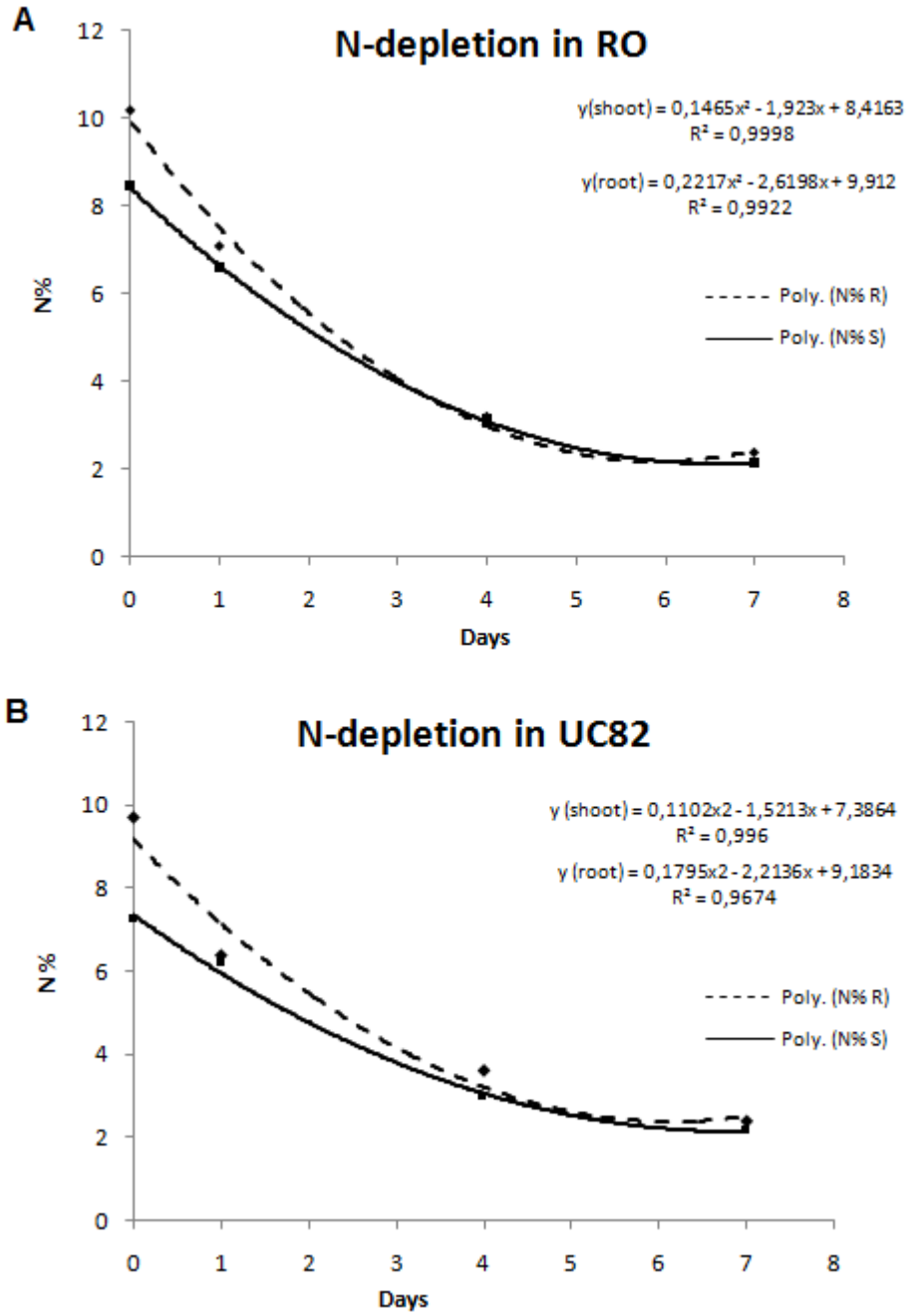

Figure S1: N-depletion in the two tomato genotypes (RO and UC82) roots and shoots grown in N free solution. The data were plotted by non linear regression.

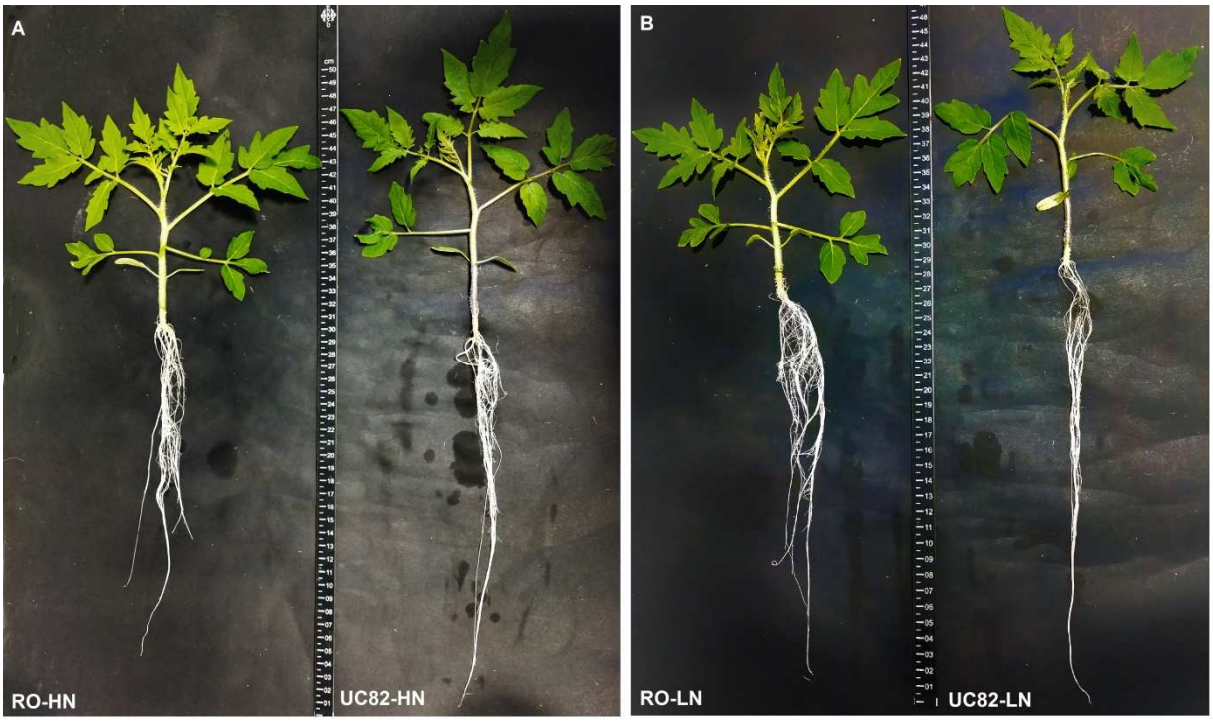

Figure S2: Phenotypic differences between tomato genotypes Regina Ostuni (RO) and UC82 grown under non-limiting (A) (10 mM $Ca(NO3)_2$) and limiting (B) (0.5 mM $Ca(NO3)_2$) NO_3^- supply.

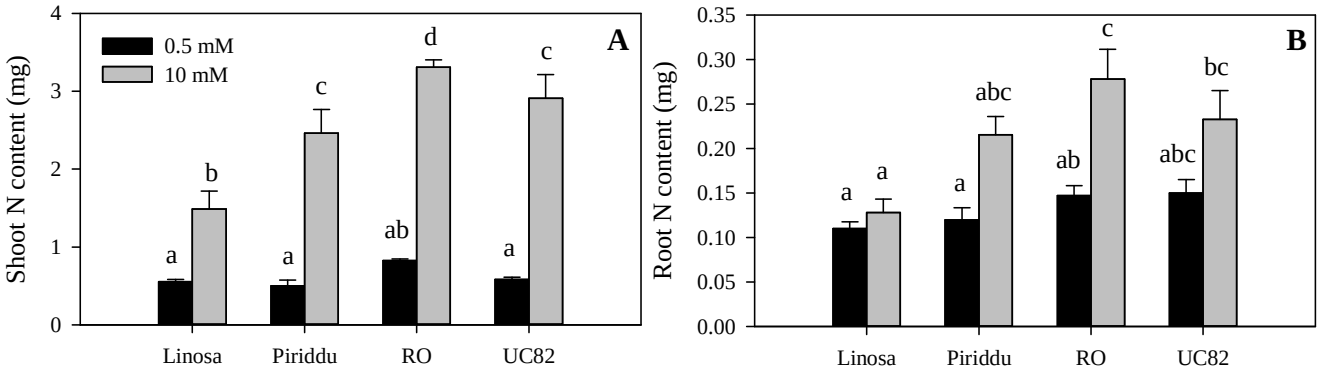

Figure S3: Shoot (A) and root N content (B) of four genotypes grown under limiting (0.5 mM $Ca(NO_3)_2$) and non-limiting NO_3^- supply (10 mM $Ca(NO_3)_2$) ($P < 0.05$, n=5).

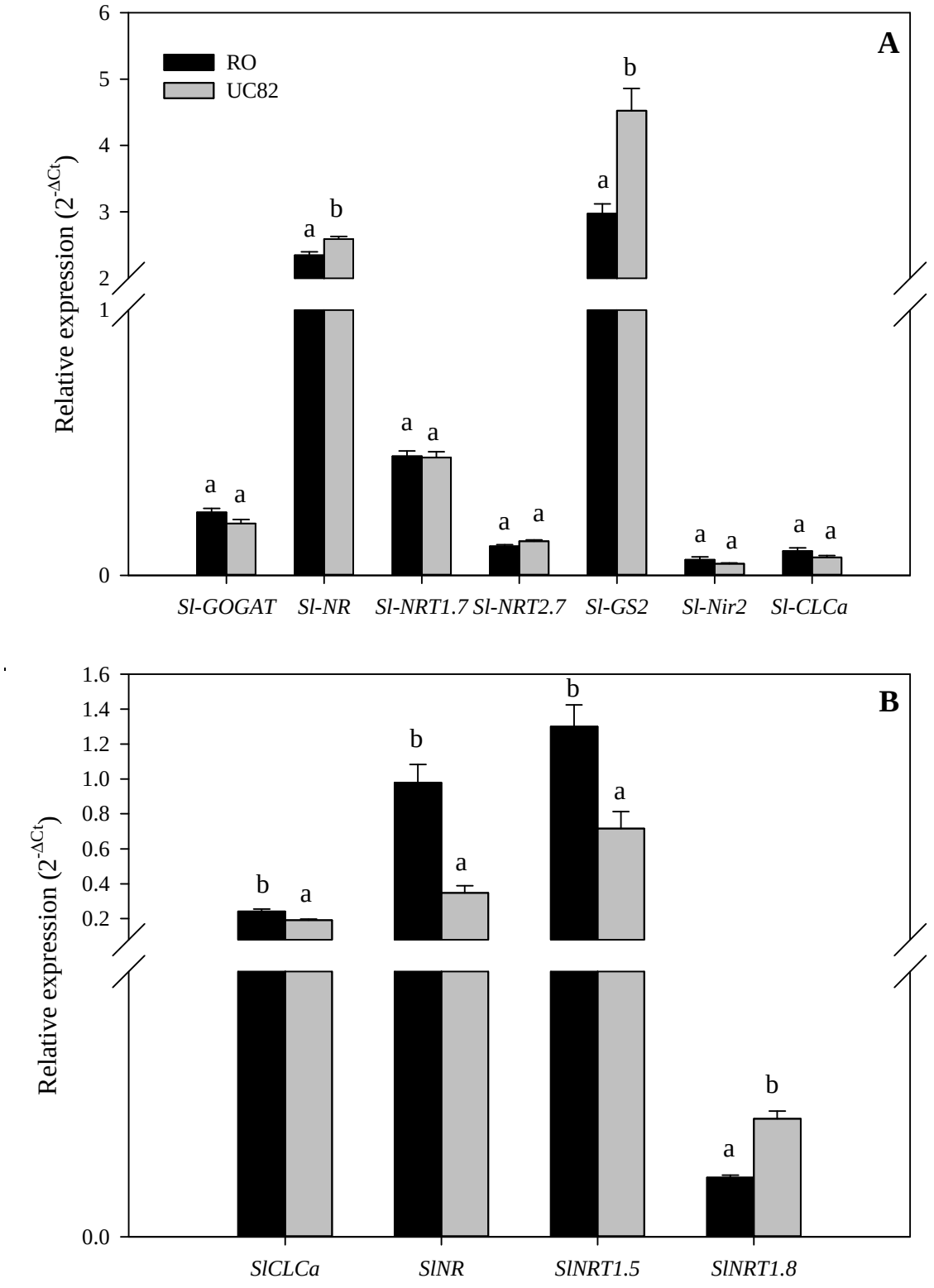

Figure S4: Differential relative expression of NO_3^- metabolism-related gene in shoot (A) and root (B) of the two tomato genotypes before NO_3^- recovery (T0, 0 mM $Ca(NO_3)_2$). The relative gene expression is represented as the normalized relative quantity of a target gene's expression with respect to the reference gene *SlActin*. Means and standard errors are shown from the analysis of three biological replicates. Different letters within each gene indicate significant differences ($P < 0.05$, n=3).

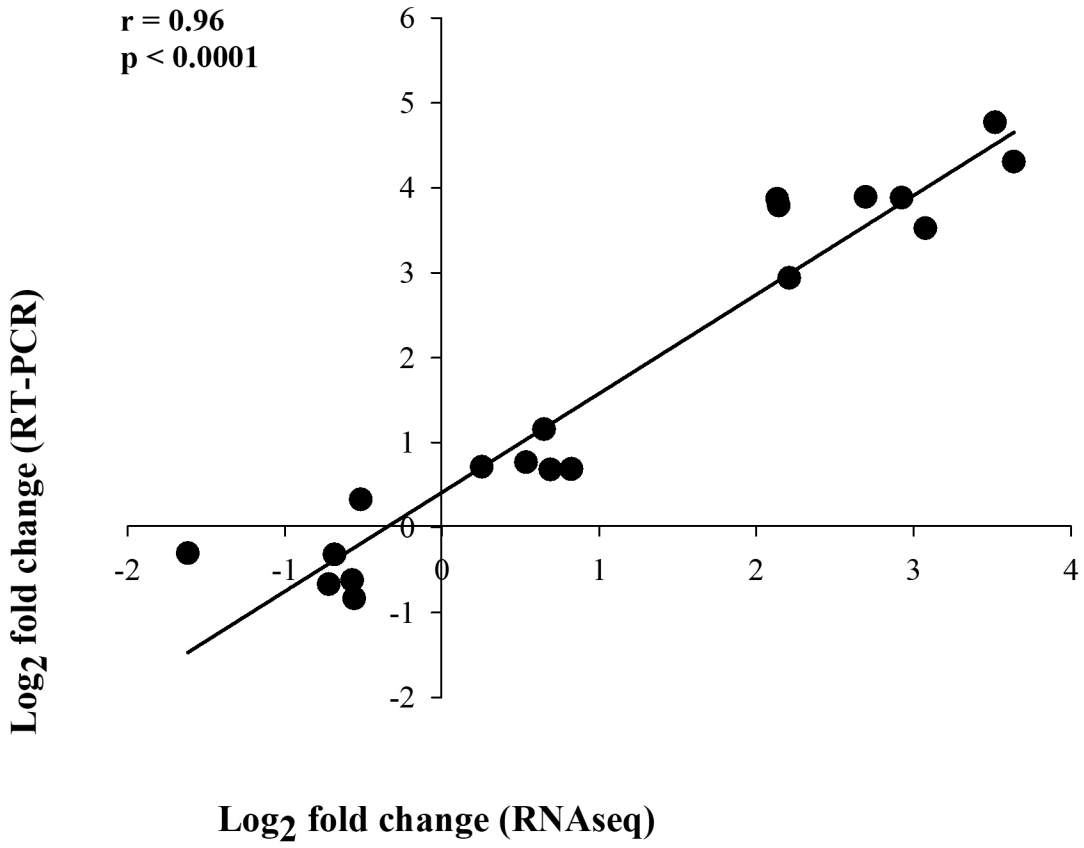

Figure S5: Scatter plot of gene expression measured by real-time qPCR and read counting in RNA-seq data in short-term analysis of 10 chosen N-metabolism related genes. Data represent Log2(FC, ration T1/T0)

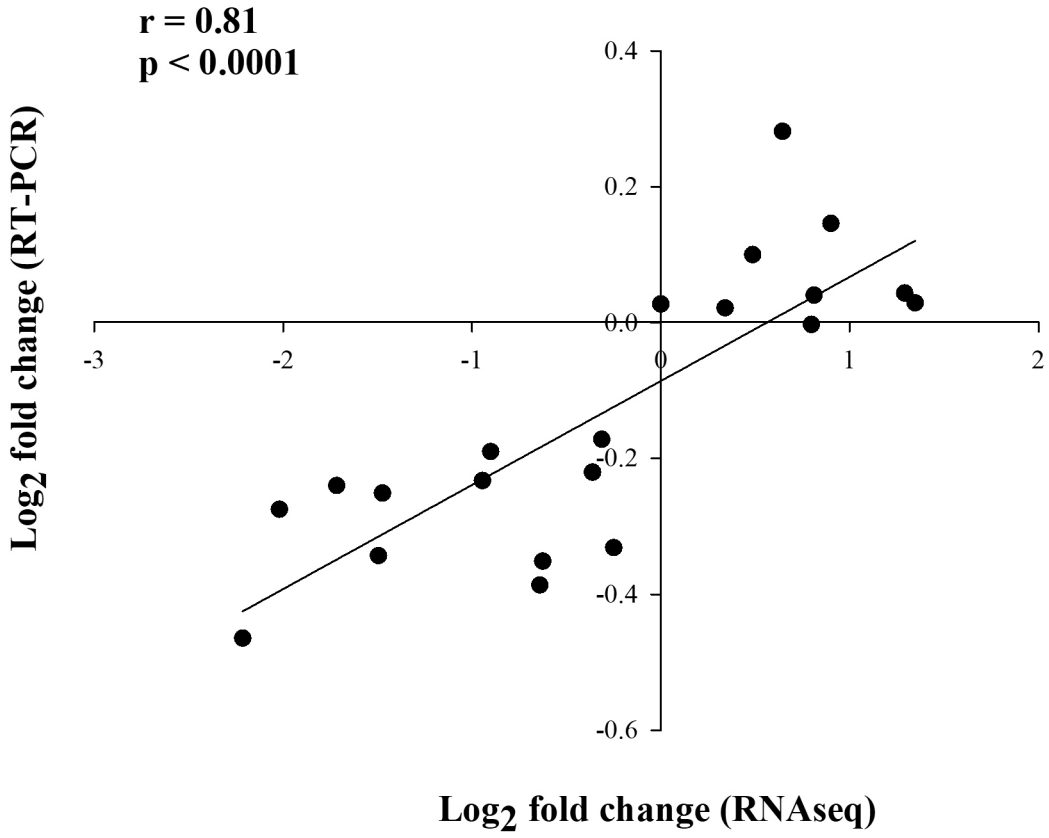

Figure S6. Scatter plot of gene expression measured by real-time qPCR and read counting in RNA-seq data in long-term analysis of 10 chosen N-metabolism related genes. Data are represented as Log2(FC, ratio T3LN/T3HN)

List of Figures

$Ca(NO_3)_2$) supply. Shoots of 32d old plants were sampled at 0h, 8h and 24 h after NO_3^- recovery. The mean fold change in expression of the target gene at each time point was calculated using the $2^{-\Delta\Delta Ct}$ method, where $\Delta\Delta CT = (C_{T,Target} - C_{,Actin})_{Time\ x} - (C_{T,Target} - C_{,Actin})_{Time\ 0,}$ SlActin was the internal control gene and time 0 was the calibrator. Means and standard errors are shown from the analysis of three biological replicates ($P < 0.05$, n=3) and different letters within each time point indicate significant differences at $P < 0.05$).

Figure 18. Differential relative expression of NO_3^- metabolism-related gene in root of RO and UC82 grown under NO_3^- limiting (0.5 mM $Ca(NO_3)_2$) and non-limiting (10 mM $Ca(NO_3)_2$) supply. Roots of 32d old plants were sampled at 0h, 8h and 24 h after NO_3^- recovery. The mean fold change in expression of the target gene at each time point was calculated using the $2^{-\Delta\Delta Ct}$ method, where $\Delta\Delta CT = (C_{T,Target} - C_{,Actin})_{Time\ x} - (C_{T,Target} - C_{,Actin})_{Time\ 0}$, SlActin was the internal control gene and time 0 was the calibrator. Means and standard errors are shown from the analysis of three biological replicates ($P < 0.05$, n=3) and different letters within each time point indicate significant differences at $P < 0.05$).

Figure 19.Heatmap of NO_3^- metabolism-related gene expressions in shoot and root, physiological NUE-related parameters and NUE and its components of RO and UC82 after one week under NO_3^- limiting (0.5 mM $Ca(NO_3)_2$) and non-limiting (10 mM $Ca(NO_3)_2$) supply.

Figure 20.Correlation matrix visualization of the correlations between NUE related parameters and NO_3^- metabolism-related gene expressions of RO and UC82 after one week under NO_3^- limiting supply (0.5 mM $Ca(NO_3)_2$). * $0.01 < p \leq 0.05$; ** $0.001 < p < 0.01$; *** $p < 0.001$

Figure 21. The proposed model describing Regina Ostuni high N-utilization efficiency (NUtE). In black and bold the different expressed key genes that could be involved in high NUE tomato genotype making it able to cope N-limiting supply. The gene expression increase or decrease are indicated with red and green arrows, respectively.

Figure 22. The N-depletion experimental setup and the schematic sampling-time.

Figure 23.N-depletion of the two tomato genotypes grown in N-free solution. The data were plotted by a non-linear regression.

Figure 24. Experimental setup adopted for the short-term RNAseq analysis

Figure 25. Principal component analysis (PCA) of the whole transcriptome data set.

Figure 26.Hierarchical clustering of normalized expression levels for the differentially expressed (DE) genes between genotypes, times, N levels and their interactions.

Annexine (ANN) in root, and Alternative Oxidase (AOX1) in shoot, which were among the central genes in both tissues regulatory networks. The antioxidant and scavenging activities of the encoded proteins might lead to shoot and root cell homestasis sustaining cell development and growth under LN stress. In shoot, plant hormone signal transduction and protein kinases (PK) signaling pathways were upregulated. Among the genes involved in these pathways a CBL-interacting PK (CIPK1), an Ethylen Responsive Transcription Factor (ERF2) and a cytokinin activating enzyme encoding gene (LOG8) were central genes in the regulatory network. CIPK1 might be involved in primary NO3- response (PNR), whereas ERF2 and LOG8 are supposed to play a pivotal role in nitrate-cytokinin signaling cross-talk. The LN-induced cytokinins activation, suppose a subsequent cell proliferation and plant tissues growth. The Asparagine synthetase (ASNS), identified as hub gene in the shoot regulatory network, was upregulated suggesting a better management of the absorbed NO3- compared to low NUE genotype. The induced metabolic pathways and the function of the encoded protein are represented in yellow and orange, respectively. The putative responses resulting from the gene expressions, genes of interest, and transcription factors (TFs) are presented in green, red and blue colors, respectively.

Figure 40.Experimental setup adopted for the long-term RNA-seq analysis.

Figure 41.Heatmap of the expression profiles of all the identified DEGs from the four pairwise comparisons for N (RO-LN*vs*.HN and UC82-LN*vs*.HN) and G effect (RO*vs*.UC82-LN and RO*vs*.UC82-HN) in shoot (A) and root (B) The values are expressed as log2FC. Venn diagram of the DEGs identified in shoot and root (C).

Figure 42.Venn diagrams of differentially expressed genes (DEGs) between the four comparisons in shoot (A) and root (B). The number of up and downregulated genes in shoot (C) and root (D).

Figure 43. Functional enrichment analysis of genotype specific DEGs in response to LN in shoot: Venn diagram (A). Top 10 Biological process GO terms (B), KEGG pathways enrichment (C).

Figure 44.Functional enrichment analysis of genotypes specific DEGs in response to LN in root: Venn diagram (A), Top 10 Biological process GO terms (B), KEGG pathways enrichment (C).

Figure 45.Functional enrichment analysis of the LN-specific DEGs identified by Venn diagrams for RO*vs*.UC82-LN comparison in shoot (A) and root (B), Top 10 Biological process terms (C), KEGG pathways enrichment (D).

Figure 46.Heatmap of the DEGs involved in the photosynthesis process GO term. The values are expressed in log2FC.

Figure 47.Distribution of DEGs encoding for different transcription factors families in shoot and root. Venn diagram for TFs total number in shoot and root (A), distribution for each TF family in shoot (B) and root (C), Venn diagrams for TFs identified in each comparison in shoot (D) and root (E).

Figure 48.Genotype-specific LN responsive DEGs encoding transcription factors and their distribution in shoot of RO (A) and UC82 (B).

Figure 49.Genotype-specific LN responsive DEGs encoding transcription factors and their distribution in root of RO (A) and UC82 (B).

Figure 50.Heatmap of LN-specific transcription factors in tomato shoot and root. The values are expressed in log2FC

Figure 51.Scale independence and Mean Connectivity (A), Clustering of module eingengenes (B), Cluster dendrogram (C) and Module-trait relationship (D) of the 3203 DEGs in the tomato shoot (see Materials and Methods).

Figure 52.Scale independence and Mean Connectivity (A), Clustering of module eingengenes (B), Cluster dendrogram (C) and Module-trait relationship (D) of the 3203 DEGs in the tomato root (see Materials and Methods).

Figure 53.Module membership (MM) *vs*. gene significance (GS) for NUE in the lightgreen module in shoot (A), Network analysis of the hub genes in the same module (B). Node size represents the connectivity degree of genes.

Figure 54.Module membership (MM) *vs*. gene significance (GS) for NUE in the greenyellow module in shoot (A), Network analysis of the hub genes in the same module (B). Node size represents the connectivity degree of genes.

Figure 55.Module membership (MM) *vs.* gene significance (GS) for SDW in the turquoise module in shoot (A), Network analysis of the hub genes in the same module (B). Node size represents the connectivity degree of genes.

Figure 56.Module memberships (MM) vs. gene significance (GS) for NUpE in the turquoise module in root (A), Network analysis of the hub genes in the same module (B). Node size represents the connectivity degree of genes.

Figure 57.Heatmaps of the expression patterns of the key genes identified for NUE, SDW and NUpE in the different comparisons for N and G effects in modules lightgreen, greenyellow and turquoise in shoot (A), and turquoise in root (B). The values are expressed in log2FC.

Figure 58. Model scheme showing the multilevel regulation of the long-term low NO3- stress in Regina Ostuni. In shoot, the photosynthesis is the main biological process upregulated by stress, including genes involved in photosynthesis light reaction (PSI, PSII, CytB6-f, FNR) as well as C fixation (Rubisco, RBC) which are central genes in the regulatory networks correlated to NUE. These results suggest the C/N balance as a potential target for NUE improvement. The results also suggest the central role played by the chloroplast in high NUE genotype, since YCF2 in chloroplast genome is strongly upregulated. Recently reported to be involved in chloroplast protein import, YCF2 is among the central genes in shoot regulatory network correlated to NUE, suggesting an ongoing and improved activity of chloroplast stroma proteins leading to a higher plant adaptation to NO3- stress. In root, the central genes identified in the regulatory networks correlated to NUpE are involved in Nitrate response and transmembrane transport activity biological processes, including two NO3- transporters (NIT1 and NIT2) and two aquaporins (PIP1.1 and PIP2.5). The overexpression of these genes should improve solute/ NO3- transport and distribution in the plant to sustain plant adaptation to long-term low NO3- stress. The induced metabolic pathways and the function of the encoded protein are presented in yellow and orange, respectively. The putative responses resulting from the gene expressions, genes of interest and transcription factors (TFs) are indicated in green, red and blue colors, respectively.

List of Tables